Rb pathway and chromatin remodeling genes that antagonize *let-60* Ras signaling during *C. elegans* vulval development

by
Craig J. Ceol

B.S./M.S., Molecular Biophysics and Biochemistry
Yale University, 1993

Submitted to the Department of Biology
in partial fulfillment of the requirements for the degree of

DOCTOR OF PHILOSOPHY

at the
MASSACHUSETTS INSTITUTE OF TECHNOLOGY
[February 2003]
September 2002

ARCHIVES

Signature of Author: _____
Department of Biology
September 12, 2002

Certified by: _____
H. Robert Horvitz
Professor of Biology
Thesis Supervisor

Accepted by: _____
Alan Grossman
Chairman of the Graduate Committee
Department of Biology

Rb pathway and chromatin remodeling genes that antagonize *let-60* Ras signaling during *C. elegans* vulval development

Craig J. Ceol

ABSTRACT

The synthetic multivulva (synMuv) class A and class B genes act redundantly to regulate Ras-mediated vulval cell fate specification in the nematode *Caenorhabditis elegans*. The class B synMuv gene *lin-35* encodes a protein similar to the mammalian pRb tumor suppressor protein. The LIN-35 Rb protein is proposed to act with HDA-1, a histone deacetylase homolog with class B synMuv activity, to remodel chromatin and repress transcription of genes that promote vulval development. To further understand how *lin-35* Rb and *hda-1* regulate vulval cell fate specification, we identified and characterized additional class B synMuv genes. We found that two of these genes, *dpl-1* and *efl-1*, encode homologs of DP and E2F DNA-binding transcription factors, respectively. Loss-of-function mutations in *dpl-1* and *efl-1* cause the same synMuv phenotype as do *lin-35* Rb loss-of-function mutations, and the DPL-1 and EFL-1 proteins interact with each other and with LIN-35 Rb *in vitro*. These data suggest that, in the context of vulval development, DPL-1 and EFL-1 recruit LIN-35 Rb, HDA-1 and other synMuv proteins to DNA to repress transcription. We found that the class B synMuv genes *lin-52* and *lin-54* encode novel, conserved proteins. The cysteine-rich LIN-54 protein is localized to nuclei and interacts with the class B synMuv protein LIN-36 *in vitro*. Homologs of *lin-52* and *lin-54* are candidate Rb pathway genes in other organisms. We performed a genetic screen for synMuv mutations and identified seven new synMuv genes. We found that one of these genes, *mep-1*, encodes a zinc-finger protein. Mutations affecting another gene identified in this screen, *trr-1*, synergize with either class A or class B mutations, thus defining a new class of synMuv gene. *trr-1* encodes a protein similar to the mammalian TRRAP transcriptional adaptor protein. We identified *hat-1* and *epc-1*, which encode homologs of TRRAP-associated histone acetyltransferase and Enhancer of Polycomb-like proteins, respectively, as additional members of this new class of synMuv genes. The synMuv activities of both *hat-1* and *hda-1* suggest that a combination of histone acetyltransferase and histone deacetylase activities are required to properly specify vulval cell fates.

Thesis Supervisor: H. Robert Horvitz
Title: Professor of Biology

ACKNOWLEDGMENTS

I thank Bob Horvitz for attracting talented people to the lab and for providing an environment that encourages intellectual curiosity and effective research and presentation. My thesis committee members Tyler Jacks and Terry Orr-Weaver have provided excellent suggestions and insights throughout the course of this work. I also thank my thesis advisor at Yale, Professor Lynne Regan, and Dr. Walt Prouty at Eli Lilly for their contributions to my scientific education.

I have benefited from the company and generosity of many past and present members of the Horvitz lab. Jeff Thomas laid much of the groundwork for my studies, and I am indebted to him. Mark Metzstein ably dealt with my initial inexperience. He and Scott Cameron showed me that one can be serious about research yet have a lot of fun in the process. Na An, Beth Castor and Colleen Asbury helped me in innumerable ways; the lab would simply not function without them. Brendan Galvin, Mark Alkema, Ignacio Perez de la Cruz, Ho-Yon Hwang, Ewa Davison, Hillel Schwartz, Peter Reddien, Zheng Zhou, Barbara Conradt, Gillian Stanfield, Melissa Hunter-Ensor, Eric Miska, Melissa Harrison, Mike Hurwitz, Erik Andersen and Frank Stegmeier provided friendship, excellent scientific discussions and interesting books and CDs.

Outside of the lab I have enjoyed the friendship of Dave Akey, Gyorgyi Csankovski, Margy Glasner and especially John Newman, with whom good beer and conversation were never a problem.

My parents Ed and Liz and my siblings and their spouses, Ed and Dawn Ceol, Beth and Matt Smith, Tracey Ceol and D'Ann and Greg Wilkes, provided continual encouragement and support. Our annual pilgrimage to the Outer Banks of North Carolina and our holidays together have never failed to recharge my battery. I am also grateful to my wife Kirsten's family, the Mayers, for great times together and for their support. My grandmother Anna Yoblonski passed away in 1998 and on an occasion like this I can't help but wish she were here.

Lastly, I am fortunate to have shared these years with Kirsten. Her companionship and unwavering support, even on those days when we'd see each other only for a morning cup of coffee, have been a constant source of strength and joy.

TABLE OF CONTENTS

Abstract 2
Acknowledgments 3
Table of contents 4
Chapter 1. Introduction: The synthetic multivulva genes and regulation of chromatin structure 13
Introductory remarks 14
Links between chromatin remodeling and *C. elegans* vulval development 15
Vulval development in *C. elegans* 15
A Ras pathway induces vulval development 15
The synthetic multivulva genes antagonize *let-60* Ras signaling 16
The class B synMuv genes encode components of an Rb pathway 17
Transcriptional regulation by chromatin remodeling is likely important for vulval development 18
Proteins that modulate chromatin structure regulate transcription 19
Chromatin structure and organization 19
ATP-dependent chromatin remodeling complexes alter DNA accessibility 20
HATs and HDACs control acetylation of histones 21
Acetylation of nucleosomal histone tails is typically correlated with transcriptional activation 23
Repressed chromatin domains are hypoacetylated 24
Some histone acetylation may be important for gene silencing 25
Recruitment of ATP-dependent remodeling and histone acetyltransferase complexes can stimulate transcription 25
Transcriptional repression can involve recruitment of ATP-dependent chromatin remodeling and histone deacetylase complexes 26
Switching between activating and repressing complexes 27
Chromatin-modifying activities are not always targeted 28
Histone methyltransferases 28
Lysine methylation of histones has different effects on transcription 29
Modified histone tails are docking sites for chromatin-binding proteins 29
Dysfunction of chromatin remodeling proteins is linked to cancer in mammals .. 30
Transcriptional regulation by the E2F and Rb families of proteins involves

chromatin remodeling 31
Future issues regarding chromatin 34
Concluding remarks 36
References 37
Table 58
Table 1. Chromatin remodeling enzymes 58
Figure 59
Figure 1. Pn.p cell fates are specified in two sequential steps 60
Chapter 2. New Genes that Interact with *lin-35 Rb* to Negatively Regulate the *let-60 ras* Pathway in *Caenorhabditis elegans* 61
Abstract 62
Introduction 63
Materials and Methods 67
Strains and general techniques 67
Mutagenesis of class A and class B mutants 67
Molecular analysis of *lin-15AB* lesions 68
Molecular analysis of *lin-13* lesions 68
Nomarski observation and P(3-8).p cell lineage analysis of *lin-54* animals 69
Construction of strains homozygous for newly isolated synMuv mutations 69
Construction of unlinked synMuv double mutants 69
Construction of linked synMuv double mutants 69
Results 71
Isolation of new synMuv strains 71
Linkage and complementation 71
Identification of *lin-15*AB double mutants 73
Identification of *lin-13* mutations 74
Phenotypes of newly isolated synMuv strains 74
New synMuv genes 76
Maternal rescue of the synMuv phenotype depends on both class A and class B genes 77
Discussion 79
Null phenotypes of synMuv genes 79
Many Class A and class B synMuv genes probably act in distinct pathways 81
Synthetic phenotypes 81

Class B synMuv genes define an Rb-mediated pathway 81
Acknowledgments 84
Literature cited 85
Tables 93
Table 1. Origins, chromosomal linkages and phenotypes of new synthetic multivulva strains 93
Table 2. Sequences of *lin-13* class B mutations 96
Table 3. Three- and four-factor crosses and deficiency heterozygotes 97
Table 4. Phenotypes of single and double mutants 99
Table 5. Maternal rescue of synMuv phenotype 100
Table 6. SynMuv genes and alleles 102
Figure 105
Figure 1. Genetic map locations of newly identified or newly characterized synMuv genes 106
Chapter 3. *dpl-1* DP and *efl-1* E2F Act with *lin-35* Rb to Antagonize Ras Signaling in *C. elegans* Vulval Development 107
Summary 108
Introduction 109
Results 111
The class B synMuv mutation *n2994* affects a DP-related gene 111
A *dpl-1* DP null allele causes a synMuv phenotype 112
DPL-1 is broadly expressed and is localized to nuclei 113
Some cell divisions are affected by loss of *dpl-1* function 113
Identification of two *C. elegans* E2F-like genes, *efl-1* and *efl-2* 115
efl-1 is a class B synMuv gene 116
DPL-1 and EFL-1 interact with each other and with LIN-35 *in vitro* 117
RTK/Ras pathway activity is required for *dpl-1* and *efl-1* Muv phenotypes 118
Discussion 120
DPL-1 and EFL-1 may repress rather than promote transcription during vulval development 120
dpl-1 and *efl-1* antagonize RTK/Ras signaling 121
Comparisons of EFL-1 with mammalian E2F family members 121
Are *dpl-1* DP and *efl-1* E2F required for entry into S phase? 122
Experimental procedures 123

Strains 123
Antibody preparation and immunocytochemistry 123
RNAi analyses 123
BrdU incorporation and detection 124
Cell lineage analysis 124
Transgenic strains 124
In vitro binding experiments 125
Acknowledgments 126
References 127
Table 133
Table 1. *dpl-1* and *efl-1* mutations cause a synMuv phenotype 133
Figures 135
Figure 1. *dpl-1* cloning 135
Figure 2. DPL-1 is expressed broadly in nuclei 137
Figure 3. Characterization of P cell descendants in *dpl-1(n3316 RNAi)* animals 139
Figure 4. Identification of *efl-1* and *efl-2* 141
Figure 5. DPL-1, EFL-1 and LIN-35 *in vitro* interactions 143
Figure 6. Model: DPL-1 and EFL-1 may repress but not activate transcription .. 145
Supplemental data 147
Isolation of deletion mutants 147
Genetic mapping 147
cDNA, RT-PCR and mutant allele analyses 147
Supplemental data references 149
Addendum 150
A *dpl-1* DP null allele causes sterility and embryonic lethality 150
Addendum references 152
Addendum table 153
Addendum table 1. Loss of *dpl-1* function causes sterility and embryonic lethality 153
Addendum figure 155
Addendum figure 1. Oocytes are fragmented during ovulation in *dpl-1(n3316)* mutants 155
Chapter 4. *lin-54* encodes a conserved cysteine-rich protein that acts in an

Rb signaling pathway to regulate vulval development in *C. elegans* 157
Abstract 158
Introduction 159
Materials and methods 161
Genetics 161
Isolation of *lin-54* deletion alleles 161
lin-54 cDNA and *in vivo* expression constructs 161
Transgenic animals 162
Heat shock analyses 162
RNAi analyses 162
Protein interaction studies 162
Results 164
Molecular identification of *lin-54* 164
LIN-54 contains two copies of a conserved cysteine-rich motif 164
LIN-54 is expressed broadly and is localized to nuclei 165
Loss of *lin-54* function causes sterility 165
let-60 Ras pathway activity is required for expression of the *lin-54; lin-15A* Muv phenotype 166
Temporal- and tissue-specific expression of a *lin-54* transgene rescues the *lin-54* Muv phenotype 166
LIN-54 interacts with LIN-36 *in vitro* 167
Discussion and future experiments 169
LIN-54 and its homologs are candidate Rb pathway proteins 169
Does *lin-54* have a role in cell cycle progression? 170
Acknowledgments 171
References 172
Tables 176
Table 1: Loss of *lin-54* function causes a synMuv phenotype 176
Table 2: *let-60* Ras pathway activity is required for the *lin-54* Muv phenotype 177
Figures 178
Figure 1. Molecular cloning of *lin-54* 178
Figure 2. *lin-54* gene structure as deduced from cDNA and genomic sequences 180
Figure 3. Alignment of LIN-54L with proteins predicted from human, mouse

and *Drosophila* cDNA and genomic sequences 182
Figure 4. *lin-54::gfp* expression 184
Figure 5. *lin-54* heat shock rescue 186
Figure 6. LIN-54 and LIN-36 *in vitro* interactions 188
Chapter 5. Newly-identified synthetic multivulva mutations affect the *lin-35* Rb pathway genes *lin-52* and *mep-1* and define genes that negatively regulate *let-60* Ras pathway signaling in *C. elegans* 190
Abstract 191
Introduction 192
Materials and methods 195
Strains and general techniques 195
Isolation of new alleles 196
Linkage group assignment 196
Complementation tests 197
Construction of deficiency heterozygotes 197
Transgenic animals 197
lin-52 cDNA isolation 197
Allele sequence 198
Results 199
Isolation of new synMuv mutants 199
Phenotypes of new mutants 200
New synMuv genes 200
Molecular identification of *lin-52* 201
Molecular identification of *mep-1* 202
Sequences of synMuv mutations 203
Discussion 205
Frequency of mutant isolation 205
The synMuv genes we identified likely act in different pathways 205
lin-52 encodes a new putative Rb pathway protein 206
Acknowledgments 208
Literature cited 209
Tables 215
Table 1. Phenotypes of synMuv mutant strains 215
Table 2. Chromosomal linkages of new synMuv mutations 218

Table 3. Map data for newly-identified synMuv loci 221
Table 4. Selected synMuv proteins and allele sequences 224
Figures 228
Figure 1. Molecular cloning of *lin-52* 228
Figure 2. *lin-52* gene structure and translation 230
Figure 3. *mep-1* physical map location and translation 232
Chapter 6. *C. elegans* TRRAP, Enhancer of Polycomb and MYST family histone acetyltransferase homologs act redundantly with *lin-35* Rb and other synthetic multivulva genes to antagonize *let-60* Ras pathway-mediated vulval induction 234
Abstract 235
Introduction 236
Materials and methods 238
Strains and genetics 238
P(3-8).p induction assay 238
trr-1 cloning 238
RNAi analyses 239
Deletion allele isolation 239
cDNA isolation 239
Allele sequence 240
Results 241
trr-1 interacts with class A and class B synMuv mutations 241
trr-1 encodes a protein similar to mammalian TRRAP 242
trr-1(RNAi) is synthetically lethal with mutations in *lin-35* Rb and other class B synMuv genes 243
trr-1 synthetically interacts with *dpl-1* DP 244
The Muv phenotype of *trr-1* mutants requires *let-60* Ras pathway activity 245
hat-1 and *epc-1*, but not *ssl-1*, loss of function phenocopies *trr-1* 246
Discussion and future experiments 249
trr-1 acts redundantly with *lin-35* Rb to antagonize *let-60* Ras signaling 249
Do *trr-1*, *hat-1* and *epc-1* share a common function? 249
Do *hat-1* mutants have defects in histone acetylation? 250
Does this putative HAT complex function in gene activation or gene silencing? 250

How might a putative TRR-1/EPC-1/HAT-1 complex be targeted to DNA? 251
Acknowledgments 252
References 253
Tables 260
Table 1. *trr-1* mutations cause a hyperinduced phenotype 260
Table 2. *trr-1(RNAi)* is synthetically lethal with class B but not with class A synMuv mutations 262
Table 3. *trr-1* acts redundantly with *dpl-1* 263
Table 4. *trr-1* epistasis with *let-23* RTK, *let-60* Ras and *lin-3* EGF 264
Table 5. *hat-1* and *epc-1* but not *ssl-1* loss of function phenocopies *trr-1* loss of function 265
Figures 266
Figure 1. *trr-1* single mutants were defective in P(8).p fate specification 266
Figure 2. *trr-1* and class B synMuv mutations are synthetically defective in P8.p cell-fate specification 268
Figure 3. *trr-1* gene structure and mutations 270
Figure 4. *hat-1* encodes a putative MYST family histone acetyltransferase that is required for P(3-8).p cell-fate specification 272
Figure 5. *epc-1* and *ssl-1* gene structures and deletion mutations 274
Figure 6. Two models of TRR-1/HAT-1/EPC-1 function with respect to class B synMuv proteins 276
Chapter 7. Discussion and future prospects 278
Investigations of synthetic multivulva gene function 279
Model for class B synMuv function 279
What is the relationship between different classes of synMuv genes? 281
Identifying synMuv targets 282
How do the synMuv genes interface with the *let-60* Ras pathway? 284
Do the synMuv genes act by regulating cell cycle progression? 286
Concluding remarks 286
References 287
Figure 290
Figure 1. Model for class B synMuv function 290
Appendix 1. The use of "wild-type" synMuv suppressor mutations to order class B synMuv genes into a genetic pathway 292

Background and rationale 293
Experimental procedures 295
RNAi analyses 295
Genetic mapping 295
Construction of *sup*, *sup; lin-15(n309)* and *dpl-1(n3316); sup; lin-15A(n767)* mutants 295
Results 296
dpl-1(RNAi) reduces the penetrance of suppression in a subset of "wild-type" suppressor strains 296
Genetic mapping of suppressor isolates 296
"Wild-type" suppressor mutations do not suppress the Muv phenotype caused by *lin-15AB(n309)* 296
Discussion and future directions 298
References 301
Tables 303
Table 1. Effect of *dpl-1(RNAi)* on the penetrance of suppression of *sup; lin-15AB(n765)* strains 303
Table 2. Chromosomal linkages of sup mutations 306
Table 3. Three- and four-factor crosses 307
Table 4. Phenotypes of *sup* single mutant, *sup; lin-15AB(n309)* double mutant and *dpl-1(n3316); sup; lin-15A(n767)* triple mutant strains 309

CHAPTER 1

INTRODUCTION:
The synthetic multivulva genes and regulation of chromatin structure

INTRODUCTORY REMARKS

During animal development a diverse array of cell types are generated. The developmental repertoire of cells arises from alternate readings of the genome. Different readings of the genome are accomplished in part through the action of proteins that govern access of the general transcription machinery to target genes. Many of these proteins act by making chromatin more exposed or refractory to factors that are involved in transcription.

In this introduction I describe how different cell types are generated during vulval development in the nematode *Caenorhabditis elegans*. Some of the genes that regulate vulval development likely act by modulating chromatin structure. These genes, termed the synthetic multivulva (synMuv) genes, negatively regulate a conserved Ras signaling pathway that is required to produce vulval tissue. To understand how modulation of chromatin might influence vulval development, I discuss properties of chromatin and how alterations of these properties affect DNA-mediated processes including transcription. A discussion integrating my findings with current models of chromatin regulation can be found in Chapter 7.

LINKS BETWEEN CHROMATIN REMODELING AND *C. elegans* VULVAL DEVELOPMENT

My studies have focused on how the fates of a subset of cells that can make vulval tissue in *C. elegans* are specified. In particular, I have investigated the synthetic multivulva (synMuv) genes, which are negative regulators of Ras-mediated vulval induction. I have identified and molecularly characterized many synMuv genes, including genes that may act by modulating chromatin structure. Prior to a discussion of chromatin structure and remodeling, this section is intended to introduce the developmental functions of synMuv genes.

Vulval development in *C. elegans*

The vulva is a structure on the ventral side of *C. elegans* hermaphrodites that functions in egg laying and copulation. It is derived from a subset of Pn.p ectodermal blast cells that are generated during the L1 larval stage. Two sequential steps specify which Pn.p cells make vulval tissue (Figure 1; Sulston and Horvitz, 1977). Initially, more anterior and posterior cells fuse with the syncytial hypodermis, leaving six unfused cells, P(3-8).p, competent to undergo further cell division. In the following step, three of these cells, P(5-7).p, are specified to divide three times and generate a total of 22 descendants that make up the adult vulva. The three other cells typically undergo one round of division, creating descendants that ultimately fuse with the hypodermis. P(5-7).p are said to adopt vulval fates, whereas P3.p, P4.p and P8.p adopt non-vulval fates. Laser ablation studies determined that all six cells are initially competent to adopt vulval fates, however, during the late L2 and early L3 larval stages, a localized signal from the gonadal anchor cell specifically induces P(5-7).p (Sulston and White, 1980; Kimble, 1981; Sternberg and Horvitz, 1986).

A Ras pathway induces vulval development

A number of genetic screens isolated two general classes of mutants defective in vulval cell-fate determination (Sulston and Horvitz, 1981; Ferguson and Horvitz, 1985; Han et al., 1990; Clark, 1992; Lackner et al., 1994; Wu and Han, 1994). Vulvaless (Vul) mutants are defective either because P(3-8).p cells are not generated or because P(3-8).p cells are generated but do not adopt vulval fates. These mutants are fertile but cannot lay eggs and are consequently consumed internally by their own progeny.

Conversely, in multivulva (Muv) mutants, more than three cells adopt vulval fates. The extra cells generated undergo morphogenesis to produce raised ventral protrusions that are readily visible under a dissecting microscope.

Molecular genetic studies of these mutants revealed that a Ras pathway controls vulval induction (reviewed by Sternberg and Han, 1998). Loss-of-function mutations that affect genes in this pathway cause a Vul phenotype, whereas mutations that increase pathway activity cause a Muv phenotype. This conserved pathway includes genes such as the *let-23* receptor tyrosine kinase, the *sem-5* SH2/SH3 adaptor, *let-60* Ras and genes that encode a MAP kinase signaling module (Aroian et al., 1990; Beitel et al., 1990; Han and Sternberg, 1990; Clark et al., 1992; Han et al., 1993; Lackner et al., 1994; Wu and Han, 1994; Kornfeld et al., 1995a; Kornfeld et al., 1995b; Sundaram and Han, 1995; Wu et al., 1995). Incidentally, a mutation that overactivates *let-60* Ras causes the same G13E substitution that is commonly observed in human oncogenic Ras (Beitel et al., 1990). An EGF-like signal from the anchor cell encoded by the *lin-3* gene stimulates the *let-60* Ras pathway (Hill and Sternberg, 1992). Ultimately this signal is transduced in the Pn.p cells, leading to the phosphorylation of the *lin-1* ETS and *lin-31* winged-helix transcription factors (Miller et al., 1993; Beitel et al., 1995; Tan et al., 1998). The *lin-39* homeobox gene is essential for vulval development (Clark et al., 1993; Wang et al., 1993) and LIN-39 protein levels are upregulated in response to *let-60* Ras signaling (Maloof and Kenyon, 1998). At this time it is unknown whether *lin-39* is directly regulated by the LIN-1 or LIN-31 proteins.

The synthetic multivulva genes antagonize *let-60* Ras signaling

Mutations in the synthetic multivulva (synMuv) genes also cause vulval cell fate transformations (Ferguson and Horvitz, 1989). However, unlike activating *let-60* Ras mutations, these mutations result in a loss of gene function. Consequently, the synMuv genes negatively regulate vulval cell fate determination, thereby antagonizing *let-60* Ras pathway activity. On the basis of genetic interactions, the synMuv genes are grouped into two classes, A and B. For an animal to be Muv, it must carry a mutation in both a class A and a class B gene. Single mutations or mutations in multiple genes of the same class do not cause vulval cell fate transformations. These interactions suggest that the two classes of synMuv genes encode functionally redundant genetic pathways. At the time my studies began, four class A genes, *lin-8*, *lin-15A*, *lin-38* and *lin-56* and ten class B genes, *lin-9*, *lin-13*, *lin-15B*, *lin-35*, *lin-36*, *lin-37*, *lin-52*, *lin-53*, *lin-54* and

dpl-1 were identified (Horvitz and Sulston, 1980; Ferguson and Horvitz, 1989, Chapter 2). *dpl-1* was originally identified by Jeff Thomas, a former graduate student in the Horvitz laboratory, and called *lin-55*, but was renamed by me in light of its similarity to genes encoding DP transcription factors (Chapters 2, 3).

Genetic epistasis experiments indicate that *let-60* Ras pathway activity is required for the synMuv phenotype. Specifically, in triple mutants, the Vul phenotype of Ras pathway loss-of-function mutations is epistatic to the Muv phenotype of class A and class B synMuv mutations (Ferguson et al., 1987; Thomas and Horvitz, 1999). On the contrary, the synMuv phenotype is epistatic to the Vul phenotype caused by loss-of-function mutations in the *lin-3* EGF ligand, and the synMuv phenotype is expressed in gonad-ablated animals (Ferguson et al., 1987; Sternberg and Horvitz, 1989; Thomas and Horvitz, 1999). These results suggest that *let-60* Ras pathway activity is essential for the ectopic vulval cell fate transformations of synMuv mutants. Additionally, it has been speculated that there exists a basal, *lin-3*-independent level of *let-60* Ras pathway activity and that this level of activity is sufficient, in combination with synMuv mutations, to cause ectopic vulval fate transformations (Thomas and Horvitz, 1999).

The class B synMuv genes may encode components of an intercellular signaling system that negatively regulates vulval development. Mosaic analyses suggest that *lin-15B* and *lin-37* act in the syncytial hypodermis, implicating this tissue as a source of signal (Herman and Hedgecock, 1990; Hedgecock and Herman, 1995). Also based on mosaic analyses, *lin-36* is proposed to act in P(3-8).p and respond to hypodermal signaling (Thomas and Horvitz, 1999). For many years these results provided a working model for class B synMuv gene action. More recently, however, the existence of a class B synMuv intercellular signaling system has been questioned in light of more refined mosaic analyses that suggest *lin-15B* can function in P(3-8).p to affect vulval development (Sanchez-Gerrichio and Sternberg, personal communication). At this point it is fair to say that this issue is unresolved but should be kept in mind when interpreting data regarding class B synMuv site of action.

The class B synMuv genes encode components of an Rb pathway

At the time my studies began, one class A gene, *lin-15A*, and four class B genes, *lin-9*, *lin-15B*, *lin-36* and *lin-37* had been cloned (Clark et al., 1994; Huang et al., 1994; Lu, 1999; Thomas and Horvitz, 1999; Beitel et al., 2000). All were found to encode novel proteins, although since this time human and *Drosophila* homologs of *lin-9* have

been identified (Beitel et al., 2000; White-Cooper et al., 2000). A few months after my joining the laboratory, another graduate student, Xiaowei Lu, made a fundamental discovery that has considerably impacted studies of the synthetic multivulva genes. She cloned the class B gene *lin-35* and found that it encodes a member of the Rb tumor suppressor protein family (Lu and Horvitz, 1998). In addition, she found that *lin-53* encodes a homolog of the Rb-interacting protein RbAp48 and that the *C. elegans* histone deacetylase *hda-1* has class B synMuv activity. As discussed below, Rb and histone deacetylases can act together to regulate transcription by remodeling chromatin. *lin-35* and *hda-1* were proposed to regulate genes involved in vulval development by a similar mechanism.

Transcriptional regulation by chromatin remodeling is likely important for vulval development

Subsequent studies have extended this model of class B synMuv function. I have identified homologs of DP and E2F transcription factors as class B synMuv genes (Chapter 3). Genes encoding a Mi-2-like ATP-dependent chromatin remodeling enzyme (Solari and Ahringer, 2000; von Zelewsky et al., 2000) and a heterochromatin protein 1 homolog (Couteau et al., 2002) also have class B synMuv activity. These genes, along with two novel genes I have identified, *lin-52* and *lin-54* (Chapters 4, 5), are likely involved in *lin-35* Rb-mediated chromatin remodeling and transcriptional regulation in *C. elegans*. In the following sections of this Introduction, I discuss chromatin remodeling and transcriptional regulation with an emphasis on studies that link homologs of class B synMuv proteins to these processes. I have also defined a third class of synMuv genes that acts in parallel to both class A and class B genes (Chapter 6). These genes encode homologs of MYST family histone acetyltransferases, the mammalian TRRAP and yeast Tra1p transcriptional regulatory proteins and the *Drosophila* Enhancer of Polycomb protein. I additionally discuss studies of the functional characterization of these homologs. Finally, I return to the synMuv genes and discuss how chromatin remodeling by these genes may influence vulval cell fate determination in *C. elegans*.

PROTEINS THAT MODULATE CHROMATIN STRUCTURE REGULATE TRANSCRIPTION

Chromatin structure and organization

The fundamental unit of chromatin is the nucleosome, which consists of DNA and a histone octamer that contains two subunits each of histones H3, H4, H2A and H2B (Wolffe, 1998). The DNA associated with a single nucleosome can vary in length but is approximately 150 base pairs and is wound almost twice around the octamer and held in place largely through electrostatic interactions with the positively charged histones. Crystallographic studies indicated that nucleosome structure is well defined and globular with the exception of the amino-terminal tails of the histones (Luger et al., 1997). Their lack of structure and their protrusion from the surface of the globular octamer is thought to expose the histone tails to a variety of proteins that modify and bind to chromatin. The sequences of nucleosomal histone proteins, including those of amino-terminal histone tails, are highly conserved in eukaryotes.

Enzymes that alter chromatin structure have traditionally been said to "remodel" chromatin. These enzymes fall into two classes (Table 1). ATP-dependent chromatin remodeling enzymes act to shift the positions of nucleosomes with respect to the underlying DNA template without chemically modifying either of these chromatin components. Chromatin modifying enzymes add or remove covalent modifications such as acetyl, methyl, phosphoryl and other groups to or from nucleosomes and DNA. These classes of enzymes and the complexes in which they function will be discussed below, and, during this discussion, I will keep with convention and use the term "chromatin remodeling" to refer to both non-covalent ATP-dependent chromatin remodeling and to covalent chromatin modification.

Two properties of nucleosomes are important in regulating chromatin structure. First of all, histone octamers are reversibly bound to nucleosomal DNA. Additionally, multiple nucleosomes can be reversibly arranged into more or less compact structures. These features allow chromatin structure to be dynamic enough for gene regulation yet able to adopt highly compact structures that are required for processes such as mitosis. Covalent modifications of histone tails may influence chromatin structure by regulating interactions between histones and DNA and interactions between adjacent nucleosomes.

Chromatin structures have been investigated using electron microscopy. Since electron microscopy must be performed under non-native conditions, it is unclear to what extent these structures represent *in vivo* conformations of chromatin. Visualization of different structures is dependent on the manner in which chromatin is prepared for microscopy. Under more disruptive conditions, chromatin adopts a decompacted "beads-on-a-string" conformation. This structure is thought to approximate chromatin that is being actively transcribed. Another well-characterized structure is the 30 nm fiber, which is observed following less stringent preparations. The 30 nm fiber, named for its diameter, contains an ordered array of nucleosomes that may be arranged in either a helical (Finch and Klug, 1976) or zigzag (Bednar et al., 1998) configuration. The stability of the 30 nm fiber is dependent on linker histones, such as histones H1 and H5, which are present in one copy per nucleosome. Linker histones reduce the linear dimension of chromatin by interacting with and bringing into apposition adjacent stretches of internucleosomal DNA (Bednar et al., 1998). The importance of linker histones in the stabilization of higher-order chromatin structure has been highlighted by assays of chromatin formation performed *in vitro* (Carruthers et al., 1998; Carruthers and Hansen, 2000). Interestingly, these assays also point to a dependence on amino-terminal histone tails in the compaction of chromatin (Garcia-Ramirez et al., 1992; Tse and Hansen, 1997; Carruthers and Hansen, 2000).

Interphase chromosomes have also been visualized using light microscopy under more native conditions. These chromosomes typically display regions of heterochromatin that are compacted like mitotic chromosomes and less condensed regions of euchromatin. These forms are thought to represent different functional structures of chromatin, with heterochromatin being more transcriptionally inert. Heterochromatin and euchromatin structures are poorly understood, although the predominant association of histone H1 with heterochromatin indicates that it contains structural elements like that of the 30 nm fiber and other more highly-ordered structures (Gorka et al., 1993).

ATP-dependent chromatin remodeling complexes alter DNA accessibility

Certain protein complexes regulate chromatin structure by utilizing the energy derived from ATP hydrolysis to break histone-DNA contacts. Sequence comparisons of their ATPase subunits have been used to divide these chromatin remodeling complexes into three classes: SWI2/SNF2, ISWI and Mi-2 (Table 1). The biochemical functions of

these complexes have been studied *in vitro* using a variety of assays, including translational repositioning of histone octamers on small linear DNA fragments (reviewed by Narlikar et al., 2002). These assays indicate that all three classes of remodeling complexes efficiently reposition octamers, although differences in substrate requirements indicate that the different classes of ATP-dependent remodelers might not act through the same mechanism. One interesting difference is the dependence, or lack thereof, on histone tails for remodeling. Whereas yeast and human SWI/SNF and the *Drosophila* Mi-2 complexes do not require histone tails for their activities (the lack of only the H4, H3 and H2A tails was investigated in the case of Mi-2), remodeling by the *Drosophila* ISWI complex NURF is strongly diminished by the lack of the histone H4 tail (Brehm et al., 2000; Clapier et al., 2001; Langst and Becker, 2001). In the latter case, the absence of the H4 amino-terminal tail does not appear to affect binding to the octamer by NURF but instead affects its rate of ATP hydrolysis (Clapier et al., 2001). Although ATP-dependent chromatin remodeling complexes can expose DNA by mobilizing nucleosomes, assays using crosslinked nucleosomes or mononucleosomes indicate that SWI/SNF and possibly other remodeling complexes may alter DNA accessibility by additional mechanisms that do not involve octamer repositioning (Lee et al., 1999; Narlikar et al., 2001). Remodeling under these circumstances appears to cause local bulging of DNA away from the histone octamer core. Whether bulging is a necessary precursor of sliding or whether these modes of remodeling are mutually exclusive is currently unknown.

The roles of ATP-dependent chromatin remodeling complexes in transcriptional regulation are discussed below. In addition, functions for ATP-dependent remodeling enzymes in processes as diverse as nucleosome assembly, homologous recombination and DNA repair have been described (reviewed by Fyodorov and Kadonaga, 2001).

HATs and HDACs control acetylation of histones

Chromatin remodeling is also characterized by the covalent modification of nucleosomal histones. Modifications include acetylation, methylation, phosphorylation, ubiquitination and ADP-ribosylation and are generally found on the amino-terminal tails of histones. The presence of acetyl and methyl groups have been shown to strongly affect transcriptional competency, and, because of my interest in the relationship between chromatin structure and transcription, I will focus on enzymes that add or remove these moieties.

Histone acetyltransferases (HATs) have been grouped into families based on sequence similarity (Table 1). The GNAT (Gcn5-related *N*-acetyltransferase) family includes the first genetically-identified HAT, Gcn5p from yeast, the first biochemically-recognized HAT, GCN5 from *Tetrahymena* (previously known as p55), and the well-characterized mammalian PCAF HAT (reviewed by Roth et al., 2001). Interestingly, these and other HATs acetylate only a subset of nucleosomal histones and often acetylate only a subset of the lysine residues of a histone tail. For example, recombinant yeast Gcn5p preferentially acetylates lysines of histone H3 over amino-terminal lysines of other nucleosomal histones (Kuo et al., 1996). In its cellular context, yeast Gcn5p functions as part of multi-subunit protein complexes, and the substrate and site specificities of yeast Gcn5p as part of the purified SAGA and ADA complexes are slightly broader than those of the recombinant protein alone (Grant et al., 1999). Such nonrandom site specificities are a feature of many types of HATs and have been confirmed in chromatin preparations from HAT mutant cells (Suka et al., 2001).

A second group of well-characterized HATs are those of the MYST family (named after its founding members MOZ; Ybf2/Sas2; Sas3; Tip60). Whereas most GNAT family members preferentially acetylate histone H3, the MYST family members Esa1p from yeast, *Drosophila* MOF and Tip60 from mammals show a preference, as either recombinant proteins or as part of protein complexes, for histone H4 as a substrate (Kimura and Horikoshi, 1998; Smith et al., 1998; Allard et al., 1999; Clarke et al., 1999; Akhtar and Becker, 2000; Smith et al., 2000). An exception to MYST family acetylation of H4 is Sas3p, which, as part of the NuA3 complex, preferentially acetylates histone H3 (John et al., 2000).

A third family of HATs is defined by the related mammalian proteins p300 and CBP. HATs in this family have been found in various metazoans but not in yeast and have been shown to be promiscuous in their substrate specificities, being able to acetylate residues on all four nucleosomal histones (Schiltz et al., 1999). Lastly, other families of HATs, for example the $TAF_{II}250$ and HAT1 families, have been identified and biochemically characterized (reviewed by Roth et al., 2001).

A similar amount of diversity characterizes enzymes that remove acetyl groups from nucleosomal histones. These histone deacetylases (HDACs) have been grouped into families, again based on sequence similarity (Table 1). Class I HDACs, which include the yeast Rpd3p HDAC, are the best characterized and are thought to function broadly in regulating chromatin structure. Class II HDACs and the Sirtuin family of

HDACs, the latter named after the Sir2p HDAC, have also been characterized. Although less biochemical and structural information is available for HDACs, the differential requirement of an NAD cofactor (class I and class II HDACs do not require an NAD cofactor, whereas Sir2p does) indicates that different classes of HDACs use different catalytic mechanisms (Imai et al., 2000; Landry et al., 2000). HDACs, like HATs, function as the catalytic subunits of multi-protein complexes *in vivo*. By contrast to most HAT complexes, HDAC complexes are promiscuous in their site specificities (Suka et al., 2001).

Acetylation of nucleosomal histone tails is typically correlated with transcriptional activation

A variety of studies established a relationship between histone acetylation and transcriptional competence. In pioneering work, Allfrey and coworkers purified hyperacetylated histones and found that they could promote transcription *in vitro* more efficiently than hypoacetylated histones (Allfrey et al., 1964). The observation that histone tails contained multiple acetylation sites focused attention on these regions, and subsequent studies of histone tail deletion mutants in yeast highlighted their importance in transcriptional regulation (Durrin et al., 1991).

The link between hyperacetylation and transcription was further strengthened by the discovery that many transcriptional regulators participate in the biochemical modification of histones. These transcriptional regulators include Gcn5p and Rpd3p, which were originally identified in screens for genes that affected transcription and were later found to be homologs of biochemically-purified HAT and HDAC proteins, respectively (Vidal and Gaber, 1991; Georgakopoulos and Thireos, 1992; Brownell et al., 1996; Taunton et al., 1996). Subsequent studies revealed that the biochemical activities of these proteins were necessary for their effects on transcription. Specifically, whereas wild-type Gcn5p promotes transcription on nucleosomal substrates *in vitro* or when overexpressed *in vivo*, mutants that are defective in histone acetyltransferase activity do not (Kuo et al., 1998; Wang et al., 1998). Likewise, Rpd3p mutants that are biochemically inactive yet retain the ability to bind other corepressor complex proteins are unable to act as transcriptional repressors (Kadosh and Struhl, 1997).

The availability of yeast mutants defective in histone acetylation and of antibodies that recognize acetylated histone isoforms have allowed the effects of modifications to be explored *in vivo*. Suka et al. investigated the extent of acetylation at

two promoters repressed by *RPD3* with respect to a promoter that is not regulated by *RPD3* (Suka et al., 2001). Their results indicate a correlation between hyperacetylation of specific histone residues in promoter nucleosomes by Gcn5p and Esa1p and the upregulation of these promoters in the absence of Rpd3p. Using the same reagents, Robyr et al. combined ChIP (chromatin immunoprecipitation) with DNA microarrays to determine a genome-wide set of promoters whose acetylation was increased by loss of *RPD3* (Robyr et al., 2002). The expression of nearly 500 of the open reading frames (ORFs) corresponding to these promoters was previously examined in *rpd3Δ* as compared to wild-type strains (Bernstein et al., 2000). This large data set again indicates a correlation between hyperacetylation (especially that of K5 and K12 of the histone H4 sites examined) and transcriptional upregulation. Of the ORFs whose promoters were hyperacetylated, 13% were upregulated in the absence of *RPD3*. A large number of ORFs were downregulated in the *rpd3Δ* mutant, leading to the suggestion that Rpd3p may have a role in transcriptional activation (Bernstein et al., 2000). A smaller proportion of the hyperacetylated set (4.9%) overlapped with these downregulated ORFs. Since a majority of studies argue for Rpd3p functioning only as a repressor, it has been speculated that the downregulation observed is a secondary effect of *RPD3* disruption (Robyr et al., 2002).

The relatively minor impact of *RPD3* disruption highlights an important point about the overall role of chromatin remodeling in gene expression. While chromatin remodeling may be important for the regulation of some genes, expression of many genes may be relatively indifferent to chromatin effects. Indeed, expression of many essential genes in yeast is likely insensitive to chromatin effects since strains lacking different chromatin remodeling enzymes, including *RPD3* and *GCN5* single mutant strains, are typically only slightly growth impaired (Vidal and Gaber, 1991; Georgakopoulos and Thireos, 1992). Whether multicellular eukaryotes rely on chromatin effects to a greater degree than yeast is currently unknown.

Repressed chromatin domains are hypoacetylated

Studies of transcriptionally silent regions have shown that these regions are characterized by a paucity of histone acetylation. As determined by immunostaining of acetylated histone isoforms, only one of the four H4 tail lysines (K12) is appreciably acetylated in *Drosophila* heterochromatin (Turner et al., 1992). In similar immunolocalization studies, centromeric heterochromatin and the inactive X

chromosome of mammals were found to be hypoacetylated at all H3 and H4 sites examined (Jeppesen et al., 1992; Jeppesen and Turner, 1993). In yeast, ChIP and quantitative PCR were used to investigate acetylation at the silenced mating-type loci and telomeric regions. In these regions, both H3 and H4 were found to be hypoacetylated, in a Sir2p-dependent fashion, at all tail lysines except for lysine 12 of histone H4 (Braunstein et al., 1996). A more recent study has led to a discrepancy regarding the acetylation state of lysine 12 of histone H4, as independently-derived anti-Ac-K12 antibodies have yielded contrasting results (Suka et al., 2001). Whether or not the yeast loci in question are acetylated at H4 K12, the results from these different species further support the link between acetylation and transcriptional competence.

Some histone acetylation may be important for gene silencing

Whereas hyperacetylation is most often correlated with gene activation, a small number of studies have shown that some acetylation may be important for gene silencing. These studies stem from the observation that deletion of a yeast MYST family histone acetyltransferase, *sas2*, causes defects in telomeric silencing and in silencing of *HML*, one of two mating type loci (Reifsnyder et al., 1996). The SAS protein complex, of which Sas2p is a subunit, is proposed to facilitate SIR-dependent silencing (Reifsnyder et al., 1996; Meijsing and Ehrenhofer-Murray, 2001; Osada et al., 2001). Acetylation of lysine 16 of histone H4 may be critical for SIR-dependent silencing, as mutation of lysine 16 to arginine, an alteration that is thought to mimic the unacetylated state, causes defects in mating type loci and telomeric silencing like those observed in a *sas2Δ* strain (Johnson et al., 1992; Meijsing and Ehrenhofer-Murray, 2001). Since lysine 16 of histone H4 is not hyperacetylated in the silenced loci, this modification may be important for the establishment but not the maintenance of SIR-dependent silencing.

Recruitment of ATP-dependent remodeling and histone acetyltransferase complexes can stimulate transcription

A large number of genetic and molecular studies have indicated that sequence-specific DNA-binding proteins target ATP-dependent remodeling and modifying complexes to promoters to regulate transcription. In many of these studies, functional interactions between a transcription factor and one type of complex, either an ATP-dependent remodeling or modifying complex, have been examined. However, some transcription factors may recruit both types of activities. This recruitment may occur

through a direct interaction with the transcription factor. For example, the glucocorticoid receptor has been shown to interact directly with both the human SWI/SNF BRG1 ATP-dependent remodeling complex and with the CBP HAT (Fryer and Archer, 1998). Transcription factors containing acidic activation domains may also recruit both types of complexes, as these domains have been shown to mediate recruitment of SWI/SNF and, via a direct interaction with their shared Tra1p subunit, of the SAGA and NuA4 HAT complexes (Neely et al., 1999; Yudkovsky et al., 1999; Brown et al., 2001). Instead of directly interacting with ATP-dependent remodeling and modifying complexes, a transcription factor may be able to recruit both types of activities by initiating a sequence of recruitment steps. Such a sequence has been suggested in the regulation of the yeast HO endonuclease gene in mother cells during cell division. Nasmyth and coworkers used ChIP to examine the temporal localization at the HO promoter of the transcriptional activator Swi5p and of the SWI/SNF ATP-dependent remodeling and SAGA HAT complexes (Cosma et al., 1999). Swi5p binding during late anaphase was followed, in mother cells, by binding of the SWI/SNF complex. Binding of SAGA occurs while SWI/SNF is present, but after Swi5p has left the promoter. This order of events suggests that SWI/SNF, either directly or indirectly, recruits SAGA to the HO promoter. Other studies have indicated that a sequence of recruitment steps may not always occur in the same order. In regulation mediated by the IFN-β enhanceosome and RAR/RXR nuclear receptor heterodimer, recruitment of HAT complexes precedes, and is required for, recruitment of ATP-dependent remodeling complexes (Agalioti et al., 2000; Dilworth et al., 2000).

Transcriptional repression can involve recruitment of ATP-dependent chromatin remodeling and histone deacetylase complexes

DNA-binding proteins that repress transcription also recruit ATP-dependent remodeling and modifying complexes to promoters. Since ATP-dependent chromatin remodeling factors were originally identified as transcriptional coactivators, their characterization as corepressors was somewhat surprising. Instead of simply opening chromatin to transcriptional activators, remodeling complexes may mediate transitions between open and closed chromatin states. ATP-dependent remodeling enzymes may act, in part, by providing energy to overcome kinetic barriers between these states.

Again, some transcription factors appear to recruit both ATP-dependent remodeling and modifying activities. Ume6p, a repressor of genes involved in meiosis

in yeast, directly interacts with the Sin3p subunit of a multimeric complex that includes Rpd3p (Kadosh and Struhl, 1997). Repression by Ume6p is dependent on this interaction and on the HDAC activity of Rpd3p. More recently, Ume6p was shown to recruit the Isw2 ATP-dependent remodeling complex to promoters (Goldmark et al., 2000). Itc1p, a subunit of this ISWI-family complex, mediates targeting by binding to Ume6p. There is no evidence to date that DNA-binding transcriptional repressors act by sequential recruitment events, although their mounting analogies to DNA-binding transcriptional activators make this possibility likely.

Some repressors target both activities by recruiting a bifunctional NuRD complex. NuRD complexes were originally characterized *in vitro* and were found to include a Mi-2 family ATPase subunit and a class I HDAC (Tong et al., 1998; Xue et al., 1998; Zhang et al., 1998). Transcriptional repression by the *Drosophila* repressor hunchback and by the lymphoid differentiation transcription factor Ikaros is thought to depend on NuRD complexes (Kehle et al., 1998; Koipally et al., 1999).

Switching between activating and repressing complexes

Transcription of many genes is differentially regulated by the recruitment of HAT and HDAC complexes. Some promoters utilize different *cis*-acting DNA elements to bind transcriptional activators and repressors, which, in turn, can recruit HAT and HDAC complexes, respectively. In other instances, the same *cis*-acting DNA element, through DNA-binding proteins, recruits both activities. The Ebox element of Myc-responsive genes accomplishes such regulation by binding two types of heterodimeric transcription factors. In proliferating mammalian cells, Myc/Max heterodimers bind to the Ebox and recruit the coactivator TRRAP and a TRRAP-associated histone acetyltransferase to stimulate transcription (Park et al., 2001). As cells begin to differentiate, levels of Mad, an alternative heterodimeric partner for Max, rise to levels at which Mad/Max heterodimers outcompete Myc/Max heterodimers for Ebox occupancy. Mad/Max heterodimers repress transcription by recruiting an mSin3-HDAC complex (Hassig et al., 1997; Laherty et al., 1997). In the case of the thyroid and other nuclear hormone receptors, the same protein bound to a *cis*-acting DNA element may mediate the shift between transcriptional activating and repressing complexes. The liganded thyroid receptor recruits the p300/CBP HAT by binding the p300/CBP-interacting protein p/CIP (Torchia et al., 1997). Release of ligand results in a conformational change that decreases the affinity of the receptor for p/CIP and increases its affinity for an mSin3-

HDAC complex (Lin et al., 1997; Torchia et al., 1997). The effects of having both types of complexes function through the same binding element are not understood, although it is possible that these mechanisms of mutually exclusive complex binding act as a switch to change the acetylation state and transcriptional competence of promoters.

Chromatin-modifying activities are not always targeted

Recent studies have addressed whether chromatin-modifying complexes act only through targeting by DNA-binding transcription factors. Two groups performed ChIP to examine the acetylation status of non-promoter regions in yeast HAT and HDAC mutant strains (Reid et al., 2000; Vogelauer et al., 2000). All of the non-promoter regions in these mutants showed substantial changes in acetylation as compared to the same regions in control strains. This phenomenon appears to be conserved, as untargeted Sin3/HDAC and NuRD activities have also been observed in *Xenopus* (Li et al., 2002).

What is the purpose of having both targeted and untargeted activities? It has been suggested that the untargeted activities set a basal level of transcriptional competence throughout the genome upon which targeted activities function (Vogelauer et al., 2000). When the competence of a specific locus needs to be changed, a DNA-binding transcription factor recruits a chromatin-modifying complex to this locus. If the competence of this locus needs to be changed back to its original state, the targeted activity vacates the locus and the untargeted activities ensure a quick transition back to the original competence. In support of this hypothesis, a recent study in yeast found the acetylation pattern of an unperturbed *tetO*-regulated promoter is rapidly altered and reestablished upon addition and removal, respectively, of a chimeric TetR-Ume6 DNA-binding transcription factor (Katan-Khaykovich and Struhl, 2002). Such a combination of targeted and untargeted activities may offer a means of quickly switching between on and off states. Whether this model can be extended to include ATP-dependent chromatin remodeling complexes has not been investigated.

Histone methyltransferases

Histone methylation has long been known to affect transcription (Allfrey, 1964), although only recently have enzymes that methylate histones been identified. On the basis of substrate specificity these enzymes fall into two classes: lysine HMTs and arginine HMTs (HMT, histone methyltransferase; Table 1). Most lysine HMTs identified to date share a common SET domain that mediates catalysis, although not all SET-

domain containing proteins appear to have HMT activity *in vitro* (Rea et al., 2000). It has been proposed that conserved groups of residues adjacent to the SET domain are important for catalysis (Rea et al., 2000). One group of SET domain-containing proteins includes SUV39H1 from mammals and Clr4p from *S. pombe* and primarily methylates lysine 9 of histone H3, whereas another group includes mammalian Set1 and Set9 and methylates lysine 4 of histone H3 (Rea et al., 2000; Nakayama et al., 2001; Nagy et al., 2002; Nishioka et al., 2002a). SET-domain proteins that methylate other lysine residues have been identified (Nishioka et al., 2002b; Strahl et al., 2002). Additional studies have identified the arginine HMTs CARM1 and PRMT1 (Chen et al., 1999; Strahl et al., 2001). Although these two proteins share a domain that may be involved in catalysis, the sites they methylate differ significantly: CARM1 preferentially methylates arginines 17 and 26 of histone H3 and PRMT1 arginine 3 of histone H4 (Schurter et al., 2001; Strahl et al., 2001).

Lysine methylation of histones has different effects on transcription

Histone methylation has varying effects on transcription. Methylation of H3 lysine 9 is generally correlated with transcriptional silencing. The *Drosophila Su(var)3-9* and *S. pombe clr4* HMT genes are known to regulate silencing at heterochromatic regions and the silent mating type locus (Ekwall and Ruusala, 1994; Tschiersch et al., 1994), respectively, and lysine 9 methylation is enriched at these sites *in vivo* (Jacobs et al., 2001; Noma et al., 2001). Methylation of H3 lysine 4 may differentially regulate transcription. H3 lysine 4 methylation is observed in transcriptionally active regions such as macronuclei of *Tetrahymena* and euchromatic regions of mammalian autosomes, but is greatly reduced in transcriptionally silent micronuclei and inactive X chromosomes (Strahl et al., 1999; Boggs et al., 2002). H3 lysine 4 methylation may keep chromatin poised for transcriptional activation by blocking H3 lysine 9 methylation through an as yet unknown mechanism (Nishioka et al., 2002a). By contrast, studies of the Set1 and COMPASS HMTs suggest that methylation at lysine 4 is required for silencing of some loci (Briggs et al., 2001; Krogan et al., 2002). Additional studies are needed to explain why methylation of H3 lysine 4 can have apparently opposite effects on transcription.

Modified histone tails are docking sites for chromatin-binding proteins

Although chromatin modifying complexes are known to affect transcription, the means of translating a modified chromatin state into a transcriptional readout are unclear. It has long been speculated that modified residues may regulate transcription by directly modulating properties intrinsic to chromatin. This modulation may include the loosening of histone-DNA contacts or the disruption of internucleosome contacts (reviewed by Annunziato and Hansen, 2000).

Recent studies have suggested an additional function of modified residues, namely, that modified residues provide docking sites for proteins that participate in transcriptional activation. Bromodomains are found in many chromatin-associated proteins and are known to bind to acetylated lysine residues (Dhalluin et al., 1999). Interestingly, $TAF_{II}250$, a subunit of the TFIID component of RNA polymerase II, was shown to interact with acetylated residues on nucleosomes through its bromodomains (Jacobson et al., 2000). An analogous mechanism may be used to target proteins involved in gene silencing. A mammalian homolog of *Drosophila* HP1, which is important for heterochromatin formation, was found to interact with methyl-lysine residues through a conserved chromodomain (Bannister et al., 2001; Lachner et al., 2001). The binding affinity for methyl-K9 was much stronger than that for methyl-K4, suggesting a modification itself does not solely determine affinity and that different residues with modifications of the same type may be able to bind non-overlapping sets of proteins (Bannister et al., 2001). Such observations have led to a 'histone code' hypothesis, whereby distinct histone modifications regulate interaction affinities of chromatin-associated proteins (Strahl and Allis, 2000; Turner, 2000).

Dysfunction of chromatin remodeling proteins is linked to cancer in mammals

Human and mouse genetic studies implicate SWI/SNF components in tumor suppression. The gene encoding hBrg1, the ATPase subunit of the human SWI/SNF complex, was found mutated, typically by deletion, in multiple types of human tumor cell lines (Wong et al., 2000). In the mouse, disruption of the *Brg1* gene caused embryonic lethality of homozygous mutants, and, in a small sample population, predisposed heterozygous mutants to epithelial tumors (Bultman et al., 2000). The tumor cells retained a *Brg1* allele of wild-type size, suggesting that the phenotype was caused either by a subtle mutation in this allele or by haploinsufficiency of the *Brg1* locus. Nonsense and deletion mutations of the human Snf5/Ini1 gene were observed in rhabdoid and other cancer cell types (Versteege et al., 1998; Sevenet et al., 1999). As

with Brg1, Snf5/Ini1 homozygous mutant mice died as embryos and heterozygous mutants were predisposed to tumors (Roberts et al., 2000; Guidi et al., 2001). These tumors were rhabdoid in nature and failed to express wild-type Snf5 protein. Little is known about why these SWI/SNF components are critical for tumor suppression.

A variety of studies indicate that misregulation of HATs and HDACs contributes to tumorigenesis. Chromosomal translocations are often observed in acute leukemias, and some of these translocations involve HAT genes (reviewed by Cairns, 2001). The catalytic domains of HAT proteins are generally preserved in translocations, suggesting that defects in proliferation result from an increased or novel gene function. One of the genes subject to translocation encodes the CBP HAT. Deletion of the corresponding mouse gene caused embryonic lethality in homozygotes and predisposed heterozygotes to different types of hematologic malignancies (Kung et al., 2000). Loss of heterozygosity was observed in these cancers, suggesting that, in this context and perhaps others, tumorigenic alterations of the CBP gene may cause a loss of gene function. Further functional characterization of human CBP fusions may resolve the natures of these mutations. Finally, HDACs are linked to tumor progression primarily because they are targeted by various anti-cancer therapies, including butyrates and trichostatin A (reviewed by Marks et al., 2001).

As discussed above, some transcriptional regulators function by recruiting chromatin remodeling complexes. These transcriptional regulators include proto-oncogenes like myc and tumor suppressor genes like Rb. Although I will not discuss the genetic data regarding their dysfunction in cancers, it should be noted that alterations of chromatin structure are likely involved in their regulation of cell proliferation.

Transcriptional regulation by the E2F and Rb families of proteins involves chromatin remodeling

Many of the mechanisms discussed above are thought to apply to the regulation of transcription by E2F and Rb family proteins. These proteins have been the subjects of intense study (reviewed by Dyson, 1998; Zhang and Dean, 2001; Trimarchi and Lees, 2002), in large part because of the role of pRb as a tumor suppressor in mammals. Early studies established that E2F proteins form heterodimers *in vivo* with DP family proteins. DP/E2F heterodimers bind DNA site-specifically and are themselves bound by Rb family proteins. Transcriptionally-activating forms of DP/E2F

heterodimers promote cell cycle progression, whereas forms of DP/E2F that are bound by Rb family proteins repress transcription and prevent cell cycle entry. These contrasting activities are thought to underlie a cell's decision to proliferate or differentiate. Many activities of these proteins have been described; I will focus on their functions in relation to chromatin remodeling and modification.

Rb family proteins are thought to mediate transcriptional repression by recruiting chromatin remodeling activities to promoters. Mammalian class I HDACs were found to interact with pRb, and the repression of Rb-regulated reporter genes was dependent on HDAC activity (Brehm et al., 1998; Luo et al., 1998; Magnaghi-Jaulin et al., 1998). In addition, the presence of an HDAC at Rb-regulated promoters caused a reduction in the acetylated forms of histone H3 and histone H4 (Luo et al., 1998; Ferreira et al., 2001). More recent studies have found that Rb can also recruit the SUV39H1 HMT to repress transcription (Nielsen et al., 2001; Vandel et al., 2001). Such a coupling of HDAC and HMT activities suggests that Rb may coordinate a two-step modification process in which acetyl groups are first removed from lysine residues and methyl groups subsequently added. The association with SUV39H1 is notable because of its specificity for lysine 9 of histone H3 and the link between this modification and transcriptional silencing. Rb is thought to repress E2F-dependent transcription by additional mechanisms. Rb binds to and is proposed to mask a transactivation domain that is present in the carboxy-terminal region of most E2F family proteins (Helin et al., 1992; Flemington et al., 1993; Helin et al., 1993; Ross et al., 1999). As a consequence, Rb may prevent association of the basal transcription machinery with E2F.

E2F-6, an atypical E2F family member, may associate with HMT activity independently of Rb. Unlike other E2F proteins, E2F-6 lacks a transactivation domain and an Rb-binding site and in place has a potent transrepression domain (Morkel et al., 1997; Gaubatz et al., 1998; Trimarchi et al., 1998). Recently, E2F-6 was found to interact with a multisubunit complex that contains the histone H3 lysine 9-specific Eu-HMTase1 (Ogawa et al., 2002). The cellular role of this interaction has not yet been reported.

In addition to chromatin modifying activities, Rb may recruit ATP-dependent chromatin remodeling activities to repress transcription. Zhang et al. found that cotransfection of Rb with the human SWI2/SNF2-like protein BRG1 in the C33a cell line caused a synergistic S-phase arrest along with a reduction in E2F reporter gene transcription (Zhang et al., 2000). Genetic data from *Drosophila* suggest a conserved

role for SWI/SNF remodeling subunits in Rb-mediated repression. Loss-of-function mutations in *osa*, *mor* and *brm*, which encode homologs of SWI3, SWI1 and the ATP-dependent catalytic subunit SWI2/SNF2, respectively, enhance the phenotype caused by overexpression of the *dE2F1* gene (Staehling-Hampton et al., 1999).

Rb may act through chromatin-binding proteins to regulate transcription. As suggested by its interaction with SUV39H1, Rb indirectly creates a binding site for the HP1 protein (Nielsen et al., 2001). Surprisingly, Rb not only appears to facilitate binding of HP1 to chromatin by promoting histone H3 lysine 9 methylation, but it also may directly interact with HP1 and recruit this protein to its binding site. As noted above, the mechanism by which HP1 alters chromatin structure is poorly understood.

As with regulation by Myc/Mad/Max proteins and nuclear hormone receptors, the same DNA regulatory sequences are involved in the switch between DP/E2F-mediated transcriptional repression and activation. As examined in cells transitioning from a quiescent G0 state and G1 phase to the S phase of the cell cycle, the replacement of DP/E2F/Rb species with forms of DP/E2F that are not bound by Rb family proteins is thought to underlie this switch. As cells progress from G1 to S phase, Rb family proteins are phosphorylated by cyclin-dependent kinases (cdks). A two step phosphorylation process may occur (reviewed by Zhang and Dean, 2001). In the first step, cyclinD/cdk(4/6) complexes phosphorylate Rb family proteins. This phosphorylation is proposed to release HDAC from DP/E2F/Rb complexes and allow binding of SWI/SNF to proceed. This initial step is thought to be sufficient for the activation of some E2F-regulated genes such as cyclin E. In the second step, cyclinE/cdk2 complexes phosphorylate Rb family proteins. This second step is proposed to dissociate Rb proteins from DP/E2F species and lead to the activation of a broader set of E2F-regulated genes that further promote S phase entry.

The range of DP/E2F species have traditionally been thought to function in both transcriptional activation and repression. However, more recent findings suggest that different classes of E2F proteins predominate in repressing and activating complexes (reviewed by Trimarchi and Lees, 2002). E2F-4 and E2F-5 are localized to the nucleus in quiescent and G1 cells, where they are found in complexes with Rb family proteins. Because E2F-4 levels exceed those of other E2Fs in these cells, E2F-4 is thought to be primarily responsible for E2F-mediated repression. As cells approach S phase E2F-4 localization shifts primarily to the cytoplasm (Muller et al., 1997; Verona et al., 1997; Gaubatz et al., 2001). E2F-4 has two nuclear export signals that may dictate its change

in localization once it dissociates from Rb family proteins (Gaubatz et al., 2001). By contrast, E2F-1, E2F-2 and E2F-3 each have a nuclear localization sequence and are never observed in the cytoplasm (Magae et al., 1996; Muller et al., 1997; Verona et al., 1997). Their presence in the nucleus and their release from Rb family proteins during S phase entry suggests that these E2Fs serve activating roles. Various lines of evidence support this model. ChIP studies indicate that E2F-4, in complexes with Rb family proteins and at least one HDAC, primarily occupies E2F-responsive promoters during G0 and G1, whereas E2F-1, E2F-2 and E2F-3 occupy these promoters as cells progress into S phase (Takahashi et al., 2000; Rayman et al., 2002). Furthermore, the opposing activities of E2F proteins suggested by this model may account for the antagonism observed between the two *Drosophila* E2F proteins (Frolov et al., 2001). Finally, cells derived from *E2F4E2F5* double mutant mice show defects in Rb protein-dependent G1 arrest, whereas *E2F1E2F2E2F3* triple knockout cells show reduced levels of E2F-regulated transcriptional activation and are unable to enter S phase (Gaubatz et al., 2000; Wu et al., 2001).

The shift from E2F-dependent repression to activation may be accompanied by a corresponding shift from repressing to activating chromatin modifying complexes. Studies of mammalian cells in culture have indicated that E2Fs may activate transcription by recruiting HATs including CBP (Trouche and Kouzarides, 1996). While E2Fs are thought to interact directly with CBP, their interaction with hGcn5 is apparently mediated by the TRRAP adaptor protein (McMahon et al., 1998; Lang et al., 2001). While these HATs cooperate with E2Fs to induce transcription of reporter genes, their requirement in E2F-dependent S phase entry is currently unknown.

Future issues regarding chromatin

The preceding sections describe the tremendous progress, achieved largely over the past decade, in understanding the links between chromatin remodeling and modification and the control of transcription. The studies described raise a number of issues that merit further investigation. For example, how does the action of targeted and untargeted enzymatic activities lead to a repressive or active chromatin structure? The identification of bromodomains and chromodomains as a modification-specific binding modules indicates that proteins containing these modules can affect transcriptional competence. However, there are likely many steps in between their binding and the creation of a refractory or open chromatin configuration. What are the

proteins that participate in these and other steps and what functions do they serve? Some studies have identified other components of remodeling and modifying complexes, however, there are likely a host of other proteins that function in remodeling, modification and other processes that modulate chromatin structure. Such proteins may act as enzymes, function as structural components of enzymatic complexes, mediate protein-protein interactions between complexes or function in some heretofore unknown capacity. An additional issue is whether all of the different mechanisms described in these disparate studies can be tied together to regulate individual genes. Studies of HO transcription by Cosma et al. have indicated that the answer may be yes. However, it will be useful to determine how general multi-mechanistic regulation is. Finally, how does modulation of chromatin specifically regulate cell cycle progression and developmental processes in multicellular animals? This question is especially relevant in light of the connection, as exemplified by the tumor suppressor Rb, between chromatin modulation and diseases including cancer.

CONCLUDING REMARKS

Proteins that modulate chromatin structure regulate gene expression. This chapter has described many of these proteins and has highlighted mechanisms, some of which may be evolutionarily conserved, by which these proteins function. Characterizing existing and identifying additional chromatin remodeling proteins will enhance our understanding of transcriptional regulation. Furthermore, knowing how these proteins regulate cell division and developmental processes will be important for understanding how their dysregulation is linked to diseases such as cancer.

The following five chapters describe the identification and characterization of synMuv genes that are putative regulators of chromatin structure in *C. elegans*. A discussion of how my and other researchers' findings regarding the synMuv genes relate to chromatin remodeling can be found in Chapter 7 (Discussion and Future Prospects).

REFERENCES

Agalioti, T., Lomvardas, S., Parekh, B., Yie, J., Maniatis, T., and Thanos, D. (2000). Ordered recruitment of chromatin modifying and general transcription factors to the IFN-beta promoter, Cell *103*, 667-78.

Akhtar, A., and Becker, P. B. (2000). Activation of transcription through histone H4 acetylation by MOF, an acetyltransferase essential for dosage compensation in Drosophila, Mol. Cell *5*, 367-75.

Allard, S., Utley, R. T., Savard, J., Clarke, A., Grant, P., Brandl, C. J., Pillus, L., Workman, J. L., and Cote, J. (1999). NuA4, an essential transcription adaptor/histone H4 acetyltransferase complex containing Esa1p and the ATM-related cofactor Tra1p, Embo J. *18*, 5108-19.

Allfrey, V., Faulkner, R. M., and Mirsky, A. E. (1964). Acetylation and methylation of histones and their possible role in the regulation of RNA synthesis, Proc. Natl. Acad. Sci. USA *51*, 786-94.

Annunziato, A. T., and Hansen, J. C. (2000). Role of histone acetylation in the assembly and modulation of chromatin structures, Gene Expr. *9*, 37-61.

Aroian, R. V., Koga, M., Mendel, J. E., Ohshima, Y., and Sternberg, P. W. (1990). The *let-23* gene necessary for *Caenorhabditis elegans* vulval induction encodes a tyrosine kinase of the EGF receptor subfamily, Nature *348*, 693-9.

Bannister, A. J., Zegerman, P., Partridge, J. F., Miska, E. A., Thomas, J. O., Allshire, R. C., and Kouzarides, T. (2001). Selective recognition of methylated lysine 9 on histone H3 by the HP1 chromodomain, Nature *410*, 120-4.

Bednar, J., Horowitz, R. A., Grigoryev, S. A., Carruthers, L. M., Hansen, J. C., Koster, A. J., and Woodcock, C. L. (1998). Nucleosomes, linker DNA, and linker histone form a unique structural motif that directs the higher-order folding and compaction of chromatin, Proc. Natl. Acad. Sci. USA *95*, 14173-8.

Beitel, G. J., Clark, S. G., and Horvitz, H. R. (1990). *Caenorhabditis elegans ras* gene *let-60* acts as a switch in the pathway of vulval induction, Nature *348*, 503-9.

Beitel, G. J., Lambie, E. J., and Horvitz, H. R. (2000). The *C. elegans* gene *lin-9*,which acts in an Rb-related pathway, is required for gonadal sheath cell development and encodes a novel protein, Gene *254*, 253-63.

Beitel, G. J., Tuck, S., Greenwald, I., and Horvitz, H. R. (1995). The *Caenorhabditis elegans* gene *lin-1* encodes an ETS-domain protein and defines a branch of the vulval induction pathway, Genes Dev. *9*, 3149-62.

Bernstein, B. E., Tong, J. K., and Schreiber, S. L. (2000). Genomewide studies of histone deacetylase function in yeast, Proc. Natl. Acad. Sci. USA *97*, 13708-13.

Boggs, B. A., Cheung, P., Heard, E., Spector, D. L., Chinault, A. C., and Allis, C. D. (2002). Differentially methylated forms of histone H3 show unique association patterns with inactive human X chromosomes, Nat. Genet. *30*, 73-6.

Braunstein, M., Sobel, R. E., Allis, C. D., Turner, B. M., and Broach, J. R. (1996). Efficient transcriptional silencing in *Saccharomyces cerevisiae* requires a heterochromatin histone acetylation pattern, Mol. Cell. Biol. *16*, 4349-56.

Brehm, A., Langst, G., Kehle, J., Clapier, C. R., Imhof, A., Eberharter, A., Muller, J., and Becker, P. B. (2000). dMi-2 and ISWI chromatin remodelling factors have distinct nucleosome binding and mobilization properties, Embo J. *19*, 4332-41.

Brehm, A., Miska, E. A., McCance, D. J., Reid, J. L., Bannister, A. J., and Kouzarides, T. (1998). Retinoblastoma protein recruits histone deacetylase to repress transcription, Nature *391*, 597-601.

Briggs, S. D., Bryk, M., Strahl, B. D., Cheung, W. L., Davie, J. K., Dent, S. Y., Winston, F., and Allis, C. D. (2001). Histone H3 lysine 4 methylation is mediated by Set1 and

required for cell growth and rDNA silencing in *Saccharomyces cerevisiae*, Genes Dev. *15*, 3286-95.

Brown, C. E., Howe, L., Sousa, K., Alley, S. C., Carrozza, M. J., Tan, S., and Workman, J. L. (2001). Recruitment of HAT complexes by direct activator interactions with the ATM-related Tra1 subunit, Science *292*, 2333-7.

Brownell, J. E., Zhou, J., Ranalli, T., Kobayashi, R., Edmondson, D. G., Roth, S. Y., and Allis, C. D. (1996). *Tetrahymena* histone acetyltransferase A: a homolog to yeast Gcn5p linking histone acetylation to gene activation, Cell *84*, 843-51.

Bultman, S., Gebuhr, T., Yee, D., La Mantia, C., Nicholson, J., Gilliam, A., Randazzo, F., Metzger, D., Chambon, P., Crabtree, G., and Magnuson, T. (2000). A *Brg1* null mutation in the mouse reveals functional differences among mammalian SWI/SNF complexes, Mol. Cell *6*, 1287-95.

Cairns, B. R. (2001). Emerging roles for chromatin remodeling in cancer biology, Trends Cell Biol. *11*, S15-21.

Carruthers, L. M., Bednar, J., Woodcock, C. L., and Hansen, J. C. (1998). Linker histones stabilize the intrinsic salt-dependent folding of nucleosomal arrays: mechanistic ramifications for higher-order chromatin folding, Biochemistry *37*, 14776-87.

Carruthers, L. M., and Hansen, J. C. (2000). The core histone N termini function independently of linker histones during chromatin condensation, J. Biol. Chem. *275*, 37285-90.

Chen, D., Ma, H., Hong, H., Koh, S. S., Huang, S. M., Schurter, B. T., Aswad, D. W., and Stallcup, M. R. (1999). Regulation of transcription by a protein methyltransferase, Science *284*, 2174-7.

Clapier, C. R., Langst, G., Corona, D. F., Becker, P. B., and Nightingale, K. P. (2001). Critical role for the histone H4 N terminus in nucleosome remodeling by ISWI, Mol. Cell. Biol. *21*, 875-83.

Clark, S. G. (1992). Intercellular signalling and homeotic genes required during vulval development in *C. elegans*, Ph.D. Thesis, Massachusetts Institute of Technology.

Clark, S. G., Chisholm, A. D., and Horvitz, H. R. (1993). Control of cell fates in the central body region of *C. elegans* by the homeobox gene *lin-39*, Cell *74*, 43-55.

Clark, S. G., Lu, X., and Horvitz, H. R. (1994). The *Caenorhabditis elegans* locus *lin-15*, a negative regulator of a tyrosine kinase signaling pathway, encodes two different proteins, Genetics *137*, 987-97.

Clark, S. G., Stern, M. J., and Horvitz, H. R. (1992). *C. elegans* cell-signalling gene *sem-5* encodes a protein with SH2 and SH3 domains, Nature *356*, 340-4.

Clarke, A. S., Lowell, J. E., Jacobson, S. J., and Pillus, L. (1999). Esa1p is an essential histone acetyltransferase required for cell cycle progression, Mol. Cell. Biol. *19*, 2515-26.

Cosma, M. P., Tanaka, T., and Nasmyth, K. (1999). Ordered recruitment of transcription and chromatin remodeling factors to a cell cycle and developmentally regulated promoter, Cell *97*, 299-311.

Couteau, F., Guerry, F., Muller, F., and Palladino, F. (2002). A heterochromatin protein 1 homologue in *Caenorhabditis elegans* acts in germline and vulval development, EMBO Rep. *3*, 235-41.

Dhalluin, C., Carlson, J. E., Zeng, L., He, C., Aggarwal, A. K., and Zhou, M. M. (1999). Structure and ligand of a histone acetyltransferase bromodomain, Nature *399*, 491-6.

Dilworth, F. J., Fromental-Ramain, C., Yamamoto, K., and Chambon, P. (2000). ATP-driven chromatin remodeling activity and histone acetyltransferases act sequentially during transactivation by RAR/RXR in vitro, Mol. Cell *6*, 1049-58.

Durrin, L. K., Mann, R. K., Kayne, P. S., and Grunstein, M. (1991). Yeast histone H4 N-terminal sequence is required for promoter activation in vivo, Cell *65*, 1023-31.

Dyson, N. (1998). The regulation of E2F by pRB-family proteins, Genes Dev. *12*, 2245-62.

Ekwall, K., and Ruusala, T. (1994). Mutations in *rik1*, *clr2*, *clr3* and *clr4* genes asymmetrically derepress the silent mating-type loci in fission yeast, Genetics *136*, 53-64.

Ferguson, E. L., and Horvitz, H. R. (1985). Identification and characterization of 22 genes that affect the vulval cell lineages of the nematode *Caenorhabditis elegans*, Genetics *110*, 17-72.

Ferguson, E. L., and Horvitz, H. R. (1989). The multivulva phenotype of certain *Caenorhabditis elegans* mutants results from defects in two functionally redundant pathways, Genetics *123*, 109-21.

Ferguson, E. L., Sternberg, P. W., and Horvitz, H. R. (1987). A genetic pathway for the specification of the vulval cell lineages of Caenorhabditis elegans, Nature *326*, 259-67.

Ferreira, R., Naguibneva, I., Mathieu, M., Ait-Si-Ali, S., Robin, P., Pritchard, L. L., and Harel-Bellan, A. (2001). Cell cycle-dependent recruitment of HDAC-1 correlates with deacetylation of histone H4 on an Rb-E2F target promoter, EMBO Rep. *2*, 794-9.

Finch, J. T., and Klug, A. (1976). Solenoidal model for superstructure in chromatin, Proc. Natl. Acad. Sci. USA *73*, 1897-901.

Flemington, E. K., Speck, S. H., and Kaelin, W. G., Jr. (1993). E2F-1-mediated transactivation is inhibited by complex formation with the retinoblastoma susceptibility gene product, Proc. Natl. Acad. Sci. USA *90*, 6914-8.

Frolov, M. V., Huen, D. S., Stevaux, O., Dimova, D., Balczarek-Strang, K., Elsdon, M., and Dyson, N. J. (2001). Functional antagonism between E2F family members, Genes Dev. *15*, 2146-60.

Fryer, C. J., and Archer, T. K. (1998). Chromatin remodelling by the glucocorticoid receptor requires the BRG1 complex, Nature *393*, 88-91.

Fyodorov, D. V., and Kadonaga, J. T. (2001). The many faces of chromatin remodeling: SWItching beyond transcription, Cell *106*, 523-5.

Garcia-Ramirez, M., Dong, F., and Ausio, J. (1992). Role of the histone "tails" in the folding of oligonucleosomes depleted of histone H1, J. Biol. Chem. *267*, 19587-95.

Gaubatz, S., Lees, J. A., Lindeman, G. J., and Livingston, D. M. (2001). E2F4 is exported from the nucleus in a CRM1-dependent manner, Mol. Cell. Biol. *21*, 1384-92.

Gaubatz, S., Lindeman, G. J., Ishida, S., Jakoi, L., Nevins, J. R., Livingston, D. M., and Rempel, R. E. (2000). *E2F4* and *E2F5* play an essential role in pocket protein-mediated G1 control, Mol. Cell *6*, 729-35.

Gaubatz, S., Wood, J. G., and Livingston, D. M. (1998). Unusual proliferation arrest and transcriptional control properties of a newly discovered E2F family member, E2F-6, Proc. Natl. Acad. Sci. USA *95*, 9190-5.

Georgakopoulos, T., and Thireos, G. (1992). Two distinct yeast transcriptional activators require the function of the GCN5 protein to promote normal levels of transcription, Embo J. *11*, 4145-52.

Goldmark, J. P., Fazzio, T. G., Estep, P. W., Church, G. M., and Tsukiyama, T. (2000). The Isw2 chromatin remodeling complex represses early meiotic genes upon recruitment by Ume6p, Cell *103*, 423-33.

Gorka, C., Fakan, S., and Lawrence, J. J. (1993). Light and electron microscope immunocytochemical analyses of histone H1(0) distribution in the nucleus of Friend erythroleukemia cells, Exp. Cell Res. *205*, 152-8.

Grant, P. A., Eberharter, A., John, S., Cook, R. G., Turner, B. M., and Workman, J. L. (1999). Expanded lysine acetylation specificity of Gcn5 in native complexes, J. Biol. Chem. *274*, 5895-900.

Guidi, C. J., Sands, A. T., Zambrowicz, B. P., Turner, T. K., Demers, D. A., Webster, W., Smith, T. W., Imbalzano, A. N., and Jones, S. N. (2001). Disruption of *Ini1* leads to peri-implantation lethality and tumorigenesis in mice, Mol. Cell. Biol. *21*, 3598-603.

Han, M., Aroian, R. V., and Sternberg, P. W. (1990). The *let-60* locus controls the switch between vulval and nonvulval cell fates in *Caenorhabditis elegans*, Genetics *126*, 899-913.

Han, M., Golden, A., Han, Y., and Sternberg, P. W. (1993). *C. elegans lin-45* raf gene participates in *let-60* ras-stimulated vulval differentiation, Nature *363*, 133-40.

Han, M., and Sternberg, P. W. (1990). *let-60*, a gene that specifies cell fates during *C. elegans* vulval induction, encodes a ras protein, Cell *63*, 921-31.

Hassig, C. A., Fleischer, T. C., Billin, A. N., Schreiber, S. L., and Ayer, D. E. (1997). Histone deacetylase activity is required for full transcriptional repression by mSin3A, Cell *89*, 341-7.

Hedgecock, E. M., and Herman, R. K. (1995). The *ncl-1* gene and genetic mosaics of *Caenorhabditis elegans*, Genetics *141*, 989-1006.

Helin, K., Harlow, E., and Fattaey, A. (1993). Inhibition of E2F-1 transactivation by direct binding of the retinoblastoma protein, Mol. Cell. Biol. *13*, 6501-8.

Helin, K., Lees, J. A., Vidal, M., Dyson, N., Harlow, E., and Fattaey, A. (1992). A cDNA encoding a pRB-binding protein with properties of the transcription factor E2F, Cell *70*, 337-50.

Herman, R. K., and Hedgecock, E. M. (1990). Limitation of the size of the vulval primordium of *Caenorhabditis elegans* by *lin-15* expression in surrounding hypodermis, Nature *348*, 169-71.

Hill, R. J., and Sternberg, P. W. (1992). The gene *lin-3* encodes an inductive signal for vulval development in *C. elegans*, Nature *358*, 470-6.

Horvitz, H. R., and Sulston, J. E. (1980). Isolation and genetic characterization of cell-lineage mutants of the nematode *Caenorhabditis elegans*, Genetics *96*, 435-54.

Huang, L. S., Tzou, P., and Sternberg, P. W. (1994). The *lin-15* locus encodes two negative regulators of *Caenorhabditis elegans* vulval development, Mol. Biol. Cell *5*, 395-411.

Imai, S., Armstrong, C. M., Kaeberlein, M., and Guarente, L. (2000). Transcriptional silencing and longevity protein Sir2 is an NAD-dependent histone deacetylase, Nature *403*, 795-800.

Jacobs, S. A., Taverna, S. D., Zhang, Y., Briggs, S. D., Li, J., Eissenberg, J. C., Allis, C. D., and Khorasanizadeh, S. (2001). Specificity of the HP1 chromodomain for the methylated N-terminus of histone H3, Embo J. *20*, 5232-41.

Jacobson, R. H., Ladurner, A. G., King, D. S., and Tjian, R. (2000). Structure and function of a human TAFII250 double bromodomain module, Science *288*, 1422-5.

Jeppesen, P., Mitchell, A., Turner, B., and Perry, P. (1992). Antibodies to defined histone epitopes reveal variations in chromatin conformation and underacetylation of centric heterochromatin in human metaphase chromosomes, Chromosoma *101*, 322-32.

Jeppesen, P., and Turner, B. M. (1993). The inactive X chromosome in female mammals is distinguished by a lack of histone H4 acetylation, a cytogenetic marker for gene expression, Cell *74*, 281-9.

John, S., Howe, L., Tafrov, S. T., Grant, P. A., Sternglanz, R., and Workman, J. L. (2000). The something about silencing protein, Sas3, is the catalytic subunit of NuA3, a yTAF(II)30-containing HAT complex that interacts with the Spt16 subunit of the yeast CP(Cdc68/Pob3)-FACT complex, Genes Dev. *14*, 1196-208.

Johnson, L. M., Fisher-Adams, G., and Grunstein, M. (1992). Identification of a non-basic domain in the histone H4 N-terminus required for repression of the yeast silent mating loci, Embo J. *11*, 2201-9.

Kadosh, D., and Struhl, K. (1997). Repression by Ume6 involves recruitment of a complex containing Sin3 corepressor and Rpd3 histone deacetylase to target promoters, Cell *89*, 365-71.

Katan-Khaykovich, Y., and Struhl, K. (2002). Dynamics of global histone acetylation and deacetylation in vivo: rapid restoration of normal histone acetylation status upon removal of activators and repressors, Genes Dev. *16*, 743-52.

Kehle, J., Beuchle, D., Treuheit, S., Christen, B., Kennison, J. A., Bienz, M., and Muller, J. (1998). dMi-2, a hunchback-interacting protein that functions in polycomb repression, Science *282*, 1897-900.

Kimble, J. (1981). Alterations in cell lineage following laser ablation of cells in the somatic gonad of *Caenorhabditis elegans*, Dev. Biol. *87*, 286-300.

Kimura, A., and Horikoshi, M. (1998). Tip60 acetylates six lysines of a specific class in core histones in vitro, Genes Cells *3*, 789-800.

Koipally, J., Renold, A., Kim, J., and Georgopoulos, K. (1999). Repression by Ikaros and Aiolos is mediated through histone deacetylase complexes, Embo J. *18*, 3090-100.

Kornfeld, K., Guan, K. L., and Horvitz, H. R. (1995a). The *Caenorhabditis elegans* gene *mek-2* is required for vulval induction and encodes a protein similar to the protein kinase MEK, Genes Dev. *9*, 756-68.

Kornfeld, K., Hom, D. B., and Horvitz, H. R. (1995b). The *ksr-1* gene encodes a novel protein kinase involved in Ras-mediated signaling in *C. elegans*, Cell *83*, 903-13.

Krogan, N. J., Dover, J., Khorrami, S., Greenblatt, J. F., Schneider, J., Johnston, M. and Shilatifard, A. (2002). COMPASS, a histone H3 (Lysine 4) methyltransferase required for telomeric silencing of gene expression, J. Biol. Chem. *277*, 10753-5.

Kung, A. L., Rebel, V. I., Bronson, R. T., Ch'ng, L. E., Sieff, C. A., Livingston, D. M., and Yao, T. P. (2000). Gene dose-dependent control of hematopoiesis and hematologic tumor suppression by CBP, Genes Dev. *14*, 272-7.

Kuo, M. H., Brownell, J. E., Sobel, R. E., Ranalli, T. A., Cook, R. G., Edmondson, D. G., Roth, S. Y., and Allis, C. D. (1996). Transcription-linked acetylation by Gcn5p of histones H3 and H4 at specific lysines, Nature *383*, 269-72.

Kuo, M. H., Zhou, J., Jambeck, P., Churchill, M. E., and Allis, C. D. (1998). Histone acetyltransferase activity of yeast Gcn5p is required for the activation of target genes in vivo, Genes Dev. *12*, 627-39.

Lachner, M., O'Carroll, D., Rea, S., Mechtler, K., and Jenuwein, T. (2001). Methylation of histone H3 lysine 9 creates a binding site for HP1 proteins, Nature *410*, 116-20.

Lackner, M. R., Kornfeld, K., Miller, L. M., Horvitz, H. R., and Kim, S. K. (1994). A MAP kinase homolog, *mpk-1*, is involved in ras-mediated induction of vulval cell fates in *Caenorhabditis elegans*, Genes Dev. *8*, 160-73.

Laherty, C. D., Yang, W. M., Sun, J. M., Davie, J. R., Seto, E., and Eisenman, R. N. (1997). Histone deacetylases associated with the mSin3 corepressor mediate mad transcriptional repression, Cell *89*, 349-56.

Landry, J., Sutton, A., Tafrov, S. T., Heller, R. C., Stebbins, J., Pillus, L., and Sternglanz, R. (2000). The silencing protein SIR2 and its homologs are NAD-dependent protein deacetylases, Proc. Natl. Acad. Sci. USA *97*, 5807-11.

Lang, S. E., McMahon, S. B., Cole, M. D., and Hearing, P. (2001). E2F transcriptional activation requires TRRAP and GCN5 cofactors, J. Biol. Chem. *276*, 32627-34.

Langst, G., and Becker, P. B. (2001). Nucleosome mobilization and positioning by ISWI-containing chromatin remodeling factors, J. Cell Sci. *114*, 2561-8.

Lee, K. M., Sif, S., Kingston, R. E., and Hayes, J. J. (1999). hSWI/SNF disrupts interactions between the H2A N-terminal tail and nucleosomal DNA, Biochemistry *38*, 8423-9.

Li, J., Lin, Q., Wang, W., Wade, P., and Wong, J. (2002). Specific targeting and constitutive association of histone deacetylase complexes during transcriptional repression, Genes Dev. *16*, 687-92.

Lin, B. C., Hong, S. H., Krig, S., Yoh, S. M., and Privalsky, M. L. (1997). A conformational switch in nuclear hormone receptors is involved in coupling hormone binding to corepressor release, Mol. Cell. Biol. *17*, 6131-8.

Lu, X. (1999). Molecular analyses of the class B synthetic multivulva genes of *Caenorhabditis elegans*, Ph.D. Thesis, Massachusetts Institute of Technology.

Lu, X., and Horvitz, H. R. (1998). *lin-35* and *lin-53*, two genes that antagonize a *C. elegans* Ras pathway, encode proteins similar to Rb and its binding protein RbAp48, Cell *95*, 981-91.

Luger, K., Mader, A. W., Richmond, R. K., Sargent, D. F., and Richmond, T. J. (1997). Crystal structure of the nucleosome core particle at 2.8 A resolution, Nature *389*, 251-60.

Luo, R. X., Postigo, A. A., and Dean, D. C. (1998). Rb interacts with histone deacetylase to repress transcription, Cell *92*, 463-73.

Magae, J., Wu, C. L., Illenye, S., Harlow, E., and Heintz, N. H. (1996). Nuclear localization of DP and E2F transcription factors by heterodimeric partners and retinoblastoma protein family members, J. Cell Sci. *109*, 1717-26.

Magnaghi-Jaulin, L., Groisman, R., Naguibneva, I., Robin, P., Lorain, S., Le Villain, J. P., Troalen, F., Trouche, D., and Harel-Bellan, A. (1998). Retinoblastoma protein represses transcription by recruiting a histone deacetylase, Nature *391*, 601-5.

Maloof, J. N., and Kenyon, C. (1998). The Hox gene *lin-39* is required during *C. elegans* vulval induction to select the outcome of Ras signaling, Development *125*, 181-90.

Marks, P., Rifkind, R. A., Richon, V. M., Breslow, R., Miller, T., and Kelly, W. K. (2001). Histone deacetylases and cancer: causes and therapies, Nat. Rev. Cancer *1*, 194-202.

McMahon, S. B., Van Buskirk, H. A., Dugan, K. A., Copeland, T. D., and Cole, M. D. (1998). The novel ATM-related protein TRRAP is an essential cofactor for the c-Myc and E2F oncoproteins, Cell *94*, 363-74.

Meijsing, S. H., and Ehrenhofer-Murray, A. E. (2001). The silencing complex SAS-I links histone acetylation to the assembly of repressed chromatin by CAF-I and Asf1 in *Saccharomyces cerevisiae*, Genes Dev. *15*, 3169-82.

Miller, L. M., Gallegos, M. E., Morisseau, B. A., and Kim, S. K. (1993). *lin-31*, a *Caenorhabditis elegans* HNF-3/fork head transcription factor homolog, specifies three alternative cell fates in vulval development, Genes Dev. *7*, 933-47.

Morkel, M., Wenkel, J., Bannister, A. J., Kouzarides, T., and Hagemeier, C. (1997). An E2F-like repressor of transcription, Nature *390*, 567-8.

Muller, H., Moroni, M. C., Vigo, E., Petersen, B. O., Bartek, J., and Helin, K. (1997). Induction of S-phase entry by E2F transcription factors depends on their nuclear localization, Mol. Cell. Biol. *17*, 5508-20.

Nagy, P. L., Griesenbeck, J., Kornberg, R. D., and Cleary, M. L. (2002). A trithorax-group complex purified from *Saccharomyces cerevisiae* is required for methylation of histone H3, Proc. Natl. Acad. Sci. USA *99*, 90-4.

Nakayama, J., Rice, J. C., Strahl, B. D., Allis, C. D., and Grewal, S. I. (2001). Role of histone H3 lysine 9 methylation in epigenetic control of heterochromatin assembly, Science *292*, 110-3.

Narlikar, G. J., Fan, H. Y., and Kingston, R. E. (2002). Cooperation between complexes that regulate chromatin structure and transcription, Cell *108*, 475-87.

Narlikar, G. J., Phelan, M. L., and Kingston, R. E. (2001). Generation and interconversion of multiple distinct nucleosomal states as a mechanism for catalyzing chromatin fluidity, Mol. Cell *8*, 1219-30.

Neely, K. E., Hassan, A. H., Wallberg, A. E., Steger, D. J., Cairns, B. R., Wright, A. P., and Workman, J. L. (1999). Activation domain-mediated targeting of the SWI/SNF complex to promoters stimulates transcription from nucleosome arrays, Mol. Cell *4*, 649-55.

Nielsen, S. J., Schneider, R., Bauer, U. M., Bannister, A. J., Morrison, A., O'Carroll, D., Firestein, R., Cleary, M., Jenuwein, T., Herrera, R. E., and Kouzarides, T. (2001). Rb targets histone H3 methylation and HP1 to promoters, Nature *412*, 561-5.

Nishioka, K., Chuikov, S., Sarma, K., Erdjument-Bromage, H., Allis, C. D., Tempst, P., and Reinberg, D. (2002a). Set9, a novel histone H3 methyltransferase that facilitates transcription by precluding histone tail modifications required for heterochromatin formation, Genes Dev. *16*, 479-89.

Nishioka, K., Rice, J. C., Sarma, K., Erdjument-Bromage, H., Werner, J., Wang, Y., Chuikov, S., Valenzuela, P., Tempst, P., Steward, R., *et al.* (2002b). PR-Set7 is a nucleosome-specific methyltransferase that modifies lysine 20 of histone H4 and is associated with silent chromatin, Mol. Cell *9*, 1201-13.

Noma, K., Allis, C. D., and Grewal, S. I. (2001). Transitions in distinct histone H3 methylation patterns at the heterochromatin domain boundaries, Science *293*, 1150-5.

Ogawa, H., Ishiguro, K., Gaubatz, S., Livingston, D. M., and Nakatani, Y. (2002). A complex with chromatin modifiers that occupies E2F- and Myc-responsive genes in G0 cells, Science *296*, 1132-6.

Osada, S., Sutton, A., Muster, N., Brown, C. E., Yates, J. R., 3rd, Sternglanz, R., and Workman, J. L. (2001). The yeast SAS (something about silencing) protein complex contains a MYST-type putative acetyltransferase and functions with chromatin assembly factor ASF1, Genes Dev. *15*, 3155-68.

Park, J., Kunjibettu, S., McMahon, S. B., and Cole, M. D. (2001). The ATM-related domain of TRRAP is required for histone acetyltransferase recruitment and Myc-dependent oncogenesis, Genes Dev. *15*, 1619-24.

Rayman, J. B., Takahashi, Y., Indjeian, V. B., Dannenberg, J. H., Catchpole, S., Watson, R. J., te Riele, H., and Dynlacht, B. D. (2002). E2F mediates cell cycle-dependent transcriptional repression in vivo by recruitment of an HDAC1/mSin3B corepressor complex, Genes Dev. *16*, 933-47.

Rea, S., Eisenhaber, F., O'Carroll, D., Strahl, B. D., Sun, Z. W., Schmid, M., Opravil, S., Mechtler, K., Ponting, C. P., Allis, C. D., and Jenuwein, T. (2000). Regulation of chromatin structure by site-specific histone H3 methyltransferases, Nature *406*, 593-9.

Reid, J. L., Iyer, V. R., Brown, P. O., and Struhl, K. (2000). Coordinate regulation of yeast ribosomal protein genes is associated with targeted recruitment of Esa1 histone acetylase, Mol. Cell *6*, 1297-307.

Reifsnyder, C., Lowell, J., Clarke, A., and Pillus, L. (1996). Yeast SAS silencing genes and human genes associated with AML and HIV-1 Tat interactions are homologous with acetyltransferases, Nat. Genet. *14*, 42-9.

Roberts, C. W., Galusha, S. A., McMenamin, M. E., Fletcher, C. D., and Orkin, S. H. (2000). Haploinsufficiency of *Snf5* (integrase interactor 1) predisposes to malignant rhabdoid tumors in mice, Proc. Natl. Acad. Sci. USA *97*, 13796-800.

Robyr, D., Suka, Y., Xenarios, I., Kurdistani, S. K., Wang, A., Suka, N., and Grunstein, M. (2002). Microarray deacetylation maps determine genome-wide functions for yeast histone deacetylases, Cell *109*, 437-46.

Ross, J. F., Liu, X., and Dynlacht, B. D. (1999). Mechanism of transcriptional repression of E2F by the retinoblastoma tumor suppressor protein, Mol. Cell *3*, 195-205.

Roth, S. Y., Denu, J. M., and Allis, C. D. (2001). Histone acetyltransferases, Annu. Rev. Biochem. *70*, 81-120.

Schiltz, R. L., Mizzen, C. A., Vassilev, A., Cook, R. G., Allis, C. D., and Nakatani, Y. (1999). Overlapping but distinct patterns of histone acetylation by the human coactivators p300 and PCAF within nucleosomal substrates, J. Biol. Chem. *274*, 1189-92.

Schurter, B. T., Koh, S. S., Chen, D., Bunick, G. J., Harp, J. M., Hanson, B. L., Henschen-Edman, A., Mackay, D. R., Stallcup, M. R., and Aswad, D. W. (2001). Methylation of histone H3 by coactivator-associated arginine methyltransferase 1, Biochemistry *40*, 5747-56.

Sevenet, N., Sheridan, E., Amram, D., Schneider, P., Handgretinger, R., and Delattre, O. (1999). Constitutional mutations of the *hSNF5/INI1* gene predispose to a variety of cancers, Am. J. Hum. Genet. *65*, 1342-8.

Smith, E. R., Eisen, A., Gu, W., Sattah, M., Pannuti, A., Zhou, J., Cook, R. G., Lucchesi, J. C., and Allis, C. D. (1998). ESA1 is a histone acetyltransferase that is essential for growth in yeast, Proc. Natl. Acad. Sci. USA *95*, 3561-5.

Smith, E. R., Pannuti, A., Gu, W., Steurnagel, A., Cook, R. G., Allis, C. D., and Lucchesi, J. C. (2000). The *Drosophila* MSL complex acetylates histone H4 at lysine 16, a chromatin modification linked to dosage compensation, Mol. Cell. Biol. *20*, 312-8.

Solari, F., and Ahringer, J. (2000). NURD-complex genes antagonise Ras-induced vulval development in *Caenorhabditis elegans*, Curr. Biol. *10*, 223-6.

Staehling-Hampton, K., Ciampa, P. J., Brook, A., and Dyson, N. (1999). A genetic screen for modifiers of E2F in *Drosophila melanogaster*, Genetics *153*, 275-87.

Sternberg, P. W., and Han, M. (1998). Genetics of RAS signaling in *C. elegans*, Trends Genet. *14*, 466-72.

Sternberg, P. W., and Horvitz, H. R. (1986). Pattern formation during vulval development in *C. elegans*, Cell *44*, 761-72.

Sternberg, P. W., and Horvitz, H. R. (1989). The combined action of two intercellular signaling pathways specifies three cell fates during vulval induction in *C. elegans*, Cell *58*, 679-93.

Strahl, B. D., and Allis, C. D. (2000). The language of covalent histone modifications, Nature *403*, 41-5.

Strahl, B. D., Briggs, S. D., Brame, C. J., Caldwell, J. A., Koh, S. S., Ma, H., Cook, R. G., Shabanowitz, J., Hunt, D. F., Stallcup, M. R., and Allis, C. D. (2001). Methylation of histone H4 at arginine 3 occurs in vivo and is mediated by the nuclear receptor coactivator PRMT1, Curr. Biol. *11*, 996-1000.

Strahl, B. D., Grant, P. A., Briggs, S. D., Sun, Z. W., Bone, J. R., Caldwell, J. A., Mollah, S., Cook, R. G., Shabanowitz, J., Hunt, D. F., and Allis, C. D. (2002). Set2 is a

nucleosomal histone H3-selective methyltransferase that mediates transcriptional repression, Mol. Cell. Biol. *22*, 1298-306.

Strahl, B. D., Ohba, R., Cook, R. G., and Allis, C. D. (1999). Methylation of histone H3 at lysine 4 is highly conserved and correlates with transcriptionally active nuclei in *Tetrahymena*, Proc. Natl. Acad. Sci. USA *96*, 14967-72.

Suka, N., Suka, Y., Carmen, A. A., Wu, J., and Grunstein, M. (2001). Highly specific antibodies determine histone acetylation site usage in yeast heterochromatin and euchromatin, Mol. Cell *8*, 473-9.

Sulston, J. E., and Horvitz, H. R. (1977). Post-embryonic cell lineages of the nematode, *Caenorhabditis elegans*, Dev. Biol. *56*, 110-56.

Sulston, J. E., and Horvitz, H. R. (1981). Abnormal cell lineages in mutants of the nematode *Caenorhabditis elegans*, Dev. Biol. *82*, 41-55.

Sulston, J. E., and White, J. G. (1980). Regulation and cell autonomy during postembryonic development of *Caenorhabditis elegans*, Dev. Biol. *78*, 577-97.

Sundaram, M., and Han, M. (1995). The *C. elegans ksr-1* gene encodes a novel Raf-related kinase involved in Ras-mediated signal transduction, Cell *83*, 889-901.

Takahashi, Y., Rayman, J. B., and Dynlacht, B. D. (2000). Analysis of promoter binding by the E2F and pRB families in vivo: distinct E2F proteins mediate activation and repression, Genes Dev. *14*, 804-16.

Tan, P. B., Lackner, M. R., and Kim, S. K. (1998). MAP kinase signaling specificity mediated by the LIN-1 Ets/LIN-31 WH transcription factor complex during *C. elegans* vulval induction, Cell *93*, 569-80.

Taunton, J., Hassig, C. A., and Schreiber, S. L. (1996). A mammalian histone deacetylase related to the yeast transcriptional regulator Rpd3p, Science *272*, 408-11.

Thomas, J. H., and Horvitz, H. R. (1999). The *C. elegans* gene *lin-36* acts cell autonomously in the *lin-35* Rb pathway, Development *126*, 3449-59.

Tong, J. K., Hassig, C. A., Schnitzler, G. R., Kingston, R. E., and Schreiber, S. L. (1998). Chromatin deacetylation by an ATP-dependent nucleosome remodelling complex, Nature *395*, 917-21.

Torchia, J., Rose, D. W., Inostroza, J., Kamei, Y., Westin, S., Glass, C. K., and Rosenfeld, M. G. (1997). The transcriptional co-activator p/CIP binds CBP and mediates nuclear receptor function, Nature *387*, 677-84.

Trimarchi, J. M., Fairchild, B., Verona, R., Moberg, K., Andon, N., and Lees, J. A. (1998). E2F-6, a member of the E2F family that can behave as a transcriptional repressor, Proc. Natl. Acad. Sci. USA *95*, 2850-5.

Trimarchi, J. M., and Lees, J. A. (2002). Sibling rivalry in the E2F family, Nat. Rev. Mol. Cell Biol. *3*, 11-20.

Trouche, D., and Kouzarides, T. (1996). E2F1 and E1A(12S) have a homologous activation domain regulated by RB and CBP, Proc. Natl. Acad. Sci. USA *93*, 1439-42.

Tschiersch, B., Hofmann, A., Krauss, V., Dorn, R., Korge, G., and Reuter, G. (1994). The protein encoded by the *Drosophila* position-effect variegation suppressor gene *Su(var)3-9* combines domains of antagonistic regulators of homeotic gene complexes, Embo J. *13*, 3822-31.

Tse, C., and Hansen, J. C. (1997). Hybrid trypsinized nucleosomal arrays: identification of multiple functional roles of the H2A/H2B and H3/H4 N-termini in chromatin fiber compaction, Biochemistry *36*, 11381-8.

Turner, B. M. (2000). Histone acetylation and an epigenetic code, Bioessays *22*, 836-45.

Turner, B. M., Birley, A. J., and Lavender, J. (1992). Histone H4 isoforms acetylated at specific lysine residues define individual chromosomes and chromatin domains in *Drosophila* polytene nuclei, Cell *69*, 375-84.

Vandel, L., Nicolas, E., Vaute, O., Ferreira, R., Ait-Si-Ali, S., and Trouche, D. (2001). Transcriptional repression by the retinoblastoma protein through the recruitment of a histone methyltransferase, Mol. Cell. Biol. *21*, 6484-94.

Verona, R., Moberg, K., Estes, S., Starz, M., Vernon, J. P., and Lees, J. A. (1997). E2F activity is regulated by cell cycle-dependent changes in subcellular localization, Mol. Cell. Biol. *17*, 7268-82.

Versteege, I., Sevenet, N., Lange, J., Rousseau-Merck, M. F., Ambros, P., Handgretinger, R., Aurias, A., and Delattre, O. (1998). Truncating mutations of *hSNF5/INI1* in aggressive paediatric cancer, Nature *394*, 203-6.

Vidal, M., and Gaber, R. F. (1991). *RPD3* encodes a second factor required to achieve maximum positive and negative transcriptional states in *Saccharomyces cerevisiae*, Mol. Cell. Biol. *11*, 6317-27.

Vogelauer, M., Wu, J., Suka, N., and Grunstein, M. (2000). Global histone acetylation and deacetylation in yeast, Nature *408*, 495-8.

von Zelewsky, T., Palladino, F., Brunschwig, K., Tobler, H., Hajnal, A., and Muller, F. (2000). The *C. elegans* Mi-2 chromatin-remodelling proteins function in vulval cell fate determination, Development *127*, 5277-84.

Wang, B. B., Muller-Immergluck, M. M., Austin, J., Robinson, N. T., Chisholm, A., and Kenyon, C. (1993). A homeotic gene cluster patterns the anteroposterior body axis of *C. elegans*, Cell *74*, 29-42.

Wang, L., Liu, L., and Berger, S. L. (1998). Critical residues for histone acetylation by Gcn5, functioning in Ada and SAGA complexes, are also required for transcriptional function in vivo, Genes Dev. *12*, 640-53.

White-Cooper, H., Leroy, D., MacQueen, A., and Fuller, M. T. (2000). Transcription of meiotic cell cycle and terminal differentiation genes depends on a conserved chromatin associated protein, whose nuclear localisation is regulated, Development *127*, 5463-73.

Wolffe, A. (1998). Chromatin, 3rd edn. (San Diego, CA, Academic Press).

Wong, A. K., Shanahan, F., Chen, Y., Lian, L., Ha, P., Hendricks, K., Ghaffari, S., Iliev, D., Penn, B., Woodland, A. M., *et al.* (2000). BRG1, a component of the SWI-SNF complex, is mutated in multiple human tumor cell lines, Cancer Res. *60*, 6171-7.

Wu, L., Timmers, C., Maiti, B., Saavedra, H. I., Sang, L., Chong, G. T., Nuckolls, F., Giangrande, P., Wright, F. A., Field, S. J., *et al.* (2001). The E2F1-3 transcription factors are essential for cellular proliferation, Nature *414*, 457-62.

Wu, Y., and Han, M. (1994). Suppression of activated Let-60 ras protein defines a role of *Caenorhabditis elegans* Sur-1 MAP kinase in vulval differentiation, Genes Dev. *8*, 147-59.

Wu, Y., Han, M., and Guan, K. L. (1995). MEK-2, a *Caenorhabditis elegans* MAP kinase kinase, functions in Ras-mediated vulval induction and other developmental events, Genes Dev. *9*, 742-55.

Xue, Y., Wong, J., Moreno, G. T., Young, M. K., Cote, J., and Wang, W. (1998). NURD, a novel complex with both ATP-dependent chromatin remodeling and histone deacetylase activities, Mol. Cell *2*, 851-61.

Yudkovsky, N., Logie, C., Hahn, S., and Peterson, C. L. (1999). Recruitment of the SWI/SNF chromatin remodeling complex by transcriptional activators, Genes Dev. *13*, 2369-74.

Zhang, H. S., and Dean, D. C. (2001). Rb-mediated chromatin structure regulation and transcriptional repression, Oncogene *20*, 3134-8.

Zhang, H. S., Gavin, M., Dahiya, A., Postigo, A. A., Ma, D., Luo, R. X., Harbour, J. W., and Dean, D. C. (2000). Exit from G1 and S phase of the cell cycle is regulated by repressor complexes containing HDAC-Rb-hSWI/SNF and Rb-hSWI/SNF, Cell *101*, 79-89.

Zhang, Y., LeRoy, G., Seelig, H. P., Lane, W. S., and Reinberg, D. (1998). The dermatomyositis-specific autoantigen Mi2 is a component of a complex containing histone deacetylase and nucleosome remodeling activities, Cell *95*, 279-89.

TABLE

Table 1. Chromatin remodeling proteins

A) ATP-dependent chromatin remodeling enzymes

Classes
SWI2/SNF2
ISWI
Mi-2

B) Chromatin modifying enzymes

- Histone acetyltransferases (HATs)

Classes
GNAT
MYST
CBP/p300

- Histone deacetylases (HDACs)

Classes
Class I
Class II
Sirtuin

- Histone methyltransferases (HMTs)

Classes
Lysine HMTs
Arginine HMTs

Major classes of ATP-dependent chromatin remodeling enzymes and chromatin modifying enzymes are shown. Details of individual proteins are described in the text.

FIGURE

Figure 1. Pn.p cell fates are specified in two sequential steps
A) During the L1 stage, more anterior and posterior Pn.p cells (open circles) fuse with the hypodermis and terminally differentiate. Cells in the midbody (colored circles), remain unfused and are competent to make vulval tissue in the subsequent vulval cell fate determination step. P3.p is depicted as half-colored because this cell occasionally fuses with the syncytial hypodermis during the L1 stage. P12.p (checkered circle) remains unfused, producing one daughter that undergoes programmed cell death and another daughter that becomes a hypodermal cell.
B) During the L2 and early L3 stages, a signal from the gonadal anchor cell induces vulval cell fates. Although P(3-8).p are competent to adopt vulval cell fates, only P(5-7).p do so in wild type animals. The lineages associated with vulval cell fates in P(5-7).p and non-vulval cell fates in P3.p, P4.p and P8.p are shown.

Figure 1

A) Pn.p cell fusions

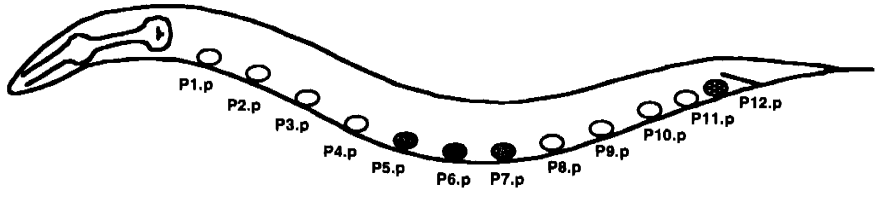

B) P(3-8).p cell lineages

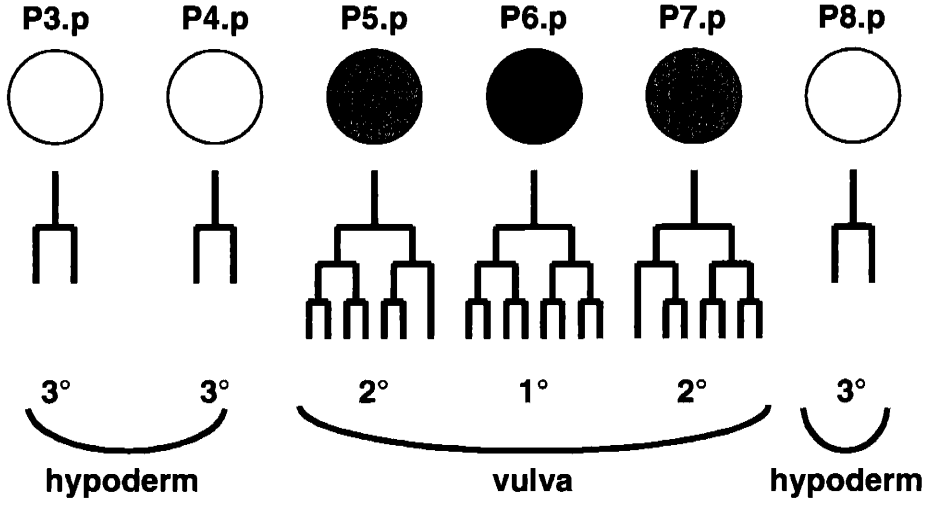

CHAPTER 2

New Genes that Interact with *lin-35 Rb* to Negatively Regulate the *let-60 ras* Pathway in *Caenorhabditis elegans*

JEFFREY H. THOMAS[1], CRAIG J. CEOL, HILLEL T. SCHWARTZ and H. ROBERT HORVITZ

This chapter has been submitted for publication. Jeff Thomas isolated all of the mutations described herein and performed much of their genetic characterization. Stemming from unrelated work, Hillel Schwartz made the initial observation that *n770* and allelic mutations affected the *lin-13* gene. I performed complementation tests and three-factor mapping experiments to confirm this observation and determined the sequences of these mutations, as described in Table 2. Through genetic mapping and complementation testing I also determined that *n2987* is a *lin-15B* allele.

[1]Current address: Department of Molecular Biology, Princeton University, Princeton, New Jersey 08544

ABSTRACT

Previous studies have shown that a synthetic multivulva phenotype results from mutations in genes that antagonize the *ras*-mediated intercellular signaling system responsible for vulval induction in *Caenorhabditis elegans*. Synthetic multivulva mutations define two classes of genes, A and B, and a mutation in a gene of each class is required to produce the multivulva phenotype. The ectopic vulval tissue in multivulva animals is generated by vulval precursor cells that in the wild type do not generate vulval tissue. One of the class B synthetic multivulva genes, *lin-35*, encodes a protein similar to the retinoblastoma (Rb) protein. In this paper, we describe the isolation and characterization of 49 synthetic multivulva mutations and the identification of new components of both the class A and class B *lin-35 Rb* pathway.

INTRODUCTION

A receptor tyrosine kinase (RTK) and Ras-mediated signal transduction pathway induces vulval cell fates during the development of the vulva of the *Caenorhabditis elegans* hermaphrodite (AROIAN *et al.* 1990; BEITEL *et al.* 1990; HAN and STERNBERG 1990). Little is known about how the activities of such pathways can be negatively regulated. The synthetic multivulva (synMuv) genes act as negative regulators of vulval development (HORVITZ and SULSTON 1980; SULSTON and HORVITZ 1981; FERGUSON and HORVITZ 1985, 1989). One of the synMuv genes, *lin-35,* is a member of the Rb gene family, one member of this family, Rb, acts as tumor suppressor gene in mammals; another synMuv gene, *lin-53,* shows similarity to RbAp48, an Rb-binding protein (LU and HORVITZ 1998). Thus, the synMuv genes provide an opportunity to analyze genetically a pathway containing an Rb-like gene, to define additional components of this pathway, and to elucidate the mechanism by which an Rb-like protein antagonizes a process stimulated by a Ras protein.

The hermaphrodite vulva of *C. elegans* is formed from the descendants of three hypodermal blast cells, P5.p, P6.p and P7.p (SULSTON and HORVITZ 1977). These cells are members of the vulval equivalence group, P(3-8).p, a set of six cells with the potential to adopt either of two vulval fates (1° or 2°) or a nonvulval fate (3°) (SULSTON and WHITE 1980; KIMBLE 1981; STERNBERG and HORVITZ 1986). These cell fates are specified by cell interactions. The gonadal anchor cell induces the nearest P(3-8).p cells to adopt vulval fates. (KIMBLE 1981; STERNBERG and HORVITZ 1986; THOMAS *et al.* 1990). Another signal, apparently from the nearby hypodermal syncytium, hyp7, acts to inhibit the adoption of vulval fates (HERMAN and HEDGECOCK 1990). It is likely that the anchor cell signal overrides this inhibitory signal to induce the cells nearest to the anchor cell to adopt vulval fates.

Genetic analysis of vulval development has led to the identification and characterization of numerous genes involved in different aspects of this process (for reviews, see HORVITZ and STERNBERG 1991; KORNFELD 1997; STERNBERG and HAN 1998). Reduction-of-function mutations in genes encoding signaling proteins reduce the output of the anchor cell signaling pathway and result in a vulvaless (Vul) phenotype in which the vulva is not formed. By contrast, some mutations result in a multivulva (Muv) phenotype in which ectopic vulva tissue is produced. The Muv phenotype of certain mutant strains results from the interaction of two different

mutations (HORVITZ and SULSTON 1980; SULSTON and HORVITZ 1981; FERGUSON and HORVITZ 1985, 1989). The mutations that interact to produce such a synthetic multivulva (synMuv) phenotype fall into two classes, A and B. Animals carrying both a class A and a class B mutation have a Muv phenotype. Animals that carry mutations in a single class have a wild-type vulval phenotype. FERGUSON and HORVITZ (1989) proposed that the synMuv genes encode the components of two functionally redundant pathways that negatively regulate vulval development.

Systematic mutagenesis of strains carrying either the class A mutation *lin-8(n111)* or the class B mutation *lin-9(n112)* as well as the mutagenesis of another strain carrying a previously undetected class A synMuv mutation allowed the identification of additional class A and class B mutations (FERGUSON and HORVITZ 1989). Both class A and class B alleles, as well as class AB alleles (which are Muv as a consequence of a single mutation), were identified for a locus named *lin-15*, indicating that *lin-15* is a complex locus with distinct class A and class B functions (FERGUSON and HORVITZ 1985; 1989). Molecular analyses of *lin-15* revealed that it consists of two adjacent genes that encode two nonoverlapping transcripts to control the A and B functions; the class AB alleles affect both genes (CLARK *et al.* 1994; HUANG *et al.* 1994). These genetic analyses resulted in the identification and characterization of three class A genes (*lin-8*, *lin-38* and *lin-15*A) and five class B genes (*lin-9*, *lin-35*, *lin-36*, *lin-37* and *lin-15*B). Three additional class B mutations (*n770*, *n771*, *n833*) were identified, but were neither further characterized nor given gene names (FERGUSON and HORVITZ 1989).

SynMuv mutants in which the anchor cell has been ablated nonetheless still display a Muv phenotype (FERGUSON *et al.* 1987). This result suggests that in the absence of synMuv gene activity, the P(3-8).p cells do not require the anchor cell signal to adopt vulval cell fates. However, reduction-of-function mutations in genes known to be involved in inductive signal transduction, *let-23 rtk*, *sem-5*, *let-60 ras*, and *lin-45 raf*, are epistatic to synMuv mutations (FERGUSON *et al.* 1987; BEITEL *et al.* 1990; HAN *et al.* 1990, CLARK *et al.* 1992; HAN *et al.* 1993; HUANG *et al.* 1994; LU and HORVITZ 1998; THOMAS and HORVITZ 1999). Thus, the activity of the RTK signal transduction cascade, but not the anchor cell-derived RTK ligand itself, is required for the adoption of vulval cell fates by P(3-8).p cells in the absence of inhibitory synMuv gene activity. Genetic mosaic analyses indicate that both *lin-15*AB and *lin-37* act non-cell autonomously and most likely in hyp7 (HERMAN and HEDGECOCK 1990;

HEDGECOCK and HERMAN 1995) while *lin-36* likely acts cell autonomously in the Pn.p cells (THOMAS and HORVITZ 1999). These observations led to the suggestion that the synMuv genes encode the components of two signaling systems by which hyp7 prevents P(3-8).p cells from adopting vulval fates. When both redundant signaling systems are disabled, P(3-8).p cells adopt vulval fates and produce a Muv phenotype.

The molecular natures of several synMuv genes have been determined. Two class B genes, *lin-15*B and *lin-36*, and one class A gene, *lin-15*A, have been cloned and shown to encode novel proteins (CLARK *et al.* 1994; HUANG *et al.* 1994; THOMAS and HORVITZ 1999). The class B gene *lin-9* encodes a protein with sequence similarity to the *Drosophila* Aly protein, which regulates the meiotic cell cycle and spermatogenesis (BEITEL *et al.* 2000; WHITE-COOPER *et al.* 2000). The class B gene *lin-35* encodes a protein with sequence similarity to the Rb protein, and the class B gene *lin-53* encodes a protein with sequence similarity to RbAp48, an Rb-binding protein (LU and HORVITZ 1998). The class B gene *dpl-1*, the discovery of which is described in this manuscript, encodes a protein similar to DP, an Rb-regulated transcription factor that regulates the G1-to-S phase transition of the cell cycle. The class B gene *efl-1* encodes a protein similar to E2F, a component of the DP/E2F heterodimeric transcription factor (CEOL and HORVITZ 2001). Another gene with class B activity, *tam-1*, encodes a RING finger and B-box protein involved in modulating gene expression (HSIEH *et al.* 1999). *lin-13*, a gene which has class B and possibly also class A synMuv activity, encodes a protein with an Rb binding motif (MELÉNDEZ and GREENWALD 2000). Genetic analysis of *let-418/chd-4*, which encodes a chromodomain helicase protein, indicates that it is a class B synMuv gene (VON ZELEWSKY *et al.* 2000). RNAi experiments suggest that *hda-1* and *hpl-2*, which encode a protein similar to class I histone deacetylases and a protein similar to heterochromatin protein 1, respectively, may have some synMuv activity (LU and HORVITZ 1998; COUTEAU *et al.* 2002). DUFOURCQ *et al.* (2002) reported that *hda-1/gon-10(e1795)* does not have class B synMuv activity but other results using stronger class A synMuv mutations suggest that *hda-1/gon-10(e1795)* does have class B synMuv activity (C. J. CEOL, E. C. ANDERSEN and H. R. HORVITZ, unpublished results). Many of these genes are known as components of a nucleosome remodeling and histone deacetylase (NuRD) complex (LU and HORVITZ 1998; VON ZELEWSKY *et al.* 2000). Some of the class B synMuv genes are involved in the promotion of early larval P3.p fusion and G1-to-S phase progression of the cell cycle (CHEN and HAN 2001; BOXEM and VAN DEN HEUVEL 2002).

In this paper, we identify and characterize 49 new synMuv mutations. Some of these mutations define new class A and new class B loci.

MATERIALS AND METHODS

Strains and general techniques: *Caenorhabditis elegans* var. Bristol strain N2 was the wild-type strain and parent of all mutants used in this study. Mutations were described by HODGKIN *et al.* (1988) unless otherwise noted.

LGI: *bli-3(e767)*; *sup-11(n403)*; *dpy-5(e61)*; *lin-35(n745)*; *unc-29(e1072)*; *dpy-14(e188)*; *unc-13(e1091)*; *lin-11(n566)*; *unc-75(e950)*; *unc-101(m1)*; *unc-54(e1092)* (WATERSTON *et al.* 1980).

LGII: *lin-8(n111)*; *lin-31(n301)*; *unc-85(e1414)*; *bli-2(e768)*; *dpy-10(e128)*; *rol-6(e187)*; *let-23(n1045, mn23, mn216)* (HERMAN 1978; SIGURDSON *et al.* 1984; FERGUSON and HORVITZ 1985); *let-240(mn209)*; *unc-4(e120)*; *unc-53(e569)*; *rol-1(e91)*; *lin-38(n751)*; *unc-52(e444)*; *mnDf67* (SIGURDSON *et al.* 1984); *mnDf85* (SIGURDSON *et al.* 1984); *mnDf46* (SIGURDSON *et al.* 1984); *mnC1 dpy-10(e128) unc-52(e444)*.

LGIII: *dpy-1(e1)*; *unc-93(e1500)*; *dpy-27(y57)* (PLENEFISCH *et al.* 1989); *unc-79(e1068)*; *dpy-17(e164)*; *lon-1(e185)*; *sma-3(e491)*; *lin-37(n758)*; *egl-5(n945)*; *lin-36(n766)*; *unc-36(e251)*; *dpy-19(e1259)*; *lin-9(n112)*; *unc-32(e189)*; *unc-16(e109)*; *unc-69(e587)*; *unc-25(e156)*; *unc-49(e382)*; *dpy-18(e364)*; *qC1* (AUSTIN and KIMBLE 1989; GRAHAM and KIMBLE 1993).

LGIV: *dpy-9(e12)*; *egl-18(n162)*; *lin-1(e1275)*; *unc-17(e245)*; *unc-5(e53)*; *dpy-20(e1282)*; *unc-22(e66)*; *unc-30(e191)*; *lev-1(x22)*; *ced-3(n717)*; *unc-26(e205)*; *dpy-4(e1166)*.

LGV: *unc-34(e566)*; *dpy-11(e224)*; *unc-51(e369)*.

LGX: *lon-2(e678)*; *unc-3(e151)*; *lin-15(n433, n744, n765, n767)* (FERGUSON and HORVITZ 1989).

Methods for the culture and genetic manipulation of *C. elegans* have been described by BRENNER (1974). Genetic nomenclature was described by HORVITZ *et al.* (1979). Nomenclature used for synMuv strains is as used by FERGUSON and HORVITZ (1989).

Mutagenesis of class A and class B mutants: Screens for new synMuv strains were conducted essentially as described by FERGUSON and HORVITZ (1989) using EMS as a mutagen, according to BRENNER (1974). Only one Muv strain was selected from each group of mutagenized P_0 hermaphrodites for subsequent analysis to ensure each mutation was independently derived. N2 males were crossed with the Muv

strains, and the F_2 progeny were scored for the Muv phenotype. The segregation of 1/16 or fewer Muv F_2 progeny indicated candidate synMuv strains. In no case did the Muv phenotype of a strain in which the original mutation was autosomal result from a synthetic interaction with a second mutation on the same linkage group, based upon either of two criteria: (1) failure of the new Muv mutation to complement a known Muv mutation, or (2) failure of the Muv phenotype to show linkage to the chromosome containing the parental mutation. In mutagenesis experiments in which the original mutation was a *lin-15* allele, strains that segregated 1/4 or fewer Muv F_2 progeny were also retained for further analysis since new *lin-15* mutations would be tightly linked to the parental mutation. All candidate synMuv strains were backcrossed to their strain of origin two to five times.

To isolate class B mutations, a *lin-8(n111)* homozygous strain and a *lin-15(n433)* homozygous strain were mutagenized. FERGUSON and HORVITZ (1989) previously mutagenized *lin-8(n111)* and *lin-15(n767)* animals to isolate class B mutations. After the mutagenesis of *lin-8(n111)* animals, we screened approximately 6,000 haploid genomes and isolated 15 synMuv strains. After the mutagenesis of *lin-15(n433)* animals, we screened approximately 10,000 haploid genomes and isolated 15 synMuv strains. To isolate class A mutations, a *lin-36(n766)* homozygous strain and a *lin-15(n744)* homozygous strain were mutagenized. FERGUSON and HORVITZ (1989) previously mutagenized *lin-9(n112)* animals to isolate class A mutations. After the mutagenesis of *lin-36(n766)* animals, we screened approximately 10,000 haploid genomes and isolated five synMuv strains. After the mutagenesis of *lin-15(n744)* animals, we screened approximately 13,000 haploid genomes and isolated 14 synMuv strains.

Molecular analysis of *lin-15*AB lesions: Genomic DNA was purified, essentially using standard methods, from *lin-15*AB strains isolated after the mutageneses of *lin-15(n744)* and *lin-15(n433)* animals (SULSTON and HODGKIN 1988). DNA was digested by *Eco*RI, separated by agarose gel electrophoresis, and probed with ^{32}P-labeled *lin-15* plasmid DNA (SAMBROOK *et al.* 1989; CLARK *et al.* 1994). Some samples of genomic DNA that showed a lesion were digested with *Eco*RI and either *Eag*I, *Sac*I, *Msc*I, *Bgl*I, *Mlu*I or *Nru*I, and probed with ^{32}P-labeled *lin-15* plasmid DNA.

Molecular analysis of *lin-13* lesions: N2 and *lin-13* strains were lysed and the *lin-13* coding regions and adjacent noncoding regions were amplified using the polymerase chain reaction (PCR). The sequences of the PCR products were

determined using an automated ABI 373A cycle sequencer (Applied Biosystems, Foster City, CA).

Nomarski observation and P(3-8).p cell lineage analysis of *lin-54* animals: P(3-8).p cells and their descendants in *lin-8(n111); lin-54(n2231)* animals were observed using Nomarski optics at different times during vulval development as described by SULSTON and HORVITZ (1977). The nomenclature and criteria of STERNBERG and HORVITZ (1986, 1989) were used to describe and assign 1°, 2° and 3° cell fates.

Construction of strains homozygous for newly isolated synMuv mutations: Strains carrying a single homozygous synMuv mutation were constructed and their genotypes confirmed essentially as described by FERGUSON and HORVITZ (1989). In these experiments, *unc-79 dpy-27* balanced *lin-13(n770)*, *unc-69* balanced *lin-52(n771)*, *unc-29* balanced *lin-53(n833)*, *unc-22 ced-3 unc-26* balanced *lin-54(n2231)*, and *rol-6 unc-4* balanced both *dpl-1(n2994)* and *lin-56(n2728)*.

Construction of unlinked synMuv double mutants: Class A; class A or class B; class B double mutants carrying a new mutation and a *lin-15* mutation of the same class were constructed essentially as described by FERGUSON and HORVITZ (1989). Class B; class B double mutants carrying a new mutation and an autosomal mutation of the same class were also constructed essentially as described by FERGUSON and HORVITZ (1989). To ensure that mutations were not lost by recombination, several independent lines were isolated for each strain.

In these constructions, *lin-15(n767)* and *lin-15(n744)* were used as the class A and class B *lin-15* alleles, respectively. The autosomal class B mutation used was *lin-36(n766)*. This allele was marked in *cis* by *unc-32*. The following markers were linked in *cis* to the new mutations: *unc-32* to *lin-13(n770)*, *unc-32* to *lin-52(n771)*, *dpy-5* to *lin-53(n833)*, *dpy-20* to *lin-54(n2231)*, *rol-6* to *dpl-1(n2994)*, and *rol-6* to *lin-56(n2728)*.

Construction of linked synMuv double mutants: To construct a class B class B double between *lin-13(n770)* and *lin-36,* hermaphrodites of genotype *lin-13 + + unc-32/+ egl-5 lin-36 +; lin-15*A were generated. The frequency of recombination between *lin-13* and *egl-5* is greater than that between *lin-36* and *unc-32* and much greater than that between *egl-5* and *lin-36*. Muv non-Unc non-Egl recombinant progeny were isolated; from these animals, Egl Muv progeny were selected and the *lin-15*A mutation crossed out, yielding animals of putative homozygous genotype *lin-13 egl-5 lin-36*. This genotype was confirmed by crossing with another class A mutation and performing

complementation tests with *lin-13* and with *lin-36* to show that the strain contained both class B mutations.

A class B class B double between *lin-36* and *lin-52(n771)* was constructed in a manner similar to that for the construction of the double between *lin-13* and *lin-36*. Hermaphrodites of genotype *+ lin-36 unc-36 +/sma-3 + + lin-52; lin-15*A were generated. The frequency of recombination between *unc-36* and *lin-52* is greater than that between *sma-3* and *lin-36* and much greater than that between *lin-36* and *unc-36*. Muv non-Sma recombinant progeny were isolated and used to generate Unc Muv progeny of putative genotype *lin-36 unc-36 lin-52; lin-15*A. *lin-15*A was removed to generate animals of homozygous genotype *lin-36 unc-36 lin-52*. This genotype was confirmed by crossing with another class A mutation and performing complementation tests with *lin-52* and with *lin-36* to show that the strain contained both class B mutations.

To construct a class A class A double between *lin-8* and *lin-56(n2728)*, animals of genotype *lin-8 unc-85 dpy-10 + +/+ + + rol-6 lin-56; lin-15*B/+ were constructed. From these animals, Unc non-Dpy non-Muv recombinant animals that did not segregate Muv progeny were isolated; these animals segregated Rol Unc animals of putative genotype *lin-8 unc-85 rol-6 lin-56*. This genotype was confirmed by conducting complementation tests, in the presence of a class B mutation, with *lin-8* and *lin-56* to show that the strain was homozygous for both class A mutations.

RESULTS

Isolation of new synMuv strains: To identify new class A mutations, we used EMS to mutagenize class B *lin-36(n766)* or class B *lin-15(n744)* homozygotes, which display wild-type vulval development. The vulval morphology of synMuv strains can be readily distinguished from that of Muv strains mutant in *lin-1* or *lin-31*. SynMuv animals usually have a vulva with wild-type morphology and have a few regularly spaced pseudovulvae. By contrast, *lin-1* animals frequently have abnormal and distinctively protruding vulvae, and *lin-31* animals are often egg-laying defective, have incomplete vulvae and have a variable number of small pseudovulval protrusions that are distinctive in number and morphology. A Muv phenotype that segregated as 1/16 or less in the F_2 generation after crossing with wild-type males was considered a candidate for being synMuv, as was a strain obtained in a *lin-15* background that segregated either as 1/16 or 1/4 because new *lin-15* mutations would be linked to the parental *lin-15* mutation. We obtained five synMuv strains from the mutagenesis of *lin-36(n766)* animals and 14 synMuv strains from the mutagenesis of *lin-15(n744)* animals. A total of 19 new class A mutations were identified in these screens (Table 1).

To identify new class B mutations, we used EMS to mutagenize animals homozygous for the class A mutations *lin-8(n111)* or *lin-15(n433)*. Muv strains were tested to determine if their phenotypes depended upon two unlinked loci as described for the isolation of class A mutations. We obtained 15 synMuv strains from the mutagenesis of *lin-8(n111)* animals and 15 synMuv strains from the mutagenesis of *lin-15(n433)* animals. A total of 30 new class B mutations were identified (Table 1).

Linkage and complementation: SynMuv mutations already shown to segregate as two unlinked loci were expected to display linkage to two loci: the parental locus and the new locus (FERGUSON and HORVITZ 1989). Mutations caused by most of the candidate synMuv strains displayed linkage to the parental locus and to another linkage group. A few *lin-15* strains, discussed below, did not display linkage to a new location (Table 1).

Newly isolated synMuv mutations were tested for complementation with alleles of the then known synMuv genes: *lin-8*, *lin-9*, *lin-15*A, *lin-15*B, *lin-35*, *lin-36*, *lin-37*, *lin-38* and *lin(n770)*, *lin(n771)*, and *lin(n833)*, three previously identified but not extensively characterized synMuv mutations (FERGUSON and HORVITZ 1989). Mutations that complemented all known synMuv complementation groups were tested against each

other after strains carrying identical parental mutations of the opposite class were constructed.

Mutations were assigned to the same complementation group only if hermaphrodites of genotype *a; b1/b2*, where *a* is the background mutation required for the synthetic interaction and *b1* and *b2* are the two mutations being tested, were Muv and segregated only Muv progeny. As described by FERGUSON and HORVITZ (1989), this approach was necessary to distinguish intragenic noncomplementation from the intergenic noncomplementation observed in some doubly heterozygous synMuv strains. Several combinations of genotype *a; b1/+; b2/+* displayed intergenic noncomplementation; in most cases, the penetrance and expressivity of the Muv phenotype produced by intergenic noncomplementation was lower than that produced by homozygosity at either of the two loci that displayed intergenic noncomplementation. Thus, animals lacking the activity of a synMuv gene of one class and having reduced doses of two genes of the other class as well as no maternal activity from one of these genes were occasionally Muv. This observation suggests that the synMuv genes are dose-sensitive. *lin-53(n833)* (see below) was notable in that it showed very strong intergenic noncomplementation with other class B mutations, consistent with the observation that this mutation causes dominant-negative activity (LU and HORVITZ 1998).

A total of 38 mutations failed to complement alleles of known synMuv genes. These mutations included eight *lin-8* alleles, eight *lin-15*A alleles, 10 *lin-15*B alleles, six *lin-35* alleles, three *lin-36* alleles, one *lin-37* allele, and two *lin-38* alleles. Another six mutations failed to complement *n770* or *n833*, mutations that had previously been isolated but not extensively characterized. The mutations that defined the *n770* complementation group failed to complement *lin-13* for class B activity. We named the other gene, defined by *n833*, *lin-53*. Our new mutations included five *lin-13* class B alleles and one *lin-53* allele. Another four mutations defined three new complementation groups, which we named *lin-54*, *dpl-1*, and *lin-56*. (The name *dpl-1* was assigned after studies by CEOL and HORVITZ (2001) showed the DPL-1 protein to be similar to mammalian DP.) There were two *lin-54* alleles, one *dpl-1* allele, and one *lin-56* allele (Table 1). We obtained no new alleles of *lin-9* nor any alleles that failed to complement *n771*, another mutation that had been previously isolated, but not extensively characterized. We named this gene *lin-52*.

Identification of *lin-15*AB double mutants: The mutations of several Muv strains isolated in a *lin-15*A or *lin-15*B background did not segregate as two loci yet displayed a Muv phenotype similar to that of synMuv strains. These strains included five isolated in a *lin-15(n433)* background and seven isolated in a *lin-15(n744)* background. These strains showed linkage to only *unc-3 X*, which marked the parental *lin-15* mutation, and failed to complement *lin-15(n765)*, a *lin-15* allele defective in both class A and class B activities. Thus, the new strains are defective in both *lin-15*A and *lin-15*B activities and they carry new *lin-15* alleles.

Six of seven *lin-15* Muv mutants that have been isolated as single mutants and analyzed, all but *lin-15(n765)*, have gross mutations that disrupt both *lin-15* mRNAs (CLARK *et al.* 1994; HUANG *et al.* 1994). *lin-15(n765)* is a deletion in the class B gene and presumably also has a point mutation in the class A gene. Several *lin-15*A and *lin-15*B mutations have been analyzed molecularly; each specifically affects only one of the two genes (CLARK *et al.* 1994).

To determine whether the Muv phenotype of each of the *lin-15*AB mutants isolated in these screens is the result of the newly induced mutation alone or rather the result of an interaction between the newly induced mutation and the parental mutation, we used Southern hybridization to analyze the *lin-15* locus in these strains. Four of the 12 mutant strains showed polymorphisms, three of which were confined to only the A or only the B region. Specifically, the *lin-15(n2993 n433)* strain has a loss of an *Eco*RI site in the B region of *lin-15*, the *lin-15(n744 n2733)* strain has a small deletion of 0.3 kb in the A region, and the *lin-15(n744 n2735)* strain has a larger deletion of several kilobases in the A region.

By contrast, the *lin-15(n744 n2726)* strain has a deletion of about 0.9 kb in an *Eco*RI-*Sac*I restriction fragment containing both A and B sequences. This region includes both the start of the class A mRNA and the end of the class B mRNA. The deletion probably eliminates the 5' end of the class A mRNA, and may eliminate some of the 3' end of the class B mRNA. This deletion may be sufficient to cause a class B defect, and the Muv phenotype of this strain may result entirely from the new mutation, *n2726*.

Polymorphisms were not detected in the other *lin-15* strains. Since the parental mutation of these strains is either a *lin-15*A or a *lin-15*B point mutation, and EMS produces predominantly point mutations (ANDERSON 1995), it is likely that the Muv

phenotype of most if not all of these *lin-15*AB strains is the result of a synthetic interaction between *lin-15* class A and class B point mutations.

Identification of *lin-13* mutations: Five newly identified putative class B mutations and *lin(n770)* failed to complement *lin-13(n387)* in a class A mutant background. *lin-13(n387)*, which causes a sterile Muv phenotype at 25°, had been shown to behave as a class B synMuv at 15° (FERGUSON and HORVITZ 1989). No class A mutations in *lin-13* were isolated.

Unlike *lin-15*, which encodes two nonoverlapping transcripts, *lin-13* encodes a single transcript encoding a nuclear protein predicted to contain 24 C2-H2 zinc fingers, one C4 zinc finger and an LXCXE potential Rb-binding motif (MELÉNDEZ and GREENWALD 2000). Sterile Muv mutations of *lin-13*, *n387* and *n388*, have been shown to be nonsense mutations at residues S524 and R857, respectively. The mutant gene products are predicted to be truncated proteins with either two or five complete zinc fingers (MELÉNDEZ and GREENWALD 2000). To determine the molecular natures of the *lin-13* mutations we isolated, we used PCR to amplify DNA from the mutants and determined the sequence changes in these strains. Three mutants carry *lin-13* nonsense mutations: *lin-13(n770)*, *lin-13(n2238)* and *lin-13(n2985)* (Table 2). These alleles are all predicted to encode truncated proteins, albeit ones longer than those generated by *lin-13(n387)* and *lin-13(n388)*. It is notable that the *lin-13(n2238)* predicted protein product of 995 amino acids is only slightly longer than the *lin-13(n388)* predicted protein product of 856 amino acids and has only one additional undisrupted zinc finger domain. Three other mutants carry *lin-13* missense mutations. *lin-13(n2988)* and *lin-13(n2981)* each encode a cysteine-to-tryptophan change in the first cysteine of the first and fifth zinc fingers, respectively (Table 2). The first zinc finger may play a more important role than the fifth zinc finger, since *lin-13(n2988)* is notably stronger at low temperature than is *lin-13(n2981)* (Table 1). The remaining missense mutation, *lin-13(n2984)*, encodes a glycine-to-glutamic acid change in the residue immediately preceding the first cysteine of the first zinc finger (Table 2). The bulky negatively charged mutant residue may partially interfere with the ability of the first cysteine to act in the coordination of zinc. Consistent with this hypothesis, the phenotype of *lin-13(n2984)* is weaker than that of *lin-13(n2988)* at lower temperatures (Table 1).

Phenotypes of newly isolated synMuv strains: Many of the newly isolated synMuv strains displayed a temperature-sensitive effect on vulval development such

that the penetrance of the Muv defect increased at higher temperatures (Table 1). Similar observations were made by FERGUSON and HORVITZ (1989). The synMuv strains also often showed temperature-sensitive growth characteristics. Many strains showed a reduced growth rate or, in some cases, lethality at 25° (Table 1). Similar observations also were made by FERGUSON and HORVITZ (1989). Although there were some differences among strains in growth at 20°, the differences were much greater at 15° and 25°. Rare synMuv animals displayed a protruding excretory pore. Some animals ruptured at the vulva or, rarely, at a pseudovulval protrusion, as adults. Strains isolated in the screen in which *lin-15(n744)* was used as the parental mutation had a fairly high percentage of rupture, often exceeding 50% of adults (data not shown).

Strains carrying *lin-54* mutations differed from other synMuv strains in that a greater proportion of these animals had a ventral protrusion that was further posterior to the vulva than was the case for most synMuv mutants. Also, a number of these strains had two ventral protrusions posterior to the vulva, a rare occurrence for other synMuv strains. This phenomenon was observed with both alleles of *lin-54*. Among *lin-8(n111); lin-54(n2231)* animals, 13% had a relatively far posterior ventral protrusion, and 11% had two posterior ventral protrusions (n=126). Among *lin-54(n2231); lin-15(n767)* animals, 26% had a ventral protrusion further posterior than ususal, and 19% had two ventral protrusions (n=75). Among *lin-54(n2990); lin-15(n433)* animals, 13% had a ventral protrusion further posterior than usual, and 10% had two ventral protrusions (n=112).

To determine the origin of these unusually far posterior pseudovulvae and two posterior pseudovulvae in *lin-54* animals, we used Nomarski optics to observe the P(3-8).p cells and their descendants in *lin-8(n111); lin-54(n2231)* animals. Our observations established that, as in the wild type, in these animals there are only six potential vulval precursor cells: P(3-8).p divided to give 1°, 2° and 3° cell fates, as in the wild type, and other Pn.p cells, such as P9.p, which lies posterior to P8.p, were not transformed into potential vulva precursor cells (as seen in "superMuv" mutants, which have extra pseudovulval protrusions in a *lin-15* background; CLARK 1992). Cell lineage analysis revealed that in *lin-8; lin-54* animals, the functional vulva sometimes formed from P(4-6).p rather than from P(5-7).p (data not shown). In these cases, the P5.p nucleus did not lie directly beneath the anchor cell nucleus; instead, the P5.p and P6.p nuclei were located to either side of and below the anchor cell nucleus (data not shown). This phenomenon has been observed in other synMuv strains, but is rare (FERGUSON *et al.*

1987, THOMAS and HORVITZ 1999). In animals in which the functional vulva was formed from the descendants of P(4-6).p, P7.p and P8.p and their descendants were posterior to the developing vulva. These cells adopted vulval fates in the mutant animals and formed either two posterior pseudovulvae or one posterior pseudovulva at a greater relative distance from the misplaced vulva than a pseudovulva formed from only P8.p relative to a properly positioned functional vulva. In one case, the vulva was observed to derive from the descendants of P5.p, P6.p and part of P7.p. The descendants of P7.p were spread over a greater distance than usual; some joined a number of P8.p descendants to form a pseudovulva, while other P8.p descendants formed a second posterior pseudovulva. Thus, the P(3-8).p cells and the anchor cell seem to be occasionally displaced relative to each other in *lin-54* animals. In some animals in which the anchor cell was located over P6.p, the descendants of P7.p and P8.p were spread over a wider distance than in the wild type. These data suggest that the posterior members of the vulval equivalence group are displaced posteriorly in a significant number of *lin-54* animals.

New synMuv genes: We mapped the six new synMuv genes, *lin-13*, *lin-52*, *lin-53*, *lin-54*, *dpl-1* (all class B) and *lin-56* (class A), using multi-factor crosses and deficiencies (Table 3; Figure 1).

dpl-1 mapped to the same linkage group II deficiency interval as *let-23*, which encodes a receptor tyrosine kinase involved in inductive vulval signaling (FERGUSON and HORVITZ 1987; AROIAN *et al.* 1990). To determine if *dpl-1(n2994)* is allelic to *let-23*, we performed complementation tests against *let-23(mn23)*, *let-23(mn216)* and *let-23(n1045).* These *let-23* alleles were chosen because *mn23* and *mn216* represent putative null alleles, and *n1045* is a viable reduction-of-function allele that causes both a Vul and a hyperinduced phenotype (Hin; P(3-8).p cells immediately adjacent to the developing vulva often adopt vulval fates, producing an abnormal vulva with adjacent Muv-like protrusions; FERGUSON and HORVITZ 1985; AROIAN and STERNBERG 1991). *dpl-1(n2994)* complemented *let-23* for all phenotypes: synMuv, Vul, Hin, and lethal (Let). The allele used in these tests, *dpl-1(n2994)*, is predicted to fail to complement a loss-of-function allele for the synMuv phenotype, since *dpl-1(n2994)/mnDf67; lin-15*A animals are Muv (Table 3).

The newly identified class B synMuv gene *dpl-1* was represented by only one mutant allele. To test whether the phenotype produced by this allele is weaker than that expected from a null phenotype, this mutation was tested in *trans* to a deficiency (Table

3). Animals of genotype *dpl-1(n2994)/mnDf67; lin-15(n433)* had a Muv phenotype and an incidence of sterility similar to those of animals of genotype *dpl-1(n2994); lin-15(n433)* when both were progeny of a mother of genotype *dpl-1(n2994)/mnDf67; lin-15(n433)*. However, the fertile animals of genotype *dpl-1(n2994)/mnDf67; lin-15(n433)* had a much greater incidence of maternal-effect lethality than did animals of genotype *dpl-1(n2994); lin-15(n433)* when both were progeny of a mother of genotype *dpl-1(n2994)/mnDf67; lin-15(n433)*. Animals of both of these genotypes had a stronger Muv phenotype and were less fertile than animals of genotype *dpl-1(n2994); lin-15(n433)* when descended from animals of genotype *dpl-1(n2994); lin-15(n433)*. These results suggest that *dpl-1(n2994)* is a weak allele of a locus that has a stronger, possibly sterile and maternal-effect lethal, null phenotype. CEOL and HORVITZ (2001) have subsequently isolated a putative null allele of *dpl-1*, which causes sterility.

To demonstrate formally that the newly defined genes are indeed synMuv genes, we conducted tests similar to those used by FERGUSON and HORVITZ (1989). First, we separated an allele of each gene from its parental mutation and showed that strains that carried only the isolated allele in homozygous condition displayed wild-type vulval development at the level of resolution of the dissecting microscope (Table 4). Double mutants were then constructed between alleles of the new synMuv genes and alleles of previously defined synMuv genes. Double mutants carrying class A and class B mutations were Muv; double mutants carrying two class A mutations or two class B mutations were wild-type for vulval development (Table 4). *lin-13(n770)* has also been shown to behave as a class B synMuv mutation by these criteria (Table 4 and data not shown).

Maternal rescue of the synMuv phenotype depends on both class A and class B genes: Many of the new synMuv strains displayed maternal rescue of the Muv phenotype, such that animals of genotype *a/a; b/b* descended from animals of genotype *a/+; b/+* had lower penetrance and reduced expressivity compared to animals of genotype *a/a; b/b* descended from animals of *a/a*; *b/b* genotype (Table 5). Similar results have been shown for other synMuv strains (FERGUSON and HORVITZ 1989). To determine whether this maternal rescue was conferred by only one of the two classes, we compared the Muv phenotypes of animals of genotype *a/a; b/b* descended from animals of genotypes *a/+; b/+* versus *a/a; b/+* versus *a/+; b/b*. Several different combinations of synMuv mutations were tested. In many cases, neither class alone produced significant maternal rescue compared to that produced by both classes

together. We concluded that maternal rescue displayed in synMuv strains is the result of a synergistic interaction between genes of the two classes rather than the result of the maternal contribution of genes of just one class (Table 5).

DISCUSSION

In this paper we describe the isolation and characterization of 49 new synMuv mutants. We define and describe three new genes, *lin-54*, *dpl-1* and *lin-56*, describe two other newly named genes, *lin-52* and *lin-53*, of which one allele each had been previously isolated, and identify class B synMuv alleles of *lin-13*. In sum, at least four class A genes (*lin-8*, *lin-15*A, *lin-38*, *lin-56*) and at least 14 class B genes (*lin-9*, *lin-13*, *lin-15*B, *lin-35 Rb*, *lin-36*, *lin-37*, *lin-52*, *lin-53 p48*, *lin-54*, *dpl-1*, *tam-1*, *let-418*, *efl-1*, *hda-1*) are now known (Table 6). We also showed that the maternal rescue of the synMuv phenotype is dependent on a synergistic interaction between the wild-type alleles of both classes.

Null phenotypes of synMuv genes: The null phenotype of most synMuv genes has not been rigorously established. Most likely, not all synMuv genes have the same null phenotypes (Table 6). Several synMuv genes are likely to have a synMuv null phenotype. The class A mutation *lin-15(n767)* is a likely null allele by molecular criteria: it is a deletion in the middle of the coding sequence with a small insertion producing a frameshift in the class A transcript (HUANG *et al.* 1994). *lin-15(n767)* mutants display a class A synMuv phenotype and are viable and fertile. The *lin-15* class B gene is also likely to have a synMuv null phenotype. The *lin-15*AB mutations *lin-15(n309)* and *lin-15(e1763)* are deletions of most of the DNA of the locus and are therefore molecular nulls for both A and B *lin-15* transcripts (CLARK *et al.* 1994; HUANG *et al.* 1994). These mutants are Muv, viable and fertile, indicating that the *lin-15* class B gene also has a synMuv null phenotype. *lin-36* is also likely to have a synMuv null phenotype: nonsense mutations isolated in a non-complementation screen are synMuv, viable and fertile (THOMAS and HORVITZ 1999).

Several other synMuv genes have a null phenotype that is either lethal or sterile. *lin-13* Muv mutants carry nonsense mutations and have a zygotic sterile and maternal effect larval arrest phenotype (MELÉNDEZ and GREENWALD 2000). It is likely that the null phenotype of *lin-9* is sterile. A non-complementation screen for *lin-9* mutants led to the isolation of *lin-9* alleles that were sterile and behaved as synMuv mutations (FERGUSON and HORVITZ 1989). These sterile *lin-9* mutations were shown to be nonsense mutations (BEITEL *et al.* 2000). The class B mutation *dpl-1(n2994)* was tested in *trans* to a deficiency that spanned the locus. *dpl-1(n2994)* mutants have a stronger Muv phenotype, are less fertile, and have a greater incidence of maternal

effect lethality when they and their mothers are *trans*-heterozygotes for a deficiency of this locus. This observation suggests that *dpl-1(n2994)* is probably a reduction-of-function mutation rather than a complete loss-of-function mutation. A null mutation of *dpl-1* isolated by CEOL and HORVITZ (2001) causes the sterile phenotype predicted by the analysis described here.

The screens described in this paper were not designed to isolate synMuv mutations that caused lethality or sterility. Thus, complete loss-of-function alleles of loci with such null phenotypes were not isolated. However, viable and fertile reduction-of-function mutations in such loci could have been isolated. Mutations in complementation groups with few alleles are candidates for being such reduction-of-function mutations. Loci that are not readily mutated to a viable synMuv phenotype may not have been identified.

From our general screens, we isolated mutations in different complementation groups at different frequencies. Class A mutations fell into either a frequently isolated group, *lin-8* and *lin-15*A (eight alleles each), or an infrequently isolated group, *lin-38* and *lin-56* (one or two alleles each). Class B mutations included 10 alleles of *lin-15*B, six of *lin-35*, five of *lin-13*, three of *lin-36*, two of *lin-54*, one each of *lin-37*, *lin-53*, *dpl-1*, and no alleles of *lin-9*, *lin-52*, *tam-1*, *let-418*, *efl-1* or *hda-1*. Given the number of haploid genomes screened and the expected frequency of mutation of the average *C. elegans* gene by EMS, $5x10^{-4}$, we expected to isolate about nine alleles of each gene with a synMuv null phenotype (BRENNER 1974; GREENWALD and HORVITZ 1980), suggesting that *lin-8*, *lin-15*A, *lin-15*B and *lin-35* are such genes. In contrast to these results, class B alleles of *lin-13*, which are not null alleles, were isolated at a relatively high frequency. *lin-13*, which encodes a protein of 2248 amino acids (MELÉNDEZ and GREENWALD 2000), may provide a large mutagenic target.

There are several reasons why mutations may have been isolated at a lower frequency than $5x10^{-4}$. Some of the genes may have a sterile or lethal loss-of-function phenotype, so that only rare reduction-of-function mutations were isolated. We probably failed to isolate any *lin-9* alleles for this reason. Mutations in such genes should be easily obtained in screens that allow the isolation of sterile and lethal mutants. Other genes may provide a small mutagenic target. Only one allele of *lin-37* was isolated in the screens described in this paper. This gene is physically small, and the allele we isolated is consistent by molecular criteria with its being a loss-of-function allele (X. LU, personal communication). In addition, there may have been a bias in our

experiments as a consequence of the parental mutations we used in our screens. The class A mutations *lin-8(n111)* and *lin-15(n433)* do not produce highly penetrant Muv phenotypes in conjunction with some class B mutations, which may have resulted in a lower frequency of isolation of alleles of certain genes.

Many Class A and class B synMuv genes probably act in distinct pathways: Most genes isolated in the screens described here or by FERGUSON and HORVITZ (1989) seem to be distinctly a member of either the class A or the class B pathway. With the exception of *lin-15* alleles, no class A and class B mutations mapped to the same site. However, the *lin-15* locus consists of two adjacent genes, a class A gene and a class B gene (CLARK *et al.* 1994; HUANG *et al.* 1994). These results suggest that most synMuv genes act in only one of the two pathways.

lin-13 is the only gene that genetic evidence suggests may act in both pathways. It was previously shown that at 25° the *lin-13(n387)* mutation produces a Muv phenotype similar to that of the synMuv double mutants but acts like a class B synMuv at 15° (FERGUSON and HORVITZ 1989; MELÉNDEZ and GREENWALD 2000). We have identified a class B allele of *lin-13, n770*. Thus, all described mutations in *lin-13* either cause a Muv phenotype or a class B synMuv phenotype. The Muv phenotype of certain *lin-13* alleles may be caused either by the elimination of both class A and class B activities of *lin-13* or by the elimination of another activity of *lin-13* that is independent of the synMuv pathways. If *lin-13* has both class A and class B activities, why might it be difficult to isolate class A alleles of *lin-13*? Particular regions of *lin-13* may be required for class A and class B activities, and class B regions may provide a larger or easier target for mutagenesis. Alternatively, some regions, possibly certain zinc fingers, are required for only class B activity while others are required for both, but none is required solely for class A activity. It is possible that *lin-13* mutations that cause a class A phenotype are not fertile or viable; however, no other class A mutations exhibit these phenotypes (Table 6). It is also possible that weaker *lin-13* alleles show only a class B synMuv phenotype. Either the class B pathway may be more sensitive to disruption or *lin-13* may play a more vital role in the class B pathway; if so, it would be impossible to get a mutation strong enough to exhibit class A activity without concomitantly exhibiting class B activity.

Synthetic phenotypes: Synthetic phenotypes are produced by combinations of mutations in different genes. Many synthetic lethal phenotypes have been studied in yeast, affecting such processes as cytoskeletal organization and secretion (HUFFAKER

et al. 1987, KAISER and SCHEKMAN 1990). Often, a synthetic phenotype is indicative of functional redundancy. There are several genes that are functionally redundant for various developmental processes in metazoa. In *Drosophila*, *achaete* and *scute* are functionally redundant for the specification of larval sense organs; however, individually each of these genes is required for the specification of a specific group adult bristles (reviewed by GHYSEN and DAMBLY-CHAUDIERE 1991). In *C. elegans*, *lin-12* and *glp-1* are molecularly similar and functionally redundant for some aspects of development, since double mutants exhibit defects not found in either single mutant (LAMBIE and KIMBLE 1991). Partial functional redundancy also is seen among *C. elegans* genes that function in the engulfment of cell corpses during programmed cell death; there are two classes of genes, such that animals carrying mutations in both classes have a more severe defect in engulfment than do animals carrying mutations in only one class (ELLIS *et al.* 1991). The three *C. elegans* genes that encode Rac-like proteins, *ced-10*, *mig-2* and *rac-2/3*, function redundantly in axon guidance and subsets of these genes function redundantly in certain cell migrations (LUNDQUIST *et al.* 2001). Whereas many synMuv genes are individually necessary for fertility or viability, others are not known to be individually required in any process other than vulval development. In contrast to lone mutations in many partially functionally redundant genes that have slight defects in a particular process, lone mutations in the synMuv genes do not have any discernable defects in vulval development (FERGUSON and HORVITZ 1989; THOMAS and HORVITZ 1999).

Functional redundancy at the genetic level suggests that two sets of genes implement the same biological effect, *e.g.* the negative regulation of vulval induction. The precise molecular mechanisms by which these genes act can be completely distinct, and the two classes of synMuv genes need not act at the same point in the pathway for vulval development. At what point(s) in the vulval pathway might the synMuv genes act? Mutations in the LET-23 receptor tyrosine kinase produce a Vul phenotype that is epistatic to the Muv phenotype caused by synMuv mutations, indicating that for the synMuv phenotype to be expressed *let-23* gene function is needed. If the Muv phenotype were caused by mutation in a single gene, this gene could act either parallel to or upstream of *let-23*. However, the synMuv phenotype is instead caused by mutations in two genes. Thus, if the effects of mutation in either of these two genes is blocked by a *let-23* mutation, the synMuv phenotype would be suppressed. These considerations indicate that at least one of the two classes of

synMuv genes (A or B) must act parallel to or upstream of *let-23*, but the other class of synMuv gene could act parallel to, upstream of or downstream of *let-23*. Specific models of how the class B synMuv genes may act in parallel to the *let-23* signal transduction pathway have been discussed by LU and HORVITZ (1998) and THOMAS and HORVITZ (1999).

Class B synMuv genes define an Rb-mediated pathway: Three of the class B synMuv genes, *lin-35*, *lin-53* and *dpl-1*, encode molecules similar to the Rb protein, RbAp48 and DP, respectively (LU and HORVITZ 1998; CEOL and HORVITZ 2001). The synMuv gene *lin-13* encodes a nuclear protein with an LXCXE motif, which has been implicated in Rb binding (MELÉNDEZ and GREENWALD 2000). These findings suggest that other class B genes likely encode components of an Rb pathway. Analyses of several other genes support this hypothesis (LU and HORVITZ 1998; VON ZELEWSKY *et al.* 2000; CEOL and HORVITZ 2001). The further analysis of the synMuv genes should help elucidate the mechanisms of action of Rb-like proteins and their regulators and effectors. The determination of how the class B synMuv genes negatively regulate the vulval induction process should provide insight concerning the antagonistic actions of an Rb-mediated and a Ras-mediated pathway.

ACKNOWLEDGMENTS

We thank BETH CASTOR for expert technical assistance. We thank EWA DAVISON for sharing unpublished data. We thank current and former members of the Horvitz laboratory, especially GREG BEITEL, KERRY KORNFELD and SHAI SHAHAM, for helpful discussions during the course of this work. We thank GREG BEITEL, KERRY KORNFELD and XIAOWEI LU for critically reading this manuscript. We thank the *Caenorhabditis* Genetics Center (supported by the National Institutes of Health National Center for Research Resources) for providing some of the strains used in this work. We thank Jonathan Hodgkin for providing the *hda-1(e1795)* strain. J.H.T. was a Predoctoral Fellow of the Howard Hughes Medical Institute. H.R.H. is an Investigator of the Howard Hughes Medical Institute.

LITERATURE CITED

ANDERSON, P., 1995 Mutagenesis, pp. 31-58 in Caenorhabditis elegans: *Modern Biological Analysis of an Organism. Methods Cell Biol.* 48, edited by H. F. EPSTEIN and D. C. SHAKES. Academic Press, New York.

AROIAN, R. V., M. KOGA, J. E. MENDEL, Y. OSHIMA, and P. W. STERNBERG, 1990 The *let-23* gene necessary for *Caenorhabditis elegans* vulval induction encodes a tyrosine kinase of the EGF receptor subfamily. Nature **348:** 693-699.

AROIAN, R. V., and P. W. STERNBERG, 1991 Multiple functions of *let-23*, a *Caenorhabditis elegans* receptor tyrosine kinase gene required for vulval induction. Genetics **128:** 251-267.

AUSTIN, J., and J. KIMBLE, 1989 Transcript analysis of *glp-1* and *lin-12*, homologous genes required for cell interactions during development of *C. elegans*. Cell **58:** 565-571.

BEITEL, G. J., E. J. LAMBIE, and H. R. HORVITZ, 2000 The *C. elegans* gene *lin-9*, which acts in an Rb-related pathway, is required for gonadal sheath cell development and encodes a novel protein. Gene **254:** 253-263.

BEITEL, G. J., S. G. CLARK, and H. R. HORVITZ, 1990 *Caenorhabditis elegans ras* gene *let-60* acts as a switch in the pathway of vulval induction. Nature **348:** 503-509.

BOXEM, M., and S. VAN DEN HEUVEL, 2002 *C.elegans* class B synthetic multivulva genes act in G1 regulation. Curr. Biol. **12:** 906-911.

BRENNER, S., 1974 The genetics of *Caenorhabditis elegans*. Genetics **77:** 71-94.

CEOL, C. J., and H. R. HORVITZ, 2001 *dpl-1* DP and *efl-1* E2F act with *lin-35* Rb to antagonize Ras signaling in *C. elegans* vulval development. Mol. Cell **7:** 461-473.

CHEN, Z., and M. HAN, 2001 *C. elegans* Rb, NuRD, and Ras regulate *lin-39*-mediated cell fusion during vulval cell fate specification. Curr. Biol. **11:** 1874-1879.

CLARK, S. G., 1992 *Intercellular Signaling and Homeotic Genes Required during Vulval Development in* C. elegans. Ph. D. Thesis, Massachusetts Institute of Technology.

CLARK, S. G., M. J. STERN, and H. R. HORVITZ, 1992 *Caenorhabditis elegans* cell-signalling gene *sem-5* encodes a protein with SH2 and SH3 domains. Nature **356:** 340-344.

CLARK, S. G., X. LU, and H.R. HORVITZ, 1994 The *Caenorhabditis elegans* locus *lin-15,* a negative regulator of a tryrosine kinase signaling pathway, encodes two different proteins. Genetics **137:** 987-997.

COUTEAU, F., F. GUERRY, F. MÜLLER, and F. PALLADINO, 2002 A heterochromatin protein 1 homologue in *Caenorhabditis elegans* acts in germline and vulval development. EMBO Rep. **3:** 235-241.

DUFOURCQ, P., M. VICTOR, F. GAY, D. CALVO, J. HODGKIN, and Y. SHI, 2002 Functional requirement for Histone Deacetylase 1 in *Caenorhabditis elegans* gonadogenesis. Mol. Cell. Biol. **22:** 3024-3034.

DESAI, C., G. GARRIGA, S. L. MCINTIRE, and H. R. HORVITZ, 1988 A genetic pathway for the development of the *Caenorhabditis elegans* HSN motor neurons. Nature **336:** 638-646.

ELLIS, R., D. M. JACOBSON, and H. R. HORVITZ, 1991 Genes required for the engulfment of cell corpses during programmed cell death in *Caenorhabditis elegans.* Genetics **129:** 79-94.

FERGUSON, E. L., and H. R. HORVITZ, 1985 Identification and genetic characterization of 22 genes that affect the vulval cell lineages of the nematode *Caenorhabditis elegans.* Genetics **110:** 17-72.

FERGUSON, E. L., and H. R. HORVITZ, 1989 The Multivulva phenotype of certain *Caenorhabditis elegans* mutants results from defects in two functionally redundant pathways. Genetics **123:** 109-121.

FERGUSON, E. L., P. W. STERNBERG, and H. R. HORVITZ, 1987 A genetic pathway for the specification of the vulval cell lineages of *Caenorhabditis elegans*. Nature **326:** 259-267.

GHYSEN, A., and C. DAMBLY-CHAUDIERE, 1988 From DNA to form: the *achaete-scute* complex. Genes Dev. **2:** 495-501.

GRAHAM, P. L., and J. KIMBLE, 1993 The *mog-1* gene is required for the switch from spermatogenesis to oogenesis in *Caenorhabditis elegans*. Genetics **133:** 919-931.

GREENWALD, I. S., and H. R. HORVITZ, 1980 *unc-93(e1500)*: a behavioral mutant of *Caenorhabditis elegans* that defines a gene with a wild-type null phenotype. Genetics **96:** 147-164.

HAN, M., and P. W. STERNBERG, 1990 *let-60*, a gene that specifies cell fates during *C. elegans* vulval induction, encodes a ras protein. Cell **63:** 921-931.

HAN, M., A. GOLDEN, Y. HAN, and P. W. STERNBERG, 1993 *C. elegans lin-45 raf* gene participates in *let-60 ras*-stimulated vulval differentiation. Nature **363:** 133-140.

HEDGECOCK, E. M., and R. K. HERMAN, 1995 The *ncl-1* gene and genetic mosaics of *Caenorhabditis elegans*. Genetics **141:** 989-1006.

HERMAN, R. K., 1978 Crossover suppressors and balanced recessive lethals in *Caenorhabditis elegans*. Genetics **88:** 49-65.

HERMAN, R. K., and E. M. HEDGECOCK, 1990 Limitation of the size of the vulval primordium of *Caenorhabditis elegans* by *lin-15* expression in the surrounding hypodermis. Nature **348:** 169-171.

HILL, R. J., and P. W. STERNBERG, 1992 The gene *lin-3* encodes an inductive signal for vulval development in *C. elegans*. Nature **358:** 470-476.

HODGKIN, J., M. EDGLEY, D. L. RIDDLE, and D. G. ALBERTSON, 1988 Appendix 4: Genetics, pp. 491-584 in *The Nematode* Caenorhabditis elegans, edited by W. B. WOOD and the Community of *C. elegans* Researchers. Cold Spring Harbor Press, Cold Spring Harbor, New York.

HORVITZ, H. R., and P. W. STERNBERG, 1991 Multiple intercellular signalling systems control the development of the *Caenorhabditis elegans* vulva. Nature **351:** 535-541.

HORVITZ, H. R., and J. E. SULSTON, 1980 Isolation and genetic characterization of cell-lineage mutants of the nematode *Caenorhabditis elegans*. Genetics **96:** 435-454.

HORVITZ, H. R., S. BRENNER, J. HODGKIN, and R. K. HERMAN, 1979 A uniform genetic nomenclature for the nematode *Caenorhabditis elegans*. Molec. Gen. Genet. **175:** 129-133.

HSIEH, J., J. LIU, S. A. KOSTAS, C. CHANG, C, P. W. STERNBERG, and A. FIRE, 1999 The RING finger/B-Box factor TAM-1 and a retinoblastoma-like protein LIN-35 modulate context-dependent gene silencing in *Caenorhabditis elegans*. Genes Dev. **13:** 2958-2970.

HUANG, L. S., P. TZOU, and P. W. STERNBERG, 1994 The *Caenorhabditis elegans lin-15* locus encodes two negative regulators of vulval development. Molec. Biol. Cell **5:** 395-412.

HUFFAKER, T. C., M. A. HOYT, and D. BOTSTEIN, 1987 Genetic analysis of the yeast cytoskeleton. Ann. Rev. Genet. **21:** 259-284.

KAISER, C. A., and R. SCHEKMAN, 1980 Distinct sets of *SEC* genes govern transport vesicle formation and fusion early in the secretory pathway. Cell **61:** 723-733.

KIMBLE, J., 1981 Alterations in cell lineage following laser ablation of cells in the somatic gonad of *Caenorhabditis elegans*. Dev. Biol. **87:** 286-300.

KORNFELD, K., 1997 Vulval development in *Caenorhabditis elegans*. Trends Genet. **13:** 55-61.

KORNFELD, K., K-L. GUAN, and H. R. HORVITZ, 1995a The *Caenorhabditis elegans* gene *mek-2* is required for vulval induction and encodes a protein similar to the protein kinase MEK. Genes Dev. **9:** 756-768.

KORNFELD, K., D. B. HOM, and H. R. HORVITZ, 1995b The *ksr-1* gene encodes a novel protein kinase involved in Ras-mediated signaling in *C. elegans*. Cell **83:** 903-913.

LACKNER, M. R., K. KORNFELD, L. M. MILLER, H. R. HORVITZ, and S. K. KIM, 1994 A MAP kinase homologue, *mpk-1*, is involved in ras-mediated induction of vulval cell fates in *Caenorhabditis elegans*. Genes Dev. **8:** 160-173.

LAMBIE, E., and J. KIMBLE, 1991 Two homologous regulatory genes, *lin-12* and *glp-1*, have overlapping functions. Development **112:** 231-240.

LUNDQUIST, E. A., P. W. REDDIEN, E. HARTWIEG, H. R. HORVITZ, and C. I. BARGMANN, 2001 Three *C. elegans* Rac proteins and several alternative Rac regulators control axon guidance, cell migration and apoptotic cell phagocytosis. Development **128:** 4475-4488.

LU, X., 1999 Molecular analyses of the class B synthetic multivulva genes of *Caenorhabditis elegans*. Ph.D. Thesis, Massachusetts Institute of Technology, USA.

LU, X., and H. R. HORVITZ, 1998 *lin-35* and *lin-53*, two genes that antagonize a *C. elegans* Ras pathway, encode proteins similar to Rb and its binding protein RbAp48. Cell **95:** 981-991.

MELÉNDEZ, A., and I. GREENWALD, 2000 *Caenorhabditis elegans lin-13*, a member of the LIN-35 Rb class of genes involved in vulval development, encodes a protein with zinc fingers and an LXCXE motif. Genetics **155:** 1127-1137.

PAGE, B. D., S. GUEDES, D. WARING, and J. R. PRIESS, 2001 The *C. elegans* E2F- and DP-related proteins are required for embryonic asymmetry and negatively regulate Ras/MAPK signaling. Mol. Cell **7:** 451-460.

PLENEFISCH, J. D., L. DELONG, and B. J. MEYER, 1989 Genes that implement the hermaphrodite mode of dosage compensation in *Caenorhabditis elegans*. Genetics **121:** 57-76.

SAMBROOK, J., E. F. FRITSCH, and T. MANIATIS, 1989 Molecular Cloning: A Laboratory Manual. Cold Spring Harbor Press, Cold Spring Harbor, New York.

SIGURDSON, D. C., G. J. SPANIER, and R. K. HERMAN, 1984 *Caenorhabditis elegans* deficiency mapping. Genetics **108:** 331-345.

STERNBERG, P. W., and M. HAN, 1998 Genetics of RAS signaling in *C. elegans*. Trends Genet. **14:** 466-472.

STERNBERG, P. W., and H. R. HORVITZ, 1986 Pattern formation during vulval development in *C. elegans*. Cell **44:** 761-772.

STERNBERG, P. W., and H. R. HORVITZ, 1989 The combined action of two intercellular signalling pathways specifies three cell fates during vulval induction in *C. elegans*. Cell **58:** 679-693.

SULSTON, J., and J. HODGKIN, 1988 Methods, pp. 587-606 in *The Nematode* Caenorhabditis elegans, edited by W. B. WOOD and the Community of *C. elegans* Researchers. Cold Spring Harbor Press, Cold Spring Harbor, New York.

SULSTON, J. E., and H. R. HORVITZ, 1977 Postembryonic cell lineages of the nematode *Caenorhabditis elegans*. Dev. Biol. **56:** 110-156.

SULSTON, J. E., and H. R. HORVITZ, 1981 Abnormal cell lineages in mutants of the nematode *Caenorhabditis elegans*. Dev. Biol. **82:** 41-55.

SULSTON, J. E., and J. G. WHITE, 1980 Regulation and cell autonomy during postembryonic development of *Caenorhabditis elegans*. Dev. Biol. **78:** 577-597.

THOMAS, J. H., and H. R. HORVITZ, 1999 The *C. elegans* gene *lin-36* acts cell autonomously in the *lin-35 Rb* pathway. Development **126:** 3449-3459.

THOMAS, J. H., M. J. STERN, and H. R. HORVITZ, 1990 Cell interactions coordinate the development of the *Caenorhabditis elegans* egg-laying system. Cell **62:** 1041-1052.

TRENT, C., N. TSUNG, and H. R. HORVITZ, 1983 Egg-laying defective mutants of the nematode *Caenorhabditis elegans*. Genetics **104:** 619-647.

VON ZELEWSKY, T., F. PALLADINO, K. BRUNSCHWIG, H. TOBLER, A. HAJNAL, and F. MÜLLER, 2000 The *C. elegans* Mi-2 chromatin-remodelling proteins function in vulval cell fate determination. Development **127:** 5277-5284.

WATERSTON, R. H., J. N. THOMSON, and S. BRENNER, 1980 Mutants with altered muscle structure in *Caenorhabditis elegans*. Develop. Biol. **77:** 271-301.

WHITE-COOPER, H., D. LEROY, A. MACQUEEN, and M. T. FULLER, 2000 Transcription of meiotic cell cycle and terminal differentiation genes depends on a conserved chromatin associated protein, whose nuclear localization is reulated. Development **127:** 5463-5473.

WU, Y., and M. HAN, 1994 Suppressors of activated Let-60 Ras protein defines a role of *Caenorhabditis elegans* Sur-1 MAP kinase in vulval differentiation. Genes Dev. **8:** 147-159.

WU, Y., M. HAN, and K-L. GUAN, 1995 MEK-2, a *Caenorhabditis elegans* MAP kinase kinase, functions in Ras-mediated vulval induction and other developmental events. Genes Dev. **9:** 742-758.

TABLES

TABLE 1

Origins, chromosomal linkages and phenotypes of new synthetic multivulva strains

	Penetrance of Muv phenotype		Strain Growth		
Genotype	15°	20°	15°	20°	25°
lin-8(n111) II; lin-13(n2238) III	65% (n=391)	100% (n=74)	Very slow	Slow	Inviable
lin-8(n111) II; lin-15(n2230) X	20% (n=254)	93% (n=376)	Slow	WT	Slow
lin-8(n111) II; lin-15(n2233) X	100% (n=235)	100% (n=385)	Slow	WT	Slow
lin-8(n111) II; lin-15(n2241) X	100% (n=130)	100% (n=238)	Slow	WT	Inviable
lin-8(n111) II; lin-15(n2244) X	91% (n=128)	99.6% (n=280)	WT	WT	Slow
lin-8(n111) II; lin-15(n2245) X	6% (n=202)	98% (n=306)	WT	WT	WT
lin-35(n2232) I; lin-8(n111) II	100% (n=200)	99.9% (n=942)	Inviable	WT	Inviable
lin-35(n2236) I; lin-8(n111) II	99% (n=96)	100% (n=97)	Inviable	Slow	Inviable
lin-35(n2239) I; lin-8(n111) II	100% (n=197)	100% (n=290)	Inviable	WT	Slow
lin-35(n2242) I; lin-8(n111) II	N.D.	100% (n=278)	Inviable	Slow	Very slow
lin-8(n111) II; lin-36(n2235) III	13% (n=279)	79% (n=313)	WT	WT	WT
lin-8(n111) II; lin-36(n2240) III	7% (n=189)	79% (n=373)	WT	WT	WT
lin-8(n111) II; lin-36(n2243) III	51% (n=115)	94% (n=593)	WT	WT	WT
lin-8(n111) II; lin-37(n2234) III	96% (n=192)	100% (n=278)	WT	WT	Inviable
lin-8(n111) II; lin-54(n2231) IV	39% (n=334)	99% (n=164)	Very slow	WT	Slow
lin-13(n2981) III; lin-15(n433) X	0% (n=237)	84% (n=241)	WT	WT	Inviable
lin-13(n2984) III; lin-15(n433) X	1% (n=217)	97% (n=239)	WT	WT	Inviable
lin-13(n2985) III; lin-15(n433) X	2% (n=229)	94% (n=213)	WT	WT	Slow
lin-13(n2988) III; lin-15(n433) X	33% (n=247)	97% (n=261)	Slow	Slow	Inviable
lin-15(n2980 n433) X[a]	2% (n=209)	99% (n=252)	WT	WT	Slow
lin-15(n2983 n433) X[a]	2% (n=232)	99% (n=227)	WT	WT	Slow
lin-15(n2987 n433) X[a]	0% (n=207)	91% (n=267)	WT	WT	WT
lin-15(n2989 n433) X[a]	0% (n=238)	100% (n=235)	WT	WT	WT
lin-15(n2991 n433) X[a]	2% (n=226)	100% (n=216)	WT	WT	WT

lin-15(n2993 n433) X[a]	0% (n=205)	79% (n=201)	WT	WT	WT
lin-35(n2977) I; lin-15(n433) X	8% (n=257)	100% (n=234)	Slow	WT	Slow
lin-35(n2996) I; lin-15(n433) X	18% (n=216)	100% (n=202)	Slow	Slow	Slow
lin-53(n2978) I; lin-15(n433) X	0% (n=211)	59% (n=203)	WT	WT	WT
lin-54(n2990) IV; lin-15(n433) X	4% (n=199)	95% (n=216)	WT	WT	Slow
dpl-1(n2994) II; lin-15(n433) X	4% (n=246)	78% (n=234)	WT	WT	Slow
lin-8(n2376) II; lin-36(n766) III	18% (n=382)	96% (n=189)	WT	WT	WT
lin-8(n2378) II; lin-36(n766) III	19% (n=456)	100% (n=125)	WT	WT	WT
lin-8(n2403) II; lin-36(n766) III	48% (n=402)	99% (n=549)	WT	WT	WT
lin-36(n766) III; lin-15(n2375) X	0% (n=544)	82% (n=675)	WT	WT	Slow
lin-38(n2402) II; lin-36(n766) III	28% (n=643)	99.7% (n=667)	WT	WT	WT
lin-8(n2724) II; lin-15(n744) X	100% (n=211)	100% (n=126)	Slow	Slow	Slow
lin-8(n2731) II; lin-15(n744) X	100% (n=217)	100% (n=167)	Slow	Slow	Slow
lin-8(n2738) II; lin-15(n744) X	100% (n=128)	100% (n=140)	Slow	Slow	Very slow
lin-8(n2739) II; lin-15(n744) X	100% (n=158)	100% (n=97)	Slow	Slow	Slow
lin-8(n2741) II; lin-15(n744) X	100% (n=157)	100% (n=155)	WT	Slow	Slow
lin-15(n744 n2725) X[a]	100% (n=152)	100% (n=177)	Slow	Slow	Very slow
lin-15(n744 n2726) X[a]	100% (n=141)	100% (n=145)	Slow	Slow	Very slow
lin-15(n744 n2733) X[a]	100% (n=193)	100% (n=140)	Slow	Slow	Inviable
lin-15(n744 n2734) X[a]	100% (n=124)	100% (n=159)	Slow	Slow	Slow
lin-15(n744 n2735) X[a]	100% (n=132)	100% (n=176)	Slow	Slow	Very slow
lin-15(n744 n2737) X[a]	99% (n=199)	100% (n=121)	Slow	Slow	Inviable
lin-15(n744 n2742) X[a]	100% (n=121)	100% (n=173)	Slow	Slow	Very slow
lin-38(n2727) II; lin-15(n744) X	100% (n=201)	100% (n=165)	Slow	Slow	Slow
lin-56(n2728) II; lin-15(n744) X	100% (n=214)	100% (n=163)	Slow	Slow	Slow

New synMuv mutations were mapped to linkage groups using strains carrying the markers *bli-3 I*; *dpy-5 I*; *unc-54 I*; *unc-85 II*; *bli-2 II*; *mnC1 dpy-10 unc-52 II*; *unc-52 II*; *dpy-1 III*; *unc-32 III*; *unc-25 III*; *dpy-9 IV*; *egl-18 IV*; *unc-5 IV*;*dpy-4 IV*; *unc-34 V*; *dpy-11 V*; *unc-51 V*; *lon-2 X* and *unc-3 X*. in a manner similar to that described previously (TRENT *et al.* 1983; FERGUSON and HORVITZ 1989).

The penetrance of the Muv phenotype of each synMuv strain was determined at 15° and 20° after growth at the indicated temperature for two or more generations. Several strains displayed a temperature-dependent reduction in viability. This reduction in viability was tested in an assay similar to that of FERGUSON and HORVITZ (1989) but differing in that exactly 10 eggs laid by hermaphrodites of the indicated genotype grown at 20° were placed on each of the four assay plates (each with a 2 cm diameter lawn of bacteria) used at each temperature. The plates were checked daily to determine when the bacterial lawn was consumed. The data are presented according to the following criteria; at 15°, WT, 8.5-14 days; Slow, 14-24 days; Very slow, 24-28 days; Inviable, lethal or more than 28 days. At 20°, WT, 5.5-9 days; Slow, 9-17 days; Very slow, 17-28 days; Inviable, lethal or more than 28 days. At 25°, WT, 5-7.5 days; Slow, 7.5-15 days; Very slow, 15-28 days; Inviable, lethal or more than 28 days. The last value of the range described was included in that category. The data obtained from the wild-type (WT) strain N2 was: 15°: 10 days, 20°: 6 days, 25°: 5 days. N. D., not determined because the strain was lethal at the listed temperature.

[a] The mutations in these strains displayed linkage only to *unc-3 X*. Linkage of the new mutation to *unc-3 X* is assumed since the mutations in these strains segregated as single locus Muv mutations and failed to complement *lin-15(n765) X*.

TABLE 2

Sequences of *lin-13* class B mutations

Allele	Wild-type sequence	Mutant sequence	Substitution
n770	CAG	TAG	Q1988amber
n2238	CAA	TAA	Q996ochre
n2981	TGC	TAC	C814Y
n2984	GGA	GAA	G360E
n2985	CAA	TAA	Q1717ochre
n2988	TGT	TAT	C361Y

Wild-type and mutant codons are shown with the mutated nucleotide underlined. All mutations were GC-to-AT transitions as expected for EMS-induced mutations (ANDERSON 1995). Amino acid substitutions are shown as wild-type residue identity, residue number, and predicted mutant residue.

TABLE 3

Three- and four-factor crosses

Gene	Genotype of heterozygote	Phenotype of selected recombinants	Genotype of selected recombinants (with respect to unselected markers)
lin-13			
	lin-13 unc-32+ +/+ + unc-49 dpy-18; lin-15(n767)	Unc-32	0/2 *unc-49 dpy-18/+ +*
		Dpy	7/7 *lin-13 unc-32/+ +*
		Unc-49	0/1 *lin-13 unc-32/+ +*
	+ + lin-13/unc-93 dpy-27 +; lin-15(n767)	Unc	30/30 *lin-13/+*
	+ + lin-13/unc-93 dpy-17 +; lin-15(n767)	Unc	8/8 *lin-13/+*
		Dpy	0/3 *lin-13/+*
	+ lin-13 +/dpy-17 + unc-32; lin-15(n767)	Dpy	1/8 *lin-13/+*
		Unc	5/10 *lin-13/+*
lin-52			
	+ + unc-32 lin-52/lon-1 sma-3 + +; lin-15(n767)	Lon	1/1 *lin-52 unc-32/ + +*
		Sma	0/4 *lin-52/+*
		Muv	7/7 *lon-1/+*
	+ + lin-52/sma-3 unc-32; lin-15(n767)	Sma	3/3 *lin-52/+*
		Unc	0/13 *lin-52/+*
	+ lin-52 +/dpy-19 + unc-69; lin-15(n767)	Dpy	17/31 *lin-52/+*
		Unc	2/11 *lin-52/+*
	+ lin-52 +/unc-16 + unc-49; lin-15(n767)	Unc-16	0/2 *lin-52/+*
		Unc-49	13/16 *lin-52/+*
lin-53			
	dpy-5 lin-53 + +/+ + lin-11 unc-75; lin-15(n767)	Dpy	7/7 *lin-11 unc-75/+ +*
		Muv	0/12 *lin-11 unc-75/+ +*
		Vul	0/10 *dpy-5 lin-53/+ +*
		Unc	8/8 *dpy-5 lin-53/+ +*
	+ lin-53 +/unc-29 + lin-11; lin-15(n767)	Unc	1/3 *lin-53/+*
		Vul	11/19 *lin-53/+*
lin-54			

	lin-8; + + lin-54/unc-22 unc-30 +	Unc-22	19/19 *lin-54/+*
		Unc-30	0/15 *lin-54/+*
	lin-8; + lin-54 +/unc-30 + dpy-4	Unc	2/11 *lin-54/+*
		Dpy	21/22 *lin-54/+*
	lin-54 + +/+ lev-1 unc-26; lin-15(n433)	Lev	0/25 *lin-54/+*
dpl-1			
	+ dpl-1 +/dpy-10 + unc-53; lin-15(n433)	Dpy	6/9 *dpl-1/+*
		Unc	6/11 *dpl-1/+*
	+ dpl-1 +/rol-6 + unc-4; lin-15(n433)	Rol	6/14 *dpl-1/+*
		Unc	9/14 *dpl-1/+*
	dpl-1 + +/+ let-240 unc-4; lin-15(n433)	Unc	25/25 *dpl-1/+*
lin-56			
	+ + lin-56/unc-85 dpy-10 +; lin-15(n744)	Unc	4/4 *lin-56/+*
		Dpy	0/6 *lin-56/+*
	+ lin-56 +/dpy-10 + unc-53; lin-15(n744)	Dpy	5/10 *lin-56/+*
		Unc	6/11 *lin-56/+*
	+ + lin-56/rol-6 unc-4 +; lin-15(n744)	Rol	16/16 *lin-56/+*
		Unc	0/9 *lin-56/+*

Deficiency heterozygotes

Gene	Genotype of heterozygote	Phenotype of heterozygote
dpl-1		
	dpy-10 dpl-1(n2994) +/+ mnDf46 unc-4; lin-15(n433)	wild-type
	dpy-10 dpl-1(n2994) +/+ mnDf85 unc-4; lin-15(n433)	wild-type
	dpy-10 dpl-1(n2994) +/+ mnDf67 unc-4; lin-15(n433)	Muv

Three-, and four-factor crosses were performed as described previously (BRENNER 1974; FERGUSON and HORVITZ 1989). Deficiency heterozygotes were constructed, and the vulval phenotype was scored. The presence of the deficiency was confirmed in each animal based upon the segregation of 1/4 dead eggs or larvae.

TABLE 4

Phenotypes of single and double mutants

			Double mutant with Class A		Double mutant with Class B	
	New Mutation	Single mutant	*lin-8(n111)*	*lin-15(n767)*	*lin-36(n766)*	*lin-15(n744)*
Class A						
	lin-56(n2728)	WT	WT	WT	Muv	Muv
Class B						
	lin-13(n770)	WT	Muv	Muv	WT	WT
	lin-52(n771)	WT	Muv	Muv	WT	WT
	lin-53(n833)	WT	Muv	Muv	WT	WT
	lin-54(n2231)	WT	Muv	Muv	WT	WT
	dpl-1(n2994)	WT	Muv	Muv	WT	WT

Mutations in new genes were separated from the original mutation present in the synMuv strain as described in MATERIALS AND METHODS. Double mutants carrying mutations in these new genes and mutations in previously known class A or class B genes were constructed as described in MATERIALS AND METHODS. WT, animals had wild-type vulval morphology as observed using a dissecting microscope, *i.e.* 0% Muv ($n > 500$). Muv, animals had a Muv phenotype of greater than 50% penetrance ($n \geq 100$). *lin-13*, *lin-52* and *lin-54* animals displayed a weaker Muv phenotype in double mutants with *lin-8(n111)* than with *lin-15(n767)*. *dpl-1* animals displayed a weaker Muv phenotype in a *lin-15(n433)* background than in a *lin-15(n767)* background. WT, animal had a wild-type vulval morphology as observed using a dissecting microscope.

TABLE 5

Maternal rescue of synMuv phenotype

Class A mutation	Class B mutation	Penetrance of the Muv phenotype in animals of *a/a; b/b* genotype descended from animals of maternal genotype			
		a/+; b/+	*a/+; b/b*	*a/a; b/+*	*a/a; b/b*[b]
lin-8(n111)	*lin-9(n112)*	72% (n=57)[a]	83% (n=141)[a]	100% (n=183)	100% (n=165)
lin-8(n111)	*lin-35(n745)*	45% (n=65)[a]	N. D.	97% (n=149)	100% (n=209)
lin-8(n111)	*lin-36(n766)*	14% (n=93)[a]	23% (n=216)[a]	84% (n=300)	98% (n=207)
lin-8(n111)	*lin-37(n758)*	31% (n=69)[a]	98% (n=133)[a]	85% (n=188)	100% (n=161)
lin-15(n433)	*lin-54(n2231)*	9% (n=89)[a]	N. D.	21% (n=211)	99% (n=164)
lin-15(n767)	*lin-13(n770)*	58% (n=64)[a]	97% (n=238)[a]	90% (n=220)	95% (n=230)
lin-15(n767)	*lin-52(n771)*	83% (n=98)[a]	103% (n=225)[a]	90% (n=294)	100% (n=211)
lin-15(n767)	*lin-53(n833)*	103% (n=76)[a]	N. D.	100% (n=64)	100% (n=116)
lin-15(n433)	*dpl-1(n2994)*	11% (n=95)*a*	75% (n=125)[a]	50% (n=298)	78% (n=234)
lin-38(n751)	*lin-9(n112)*	81% (n=65)[a]	100% (n=146)	99% (n=189)[a]	100% (n=165)
lin-56(n2728)	*lin-15(n744)*	93% (n=92)[a]	99% (n=200)	N. D.	100% (n=163)

The contribution of class A and class B genes to the maternal rescue of the synMuv phenotype of doubly homozygous animals descended from either singly or doubly heterozygous mothers was determined by counting the number of Muv animals of phenotype R, where R is the phenotype produced by the *cis* marker *r*. Doubly heterozygous mothers were obtained by mating N2 males with marked doubly homozygous hermaphrodites. Singly heterozygous mothers were obtained by mating males homozygous for one of the synMuv mutations with marked doubly homozygous hermaphrodites. A strain homozygous for *lin-35* was obtained by the general procedure used for the isolation of strains homozygous for single synMuv mutations. *dpy-14* was used to balance *lin-35*. The *lin-8; lin-9* strain was marked with *lon-1*. The *lin-35; lin-8* strain was marked with *unc-13*. The *lin-8; lin-36* strain was marked with *unc-32*. The *lin-8; lin-37* strain was marked with *lon-1*. The *lin-38; lin-9* strain was marked with *unc-52*. The *lin-13; lin-15(n767)* strain was marked with *unc-93* or *unc-32*. The *lin-52; lin-15(n767)* strain was marked with *sma-3*. The *lin-53; lin-15(n767)* strain was marked

with *dpy-5* or *lin-11*. The *lin-54; lin-15(n433)* strain was marked with *dpy-20*. The *dpl-1; lin-15(n433)* strain was marked with *rol-6*. The *lin-56; lin-15(n744)* strain was marked with *rol-6*.

[a]These data were obtained by estimating the penetrance and by assuming that the number of doubly homozygous animals were 1/4 of the R progeny.

[b]These data are from Table 1 of FERGUSON and HORVITZ (1989).

TABLE 6

SynMuv genes and alleles

	Gene	No. of alleles	Mutant alleles	Probable null phenotype (evidence)
Class A				
	lin-8	9	*n111*, *n2376*, *n2378*, *n2403*, *n2724*, *n2731*, *n2738*, *n2739*, *n2741*	SynMuv[a] (no. alleles)
	*lin-15*A	13	*n433*, *n749*, *n767*, *n2375*, *n2725*, *n2726*, *n2733*, *n2734*, *n2735*, *n2737*, *n2742*, *sy211*, *sy212*	SynMuv (molecular data[b], no. alleles)
	lin-38	4	*n751*, *n761*, *n2402*, *n2727*	Unknown
	lin-56	1	*n2728*	Unknown
Class B				
	lin-9	3	*n112*, *n942*, *n943*	SynMuv, sterile (molecular data[c], non-complementation screen[d])
	lin-13	8	*n770*, *n2238*, *n2981*, *n2984*, *n2985*, *n2988*, (*n387* and possibly *n388* at 15°[d])	SynMuv, sterile, maternal-effect lethal[a] (molecular data[e])
	*lin-15*B	14	*n374*, *n743*, *n744*, *n2230*, *n2233*, *n2241*, *n2244*, *n2245*, *n2980*, *n2983*, *n2987*, *n2989*, *n2991*, *n2993*	SynMuv (molecular data[b], no. alleles)
	lin-35	8	*n373*, *n745*, *n2232*, *n2236*, *n2239*, *n2242*, *n2977*, *n2996*	SynMuv (molecular data[f], no. alleles)
	lin-36	13	*n747*, *n750*, *n766*, *n772*, *n2235*, *n2240*, *n2243*, *n3090*, *n3093*, *n3094*, *n3095*, *n3096*, *n3097*	SynMuv (molecular data[g], non-complementation screen[g])
	lin-37	2	*n758*, *n2234*	SynMuv (molecular data[h])
	lin-52	1	*n771*	Unknown

lin-53	3	*n833*, *n2978*, *n3386*[i]	SynMuv, sterile, protruding vulva (molecular data[i], *n833* and *n2978* are dominant negative[j])
lin-54	2	*n2231*, *n2990*	Unknown
dpl-1	4	*n2994*, *n3316*, *n3643*, *zu355*	SynMuv, sterile, maternal-effect lethal (phenotype enhanced by Df, molecular data[k], *zu355* isolated in maternal-effect lethal screen[l])
tam-1[m]	18	*cc566*, *cc567*, *cc587*, *sy272* and 14 others	synMuv (molecular data[n], no. alleles[n], phenotype not enhanced by Df[m])
let-418	3	*ar113*, *ar114*, *s1617*	SynMuv, sterile, maternal-effect lethal, everted vulva (molecular data[o], phenotype not enhanced by Df[o])
efl-1	3	*n3318*, *n3639*, *se1*	SynMuv, sterile, maternal-effect lethal[p] (molecular data[k], *se1* isolated in maternal-effect lethal screen[l])
hda-1	1	*e1795*[q]	SynMuv, sterile, protruding vulva (molecular data[r])

Mutant alleles not described in the text are described by HORVITZ and SULSTON (1980), FERGUSON and HORVITZ (1985, 1989), DESAI *et al.* (1988), HUANG *et al.* (1994), THOMAS and HORVITZ (1999), HSIEH *et al.* (1999), VON ZELEWSKY *et al.* (2000), CEOL and HORVITZ (2001), PAGE *et al.* (2001). Probable null phenotype is given at 20°; see Table 1. Under evidence, no. alleles indicates that a high number of mutations were isolated in the screens described in the text, consistent with the hypothesis that some of these alleles are null alleles.

[a]See FERGUSON and HORVITZ (1985) for possibly contradictory deficiency data.

[b]CLARK *et al.* (1994), HUANG *et al.* (1994).

[c]BEITEL *et al.* (2000).

[d]FERGUSON and HORVITZ (1989).

[e]MELÉNDEZ and GREENWALD (2000).

[f]LU and HORVITZ (1998).

[g]THOMAS and HORVITZ (1999).

[h]LU (1999).

[i]X. LU and H. R. H. (personal communication).

[j]Text and LU and HORVITZ (1998).

[k]CEOL and HORVITZ (2001).

[l]PAGE *et al.* (2001).

[m]This gene does not act as a class B synMuv in double mutants with *lin-8*, but does with *lin-15*A and *lin-38* (HSIEH *et al.* 1999). Such an interaction had not been previously observed for the synMuv genes, but *lin-8(n111)* synMuv double mutants have occasionally been observed to be weaker than corresponding synMuv double mutants carrying other class A mutations. (THOMAS and HORVITZ 1999).

[n]HSIEH *et al.* (1999).

[o]VON ZELEWSKY *et al.* (2000).

[p]PAGE *et al.* (2001), C. J. CEOL and H. R. HORVITZ (unpublished results).

[q] *hda-1* is also known as *gon-10* (DUFOURCQ *et al.* 2002). The *hda-1(e1795)* mutation alone causes a weakly penetrant Muv phenotype (DUFOURCQ *et al.* 2002), but in combination with the class A mutation *lin-15(n767)* this phenotype is fully penetrant and displays stronger expressivity (C. J. CEOL, E. C. ANDERSEN and H. R. HORVITZ, unpublished results).

[r] DUFOURCQ *et al.* (2002).

FIGURE

FIGURE 1.--Partial genetic map of *C. elegans* showing the locations of newly identified or newly characterized synMuv genes and the markers that were used to position these genes on the map. New synMuv genes are shown above the line representing the linkage group; marker genes are shown below the line. Deficiencies are drawn below the line and indicate which genes are deleted.

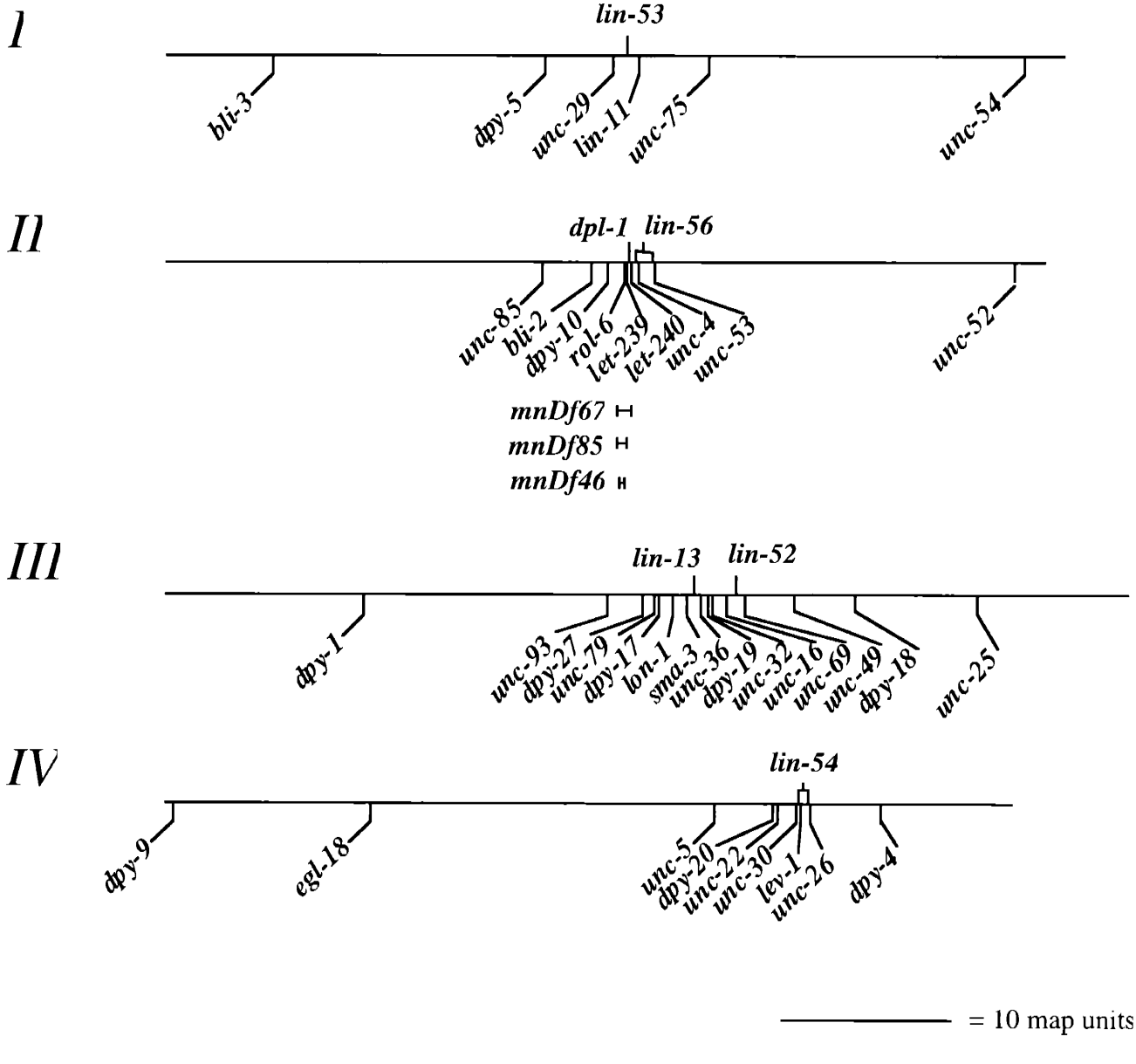
I
lin-53
bli-3
dpy-5
unc-29
lin-11
unc-75
unc-54
II
dpl-1
lin-56
unc-85
bli-2
dpy-10
rol-6
let-239
let-240
unc-4
unc-53
unc-52
mnDf67
mnDf85
mnDf46
III
lin-13
lin-52
dpy-1
unc-93
dpy-27
unc-79
dpy-17
lon-1
sma-3
unc-36
dpy-19
unc-32
unc-16
unc-69
unc-49
dpy-18
unc-25
IV
lin-54
dpy-9
egl-18
unc-5
dpy-20
unc-22
unc-30
lev-1
unc-26
dpy-4
= 10 map units

CHAPTER 3

dpl-1 DP and *efl-1* E2F Act with *lin-35* Rb to Antagonize Ras Signaling in *C. elegans* Vulval Development

Craig J. Ceol and H. Robert Horvitz

Published as Ceol and Horvitz (2001), Molecular Cell 7: 461-73. The data described in the Addendum were excluded from the published manuscript due to space limitations.

SUMMARY

The synthetic multivulva (synMuv) genes define two functionally redundant pathways that antagonize RTK/Ras signaling during *Caenorhabditis elegans* vulval induction. The synMuv gene *lin-35* encodes a protein similar to the mammalian tumor suppressor pRB and has been proposed to act as a transcriptional repressor. Studies using mammalian cells have shown that pRB can prevent cell cycle progression by inhibiting DP/E2F-mediated transcriptional activation. We identified *C. elegans* genes that encode proteins similar to DP or E2F. Loss-of-function mutations in two of these genes, *dpl-1* DP and *efl-1* E2F, caused the same vulval abnormalities as do *lin-35* Rb loss-of-function mutations. We propose that rather than being inhibited by *lin-35* Rb, *dpl-1* DP and *efl-1* E2F act with *lin-35* Rb in transcriptional repression to antagonize RTK/Ras signaling during vulval development.

INTRODUCTION

Signal transduction pathways can control the specification of cell fates during metazoan development. Some of the pathways used for cell-fate specification also act in tumorigenesis in mammals (Potter et al., 2000). Such signal transduction pathways include both proto-oncogenes and tumor suppressor genes.

Counterparts of mammalian proto-oncogenes and tumor suppressor genes play opposing roles in the determination of cell fates during the development of the hermaphrodite vulva of the nematode *Caenorhabditis elegans*. A receptor tyrosine kinase (RTK)- and Ras-mediated signal transduction pathway induces the development of the vulva (Ferguson et. al., 1987; reviewed by Sternberg and Han, 1998). During the second larval stage of *C. elegans* development, a set of six ectodermal blast cells, P(3-8).p, are present along the ventral midline. Each of these six cells has the capacity to adopt either 1° or 2° vulval cell fates or a 3° non-vulval cell fate. In the wild type, P(5-7).p are induced by a signal from the neighboring gonadal anchor cell to adopt vulval fates, and these cells divide to together generate the 22 descendants that make up the adult vulva. P3.p, P4.p and P8.p are not induced and adopt a non-vulval fate, dividing once and fusing with the syncytial hypodermis. The anchor cell signal activates an RTK/Ras pathway in P(5-7).p. Mutations that reduce RTK/Ras pathway activity, including loss-of-function mutations in *let-23* RTK or *let-60* Ras, cause P(5-7).p to adopt non-vulval fates, result in a vulvaless (Vul) phenotype. By contrast, mutations that increase RTK/Ras pathway activity, such as gain-of-function mutations in *let-60* Ras, cause P3.p, P4.p and P8.p to ectopically adopt vulval fates, resulting in a multivulva (Muv) phenotype.

The activity of the RTK/Ras pathway is antagonized by the synthetic multivulva (synMuv) genes (Horvitz and Sulston, 1980; Ferguson and Horvitz, 1989). On the basis of genetic interactions, the synMuv genes have been grouped into two classes, A and B. Animals with loss-of-function mutations in a class A and a class B gene are Muv, whereas animals mutant in a single gene or genes of a single class are non-Muv. Mutations identifying five class A and 17 class B genes have been isolated (Horvitz and Sulston, 1980; Ferguson and Horvitz, 1989; Hsieh et al., 1999; Solari and Ahringer, 2000; von Zelewsky et al., 2000; H. R. H., C. C., X. Lu and P. Sternberg, unpublished results). Classes A and B are proposed to define functionally redundant pathways that negatively regulate vulval induction (Ferguson and Horvitz, 1989).

A molecular mechanism by which some of the class B synMuv genes act was revealed by the finding that the class B gene *lin-35* encodes a protein similar to the mammalian tumor suppressor pRB (Lu and Horvitz, 1998). Among other functions, pRB and the related proteins p107 and p130 bind to and modulate the activities of DP/E2F heterodimeric transcription factors (reviewed by Dyson, 1998; Lavia and Jansen-Durr, 1999). DP/E2F heterodimers are proposed to be regulators of the G_1-to-S phase transition of the cell cycle. "Free" DP/E2F heterodimers that are not bound by pRB, p107 or p130 activate the transcription of genes required for S phase. However, when associated with DP/E2F heterodimers, pRB family proteins are thought to repress DP/E2F-regulated genes, thereby inhibiting premature expression of genes required for S phase and preventing inappropriate S phase entry. pRB can recruit proteins involved in chromatin modification and transcriptional repression, including the histone deacetylase HDAC1, to promoters containing DP/E2F-binding sites (Brehm et al., 1998; Luo et al., 1998; Magnaghi-Jaulin et al., 1998). This latter function appears to be conserved in *C. elegans*, as two genes with class B synMuv activity, *hda-1* and *lin-53*, encode proteins similar to the class I histone deacetylase HDAC1 and the histone deacetylase-associated protein RbAp48, respectively (Lu and Horvitz, 1998). Based on these findings, the class B synMuv genes are proposed to repress the transcription of genes required for vulval cell fate specification.

Here we report the identification and characterization of *C. elegans* genes encoding DP and E2F family members. *dpl-1* (*dpl*, DP-like) and *efl-1* (*efl*, E2F-like) are class B synMuv genes that act with *lin-35* Rb to negatively regulate vulval induction, thereby antagonizing *let-23* RTK/*let-60* Ras signaling.

RESULTS

The class B synMuv mutation *n2994* affects a DP-related gene

The class B synMuv mutation *n2994* was isolated in a screen for synMuv mutants and was mapped using deficiencies to a region of LGII between the cloned genes *rol-6* and *eat-3* (J. Thomas and H.R.H., unpublished results). We injected genomic DNA clones (Mello et al., 1991) from this region into *n2994*; *lin-15A(n433)* mutants to obtain transformation rescue. (*lin-15* is a complex locus of two genes, *lin-15A* and *lin-15B*, which encode class A synMuv and class B synMuv genes, respectively; Clark et al., 1994; Huang et al., 1994). The Muv phenotype was rescued both by the cosmid C32F7 and by a 5.2 kb PvuII-PvuII subclone of C32F7 (Figure 1A). The DNA sequence of this subclone contains one complete predicted gene, T23G7.1, which encodes a protein similar to human DP-1 and other DP family proteins (*C. elegans* Genome Sequencing Consortium, 1998). We named this gene *dpl-1* (*dpl*, *DP-l*ike). We obtained *dpl-1* cDNA clones (see Supplemental Materials), the longest of which contains a single open reading frame that encodes a protein of 598 amino acids. An in-frame stop codon precedes the putative initiator methionine codon, suggesting that this open reading frame is full-length. We determined the sequence of *dpl-1* in *n2994* mutants and found a splice-acceptor mutation preceding the fifth exon (Figures 1B and 1C). We isolated another *dpl-1* allele, *n3643*, in a screen for synMuv mutants (C.J.C and H.R.H., unpublished results) and found two alterations in the *dpl-1* locus: a nonsense mutation predicted to truncate the DPL-1 protein after 340 amino acids and a missense mutation 192 residues downstream of the nonsense mutation (Figures 1B and 1C). The gene affected by *n2994* was previously known as *lin-55* (Lu and Horvitz, 1998).

The DPL-1 protein shares extensive sequence similarity with DP family proteins, particularly in domains required by DP-1 for dimerization with E2F-1 and for enhanced DNA binding of the resultant DP-1/E2F-1 complex (Figure 1C; Girling et al., 1993; Helin et al., 1993). DPL-1 is the only DP family member predicted by the nearly complete *C. elegans* genome sequence (*C. elegans* Sequencing Consortium, 1998).

A *dpl-1* DP null allele causes a synMuv phenotype

Mammalian DP proteins participate both in transcriptional activation and, by targeting pRB-family proteins to promoters, in transcriptional repression (reviewed by Lavia and Jansen-Durr, 1999). Given the potential dual activation and repression functions of DPL-1, we sought to determine if the synMuv phenotype caused by *dpl-1(n2994)*, which is similar to the phenotype caused by *lin-35* Rb loss-of-function mutations, was caused by a gain of *dpl-1* function, suggesting antagonism by *lin-35* Rb, or was caused by a loss of *dpl-1* function, indicating *dpl-1* action with *lin-35* Rb.

Gene dosage experiments indicate that *n2994* causes a loss rather than a gain of *dpl-1* function. Specifically, *dpl-1(n2994)/+; lin-15A(n433)* animals are non-Muv, whereas *dpl-1(n2994)/mnDf67; lin-15A(n433)* mutants, like *dpl-1(n2994); lin-15A(n433)* mutants, have a highly penetrant Muv phenotype (Table 1). *mnDf67* is a deficiency that removes the *dpl-1* locus (J. Thomas and H.R.H., unpublished results).

To confirm these findings and to study further the consequences of a *dpl-1* loss of function, we isolated the *dpl-1* deletion allele *n3316* (see Supplemental Materials). *n3316* removes 1421 base pairs of the *dpl-1* locus, deleting exons that encode the conserved DPL-1 DNA-binding and dimerization domains (Figure 1B). The predicted DPL-1 protein in *n3316* mutants contains the first three amino acids of DPL-1 followed by four unrelated amino acids prior to truncation.

dpl-1(n3316) caused a Muv phenotype in a class A synMuv background but not in a class B synMuv background (Table 1), confirming that *dpl-1* is a class B synMuv gene. In addition, *dpl-1(n3316)* caused hermaphrodite sterility as a consequence of defects in ovulation and in *trans* to partial loss-of-function *dpl-1* alleles caused embryonic lethality (C.J.C. and H.R.H., unpublished results). The severe effect of the *n3316* deletion on the *dpl-1* locus combined with our observation that *dpl-1(n3316)* behaves genetically like the deficiency *mnDf67* (in heterozygotes with the *dpl-1(n2994)* and *dpl-1(n3316)* alleles) for the synMuv and sterile phenotypes indicate that *n3316* is a null allele of *dpl-1* (Table 1; C.J.C. and H.R.H., unpublished observations).

DPL-1 is broadly expressed and is localized to nuclei

We obtained a crude rabbit polyclonal antiserum raised against DPL-1 (kindly provided by B. Page and J. Priess; Page et al., 2000). We purified these antibodies against a carboxy-terminal fragment of DPL-1 (see Experimental Procedures) predicted to be truncated by the *dpl-1(n3643)* premature stop codon. The purified antibodies recognized a single band of about 70 kD on western blots of wild-type protein extracts; this band was absent in extracts from *dpl-1(n3643)* mutants (Figure 2A).

We used the purified antibodies for immunostaining of fixed worms. The purified antibodies did not stain fixed *dpl-1(n3643)* mutant worms of any stage (data not shown). In wild-type animals, DPL-1 protein was expressed in most and perhaps all cells throughout development and was localized to nuclei. The P(3-8).p nuclei and nuclei of the hypodermal syncytium, hyp7, two proposed sites of synMuv gene function during vulval development (Herman and Hedgecock, 1990; Hedgecock and Herman, 1995; Thomas and Horvitz, 1999), both expressed DPL-1 (Figure 2B and data not shown). DPL-1 was also present in the descendants of P(3-8).p (Figure 2C). In addition to somatic nuclei, immature germ cell and oocyte nuclei were also sites of strong DPL-1 expression (Figure 2D).

We assessed the maternal contribution of DPL-1 protein by staining *dpl-1(n3643)* homozygous progeny of heterozygous *dpl-1(n3643)/+* mothers. DPL-1 was present in *dpl-1(n3643)* embryos but was absent from *dpl-1(n3643)* larvae generated by *dpl-1(n3643)/+* mothers (Figure 2E and data not shown). These results suggest that maternally-provided DPL-1 protein or DPL-1 protein synthesized from maternally-provided RNA is present during embryonic development but does not persist at comparable levels into larval development.

Some cell divisions are affected by loss of *dpl-1* function

DP/E2F heterodimers can promote cell cycle progression by activating the transcription of genes required for S phase (reviewed by Lavia and Jansen-Durr, 1999). We therefore wanted to determine if loss of *dpl-1* function could prevent cell division. We sought to characterize animals in which both maternally- and zygotically-provided *dpl-1* activities were severely reduced or eliminated. For this reason we combined *dpl-1(RNAi)* with the *dpl-1(n3316)* mutation. *dpl-1(RNAi)* effectively reduced the maternal contribution of *dpl-1* activity and DPL-1 protein. First, *dpl-1(RNAi)* eliminated maternal rescue (J. Thomas and H.R.H., unpublished results) of the *dpl-1* synMuv

phenotype: 55.1% (n=156) of *dpl-1(n2994); lin-15(n433)* mutants descended from *dpl-1(n2994)/+; lin-15(n433)* mothers were Muv, whereas 100% (n=147) of *dpl-1(n2994); lin-15(n433)* mutants descended from *dpl-1(n2994)/+; lin-15(n433)* mothers injected with *dpl-1* RNA were Muv. Second, we did not detect DPL-1 protein in embryos descended from mothers injected with *dpl-1* RNA (data not shown).

dpl-1(n3316 RNAi) animals developed into morphologically normal adults. Direct examination and DAPI staining indicated that the cellular divisions that generated many tissues, including the vulva and the gonad, likely occurred normally. To confirm that S phase occurred in generating these postembronically-derived structures, we monitored incorporation of the thymidine analog 5-bromo-2'-deoxyuridine (BrdU) (see Experimental Procedures). BrdU was incorporated in the P(3-8).p descendants of *dpl-1(n3316 RNAi)* animals (Figure 3A). We also observed BrdU incorporation in other cells that are generated or that synthesize DNA during the L3 larval stage, including seam cell descendants, germ cell precursors and intestinal nuclei (Figure 3A and data not shown). These results indicate that loss of *dpl-1* function does not result in a general block in cell division or S phase.

Interestingly, *dpl-1(n3316 RNAi)* animals were uncoordinated (Unc), especially in backward movement. Such Unc mutants are often defective in the generation or function of ventral cord neurons, many of which are postembryonically derived from Pn.a neuroblasts. To determine if the number of ventral cord neurons was affected in *dpl-1(n3316 RNAi)* animals, we counted ventral cord nuclei in DAPI-stained individuals. Newly-hatched *dpl-1(n3316 RNAi)* and wild-type L1 animals had similar numbers of embryonically-derived ventral cord nuclei (Figure 3D). However, the number ventral cord nuclei in *dpl-1(n3316 RNAi)* adults was substantially reduced as compared to in the wild type. Some of the nuclei in *dpl-1(n3316 RNAi)* adults that we scored as ventral cord neurons based on morphology were larger than wild-type ventral cord nuclei and possibly polyploid (Figure 3B, 3C). The reduced number and larger size of postembryonically-derived ventral cord nuclei is consistent with a defect in the Pn.a neuroblast lineages (Sulston and Horvitz, 1981).

We directly examined the P(6-10).a lineages of three *dpl-1(n3316 RNAi)* animals. In the wild type, P(6-8).a each generate five neurons and P(9-10).a each generate four neurons and one cell that undergoes programmed cell death. All 15 of the Pn.a lineages we observed in *dpl-1(n3316 RNAi)* animals were abnormal. In ten cases, the Pn.a cell generated only two cells (Pn.aa and Pn.ap) and in five cases generated only

three cells (Pn.aaa, Pn.aap and Pn.ap). In addition, the times between cell divisions in these mutant lineages were often delayed. For example, the average time between the generation and division of Pn.a cells was 4.5 hours as compared to approximately 2 hours in the wild type (Sulston and Horvitz, 1977). The cells produced by these abnormal lineages often assumed the appearance, as visualized with Nomarski optics, characteristic of terminally-differentiated neurons, although some cells retained, often for more than an hour, the clear and swelled appearance of a cell undergoing mitosis. Characteristics of terminally-differentiated neurons have previously been observed in undivided cells in mutants with Pn.a cell-lineage defects (Albertson et al., 1978; White et al., 1982). The failure to complete Pn.a lineages in *dpl-1(n3316 RNAi)* animals may reflect a requirement for *dpl-1* activity in cell cycle progression in these lineages.

Identification of two *C. elegans* E2F-like genes, *efl-1* and *efl-2*

Since E2F proteins interact with DP family members in mammals, we sought to identify *C. elegans* E2F-like genes. From *C. elegans* EST and genomic sequence databases we identified two genes, *efl-1* and *efl-2* (*efl*, *E2F-l*ike), that are predicted to encode E2F family proteins. We obtained full-length cDNA clones of *efl-1* and *efl-2* (see Supplemental Materials), as indicated by the presence of *trans*-spliced leader sequences and a poly-A tails. We deduced the gene structures of *efl-1* and *efl-2* by comparison of genomic DNA and cDNA sequences (Figure 4A).

The EFL-1 protein is similar to mammalian E2F proteins in domains required for DNA binding and for heterodimerization with DP family members (Figure 4B). The DNA-binding domains of different mammalian E2F proteins are highly conserved but the dimerization domains of these proteins are more divergent. The putative dimerization domain of EFL-1 is most similar to the dimerization domains of human E2F-4 (38% identity) and E2F-5 (38%) and less similar to the dimerization domains of E2F-1 (22%), E2F-2 (23%), E2F-3 (26%) and E2F-6 (26%). EFL-1 is also similar to E2F-4 and E2F-5 in that it lacks a nuclear localization signal found in E2F-1, E2F-2 and E2F-3 (Muller et al., 1997; Verona et al., 1997). Because E2F-4 lacks this nuclear localization signal, this protein is proposed to function only when it is recruited to the nucleus, which occurs only in G_0 and G_1 cells. With the exception of E2F-6, mammalian E2F proteins also have a small carboxy-terminal domain that interacts with pRB, p107 and p130. The EFL-1 carboxy terminus is similar to those of E2F-1, E2F-2, E2F-3, E2F-4 and E2F-5 but is not similar to that of E2F-6. Together, these comparisons suggest that EFL-1

may interact with LIN-35 Rb and may be most closely related to mammalian E2F-4 and E2F-5.

The putative dimerization domain of EFL-2 is most similar to the dimerization domains of human E2F-3 (31% identity) and E2F-6 (31%) and is somewhat less similar to the dimerization domains of E2F-1 (22%), E2F-2 (24%), E2F-4 (27%) and E2F-5 (25%). The carboxy-terminal region of EFL-2 is similar to the pRB-family interaction domains of mammalian E2F proteins. These comparisons indicate that EFL-2 is an E2F family member that may interact with LIN-35 Rb.

efl-1 is a class B synMuv gene

We used RNAi to investigate the functions of *efl-1* and *efl-2*. RNAi of *efl-1* caused a Muv phenotype in *lin-15A(n767)* mutants but not in the wild type or in *lin-15B(n744)* mutants (data not shown), indicating that *efl-1* may be a class B synMuv gene. *efl-1(RNAi)* also caused defects in backward movement similar to those observed in *dpl-1(RNAi)* animals. *efl-2(RNAi)* did not cause Muv or Unc phenotypes in a wild-type background or in either a *lin-15A(n767)* or a *lin-15B(n744)* mutant background (data not shown).

To analyze *efl-1*, we sought deletions that affected the *efl-1* locus (Supplemental Materials). We obtained a single allele, *n3318*, that removes 1152 base pairs, deleting 268 base pairs of sequence prior to the putative translation start site and the first three exons (Figure 4A). P(3-8).p cell divisions, germ cell divisions and adult morphology were all normal in *efl-1(n3318)* mutants (data not shown). We isolated another *efl-1* allele, *n3639* (C.J.C and H.R.H., unpublished results), and found a nonsense mutation predicted to truncate the EFL-1 protein after 174 amino acids (Figures 4B and 4C).

efl-1(n3318) caused a Muv phenotype as a double mutant with *lin-38(n751)*, *lin-15A(n433)* and *lin-15A(n767)*, all alleles of class A synMuv genes, whereas *efl-1(n3318); lin-15B(n744)* double mutants had wild-type vulvae (Table 1). Expression of the *efl-1* cDNA under its endogenous promoter rescued the Muv phenotype of *efl-1(n3318); lin-15A(n433)* mutants, indicating that the Muv phenotype of these mutants was caused by the *efl-1(n3318)* deletion (see Experimental Procedures). That both the *efl-1(n3318)* mutation and *efl-1*(RNAi) cause a Muv phenotype specifically in the presence of a class A synMuv mutation indicates that *efl-1* is a class B synMuv gene. The class B synMuv activity of *efl-1* is neither redundant with nor is inhibited by *efl-2*, as *efl-2(RNAi)* had little effect on the penetrance of the Muv phenotype of *efl-1(n3318);*

lin-15A(n433) mutants. In addition to the Muv phenotype, *efl-1* mutations caused sterility and embryonic lethality (C.J.C. and H.R.H., unpublished results).

DPL-1 and EFL-1 interact with each other and with LIN-35 *in vitro*

Since mammalian DP, E2F and pRB family proteins physically interact we sought to determine if DPL-1, EFL-1 and LIN-35 likewise associate. We were specifically interested in understanding the consequences of the *dpl-1(n3643)* mutation on DPL-1 protein-protein interactions. *n3643* introduces a stop codon that is predicted to truncate DPL-1 after 340 amino acids. Western blots of extracts from *dpl-1(n3643)* mutants with crude DPL-1 antiserum indicate that this truncated protein is stably expressed *in vivo* (C.J.C. and H.R.H., unpublished results). The truncated protein retains domains similar to those used by DP family members for both DNA and E2F binding. Although these domains are present in the truncated protein, *dpl-1(n3643); lin-15A(n433)* mutants are partially defective in vulval development (Table 1).

To assess DPL-1 protein-protein interactions in *dpl-1(n3643)* mutants, we compared binding properties of a DPL-1 amino-terminal fragment to those of a DPL-1 carboxy-terminal fragment. We found that GST-tagged DPL-1(31-343) but not GST-DPL-1(344-598) bound *in vitro* translated EFL-1 (Figure 5A). Therefore, DPL-1 and EFL-1 can interact, and this interaction may be mediated by a domain of DPL-1 that is similar to the domain of mammalian DP-1 important for interaction with E2F proteins.

We next tested for interactions of DPL-1 fragments with LIN-35 Rb. The 961 amino acid LIN-35 protein contains a domain (amino acids 496-897) that is similar to the A/B pocket, a protein-protein interaction domain of pRB, p107 and p130 (Lu and Horvitz, 1998). GST-DPL-1(31-343) did not bind either LIN-35(1-555) or LIN-35(270-961) fragments (Figure 5A). However, GST-DPL-1(344-598) specifically bound the LIN-35(270-961) fragment (Figure 5A), indicating that the interaction of GST-DPL-1(344-598) with LIN-35 is dependent on a carboxy-terminal region of LIN-35. Together these results indicate that a DPL-1 amino-terminal domain interacts with EFL-1 and a DPL-1 carboxy-terminal domain interacts with the LIN-35 Rb carboxy-terminus.

We next tested the interaction between EFL-1 and LIN-35 Rb. GST-EFL-1(214-342) interacted *in vitro* with LIN-35(270-961) (Figure 5B). Like the interaction of LIN-35 Rb with GST-DPL-1(344-598), this interaction was dependent upon a carboxy-terminal region of LIN-35 Rb, since LIN-35(1-555) did not bind

GST-EFL-1(214-342) (Figure 5B). We propose that the carboxy-terminal tail of EFL-1 binds the predicted A/B pocket domain of LIN-35 Rb.

We also examined the possible formation of a DPL-1/EFL-1/LIN-35 ternary complex. To address this issue, we asked whether GST-DPL-1(31-343), which does not interact directly with LIN-35(270-961), would in the presence of EFL-1 associate with LIN-35(270-961). When incubated in a single binding reaction, both EFL-1 and LIN-35(270-961) associated with GST-DPL-1(31-343) (Figure 5C). These interactions indicate the formation of a GST-DPL-1(31-343)/EFL-1/LIN-35(270-961) ternary complex.

Together these results suggest that DPL-1 and EFL-1 interact with each other and with LIN-35 Rb *in vivo*. We speculate that the mutant DPL-1/EFL-1 heterodimer in *dpl-1(n3643)* animals interacts with LIN-35 Rb only through EFL-1 and that the affinity of this interaction is not sufficient for the full function of a DPL-1/EFL-1/LIN-35 complex during vulval development. It is possible that the truncated DPL-1 protein in *dpl-1(n3643)* mutants is defective in another putative DPL-1 function, for example DNA binding, and that this defect contributes to an impaired DPL-1/EFL-1/LIN-35 complex function.

RTK/Ras pathway activity is required for *dpl-1* and *efl-1* Muv phenotypes

We conducted genetic epistasis tests to investigate the relationship between *dpl-1* and *efl-1* and genes involved in RTK/Ras signaling. Animals bearing *dpl-1(n3316)* and *lin-15A(n767)* mutations as well as either *sem-5* Grb2, *let-60* Ras, *lin-45* Raf or *mpk-1* MAPK mutant alleles were Vul, indicating that RTK/Ras pathway activity is required for the *dpl-1(n3316); lin-15A(n767)* Muv phenotype. (A *dpl-1* double mutant with *let-23* RTK was not constructed because of tight linkage and a lack of suitable markers.) We also observed a Vul phenotype in triple mutants containing *efl-1(n3318)* and *lin-15A(n767)* as well as either *let-23* RTK, *sem-5* Grb2, *let-60* Ras, *lin-45* Raf or *mpk-1* MAPK alleles. These data suggest that *dpl-1* and *efl-1* act upstream of or in parallel to the RTK/Ras pathway in vulval development.

By contrast, *dpl-1(n3316); lin-3* EGF*; lin-15A(n767)* and *lin-3* EGF*; efl-1(n3318); lin-15A(n767)* triple mutants were Muv. *lin-3* encodes an EGF-like protein that presumably binds LET-23 RTK and activates RTK/Ras signaling in P(5-7).p (Hill and Sternberg, 1992). In *lin-3* mutants, RTK/Ras signaling is not activated and P(5-7).p do not adopt vulval cell fates (Horvitz and Sulston, 1980). Consistent with our

observations, previous studies have shown that other synMuv mutants do not require either *lin-3* function or the gonadal anchor cell, the source of LIN-3 protein, for expression of a Muv phenotype (Ferguson et al., 1987; Sternberg and Horvitz, 1989; Lu and Horvitz, 1998).

There are at least two possible explanations why P(3-8).p can adopt vulval cell fates when *dpl-1*, *efl-1* and other synMuv mutations are combined with a *lin-3* mutation but cannot adopt vulval cell fates when *dpl-1*, *efl-1* and other synMuv mutations are combined with RTK/Ras pathway mutations. Both explanations assume that some RTK/Ras signaling can occur in a ligand-independent fashion, that is, in a *lin-3* mutant. First, loss of synMuv function may result in ectopic activation of RTK/Ras signaling, via a *lin-3*-independent mechanism, to a level that is sufficient to induce vulval cell fates. Alternatively, loss of synMuv function may lower the threshold of activity required for vulval cell fate specification to a point that can be exceeded by basal, uninduced RTK/Ras pathway activity. In either case, these results indicate that *dpl-1* and *efl-1* can affect cell-fate determination not only in P3.p, P4.p and P8.p but also in P(5-7).p.

DISCUSSION

DPL-1 and EFL-1 may repress rather than promote transcription during vulval development

A number of proteins with class B synMuv activity are similar to proteins implicated in chromatin modification, nucleosome remodeling and transcriptional repression. In mammals, pRB regulates expression of DP/E2F-responsive genes, in part, by recruiting the histone deacetylase HDAC1 (Brehm et al., 1998; Luo et al., 1998; Magnaghi-Jaulin et al., 1998). A pRB-associated complex that includes HDAC1 and an associated subunit, RbAp48, has been shown to deacetylate polynucleosomal substrates *in vitro*, reflecting a role of this complex in pRB-mediated repression (Nicolas et al., 2000). The *C. elegans* counterparts of these proteins, LIN-35 Rb, HDA-1 HDAC and LIN-53 p48, physically interact *in vitro* and act together in vulval development, indicating that a functional relationship as transcriptional repressors may be conserved (Lu and Horvitz, 1998). Other studies have suggested that RBA-1, CHD-3, CHD-4, and EGR-1, proteins similar to components of the NURD (nucleosome remodeling and histone deacetylase) complex, may also act in synMuv-mediated repression (Solari and Ahringer, 2000; Walhout et al., 2000).

By analogy to their mammalian counterparts, DPL-1 and EFL-1 may form a heterodimer and bind DNA to modulate gene expression by tethering to DNA a protein complex containing LIN-35 Rb, LIN-53 p48, HDA-1 HDAC and other proteins (Figure 6). Since the mammalian counterparts of LIN-35, LIN-53 and HDA-1 appear to function as transcriptional repressors, we propose that DPL-1 and EFL-1 target a repressor complex to genes required in P(3-8).p for vulval cell-fate specification, thereby antagonizing Ras signaling during vulval development. In this model, the transcription of genes required for vulval specification is ectopically activated in synMuv mutants, that is, such genes are transcribed in *dpl-1* and *efl-1* loss-of-function mutants (Figure 6). Consequently, while DPL-1/EFL-1 activity may be important for repression of target genes, we propose that, at least in the context of vulval development, DPL-1/EFL-1 activity does not appear to be required for activation of these same targets.

dpl-1 and *efl-1* antagonize RTK/Ras signaling

Mammalian Rb and Ras can act antagonistically to regulate the G_1-to-S phase transition (Mittnacht et al., 1997; Peeper et al., 1997), and E2F-4 and E2F-5 can function redundantly in mouse embryonic fibroblasts to oppose the effects of Ras on S phase entry (Gaubatz et al., 2000). In *C. elegans*, *dpl-1* and *efl-1* normally inhibit, whereas RTK/Ras signaling normally promotes, vulval cell-fate specification. Therefore, *dpl-1* and *efl-1* antagonize RTK/Ras pathway function in vulval development. As discussed above, the function of DPL-1 and EFL-1 as transcriptional repressors may be important for the regulation of vulval development, and, consequently, for the antagonism of Ras signaling. It is possible that DPL-1/EFL-1 heterodimers converge on the same targets as controlled by the *let-23* RTK/*let-60* Ras-regulated LIN-1 ETS and LIN-31 winged helix transcription factors. LIN-1 and LIN-31 form a protein complex that inhibits vulval induction; when phosphorylated by MPK-1 MAPK, this complex dissociates to release phosphorylated LIN-31, which is believed to promote vulval cell-fate specification (Tan et al., 1998). That RTK/Ras pathway activity is required for vulval cell-fate specification in *dpl-1* and *efl-1* mutants is consistent with the requirement for LIN-31 phosphorylation and activation by RTK/Ras: loss of *dpl-1* or *efl-1* function in the absence of RTK/Ras signaling would not activate transcription by an unphosphorylated LIN-31 protein. However, the existing data do not preclude models in which *dpl-1* and *efl-1* antagonize RTK/Ras signaling at another point in the pathway.

Comparisons of EFL-1 with mammalian E2F family members

Although E2F-1, E2F-2, E2F-3, E2F-4 and E2F-5 all have transactivation and pRB-family protein binding domains and hence might all function in both transcriptional activation and repression, it is possible that each E2F protein performs only one of these functions *in vivo*. E2F-4 and E2F-5 may act primarily in repression. Specifically, E2F-4 is present at the promoters of DP/E2F-responsive genes in G_0 and in early G_1, when these genes are repressed (Takahashi et al., 2000). In addition, *E2f4* and *E2f5* single and *E2f4 E2f5* double mutant mice exhibit defects in cellular differentiation events that are thought to be caused by the loss of E2F4 and E2F5 repressor complexes with pRb, p107 and p130 (Lindeman et al., 1998; Gaubatz et al., 2000; Humbert et al., 2000; Rempel et al., 2000). EFL-1 is structurally most similar to the mammalian E2F-4 and E2F-5 proteins. The role we propose for EFL-1 as a transcriptional repressor during vulval development is similar to the suspected roles of E2F-4 and E2F-5.

Are *dpl-1* DP and *efl-1* E2F required for entry into S phase?

Considerable evidence indicates that mammalian DP and E2F proteins can promote the entry of cells into S phase, thereby stimulating cell cycle progression. Our observations of *dpl-1(n3316 RNAi)* animals, which presumably are deficient in both the zygotic and maternal contribution of DPL-1, suggest that DPL-1 activity is not essential in every cell for cell cycle progression. Since *dpl-1* is the only predicted *C. elegans* DP family member and since DP protein function is thought to be necessary for DP/E2F heterodimer function, DP/E2F activity in *C. elegans* may not be generally required for cell cycle progression. However, *dpl-1* and *efl-1* may be required to promote S phase entry in some cell types. Specifically, the Pn.a neuroblasts of *dpl-1(n3316 RNAi)* animals did not complete their divisions and sometimes generated large polyploid descendants. We conclude that *dpl-1* and possibly *efl-1* may act in but are not essential for the cell cycle in *C. elegans*. We note the possibility that undetectable levels of *dpl-1* activity and DPL-1 protein may be present in *dpl-1(n3316 RNAi)* animals and may fulfill a broader requirement for *dpl-1* in promoting cell cycle progression.

As discussed above, loss-of-function mutations in *dpl-1* and *efl-1*, like loss-of-function mutations in *lin-35* Rb, cause cell-fate transformations that result in supernumerary cell divisions in the P(3,4,8).p lineages. The extra cell divisions in these mutants are consistent with the possibility that a DPL-1/EFL-1/LIN-35 protein complex normally inhibit cell cycle progression in P(3,4,8).p. Thus, while *dpl-1* and *efl-1* promote cell division in some cell types, e.g. in Pn.a descendants, *dpl-1* and *efl-1* may prevent cell division in other cell types, e.g. in P(3,4,8).p descendants.

While it is tempting to speculate that *dpl-1* and *efl-1* are cell cycle regulators in *C. elegans*, we do not yet know if the effects of these genes on cell division are caused by the direct regulation of the cell cycle machinery or are caused by the regulation of cell-fate determining factors that subsequently impinge on the cell cycle machinery. We hope that further studies of *dpl-1* and *efl-1* mutants will help establish the *in vivo* functions not only of these *C. elegans* genes but also of DP and E2F genes in other organisms, including humans.

EXPERIMENTAL PROCEDURES

Strains

All strains were cultured at 20°C on NGM agar seeded with *E. coli* strain OP50 as described by Brenner (1974). Bristol N2 was the wild-type strain. Mutant alleles used are listed below and are described by Riddle et al. (1997) unless noted otherwise: LGII *dpy-10(e128)*, *dpl-1(n2994, n3316, n3643)* (J. Thomas and H.R.H., unpublished results; this study), *let-23(sy97)*, *unc-4(e120)*, *lin-38(n751)*, *mnC1*[*dpy-10(e128) unc-52(e444)*] (Herman, 1978), *mIn1*[*dpy-10(e128) mIs14*] (M.L. Edgley, J.K. Liu, D.L. Riddle and A. Fire, unpublished results); LGIII *mpk-1(oz140)*, *dpy-17(e164)*; LGIV *lin-45(sy96)*; *lin-3(n378)*; *let-60(n2021)*; LGV *rol-4(sc8)*, *unc-76(e911)*, *efl-1(n3318, n3639)* (this study), *dpy-21(e428)*; LGX *sem-5(n2030)*, *lin-15B(n744)*, *lin-15A(n433)* (Ferguson and Horvitz, 1989), *lin-15A(n767)*. The deficiency *mnDf67* was also used (Sigurdson et al., 1984). *dpl-1(n3643)* and *efl-1(n3639)* were isolated in a screen for mutations that caused a Muv phenotype in a *lin-15A(n767)* background (C.J.C., F. Stegmeier and H.R.H., unpublished results).

Antibody preparation and immunocytochemistry

Crude anti-DPL-1 antiserum was provided by B. Page and J. Priess. This antiserum was generated by injecting purified 6His-DPL-1(294-598) into rabbits. We affinity purified anti-DPL-1 antibodies by applying this antiserum to nitrocellulose strips containing GST-DPL-1(344-598) fusion protein, and we washed and eluted bound antibody as described by Koelle and Horvitz (1996). Antibodies were further purified by preadsorption to an acetone precipitate of proteins from *dpl-1(n3643)* mutant animals, which was prepared essentially as described by Harlow and Lane (1988). Antibodies were used at a 1:500 dilution on western blots. Larvae and adults for whole-mount staining were fixed for 30 minutes as described by Nonet (1997) and embryos were fixed for 30 minutes as described by Finney and Ruvkun (1990). Fixed animals were incubated with affinity-purified preadsorbed DPL-1 antibodies at a 1:50 dilution, and FITC-conjugated goat anti-rabbit secondary antibody (Jackson Laboratories) was used for detection.

RNAi analyses

Templates for *in vitro* transcription reactions were made by PCR amplification of cDNA inserts and their flanking T3 and T7 promoter sequences. *In vitro* transcribed RNA was annealed and injected as described by Fire et al. (1998). Injected animals were transferred 10-15 hours after injection, and their progeny were analyzed. The *dpl-1* gene is located within a large intron of the gene T23G7.2. To determine if *dpl-1* mutations or *dpl-1(RNAi)* perturb T23G7.2 function, we performed RNA interference of T23G7.2. T23G7.2*(RNAi)* animals did not display the Muv, Unc or sterile phenotypes caused by *dpl-1(RNAi)* or by *dpl-1* mutations.

BrdU incorporation and detection

BrdU application and detection were performed as described by Boxem et al. (1999), except that BrdU was applied to *dpl-1(n3316 RNAi) unc-4(e120)* L2 larvae after ventral cord divisions had been completed and animals were harvested as L3 larvae after P(3-8).p divisions had commenced.

Cell lineage analysis

Animals were mounted for Nomarski microscopy and observed as described by Sulston and Horvitz (1977) for at least four hours following recovery from lethargus, during which time most nuclei in *dpl-1(n3316 RNAi)* animals adopted morphologies like those of differentiated neurons.

Transgenic strains

Germline transformations were performed as described by Mello et al. (1991). For rescue of the *dpl-1(n2994); lin-15A(n433)* Muv phenotype, we injected C32F7 (10 ng/μl) or a 5.2 kb PvuII-PvuII subclone of C32F7 (50 ng/μl) with pRF4 (80 ng/μl) as a coinjection marker. Expression of the mutant *rol-6* gene encoded by pRF4 causes a roller (Rol) phenotype (Mello et al., 1991). 3/3 C32F7 and 4/4 5.2kb PvuII-PvuII subclone transgenic lines were rescued. To rescue the Ste phenotype caused by *dpl-1(n3316)*, we injected *dpl-1(n3316) unc-4(e120)/mnC1* mutants with C32F7 (10 ng/μl) and pRF4 (80 ng/μl). We recovered F_1 and F_2 transgenic Unc animals which themselves produced dead eggs and rare live transgenic Unc progeny. To rescue the Muv phenotype of *efl-1(n3318); lin-15A(n433)* mutants we used pEFL-1.MG, a minigene construct containing the *efl-1* cDNA flanked by 1.8 kb of upstream genomic sequence and 2.1 kb of downstream genomic sequence. pEFL-1.MG (50 ng/μl) and the

coinjection marker pPD93.97 (80 ng/μl), which contains *gfp* under the control of the *myo-3* promoter, were injected into + *unc-76(e911) efl-1(n3318)* +/*rol-4(sc8)* + + *dpy-21(e428)*; *lin-15A(n433)* animals. Unc animals of transgenic lines were scored, and 5/6 lines were rescued for the Muv phenotype. To obtain genomic DNA clones of the *efl-1* locus we used an *efl-1* cDNA fragment to screen a library of *C. elegans* genomic DNA cloned into the λ2001 vector (A. Coulson, personal communication). We obtained two clones, λE4-1 and λE11-1, that together spanned the *efl-1* locus. To rescue the Ste Mel phenotype caused by *efl-1(n3318)*, we injected + *unc-76(e911) efl-1(n3318)* +/*rol-4(sc8)* + + *dpy-21(e428)* mutants with λE4-1 (20 ng/μl), λE11-1 (20 ng/μl) and pPD93.97 (80 ng/μl). 5/7 Unc transgenic lines were rescued.

In vitro binding experiments

Constructs encoding GST-DPL-1(31-343) and GST-DPL-1(344-598) were made by subcloning portions of the *dpl-1* cDNA into pGEX-5X-1 and pGEX-3X (Pharmacia), respectively. The construct encoding GST-EFL-1(214-342) was made by subcloning a portion of the *efl-1* cDNA into pGEX-2T (Pharmacia). Fusion proteins were expressed in BL21(DE3) cells and purified using glutathione sepharose resin according to the manufacturer's recommendations (Pharmacia). A portion of the *efl-1* cDNA encoding amino acids 8-342 was cloned into pCITE-4a(+) (Novagen). Constructs encoding LIN-35(1-555), and LIN-35(270-961), were described previously (Lu and Horvitz, 1998). These constructs were used as templates for in vitro synthesis of ^{35}S-labeled proteins (TNT Coupled Reticulocyte Lysate System, Promega). Binding experiments were performed as described by Reddien and Horvitz (2000), and bound proteins were analyzed by SDS-PAGE and autoradiography.

ACKNOWLEDGMENTS

We thank Mark Alkema, Scott Cameron, Ewa Davison, Brad Hersh, Jackie Lees and Eric Miska for comments concerning this manuscript; Mark Metzstein and Jeff Thomas for helpful discussions during the course of this work; and Barbara Page and Jim Priess for providing crude anti-DPL-1 antiserum and for communicating results prior to publication. We also thank Frank Stegmeier for assistance in isolating *dpl-1(n3643)* and *efl-1(n3639)*; Beth Castor for DNA sequence determination; Na An for strain management; Rajesh Ranganathan, Peter Reddien and other members of the Horvitz laboratory for constructing the deletion library; Alan Coulson for the λ genomic library; Andy Fire for pPD93.97; Yuji Kohara for cDNA clones; Peter Okkema for *C. elegans* cDNA libraries; the *C. elegans* Genome Sequencing Consortium for genome sequence of the *dpl-1* and *efl-2* loci; and the *C. elegans* Genetics Center for strains used in this work. This work was supported by NIH grant GM24663. C.J.C. was a Koch Graduate Fellow. H.R.H. is an Investigator of the Howard Hughes Medical Institute.

REFERENCES

Albertson, D. G., Sulston, J. E., and White, J. G. (1978). Cell cycling and DNA replication in a mutant blocked in cell division in the nematode *Caenorhabditis elegans*. Dev. Biol. *63*, 165-178.

Boxem, M., Srinivasan, D. G., and van den Heuvel, S. (1999). The *Caenorhabditis elegans* gene *ncc-1* encodes a cdc2-related kinase required for M phase in meiotic and mitotic cell divisions, but not for S phase. Development *126*, 2227-2239.

Brehm, A., Miska, E. A., McCance, D. J., Reid, J. L., Bannister, A. J., and Kouzarides, T. (1998). Retinoblastoma protein recruits histone deacetylase to repress transcription. Nature *391*, 597-601.

Brenner, S. (1974). The genetics of *Caenorhabditis elegans*. Genetics *77*, 71-94.

C. elegans Sequencing Consortium. (1998). Genome sequence of the nematode *C. elegans*: a platform for investigating biology. Science *282*, 2012-2018.

Clark, S. G., Lu, X., and Horvitz, H. R. (1994). The *Caenorhabditis elegans* locus *lin-15*, a negative regulator of a tyrosine kinase signaling pathway, encodes two different proteins. Genetics *137*, 987-997.

Dyson, N. (1998). The regulation of E2F by pRB-family proteins. Genes Dev. *12*, 2245-2262.

Ferguson, E. L., and Horvitz, H. R. (1989). The multivulva phenotype of certain *Caenorhabditis elegans* mutants results from defects in two functionally redundant pathways. Genetics *123*, 109-121.

Ferguson, E. L., Sternberg, P. W., and Horvitz, H. R. (1987). A genetic pathway for the specification of the vulval cell lineages of *Caenorhabditis elegans*. Nature *326*, 259-267.

Finney, M., and Ruvkun, G. (1990). The *unc-86* gene product couples cell lineage and cell identity in *C. elegans*. Cell *63*, 895-905.

Fire, A., Xu, S., Montgomery, M. K., Kostas, S. A., Driver, S. E., and Mello, C. C. (1998). Potent and specific genetic interference by double-stranded RNA in *Caenorhabditis elegans*. Nature *391*, 806-811.

Gaubatz, S., Lindeman, G. J., Ishida, S., Jakoi, L., Nevins, J. R., Livingston, D. M., and Rempel, R. E. (2000). E2F4 and E2F5 play an essential role in pocket protein-mediated G1 control. Mol. Cell *6*, 729-735.

Girling, R., Partridge, J. F., Bandara, L. R., Burden, N., Totty, N. F., Hsuan, J. J., and La Thangue, N. B. (1993). A new component of the transcription factor DRTF1/E2F. Nature *362*, 83-87.

Harlow, E., and Lane, D. P. (1988). Antibodies: A Laboratory Manual (Cold Spring Harbor, New York: Cold Spring Harbor Laboratory Press).

Hedgecock, E. M., and Herman, R. K. (1995). The *ncl-1* gene and genetic mosaics of *Caenorhabditis elegans*. Genetics *141*, 989-1006.

Helin, K., Wu, C. L., Fattaey, A. R., Lees, J. A., Dynlacht, B. D., Ngwu, C., and Harlow, E. (1993). Heterodimerization of the transcription factors E2F-1 and DP-1 leads to cooperative *trans*-activation. Genes Dev. *7*, 1850-1861.

Herman, R. K. (1978). Crossover suppressors and balanced recessive lethals in *Caenorhabditis elegans*. Genetics *88*, 49-65.

Herman, R. K., and Hedgecock, E. M. (1990). Limitation of the size of the vulval primordium of *Caenorhabditis elegans* by *lin-15* expression in surrounding hypodermis. Nature *348*, 169-171.

Hill, R. J., and Sternberg, P. W. (1992). The gene *lin-3* encodes an inductive signal for vulval development in *C. elegans*. Nature *358*, 470-476.

Horvitz, H. R., and Sulston, J. E. (1980). Isolation and genetic characterization of cell-lineage mutants of the nematode *Caenorhabditis elegans*. Genetics *96*, 435-454.

Hsieh, J., Liu, J., Kostas, S. A., Chang, C., Sternberg, P. W., and Fire, A. (1999). The RING finger/B-box factor TAM-1 and a retinoblastoma-like protein LIN-35 modulate context-dependent gene silencing in *Caenorhabditis elegans*. Genes Dev. *13*, 2958-2970.

Huang, L. S., Tzou, P., and Sternberg, P. W. (1994). The *lin-15* locus encodes two negative regulators of *Caenorhabditis elegans* vulval development. Mol. Biol. Cell *5*, 395-411.

Humbert, P. O., Rogers, C., Ganiatsas, S., Landsberg, R. L., Trimarchi, J. M., Dandapani, S., Brugnara, C., Erdman, S., Schrenzel, M., Bronson, R. T., and Lees, J. A. (2000). E2F4 is essential for normal erythrocyte maturation and neonatal viability. Mol. Cell *6*, 281-291.

Koelle, M. R., and Horvitz, H. R. (1996). EGL-10 regulates G protein signaling in the *C. elegans* nervous system and shares a conserved domain with many mammalian proteins. Cell *84*, 115-125.

Lavia, P., and Jansen-Durr, P. (1999). E2F target genes and cell-cycle checkpoint control. Bioessays *21*, 221-230.

Lindeman, G. J., Dagnino, L., Gaubatz, S., Xu, Y., Bronson, R. T., Warren, H. B., and Livingston, D. M. (1998). A specific, nonproliferative role for E2F-5 in choroid plexus function revealed by gene targeting. Genes Dev. *12*, 1092-1098.

Lu, X., and Horvitz, H. R. (1998). *lin-35* and *lin-53*, two genes that antagonize a *C. elegans* Ras pathway, encode proteins similar to Rb and its binding protein RbAp48. Cell *95*, 981-991.

Luo, R. X., Postigo, A. A., and Dean, D. C. (1998). Rb interacts with histone deacetylase to repress transcription. Cell *92*, 463-473.

Magnaghi-Jaulin, L., Groisman, R., Naguibneva, I., Robin, P., Lorain, S., Le Villain, J. P., Troalen, F., Trouche, D., and Harel-Bellan, A. (1998). Retinoblastoma protein represses transcription by recruiting a histone deacetylase. Nature *391*, 601-605.

Mello, C. C., Kramer, J. M., Stinchcomb, D., and Ambros, V. (1991). Efficient gene transfer in *C. elegans*: extrachromosomal maintenance and integration of transforming sequences. EMBO J. *10*, 3959-3970.

Mittnacht, S., Paterson, H., Olson, M. F., and Marshall, C. J. (1997). Ras signalling is required for inactivation of the tumour suppressor pRb cell-cycle control protein. Curr. Biol. *7*, 219-221.

Muller, H., Moroni, M. C., Vigo, E., Petersen, B. O., Bartek, J., and Helin, K. (1997). Induction of S-phase entry by E2F transcription factors depends on their nuclear localization. Mol. Cell. Biol. *17*, 5508-5520.

Nicolas, E., Morales, V., Magnaghi-Jaulin, L., Harel-Bellan, A., Richard-Foy, H., and Trouche, D. (2000). RbAp48 belongs to the histone deacetylase complex that associates with the retinoblastoma protein. J. Biol. Chem. *275*, 9797-9804.

Nonet, M. L., Staunton, J. E., Kilgard, M. P., Fergestad, T., Hartwieg, E., Horvitz, H. R., Jorgensen, E. M., and Meyer, B. J. (1997). *Caenorhabditis elegans rab-3* mutant synapses exhibit impaired function and are partially depleted of vesicles. J. Neurosci. *17*, 8061-8073.

Page, B. D., Guedes, S., Waring, D., and Priess, J. R. (2000). The *C. elegans* E2F- and DP-related proteins are required for embryonic asymmetry and negatively regulate Ras/Mapk signaling. Submitted for publication.

Peeper, D. S., Upton, T. M., Ladha, M. H., Neuman, E., Zalvide, J., Bernards, R., DeCaprio, J. A., and Ewen, M. E. (1997). Ras signalling linked to the cell-cycle machinery by the retinoblastoma protein. Nature *386*, 177-181.

Potter, C. J., Turenchalk, G. S., and Xu, T. (2000). *Drosophila* in cancer research. An expanding role. Trends Genet. *16*, 33-39.

Reddien, P. W., and Horvitz, H. R. (2000). CED-2/CrkII and CED-10/Rac control phagocytosis and cell migration in *Caenorhabditis elegans*. Nat. Cell Biol. *2*, 131-136.

Rempel, R. E., Saenz-Robles, M. T., Storms, R., Morham, S., Ishida, S., Engel, A., Jakoi, L., Melhem, M. F., Pipas, J. M., Smith, C., and Nevins, J. R. (2000). Loss of E2F4 activity leads to abnormal development of multiple cellular lineages. Mol. Cell *6*, 293-306.

Riddle, D. L., Blumenthal, T., Meyer, B. J., and Priess, J. R., eds. (1997). *C. elegans* II (Cold Spring Harbor, New York: Cold Spring Harbor Laboratory Press).

Sigurdson, D. C., Spanier, G. J., and Herman, R. K. (1984). *Caenorhabditis elegans* deficiency mapping. Genetics *108*, 331-345.

Solari, F., and Ahringer, J. (2000). NURD-complex genes antagonise Ras-induced vulval development in *Caenorhabditis elegans*. Curr. Biol. *10*, 223-226.

Sternberg, P. W., and Han, M. (1998). Genetics of RAS signaling in *C. elegans*. Trends Genet. *14*, 466-472.

Sternberg, P. W., and Horvitz, H. R. (1989). The combined action of two intercellular signaling pathways specifies three cell fates during vulval induction in *C. elegans*. Cell *58*, 679-693.

Sulston, J. E., and Horvitz, H. R. (1977). Post-embryonic cell lineages of the nematode, *Caenorhabditis elegans*. Dev. Biol. *56*, 110-156.

Sulston, J. E., and Horvitz, H. R. (1981). Abnormal cell lineages in mutants of the nematode *Caenorhabditis elegans*. Dev. Biol. *82*, 41-55.

Takahashi, Y., Rayman, J. B., and Dynlacht, B. D. (2000). Analysis of promoter binding by the E2F and pRB families in vivo: distinct E2F proteins mediate activation and repression. Genes Dev *14*, 804-816.

Tan, P. B., Lackner, M. R., and Kim, S. K. (1998). MAP kinase signaling specificity mediated by the LIN-1 Ets/LIN-31 WH transcription factor complex during *C. elegans* vulval induction. Cell *93*, 569-580.

Thomas, J. H., and Horvitz, H. R. (1999). The *C. elegans* gene *lin-36* acts cell autonomously in the *lin-35* Rb pathway. Development *126*, 3449-3459.

Verona, R., Moberg, K., Estes, S., Starz, M., Vernon, J. P., and Lees, J. A. (1997). E2F activity is regulated by cell cycle-dependent changes in subcellular localization. Mol. Cell. Biol. *17*, 7268-7282.

von Zelewsky, T., Palladino, F., Brunschwig, K., Tobler, H., Hajnal, A., and Muller, F. (2000). The C. elegans Mi-2 chromatin-remodelling proteins function in vulval cell fate determination. Development *127*, 5277-5284.

Walhout, A. J., Sordella, R., Lu, X., Hartley, J. L., Temple, G. F., Brasch, M. A., Thierry-Mieg, N., and Vidal, M. (2000). Protein interaction mapping in *C. elegans* using proteins involved in vulval development. Science *287*, 116-122.

White, J. G., Horvitz, H. R., and Sulston, J. E. (1982). Neurone differentiation in cell lineage mutants of *Caenorhabditis elegans*. Nature *297*, 584-587.

Wu, C. L., Zukerberg, L. R., Ngwu, C., Harlow, E., and Lees, J. A. (1995). In vivo association of E2F and DP family proteins. Mol. Cell. Biol. *15*, 2536-2546.

TABLE

Table 1. *dpl-1* and *efl-1* mutations cause a synMuv phenotype

Genotype	Percent Muv (n)
N2	0 (221)
lin-15A(n433)	0 (143)
lin-15A(n767)	0 (155)
lin-15B(n744)	0 (108)
dpl-1(n2994)	0.6 (173)
dpl-1(n3316)	0 (112)
dpl-1(n3643)	0 (132)
dpl-1(RNAi)	0 (102)
dpl-1(n3316 RNAi)	1.6 (123)
efl-1(n3318)	0 (202)
efl-1(n3639)	0 (84)
mnDf67/+	0 (116)
dpl-1(n2994)/+	0 (167)
dpl-1(n3316)/+	0 (126)
dpl-1(n2994)/dpl-1(n3316)	0 (101)
dpl-1(n2994)/mnDf67	0 (101)
dpl-1(n3316)/mnDf67	0 (113)
dpl-1(n2994); lin-15A(n433)	100 (366)
dpl-1(n3316); lin-15A(n433)	99 (103)
dpl-1(n3316); lin-15B(n744)	0 (150)
dpl-1(n3643); lin-15A(n433)	81 (229)
mnDf67/+; lin-15A(n433)	0 (221)
dpl-1(n2994)/+; lin-15A(n433)	0 (170)
dpl-1(n3316)/+; lin-15A(n433)	0 (105)
dpl-1(n2994)/dpl-1(n3316); lin-15A(n433)	99 (127)
dpl-1(n2994)/mnDf67; lin-15A(n433)	99 (200)
dpl-1(n3316)/mnDf67; lin-15A(n433)	98 (102)
lin-38(n751); efl-1(n3318)	100 (129)
efl-1(n3318); lin-15A(n433)	88 (193)

efl-1(n3318); lin-15A(n767)	100 (112)
efl-1(n3318); lin-15B(n744)	1 (176)
*efl-1(n3318); efl-2(*RNAi*)*	0 (214)
*efl-1(n3318); lin-15A(n433); efl-2(*RNAi*)*	84 (238)
efl-1(n3639); lin-15A(n767)	100 (51)

To analyze the Muv phenotype of *dpl-1* mutants, L4 larvae were scored for the presence of pseudovulval invaginations using Nomarski DIC optics. The complete genotypes of animals scored, in either *lin-15A(+)* or *lin-15A(n433)* backgrounds, were, from top to bottom, as follows: *dpl-1(n2994)*, *dpy-10(e128) dpl-1(n3316)* +/+ *dpl-1(n3316) unc-4(e120)*, *dpl-1(n3643)*, *dpl-1(RNAi)*, + *mnDf67 unc-4(e120)/dpy-10(e128)* + +, *dpy-10(e128) dpl-1(n2994)*/+ +, + *dpl-1(n3316) unc-4(e120)/dpy-10(e128)* + +, *dpy-10(e128) dpl-1(n2994)* +/+ *dpl-1(n3316) unc-4(e120)*, *dpy-10(e128) dpl-1(n2994)* +/+ *mnDf67 unc-4(e120)*, *dpy-10(e128) dpl-1(n3316)* +/+ *mnDf67 unc-4(e120)*. NA = not applicable; ND = not determined. To analyze the Muv phenotype of *efl-1(n3318)* and *efl-1(n3639)* homozygotes in the specified genetic backgrounds, we scored L4 Unc progeny from + *unc-76(e911) efl-1(n3318)* +/*rol-4(sc8)* + + *dpy-21(e428)* and from + *efl-1(n3639)* +/*rol-4(sc8)* + *dpy-21(e428)* mothers, respectively, for the presence of pseudovulval invaginations using Nomarski DIC optics. Animals were recovered from microscope slides and scored for the Ste Mel and Ste phenotypes to confirm the presence of *efl-1(n3318)* and *efl-1(n3639)*, respectively. To analyze interaction between *efl-1* and *efl-2*, + *unc-76(e911) efl-1(n3318)* +/*rol-4(sc8)* + + *dpy-21(e428); lin-15(n433)* mothers were injected with *efl-2* RNAi and their progeny were scored as described above.

FIGURES

Figure 1. *dpl-1* cloning

(A) (top) Genetic map location of the class B synMuv allele *n2994* on linkage group II. (bottom) Segment of the rescuing cosmid C32F7 containing the *dpl-1* gene and other predicted genes. Arrows indicate the direction of transcription. The PvuII-PvuII subclone derived from C32F7 that rescues the Muv phenotype of *n2994; lin-15A(n433)* mutants is indicated.

(B) Gene structure of *dpl-1* as derived from cDNA and genomic sequences. Coding sequences are shaded. Translation initiation and termination codons and the poly(A) tail are indicated. An in-frame stop codon upstream of the translation initiation codon is also shown. The positions of and changes caused by *dpl-1* point mutations are indicated above (arrows) and sequence deleted in the *n3316* mutant is indicated below (bracket). *n3643* has two point mutations, one causing a tyrosine-to-ochre substitution and the other a glycine-to-arginine substitution.

(C) Alignment of DPL-1 with human DP-1 (accession number NP 009042), human DP-2 (Q14188) and *Drosophila* DP (B55745). Solid boxes indicate identities with DPL-1. Arrowheads indicate the site of the splice junction affected by *n2994* and the sites of the two *n3643* mutations. The sequence removed by *n3316* is indicated by brackets. The DNA-binding and E2F-binding domains of human DP-1 are underlined with solid and hatched lines, respectively (Girling et al., 1993; Wu et al., 1995).

Figure 1

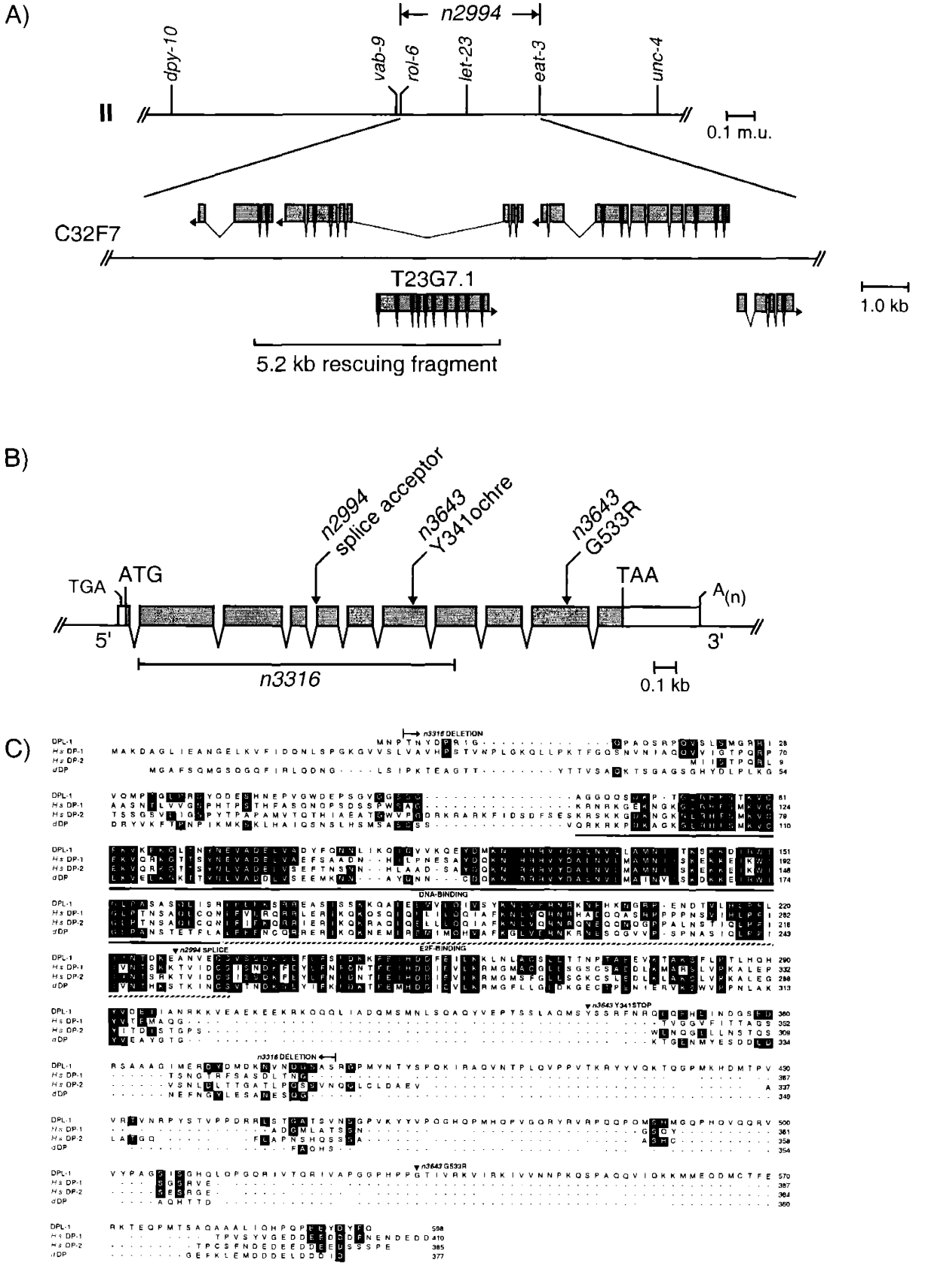
A)
n2994
dpy-10
vab-9
rol-6
let-23
eat-3
unc-4
II
0.1 m.u.
C32F7
T23G7.1
1.0 kb
5.2 kb rescuing fragment
B)
n2994 splice acceptor
n3643 Y341ochre
n3643 G533R
TGA
ATG
TAA
A(n)
5'
3'
n3316
0.1 kb
C)
n3316 DELETION
DNA-BINDING
n2994 SPLICE
E2F-BINDING
n3643 Y341STOP
n3316 DELETION
n3643 G533R

Figure 2. DPL-1 is expressed broadly in nuclei

(A) Western blot of wild type and *dpl-1(n3643)* protein extracts with purified anti-DPL-1 antiserum.

(B-E) Whole-mount staining with anti-DPL-1 antiserum.

(B) Staining of a wild-type L2 larva. P(3-8).p nuclei are indicated by arrowheads.

(C) DPL-1 expression in nuclei of P(3-8).p descendants (arrows) in a wild-type L4 larva.

(D) DPL-1 expression in immature germ nuclei and oocyte nuclei of a wild-type adult.

(E) Staining of a *dpl-1(n3643)* pretzel-stage embryo derived from a *dpl-1(n3643)/+* mother. We recognized *dpl-1(n3643)* homozygotes as non-GFP progeny of *dpl-1(n3643)/mln1*[*dpy-10(e128) mls14*] mothers. *mls14*, an integrated transgene linked to the chromosomal inversion *mln1*, consists of a combination of GFP-expressing transgenes that allow *mls14*-containing animals to be scored beginning at the 4-cell stage of embryogenesis (M.L. Edgley, J.K. Liu, D.L. Riddle and A. Fire, personal communication).

The scale bar in each panel represents 5 μm.

Figure 2

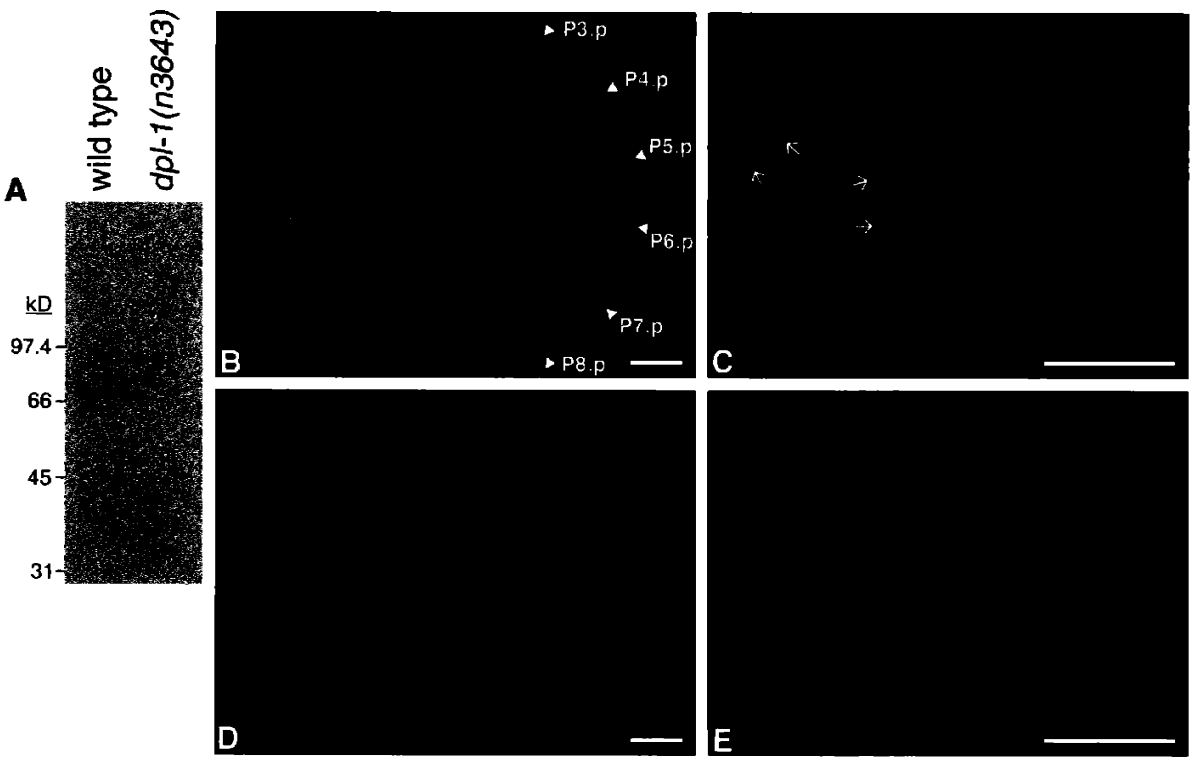
A
wild type
dpl-1(n3643)
kD
97.4
66
45
31
B
P3.p
P4.p
P5.p
P6.p
P7.p
P8.p
C
D
E

Figure 3. Characterization of P cell descendants in *dpl-1(n3316 RNAi)* animals
(A) BrdU incorporation in L3 stage *dpl-1(n3316 RNAi)* animals. Pn.px and Pn.pxx cells are shown as descendants of their respective Pn.p precursor cells. An intestinal cell nucleus (arrow) and a germ cell nucleus (arrowhead) are indicated. All of these cell types incorporate BrdU in wild-type animals (data not shown). Anterior is to the left, and ventral is down.
(B, C) DAPI-stained ventral cord nuclei in wild-type (B) and in *dpl-1(n3316 RNAi)* (C) animals. Neurons with normal morphology (arrows); an abnormally large and polyploid neuronal-like nucleus (arrowhead).
The scale bar in each panel represents 5 μm.
(D) Numbers of ventral cord nuclei in the wild type and in *dpl-1(n3316 RNAi)* animals. Animals were stained with DAPI and nuclei between the retrovesicular ganglion and P10.p were counted.

Figure 3

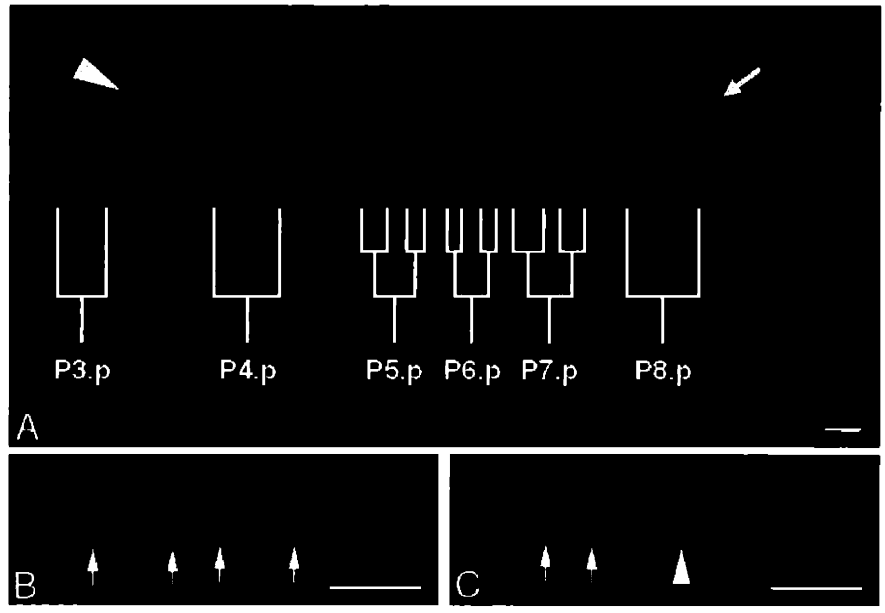

D. *dpl-1(n3316 RNAi)* adults have a reduced number of ventral cord neurons

Genotype	Stage	No. neurons ± SD
wild type	L1	15.0 ± 0.2 (n=36)
dpl-1(n3316 RNAi)	L1	14.9 ± 0.3 (n=30)
wild type	adult	56.3 ± 2.2 (n=48)
dpl-1(n3316 RNAi)	adult	25.5 ± 3.3 (n=44)

Figure 4. Identification of *efl-1* and *efl-2*

(A) Gene structures of *efl-1* and *efl-2* as deduced from cDNA and genomic sequences. Coding sequences are shaded. Translation initiation and termination codons, SL1 and SL2 *trans*-spliced leaders and poly(A) tails are indicated. The region deleted in *efl-1(n3318)* mutants is bracketed.

(B) Alignment of EFL-1 and EFL-2 with human E2F proteins (human E2F-4, accession number NP 001941; E2F-5, NP 001942; E2F-1, Q01094; E2F-2, NP 004082; E2F-3, NP001940; E2F-6, O75461). Solid boxes indicate identities between EFL-1 and another protein. Shaded boxes indicate identities between EFL-2 and a human E2F protein. EFL-1 sequence removed by *n3318* is indicated by brackets. The DNA-binding (solid lines), DP-binding (hatched lines) and pRB-binding (dotted line) domains and the nuclear localization signals (NLS; asterisks) of mammalian E2F proteins are indicated.

Figure 4

A)

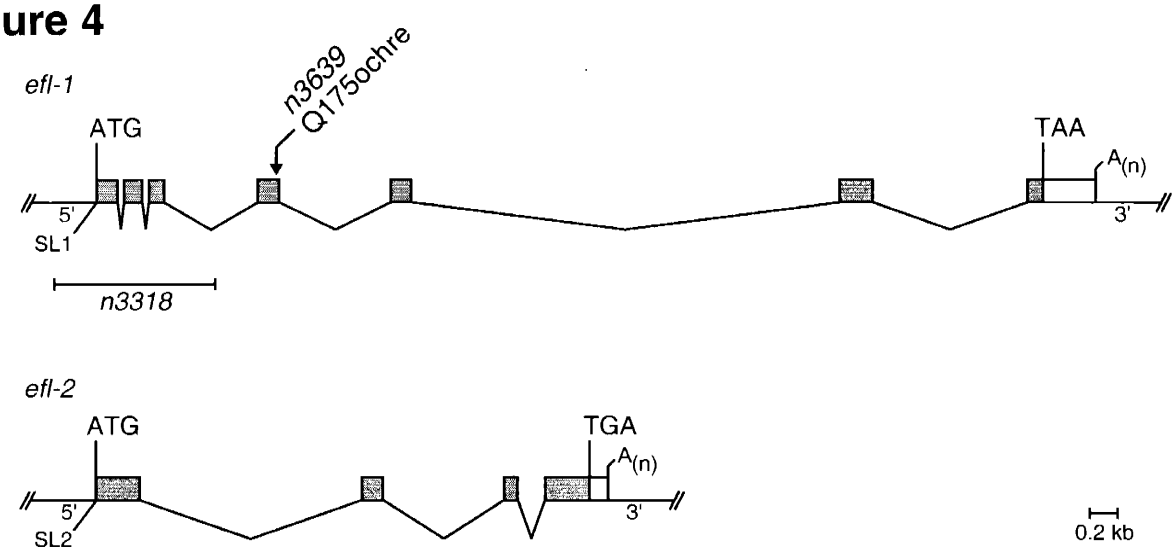
efl-1
n3639
Q175ochre
ATG
TAA
A(n)
5'
3'
SL1
n3318
efl-2
ATG
TGA
A(n)
5'
3'
SL2
0.2 kb

B)

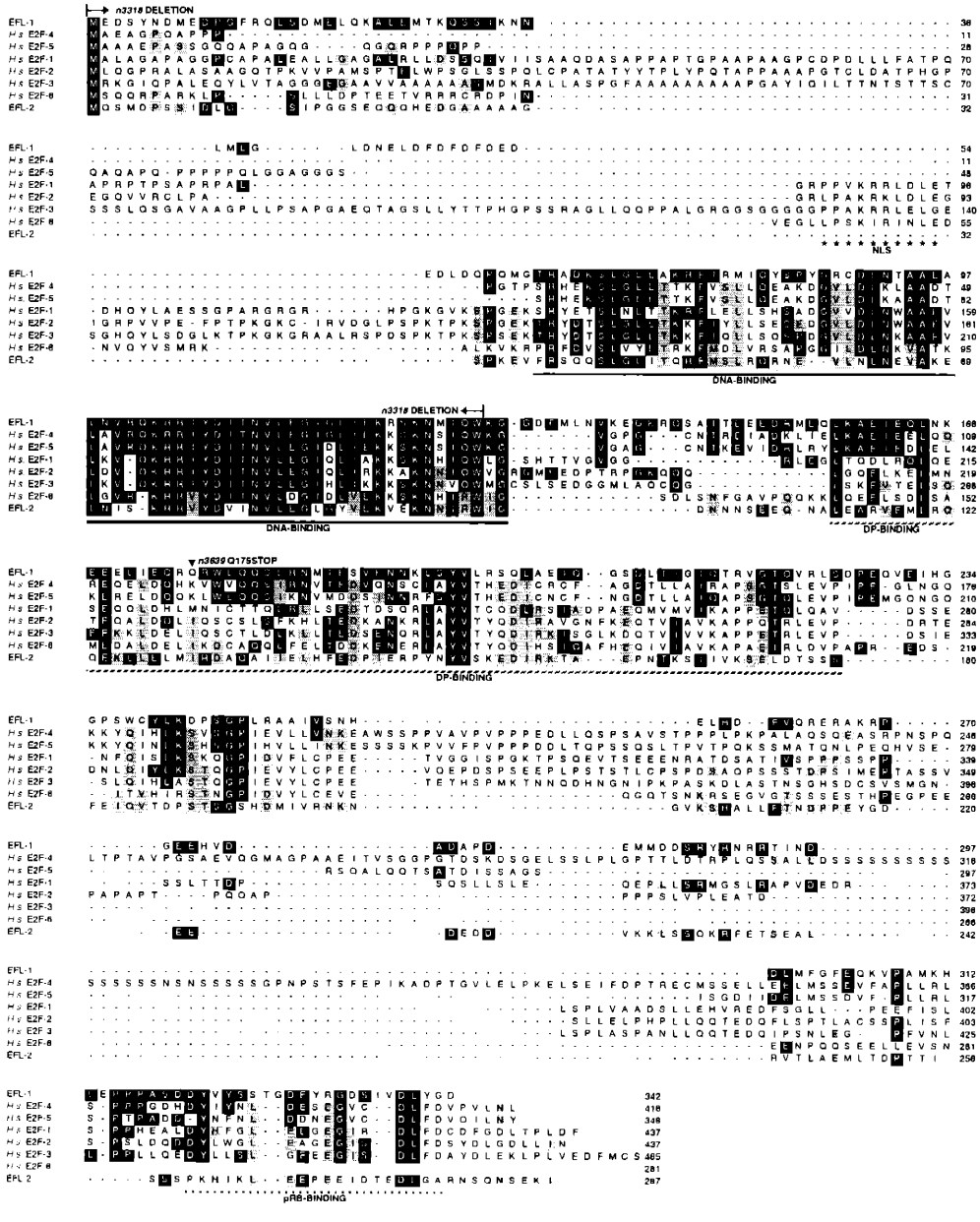
n3318 DELETION
NLS
DNA-BINDING
n3639 Q175STOP
DP-BINDING
pRB-BINDING

Figure 5. DPL-1, EFL-1 and LIN-35 *in vitro* interactions

(A) The DPL-1 amino terminus interacted with EFL-1 and the DPL-1 carboxy terminus interacted with LIN-35. GST-DPL-1 (amino acids 31-343) and GST-DPL-1 (amino acids 344-598) were incubated with ^{35}S-labeled EFL-1 , LIN-35 (amino acids 1-555), LIN-35 (amino acids 270-961) and luciferase.

(B) The EFL-1 carboxy-terminus interacted with LIN-35. GST-EFL-1 (amino acids 214-342) was incubated with ^{35}S-labeled LIN-35(1-555), LIN-35(270-961) and luciferase. None of the ^{35}S-labeled proteins interacted with GST alone.

(C) LIN-35 interaction with the DPL-1 amino-terminus was dependent on EFL-1. GST-DPL-1(31-343) was incubated with ^{35}S-labeled EFL-1 and LIN-35(1-555) and with ^{35}S-labeled EFL-1 and LIN-35(270-961).

(D) 20% of the ^{35}S-labeled proteins used in the binding reactions is shown.

(E) Coomassie blue staining of purified GST-DPL-1(31-343), GST-DPL-1(344-598), GST-EFL-1(214-342) and GST proteins used in the binding reactions.

Binding reactions (panels A-C) were performed as described by Reddien and Horvitz (2000). ^{35}S-labeled bound proteins (panels A-C) or input proteins (panel D) were resolved by 10% SDS-PAGE and analyzed by autoradiography. GST-tagged proteins (panel E) were resolved by 10% SDS-PAGE and stained with Coomassie blue.

Figure 5

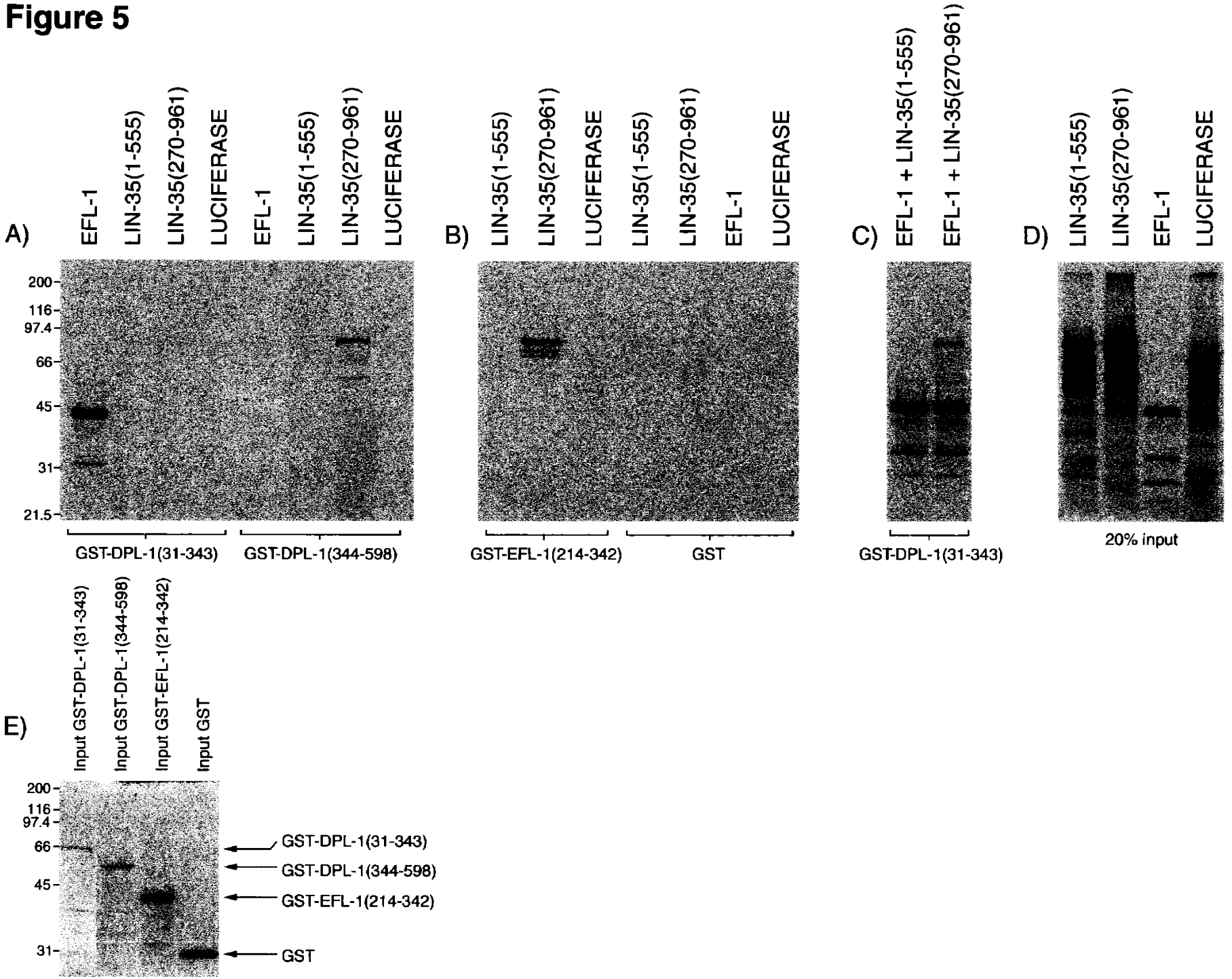
A)
EFL-1
LIN-35(1-555)
LIN-35(270-961)
LUCIFERASE
EFL-1
LIN-35(1-555)
LIN-35(270-961)
LUCIFERASE
200
116
97.4
66
45
31
21.5
GST-DPL-1(31-343)
GST-DPL-1(344-598)
B)
LIN-35(1-555)
LIN-35(270-961)
LUCIFERASE
LIN-35(1-555)
LIN-35(270-961)
EFL-1
LUCIFERASE
GST-EFL-1(214-342)
GST
C)
EFL-1 + LIN-35(1-555)
EFL-1 + LIN-35(270-961)
GST-DPL-1(31-343)
D)
LIN-35(1-555)
LIN-35(270-961)
EFL-1
LUCIFERASE
20% input
E)
Input GST-DPL-1(31-343)
Input GST-DPL-1(344-598)
Input GST-EFL-1(214-342)
Input GST
200
116
97.4
66
45
31
GST-DPL-1(31-343)
GST-DPL-1(344-598)
GST-EFL-1(214-342)
GST

Figure 6. Model: DPL-1 and EFL-1 may repress but not activate transcription. DNA sequences bound by transcription factors are indicated by black boxes, and a representative vulval specification gene is shown as an open box. In this model, a DPL-1/EFL-1 heterodimer tethers LIN-35 Rb and a complex containing LIN-53 p48, HDA-1 HDAC and proteins that repress transcription, denoted as "X", to DNA. In wild-type P3.p, P4.p and P8.p cells (top), this complex is active and represses transcription of vulval specification genes. In *lin-35; synmuvA* mutants (middle), the transcriptional repressor complex is uncoupled from DPL-1/EFL-1 and transcription of vulval specification genes is activated. Since P3.p, P4.p and P8.p adopt 1°/2° fates in *dpl-1; synmuvA* and *efl-1; synmuvA* we propose that vulval specification genes are also activated in these mutants, presumably by another transcriptional activator, denoted here as "Act" (bottom).

Figure 6

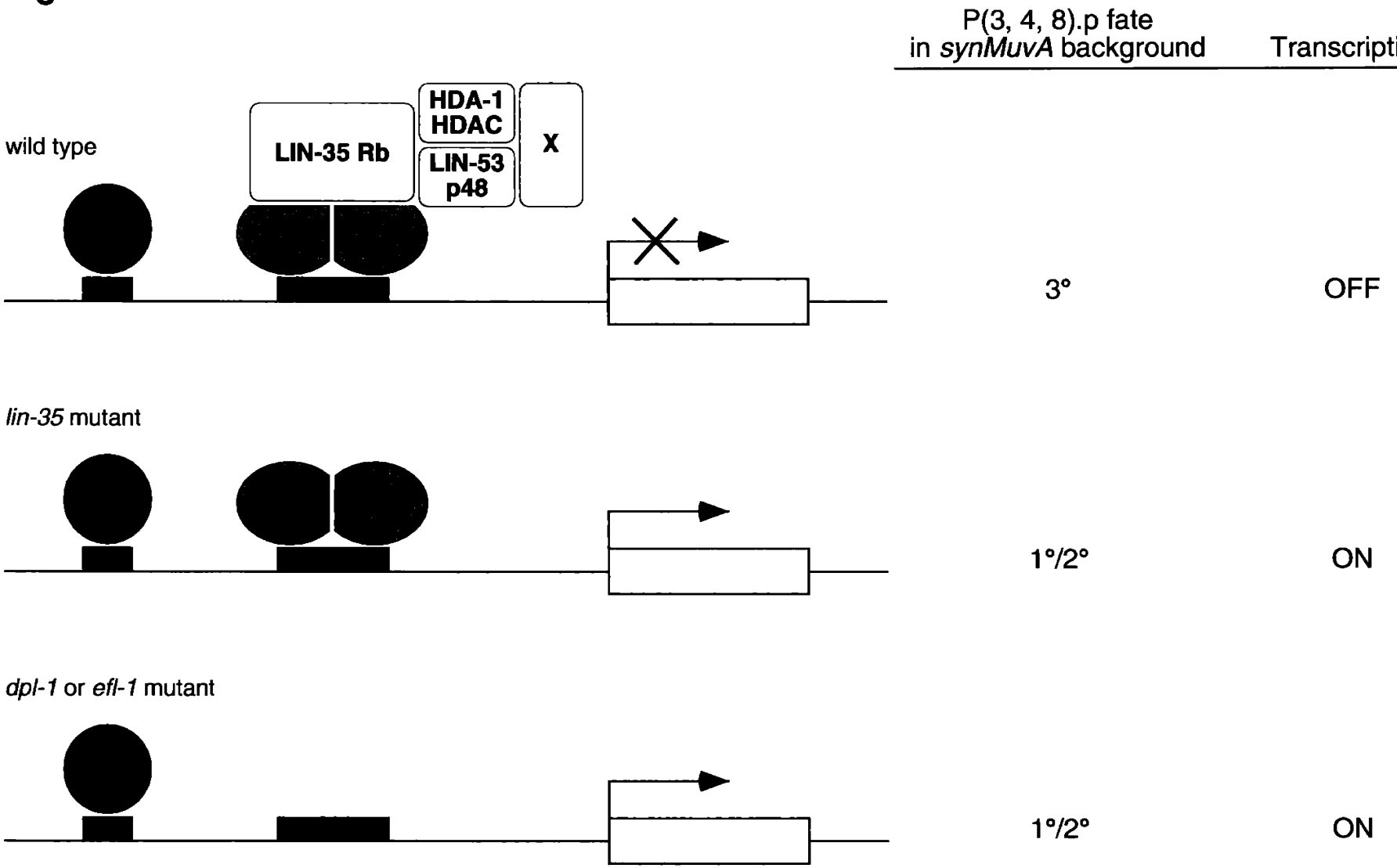
P(3, 4, 8).p fate
in synMuvA background
Transcription
wild type
LIN-35 Rb
HDA-1
HDAC
LIN-53
p48
X
3°
OFF
lin-35 mutant
1°/2°
ON
dpl-1 or efl-1 mutant
1°/2°
ON

SUPPLEMENTAL DATA

Isolation of deletion mutants

Using PCR we screened 1.47×10^6 chemically mutagenized haploid genomes for deletions in *dpl-1* and *efl-1*. Screening was performed essentially as described by Jansen *et al.* (1997). Our laboratory's deletion library was based on a design described by Liu *et al.* (1999). Both *dpl-1(n3316)* and *efl-1(n3318)* were backcrossed eight times to N2 prior to phenotypic characterization and strain construction.

Genetic mapping

We mapped both the *dpl-1(n3316)* deletion (using PCR as above) and its associated Ste phenotype to LGII between *dpy-10* and *unc-4* using standard methods. Among the progeny of *dpl-1(n3316)/dpy-10 unc-4* mothers, 10/22 Dpy non-Unc and 11/23 Unc non-Dpy F_1s were *dpl-1(n3316)/dpl-1(+)* and segregated Ste animals, and 12/22 Dpy non-Unc and 12/23 Unc non-Dpy F_1s were *dpl-1(+)/dpl-1(+)* and did not segregate Ste animals. Since *dpy-10* and *unc-4* are 1.75 map units apart, these data indicate that the *ste* mutation lies within about 0.04 map units of *dpl-1(n3316)*.

Using a similar strategy, we mapped *efl-1(n3318)* and its associated Ste Mel phenotype to LGV between *unc-76* and *dpy-21*. From *efl-1(n3318)/unc-76 dpy-21* mothers, 9/13 Unc non-Dpy and 18/34 Dpy non-Unc F_1s were *efl-1(n3318)/efl-1(+)* and segregated Ste Mel animals, and 4/13 Unc non-Dpy and 16/34 Dpy non-Unc F_1s were *efl-1(+)/efl-1(+)* and did not segregate Ste Mel animals. Since *unc-76* and *dpy-21* are 6 map units apart, these data indicate that the *ste mel* mutation lies within about 0.13 map units of *efl-1(n3318)*.

cDNA, RT-PCR and mutant allele analyses

We recovered 15 *dpl-1* and 13 *efl-1* cDNAs by screening a *C. elegans* embryonic cDNA library (Okkema and Fire, 1994) using probes derived from partial *dpl-1* and *efl-1* cDNA clones (generously provided by Yuji Kohara), respectively. For both *dpl-1* and *efl-1*, we determined end sequences of each clone and full sequences of two clones to confirm splicing patterns. Sequences of mutant alleles were determined using PCR-amplified genomic DNA. We screened *C. elegans* embryonic and mixed-stage libraries (Okkema and Fire, 1994) with a probe derived from PCR-amplified genomic DNA for *efl-2* cDNAs and recovered two clones of identical sequence from the

mixed-stage library. We used the 5' RACE system v2.0 (GIBCO-BRL) to determine the 5' end of the *efl-2* transcript. We found two variants of the SL2 *trans*-spliced leader sequence on *efl-2* 5' RACE products: 5' GGTTTTAACCCAGTTAGTCAAG 3' and 5' GGTTTTAACCCAGTTATTCAAG 3'. All sequences were determined using an automated ABI 373 DNA sequencer (Applied Biosystems).

SUPPLEMENTAL DATA REFERENCES

Jansen, G., Hazendonk, E., Thijssen, K. L., and Plasterk, R. H. (1997). Reverse genetics by chemical mutagenesis in *Caenorhabditis elegans.* Nat. Genet. *17*, 119-121.

Liu, L. X., Spoerke, J. M., Mulligan, E. L., Chen, J., Reardon, B., Westlund, B., Sun, L., Abel, K., Armstrong, B., Hardiman, G., *et al.* (1999). High-throughput isolation of *Caenorhabditis elegans* deletion mutants. Genome Res. *9*, 859-867.

Okkema, P. G., and Fire, A. (1994). The *Caenorhabditis elegans* NK-2 class homeoprotein CEH-22 is involved in combinatorial activation of gene expression in pharyngeal muscle. Development *120*, 2175-2186.

ADDENDUM

A *dpl-1* DP null allele causes sterility and embryonic lethality

dpl-1(n3316) hermaphrodites were self-sterile and also could not be fertilized by males (Addendum table 1 and data not shown). The sterile phenotype was tightly linked to the *dpl-1(n3316)* deletion and was partially rescued by the cosmid C32F7 (see Supplemental Data). In addition, *dpl-1(n2994)*, *dpl-1(n2994)/dpl-1(n3316)* and *dpl-1(n2994)/mnDf67* mutants and animals in which *dpl-1* was inactivated by RNA-mediated interference (RNAi) (Fire et al., 1998) all displayed partially penetrant sterility (Addendum table 1), indicating that sterility is more generally associated with *dpl-1* loss of function.

We characterized the sterile phenotype by examining germ cell nuclei using 4,6-Diamidino-2-phenylindole (DAPI) staining. In a wild-type hermaphrodite germ cells are located within two tubular halves of the somatic gonad (Hirsh et al., 1976). The gonads of *dpl-1(n3316)* mutants contained immature mitotic and meiotic germ nuclei in the same positions and in the same approximate numbers as in the wild type (data not shown). However, the gonad arms of these mutants occasionally contained oocyte fragments with polyploid nuclei (data not shown). Such polyploid nuclei arise from the endomitotic replication of DNA within the oocyte (Iwasaki et al., 1996). We also observed endomitotic oocytes in the uteri of *dpl-1(n3316)* mutants (data not shown).

In *C. elegans*, such endomitotic oocytes have been seen in mutants defective in ovulation (Iwasaki et al., 1996; Clandinin et al., 1998). To determine if ovulation was defective in *dpl-1(n3316)* mutants, we observed oocytes during the process of ovulation as they transited from the gonad arm to the spermatheca. We found that gonadal sheath cell contractions in *dpl-1(n3316)* mutants were not as vigorous or frequent as in the wild type (C.C. and H.R.H., unpublished observations). In addition, the opening from the gonad arm to the spermatheca was abnormal. It appeared to be reduced in diameter, as judged by the size of an oocyte during attempted ovulation, and it constricted inappropriately, fragmenting oocytes in the process (Addendum figure 1). We observed defects in sheath cell contraction and oocyte fragmentation during 13/16 ovulations in *dpl-1(n3316)* mutants but in 0/11 ovulations in *dpl-1(+)* control animals.

Similar defects in ovulation occur following laser ablation of sheath cell precursors (McCarter et al., 1997). In addition, mutation of the class B synMuv gene *lin-9* reduces sheath cell number (Beitel et al., 2000). Therefore, we scored numbers of

sheath cell nuclei in *dpl-1(n3316)* mutants to determine if a reduction in sheath cell number was responsible for the ovulation defect. We visualized sheath cell nuclei with an antiserum that recognizes the homeobox protein CEH-18 (Greenstein et al., 1994) and observed ≥ 8 CEH-18-positive nuclei in 49/51 dissected gonads of *dpl-1(n3316)* mutants. Since 8 of 10 possible sheath cell nuclei can be reliably scored using this method, we conclude that sheath cell numbers are normal in *dpl-1(n3316)* mutants.

dpl-1 also appears to play a role in embryonic development. 16.4% of eggs laid by homozygous *dpl-1(n2994)* mothers died during embryogenesis (Addendum table 1). We suspect that this embryonic lethality was caused by a reduction of maternally-supplied *dpl-1* activity. First, 27.8% of eggs laid by heterozygous *dpl-1(n2994)/dpl-1(n3316)* mothers died during embryogenesis, suggesting that this phenotype resulted from a loss of *dpl-1* function and that *dpl-1(n2994)* partially impairs *dpl-1* function in embryogenesis. Second, 0% of eggs laid by either *dpl-1(n2994)/+* or *dpl-1(n3316)/+* mothers died, indicating that maternally supplied wild-type *dpl-1* activity is sufficient for embryogenesis even when zygotically-provided *dpl-1* activity is reduced or absent.

ADDENDUM REFERENCES

Beitel, G. J., Lambie, E. J., and Horvitz, H. R. (2000). The *C. elegans* gene *lin-9*, which acts in an Rb-related pathway, is required for gonadal sheath cell development and encodes a novel protein. Gene *254*, 253-263.

Clandinin, T. R., DeModena, J. A., and Sternberg, P. W. (1998). Inositol trisphosphate mediates a RAS-independent response to LET-23 receptor tyrosine kinase activation in *C. elegans*. Cell *92*, 523-533.

Fire, A., Xu, S., Montgomery, M. K., Kostas, S. A., Driver, S. E., and Mello, C. C. (1998). Potent and specific genetic interference by double-stranded RNA in *Caenorhabditis elegans*. Nature *391*, 806-811.

Greenstein, D., Hird, S., Plasterk, R. H., Andachi, Y., Kohara, Y., Wang, B., Finney, M., and Ruvkun, G. (1994). Targeted mutations in the *Caenorhabditis elegans* POU homeo box gene *ceh-18* cause defects in oocyte cell cycle arrest, gonad migration, and epidermal differentiation. Genes Dev. *8*, 1935-1948.

Hirsh, D., Oppenheim, D., and Klass, M. (1976). Development of the reproductive system of *Caenorhabditis elegans*. Dev. Biol. *49*, 200-219.

Iwasaki, K., McCarter, J., Francis, R., and Schedl, T. (1996). *emo-1*, a *Caenorhabditis elegans* Sec61p gamma homologue, is required for oocyte development and ovulation. J. Cell Biol. *134*, 699-714.

McCarter, J., Bartlett, B., Dang, T., and Schedl, T. (1997). Soma-germ cell interactions in *Caenorhabditis elegans*: multiple events of hermaphrodite germline development require the somatic sheath and spermathecal lineages. Dev. Biol. *181*, 121-143.

ADDENDUM TABLE

Addendum table 1. Loss of *dpl-1* function causes sterility and embryonic lethality

Genotype	Percent Ste (n)	Percent dead embryos (n)
N2	0 (many)	0 (5544)
dpl-1(n2994)	10.2 (164)	16.4 (6739)
dpl-1(n3316)	100 (303)	NA
dpl-1(n3643)	0 (233)	2.4 (4533)
*dpl-1(*RNAi*)*	51.6 (161)	17.7 (813)
*dpl-1(n3316); dpl-1(*RNAi*)*	100 (188)	NA
mnDf67/+	0 (many)	25.3 (5917)
dpl-1(n2994)/+	0 (155)	0 (5045)
dpl-1(n3316)/+	0 (289)	0 (5672)
dpl-1(n2994)/dpl-1(n3316)	17.2 (128)*	27.8 (486)
dpl-1(n2994)/mnDf67	15.0 (133)*	59.0 (1284)
dpl-1(n3316)/mnDf67	100 (63)	NA
lin-15A(n433)	1.1 (92)	0.3 (770)
dpl-1(n2994); lin-15A(n433)	13.6 (250)	9.6 (866)
dpl-1(n3316); lin-15A(n433)	100 (155)	NA
dpl-1(n3643); lin-15A(n433)	1.4 (142)	4.1 (798)

The complete genotypes of animals scored, in either *lin-15A(+)* or *lin-15A(n433)* backgrounds, were, from top to bottom, as follows: *dpl-1(n2994)*, *dpy-10(e128) dpl-1(n3316) +/+ dpl-1(n3316) unc-4(e120)*, *dpl-1(n3643)*, *dpl-1(RNAi)*, *+ mnDf67 unc-4(e120)/dpy-10(e128) + +*, *dpy-10(e128) dpl-1(n2994)/+ +*, *+ dpl-1(n3316) unc-4(e120)/dpy-10(e128) + +*, *dpy-10(e128) dpl-1(n2994) +/+ dpl-1(n3316) unc-4(e120)*, *dpy-10(e128) dpl-1(n2994) +/+ mnDf67 unc-4(e120)*, *dpy-10(e128) dpl-1(n3316) +/+ mnDf67 unc-4(e120)*. NA = not applicable. *The average brood sizes of these animals were greatly reduced in comparison to control animals and were as follows: 56 (n=23) for *dpl-1(n2994)/mnDf67*; 29 (n=17) for *dpl-1(n2994)/dpl-1(n3316)*; as compared to 280 (n=18) for *dpl-1(n2994)/+*; 296 (n=20) for *mnDf67/+*; 284 (n=20) for *dpl-1(n3316)/+*; and 259 (n=20) for *dpl-1(n2994)* animals. Reductions in the dosage of *dpl-1* both increase the penetrance of sterility and cause severe fertility defects in non-

sterile animals. These data are consistent with our conclusion that the sterility caused by the *dpl-1(n3316)* deletion resulted from a loss of *dpl-1* function as opposed to an effect of the deletion on a neighboring gene.

ADDENDUM FIGURE

Addendum figure 1. Oocytes are fragmented during ovulation in *dpl-1(n3316)* mutants
(A-C) Time series of Nomarski DIC photomicrographs of a normal ovulation in a *dpl-1(+)* hermaphrodite. Ventral is down, the proximal gonad arm is to the left and the uterus is to the right in each panel. The scale bar represents 5 μm.
(D-F) Schematic diagrams of images in panels A-C. The oocyte nucleus in panels B and C is out of the plane of focus and is indicated in E and F by a dashed circle. The spermatheca in each diagram is hatched. spt, spermatheca; oo, oocyte.
(G-I) Time series of Nomarski DIC photomicrographs of a defective ovulation in a *dpl-1(n3316)* hermaphrodite.
(J-L) Schematic diagrams of images in panels G-I. oo', oocyte fragment
The complete genotypes of the animals shown were *unc-4(e120)* (panels A-C) and *dpl-1(n3316) unc-4(e120)* (panels G-I).

Addendum figure 1

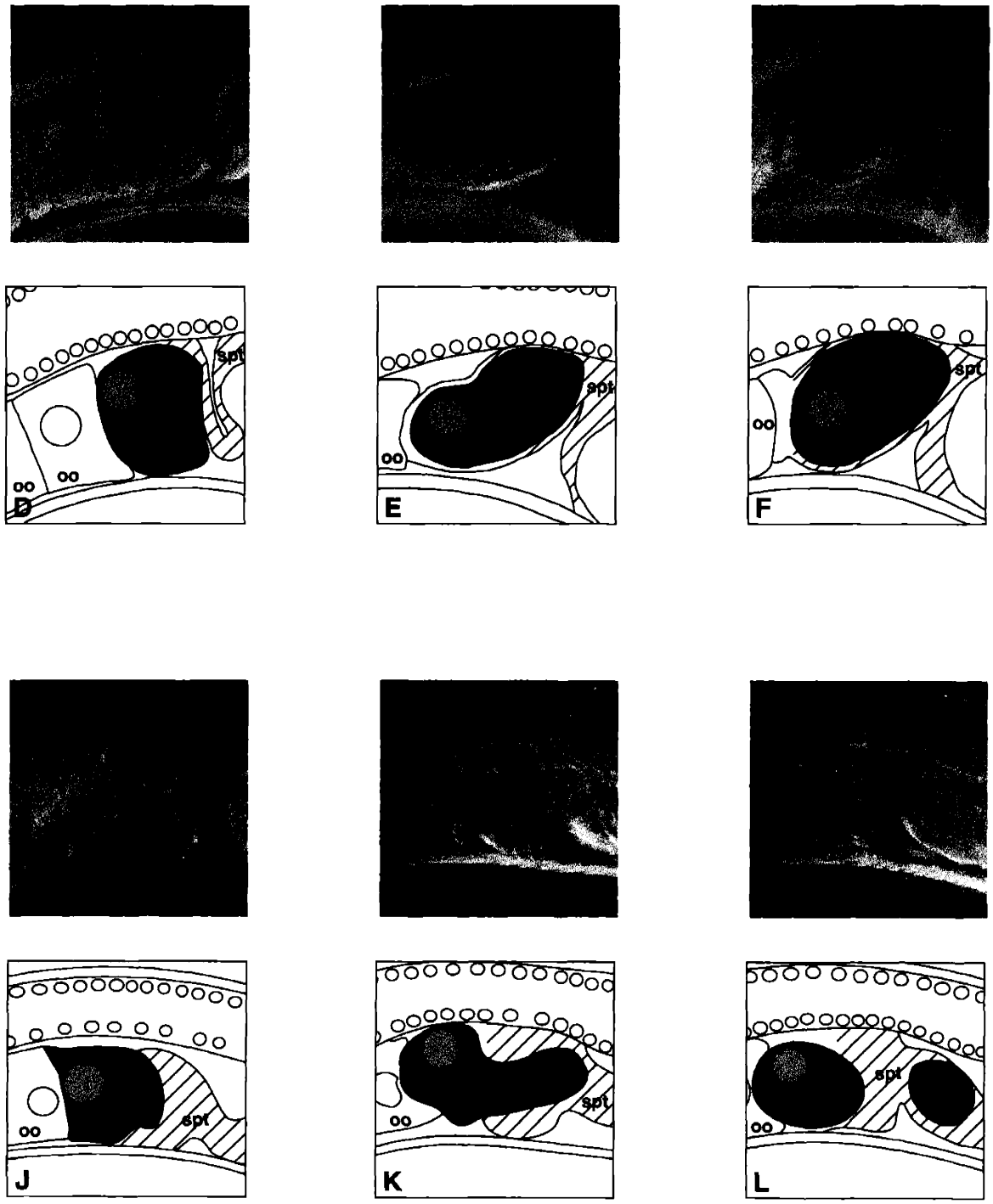

CHAPTER 4

lin-54 encodes a conserved cysteine-rich protein that acts in an Rb signaling pathway to regulate vulval development in *C. elegans*

Craig Ceol and H. Robert Horvitz

This manuscript is being prepared for publication.

ABSTRACT

The *C. elegans* gene *lin-54* acts with *lin-35* Rb, *efl-1* E2F, *dpl-1* DP, *hda-1* HDAC and other class B synthetic multivulva genes to negatively regulate Ras-mediated vulval induction. We cloned *lin-54* and found that it encodes a novel protein that is expressed in nuclei and interacts *in vitro* with the class B synMuv protein LIN-36. LIN-54 contains two cysteine-rich domains that are present in predicted proteins from other species. A subset of these proteins are additionally similar to LIN-54 in regions outside of the cysteine-rich domains and therefore are candidate LIN-54 orthologs and Rb pathway proteins in other species.

INTRODUCTION

The mammalian tumor suppressor Rb and the related p107 and p130 proteins play important roles in cell-cycle progression and differentiation in mammals (Harbour and Dean, 2000). To properly regulate these processes, Rb family proteins interact, either directly or indirectly, with a host of other proteins. Identifying and understanding the functions of these proteins has helped to elucidate the of role of Rb in tumor suppression.

The *C. elegans lin-35* gene encodes an Rb homolog, and genetic studies have identified a group of genes with which *lin-35* Rb acts (Ferguson and Horvitz, 1989; Lu and Horvitz, 1998; Hsieh et al., 1999; Solari and Ahringer, 2000; von Zelewsky et al., 2000; Ceol and Horvitz, 2001; Couteau et al., 2002; Chapters 2, 5). This group of genes, termed the class B synthetic multivulva (synMuv) genes, negatively regulates hermaphrodite vulval development. The vulva is formed from the descendants of three ectodermal blast cells, P(5-7).p (Sulston and Horvitz, 1977). These three cells and the neighboring cells P3.p, P4.p and P8.p are generated in the L1 larval stage, each initially capable of producing vulval tissue (Sternberg and Horvitz, 1986). However, during the L2 stage a localized signal from the gonadal anchor cell specifically induces P(5-7).p to adopt vulval cell fates (Sulston and White, 1980; Kimble, 1981). Such fates are characterized by three rounds of division that produce seven or eight cells. P3.p, P4.p and P8.p are not induced and consequently adopt non-vulval cell fates in which they typically divide once to produce two descendants that fuse with the hypodermal syncytium. A conserved receptor tyrosine kinase (RTK)/Ras pathway controls vulval induction (reviewed by Sternberg and Han, 1998). Mutations that disable this pathway cause P(5-7).p to adopt non-vulval fates, leading to vulvaless (Vul) adult animals. Mutations that increase Ras pathway activity, for instance G13E substitutions in LET-60 Ras, substitutions that are also found in oncogenic forms of mammalian Ras, lead to a multivulva (Muv) phenotype by causing P3.p, P4.p and P8.p, in addition to P(5-7).p, to adopt induced fates (Beitel et al., 1990). The class B synMuv genes and the functionally redundant class A synMuv genes antagonize Ras pathway signaling (Ferguson and Horvitz, 1989). Whereas mutations in genes of one class do not affect vulval development, animals that have lost function in both class A and class B genes exhibit a Muv phenotype.

The mechanism by which *lin-35* Rb and other class B synMuv genes function is likely conserved in other organisms. Many genes with class B synMuv activity encode homologs of proteins that function with mammalian Rb family members. These genes include: *dpl-1* and *efl-1*, which encode homologs of DP and E2F transcription factors, respectively (Ceol and Horvitz, 2001), *hda-1* and *lin-53*, which encode homologs of class I histone deacetylases and the Rb- and histone deacetylase-associated protein RbAp48, respectively (Lu and Horvitz, 1998) and *hpl-2*, which encodes a homolog of the *Drosophila* and mammalian HP1 family of proteins that, through a conserved chromodomain motif, are proposed to bind to methyl-lysine residues of nucleosomal histones and subsequently mediate transcriptional silencing (Couteau et al., 2002). Based on the functions of the mammalian proteins and on conserved interactions amongst the *C. elegans* proteins, we previously proposed that a DNA-bound DPL-1/EFL-1 heterodimer recruits LIN-35 Rb to promoters of genes that are required for vulval development (Ceol and Horvitz, 2001). LIN-35, in turn, is proposed to recruit HDA-1, LIN-53, HPL-2 and other class B synMuv proteins to repress transcription of these target genes.

Additional class B synMuv genes have been identified. Given the similarities of Rb function in *C. elegans* and mammals, these genes may define conserved members of Rb signaling pathways. In this paper, we present genetic and molecular characterization of the class B synMuv gene *lin-54*. *lin-54* displays genetic interactions and an expression pattern like those of other *lin-35* Rb pathway members. *lin-54* encodes a protein with cysteine-rich domains that are also found in proteins from plants, flies, mammals and other species. A subset of these proteins are similar to LIN-54 in regions outside these cysteine-rich domains and therefore are candidate LIN-54 orthologs and Rb pathway members.

MATERIALS AND METHODS

Genetics

Strains were cultured as described by Brenner (1974) and maintained at 20°C unless otherwise specified. The following mutations were used: LGII: *rol-6(e187)*, *let-23(sy97)*, *unc-4(e120)*; LGIV: *lin-3(n378)*, *let-60(n1876)* (Beitel et al., 1990), *unc-22(e66)*, *unc-30(e191)*, *lin-54(n2231, n2990, n3423, n3424)* (Chapter 2; this study); LGX: *lin-15A(n433)* (Ferguson and Horvitz, 1989), *lin-15(n767)* and, unless otherwise noted, are described in Riddle (1997). In addition, we used strains containing the *nT1 (IV;V)* (Ferguson and Horvitz, 1985) and *mIn1[dpy-10(e128) mIs14] II* (Edgley and Riddle, 2001) chromosomal rearrangements. *mIs14*, an integrated transgene linked to the chromosomal inversion *mIn1*, consists of a combination of GFP-expressing transgenes that allow *mIs14*-containing animals to be scored beginning at the 4-cell stage of embryogenesis (Edgley and Riddle, 2001).

Isolation of *lin-54* deletion alleles

Genomic DNA from pools of mutagenized worms was screened for deletions essentially as described by Plasterk (1997). Deletion mutant animals were isolated from frozen stocks and were backcrossed eight times prior to analysis. *lin-54(n3423)* removes nucleotides -280 to +2058 and *lin-54(n3424)* removes nucleotides +1804 to +2944 of genomic DNA relative to the predicted *lin-54* translational start site.

lin-54 cDNA and *in vivo* expression constructs

lin-54 cDNA sequence was determined from the clones yk414a8 and yk454f3 (kindly provided by Y. Kohara). 5' ends of *lin-54* transcripts were determined using the 5' RACE system v2.0 (GIBCO) according to the manufacturer's recommendations. We found SL1 splice-leader sequence on 5' RACE isolates and detected two alternative SL1 splice sites: gtttaattacccaagtttgagtattttcagtgttgacaATG and gtttaattacccaagtttgagtgttgacaATG, where SL1 sequence is underlined and the predicted translational start site is in uppercase. The *lin-54* open reading frame was PCR amplified and cloned into the vectors pSCL2 (P. Olsen and V. Ambros, personal communication) to generate the $P_{col\text{-}10}$::*lin-54* expression construct and pPD48.78 and pPD48.83 (A. Fire, personal communication) to generate the P_{hs}::*lin-54* expression constructs. The *lin-54::gfp* construct contained the *lin-54* genomic locus flanked by 0.8

kb of upstream and 1.8 kb of downstream genomic sequence. The *gfp* coding sequence was inserted in frame into a XhoI site in the 2nd exon of *lin-54*, at a site corresponding to amino acid 54 of the LIN-54L protein.

Transgenic animals

Germline transformation was performed, as described by Mello (1991), by injecting cosmid (5-10 ng/μL) or plasmid (50-80 ng/μL) DNA into *lin-54; lin-15A* mutants. pRF4, which causes a dominant Rol phenotype, was used as a coinjection marker except for $P_{col\text{-}10}$::*lin-54* and P_{hs}::*lin-54* transgenic lines, in which p76-16B, an *unc-76* rescuing plasmid (Bloom and Horvitz, 1997), was used for injection into *lin-54; unc-76; lin-15A* mutants. Rol and non-Unc transgenic lines, respectively, were established and scored.

Heat shock analyses

Animals were developmentally synchronized as described (Hodgkin and Sulston, 1988). Heat shock was performed by incubating animals of a desired stage at 33°C for one hour. Heat-shocked animals were allowed to develop and were scored as adults for vulval abnormalities.

RNAi analyses

The full-length *lin-54* cDNA was cloned, using *in vitro* recombination (Gateway system, Invitrogen), into pDEST-L4440, a vector suitable for producing double-stranded RNA. The resulting construct was transformed into the HT115 *E. coli* strain, and *lin-54* feeding RNAi was performed as described by Timmons and Fire (1998). RNAi of *lin-54* by feeding or injection were similarly efficacious (data not shown). RNAi negative controls were performed by feeding animals HT115 bacteria containing the empty pDEST-L4440 vector.

Protein interaction studies

Constructs encoding MBP-LIN-36 and MBP-LIN-54 were made by cloning the *lin-36* and *lin-54* coding sequences, respectively, into the Gateway system-compatible vector pDEST-MAL. Fusion proteins were expressed in BL21(DE3) cells and purified using amylose resin according to the manufacturer's recommendations (New England Biolabs). The full-length cDNAs of *lin-36*, *lin-54* and other synMuv genes were cloned into the Gateway system vector pDEST14, and the resulting constructs were used as a

templates for *in vitro* syntheses of ^{35}S-labeled proteins (TNT Coupled Reticulocyte Lysate System, Promega). Binding experiments were performed as described by Reddien and Horvitz (2000), and bound proteins were analyzed by 8% SDS-PAGE followed by autoradiography.

RESULTS

Molecular identification of *lin-54*

lin-54 was previously mapped to an interval on LGIV between *unc-30* and *unc-26* (Chapter 2). We performed germline transformation experiments using genomic DNA clones from this interval and found that two overlapping cosmids, MMMC1 and JC8, independently rescued the Muv phenotype of *lin-54(n2231); lin-15A(n433)* mutants (Figure 1). DNA subclones of the overlapping region that contained the predicted gene JC8.6, including a subclone that contained JC8.6 as the only complete predicted gene, rescued the *lin-54(n2231); lin-15A(n433)* Muv phenotype, whereas subclones that lacked or disrupted JC8.6 failed to rescue. RNA-mediated interference (RNAi) of JC8.6 in a *lin-15A* background resulted in a Muv phenotype similar to that observed in *lin-54; lin-15A* mutants (Table 1). *JC8.6(RNAi)* did not cause a Muv phenotype in a *lin-15B* or wild-type background, thus showing the same genetic interactions as *lin-54* and other class B synMuv mutations. We determined the DNA sequence of JC8.6 in strains containing *lin-54(n2231)* and *lin-54(n2990)* and found missense mutations in both (Figure 2). The combination of transformation rescue, RNAi phenocopy and the presence of mutations indicate that JC8.6 is *lin-54*. In addition, the recessive natures of *lin-54(n2231)* and *lin-54(n2990)* and the similarity of their phenotype to that caused by *lin-54(RNAi)* suggests that these alleles result in a loss of *lin-54* function.

LIN-54 contains two copies of a conserved cysteine-rich motif

We determined the end and internal sequences of *lin-54* cDNAs (Figure 2; see Materials and Methods). Due to alternative splicing, the large open reading frames of *lin-54* cDNAs predict proteins of 438 (LIN-54L) and 432 (LIN-54S) amino acids in length (Figure 3). LIN-54 proteins are rich in cysteines, which are clustered into two domains that have a nearly identical pattern and spacing. Domains with this cysteine signature, $CXCX_4CX_4CXCX_6CX_{2\text{-}3}CXCX_2C$, are found in proteins from mammals, plants, flies and other organisms, however a biochemical activity for this domain has not yet been described. Like LIN-54 proteins, many of these proteins contain two closely apposed copies of this cysteine-rich domain. A subset of these proteins are similar to LIN-54 proteins not only in the cysteine-rich domains but also in other regions of the protein. Most notably, predicted proteins from humans (AAD24668) and from the mouse (XP_132238) share similarity to LIN-54 in their sequence between the two cysteine-rich

domains and in their C-termini, indicating that these proteins may be closer functional homologs to LIN-54 than other proteins that contain these cysteine-rich-domains.

LIN-54 is expressed broadly and is localized to nuclei

To determine where LIN-54 might function, we examined the expression pattern and subcellular localization of a LIN-54 fusion with the green fluorescent protein (GFP) . The transgene we built for this purpose contains 0.8 kb of *lin-54* promoter sequence and the entire *lin-54* coding sequence, with the *gfp* gene inserted in frame into the second exon of *lin-54* (see Materials and Methods). This transgene rescued the Muv phenotype of *lin-54(n2231); lin-15A(n433)* mutants, indicating that the GFP insertion did not severely perturb LIN-54 function. LIN-54::GFP was present in all tissues except the germline and was localized to nuclei. The nuclei of P(3-8).p and hyp7, two proposed sites of synMuv gene action, both expressed LIN-54::GFP (Figure 4; data not shown). Similar broad expression patterns and nuclear localizations have been observed for other class B synMuv proteins including LIN-36, LIN-53 and DPL-1 (Lu and Horvitz, 1998; Thomas and Horvitz, 1999; Ceol and Horvitz, 2001). Since transgenes generally are silenced in the *C. elegans* germline (Kelly et al., 1997), lack of expression in this tissue should not imply that endogenous *lin-54* is not expressed in the germ cells. On the contrary, because *lin-54* shows maternal rescue, that is, because the penetrance of the *lin-54(n2231); lin-15A(n433)* Muv phenotype is reduced when these animals are derived from heterozygous as compared to homozygous mutant mothers (Chapter 2), we speculate that endogenous LIN-54 is present in the germline and is passed from mother to progeny.

Loss of *lin-54* function causes sterility

We sought to determine whether *lin-54* function is required for processes other than vulval development. Towards this end, we screened for and isolated two deletion alleles, *lin-54(n3423)* and *lin-54(n3424)*, that are predicted to have severe effects on *lin-54* function. *lin-54(n3423)* removes 2338 base pairs beginning 280 base pairs upstream of the predicted *lin-54* initiator codon and ending to leave only the final ten *lin-54* codons intact (Figures 2, 3). *lin-54(n3424)* removes 1140 base pairs beginning late in the *lin-54* gene, after sequence encoding the first 360 amino acids of LIN-54L, and ends 853 base pairs downstream of the predicted *lin-54* terminator codon (Figures 2, 3). Both deletions cause a Muv phenotype specifically in a class A synMuv

background, confirming that the synMuv phenotype caused by mutations in *lin-54* results from a loss of gene function (Table 1). Both deletions also cause a fully-penetrant sterile phenotype. To investigate the nature of this phenotype, we stained *lin-54(n3423)* and *lin-54(n3424)* mutants with 4,6-Diamidino-2-phenylindole (DAPI). In a wild-type hermaphrodite germ cells are located within two tubular halves of the somatic gonad (Hirsh et al., 1976). The gonads of *lin-54* deletion mutants contained immature mitotic and meiotic germ nuclei in the same positions and in the same approximate numbers as in the wild type (data not shown). However, the gonad arms of these mutants contained oocytes and occasionally oocyte fragments with polyploid nuclei (data not shown). Such polyploid nuclei arise from the endomitotic replication of DNA within the oocyte (Iwasaki et al., 1996). We also observed endomitotic oocytes in the uteri of *lin-54* deletion mutants (data not shown). This phenotype is similar to that observed in *dpl-1* null mutant animals. In *dpl-1* mutants, endomitotic oocytes and oocyte fragments are likely produced by defects in ovulation (Chapter 3).

let-60 Ras pathway activity is required for expression of the *lin-54; lin-15A* Muv phenotype

A conserved RTK/Ras signaling pathway can act in P(3-8).p to induce vulval cell fates (Sternberg and Han, 1998). This pathway responds to the LIN-3 EGF ligand that is produced by the neighboring anchor cell and acts cell non-autonomously. In wild-type animals, LIN-3 EGF is localized nearest to P(5-7).p and consequently specifically induces these cells. We wished to determine if the vulval cell fate transformations we observed in *lin-54* mutants require RTK/Ras pathway or *lin-3* activity. When we combined *lin-54(RNAi)* with *lin-15A(n767)* and a mutation in either *let-23* RTK or *let-60* Ras we found that these mutant animals had a Vul phenotype like that of *let-23* RTK or *let-60* Ras single mutants (Table 2). The combination of *lin-54(RNAi), lin-15A(n767)* and a *lin-3* EGF mutation, however, caused a Muv phenotype like that of *lin-54(RNAi); lin-15A(n767)* mutants. These results suggest that a basal, *lin-3*-independent level of RTK/Ras pathway activity is sufficient for the *lin-54; lin-15A* Muv phenotype and that the Muv phenotype depends on at least some RTK/Ras signaling.

Temporal- and tissue-specific expression of a *lin-54* transgene rescues the *lin-54* Muv phenotype

The Muv phenotype of *lin-54* mutants can be partially rescued by maternal contribution of wild-type gene activity (Chapter 2). Maternal gene activity may be expected to persist only temporarily, raising the possibility that *lin-54* may normally function early in development and may not be required at the time of vulval cell-fate specification. To address this possibility, we expressed *lin-54* under the control of the *C. elegans* heat shock promoters and determined developmental stages during which *lin-54* could function (Figure 5). In this experiment, *lin-54(n2231); lin-15A(n433)* mutants containing P_{hs}*lin-54* transgenes were raised under standard conditions, except for a one-hour heat shock treatment at a specific developmental stage, and scored as adults for rescue of the Muv phenotype. Animals that were heat shocked as embryos showed a weak degree of rescue. Later heat shock treatments during the L1 and early L2 larval stages slightly increased the degree of rescue to 22 and 28 percent, respectively. The penetrance of rescue peaked to 74 percent when animals were heat shocked during the late L2 stage and diminished to 26 percent following heat shock at the L3 stage. Because exogenous LIN-54 protein may perdure after being expressed early in development, these results do not elucidate the earliest time during which *lin-54* might function. However, the rescue observed after L2 and L3 heat shock treatments indicates that *lin-54* can function as late as these times. This result, together with the knowledge that *lin-54* is expressed throughout development, suggests that *lin-54* functions during the L2 and at least the early L3 larval stages in the specification of vulval cell fates.

We also wanted to determine if *lin-54* could function in a tissue-specific manner. The promoter for the *col-10* gene is expressed in ectodermal blast cells that give rise to the vulva and hypodermis (P. Olson and V. Ambros, personal communication). *lin-54(n2231); lin-15A(n433)* animals containing a $P_{col\text{-}10}$*lin-54* transgene were strongly rescued, indicating that *lin-54* can function in ectodermal tissues to carry out its role in vulval development.

LIN-54 interacts with LIN-36 *in vitro*

Because of their specific genetic interactions, the class B synMuv genes were proposed to act together as a functional unit to negatively regulate vulval cell fates (Ferguson and Horvitz, 1989). Characterization of the proteins encoded by some of these genes revealed that this function is likely mediated, in part, by protein-protein interactions (Lu and Horvitz, 1998; Ceol and Horvitz, 2001). To investigate whether LIN-54 interacts

with other synMuv proteins, we performed binding assays using maltose binding protein-tagged LIN-54 (MBP-LIN-54) and *in vitro* translated class B synMuv proteins. In these assays, MBP-LIN-54 specifically interacted with the class B synMuv protein LIN-36 but not with luciferase or the class B synMuv proteins LIN-15B, LIN-35, LIN-52, LIN-53 and EFL-1 (Figure 6; data not shown). In the converse experiment, MBP-LIN-36 interacted with *in vitro* translated LIN-54 but not with luciferase or LIN-15B, LIN-35, LIN-52, LIN-53 and EFL-1. LIN-36 is a novel protein that contains an amino-terminal cysteine and histidine-rich domain and also has a carboxy-terminal polyglutamine sequence. We are currently attempting to determine which domains of LIN-54 and LIN-36 mediate their interaction and whether previously identified missense mutations in either protein abrogate their binding.

DISCUSSION AND FUTURE EXPERIMENTS

LIN-54 and its homologs are candidate Rb pathway proteins

In its effects on vulval development, *lin-54* shows genetic interactions that are highly specific and similar to those of the *C. elegans* Rb homolog *lin-35*. The LIN-54 protein is broadly expressed and is localized to nuclei much like other class B synMuv proteins. These observations suggest that LIN-54 acts with LIN-35 Rb and other class B synMuv proteins to antagonize Ras-mediated vulval induction. By extension, homologs of LIN-54 may act in Rb-mediated processes in other systems. Mammalian Rb and the related proteins p107 and p130 are well characterized and have been ascribed a variety of functions (Dyson, 1998; Harbour and Dean, 2000). Among these functions are the abilities of Rb and Rb family proteins to actively repress transcription of E2F-regulated genes. In this capacity, Rb binds to DP/E2F heterodimers and recruits proteins such as histone deacetylases and heterochromatin protein 1 (HP1) that are thought to repress transcription by remodeling chromatin into a structure less accessible to the general transcription machinery (Brehm et al., 1998; Luo et al., 1998; Magnaghi-Jaulin et al., 1998; Bannister et al., 2001). The description of class B synMuv activity for the DP and E2F homologs *dpl-1* and *efl-1*, the histone deacetylase *hda-1* and the HP1 homolog *hpl-2* indicates that this function is conserved in *C. elegans* and has a role in class B synMuv function (Lu and Horvitz, 1998; Ceol and Horvitz, 2001; Couteau et al., 2002). We therefore propose a role for *lin-54* in *lin-35* Rb-mediated transcriptional repression.

Although we cannot yet ascribe an *in vivo* activity to the LIN-54 protein, there are some intriguing possibilities. LIN-54 has two cysteine-rich domains that are conserved in proteins from other systems. These domains may be modular since they are found in single or multiple copies in a given protein. Such modularity is commonly observed for protein-protein interaction domains but is atypical of enzymatic domains. If the cysteine-rich domains of LIN-54 were interaction domains, what would they bind? One possibility is that they interact with chromatin. In this regard, they may function like bromodomains or chromodomains, which bind acetylated and methylated lysine residues, respectively, of histones (Jacobson et al., 2000; Rea et al., 2000), and are present in single or multiple copies in chromatin-binding proteins. Another possibility is that the LIN-54 cysteine-rich domains mediate interactions with other synMuv proteins. Indeed, we are currently testing whether these domains mediate the interaction LIN-54 with LIN-36.

Does *lin-54* have a role in cell cycle progression?

The vulval abnormalities observed in *lin-54* mutants reflect a defect in cell-fate determination. The fates to which P3.p, P4.p and P8.p are transformed in *lin-54* mutants are characterized by extra cell divisions and altered differentiation. Because of this cell division defect *lin-54* may function, in part, by regulating cell cycle progression. The roles of mammalian Rb, E2F and DP proteins in regulating progression from the G1 to S phase of the cell cycle are well documented (Dyson, 1998; Trimarchi and Lees, 2002). In cells entering G1, the majority of DP/E2F heterodimers are bound by Rb family proteins, resulting in the repression of E2F-regulated genes. As cells approach S phase, Rb proteins are phosphorylated by cyclin D/cdk4 complexes and later cyclin E/cdk2 complexes and released from DP/E2F heterodimers. Free DP/E2F heterodimers are thought to promote S phase entry by stimulating the transcription of genes that are required for cell cycle progression. The repressive roles of Rb, E2F and DP proteins may be conserved in *C. elegans* as loss of *lin-35* Rb, *efl-1* E2F or *dpl-1* DP partially alleviates defects in cell cycle progression caused by RNA-mediated interference of the cyclin D homolog *cyd-1* (Boxem and van den Heuvel, 2002). We are currently testing whether loss of *lin-54* function can similarly suppress defects caused by *cyd-1(RNAi)*.

ACKNOWLEDGMENTS

We thank Na An and Beth Castor for expert technical assistance, Ignacio Perez de la Cruz for critical review of this manuscript, Peter Reddien, Rajesh Ranganathan and members of the laboratory for constructing the deletion library, Alan Coulson and Yuji Kohara for providing cosmid and cDNA clones, respectively, and Marc Vidal and Simon Boulton for providing some Gateway system-compatible plasmids. This work was supported by NIH grant GM24663. C.J.C. was a Koch Graduate Fellow. H.R.H. is an investigator of the Howard Hughes Medical Institute.

REFERENCES

Bannister, A. J., Zegerman, P., Partridge, J. F., Miska, E. A., Thomas, J. O., Allshire, R. C., and Kouzarides, T. (2001). Selective recognition of methylated lysine 9 on histone H3 by the HP1 chromodomain, Nature *410*, 120-4.

Beitel, G. J., Clark, S. G., and Horvitz, H. R. (1990). *Caenorhabditis elegans ras* gene *let-60* acts as a switch in the pathway of vulval induction, Nature *348*, 503-9.

Bloom, L., and Horvitz, H. R. (1997). The *Caenorhabditis elegans* gene *unc-76* and its human homologs define a new gene family involved in axonal outgrowth and fasciculation, Proc. Natl. Acad. Sci. USA *94*, 3414-9.

Boxem, M., and van den Heuvel, S. (2002). *C. elegans* Class B Synthetic Multivulva Genes Act in G(1) Regulation, Curr. Biol. *12*, 906-11.

Brehm, A., Miska, E. A., McCance, D. J., Reid, J. L., Bannister, A. J., and Kouzarides, T. (1998). Retinoblastoma protein recruits histone deacetylase to repress transcription, Nature *391*, 597-601.

Brenner, S. (1974). The genetics of *Caenorhabditis elegans*, Genetics *77*, 71-94.

Ceol, C. J., and Horvitz, H. R. (2001). *dpl-1* DP and *efl-1* E2F act with *lin-35* Rb to antagonize Ras signaling in *C. elegans* vulval development, Mol. Cell *7*, 461-73.

Couteau, F., Guerry, F., Muller, F., and Palladino, F. (2002). A heterochromatin protein 1 homologue in *Caenorhabditis elegans* acts in germline and vulval development, EMBO Rep. *3*, 235-41.

Dyson, N. (1998). The regulation of E2F by pRB-family proteins, Genes Dev. *12*, 2245-62.

Edgley, M. L., and Riddle, D. L. (2001). LG II balancer chromosomes in *Caenorhabditis elegans*: *mT1(II;III)* and the *mIn1* set of dominantly and recessively marked inversions, Mol. Genet. Genomics *266*, 385-95.

Ferguson, E. L., and Horvitz, H. R. (1985). Identification and characterization of 22 genes that affect the vulval cell lineages of the nematode *Caenorhabditis elegans*, Genetics *110*, 17-72.

Ferguson, E. L., and Horvitz, H. R. (1989). The multivulva phenotype of certain *Caenorhabditis elegans* mutants results from defects in two functionally redundant pathways, Genetics *123*, 109-21.

Harbour, J. W., and Dean, D. C. (2000). The Rb/E2F pathway: expanding roles and emerging paradigms, Genes Dev. *14*, 2393-409.

Hirsh, D., Oppenheim, D., and Klass, M. (1976). Development of the reproductive system of *Caenorhabditis elegans*, Dev. Biol. *49*, 200-19.

Hodgkin, J., and Sulston, J. E. (1988). Methods. In The Nematode *Caenorhabditis elegans*, W. B. Wood, ed. (Cold Spring Harbor, New York: Cold Spring Harbor Laboratory Press).

Hsieh, J., Liu, J., Kostas, S. A., Chang, C., Sternberg, P. W., and Fire, A. (1999). The RING finger/B-box factor TAM-1 and a retinoblastoma-like protein LIN-35 modulate context-dependent gene silencing in *Caenorhabditis elegans*, Genes Dev. *13*, 2958-70.

Iwasaki, K., McCarter, J., Francis, R., and Schedl, T. (1996). *emo-1*, a *Caenorhabditis elegans* Sec61p gamma homologue, is required for oocyte development and ovulation, J. Cell Biol. *134*, 699-714.

Jacobson, R. H., Ladurner, A. G., King, D. S., and Tjian, R. (2000). Structure and function of a human TAFII250 double bromodomain module, Science *288*, 1422-5.

Jansen, G., Hazendonk, E., Thijssen, K. L., and Plasterk, R. H. (1997). Reverse genetics by chemical mutagenesis in *Caenorhabditis elegans*, Nat. Genet. *17*, 119-21.

Kelly, W. G., Xu, S., Montgomery, M. K., and Fire, A. (1997). Distinct requirements for somatic and germline expression of a generally expressed *Caernorhabditis elegans* gene, Genetics *146*, 227-38.

Kimble, J. (1981). Alterations in cell lineage following laser ablation of cells in the somatic gonad of *Caenorhabditis elegans*, Dev. Biol. *87*, 286-300.

Lu, X., and Horvitz, H. R. (1998). *lin-35* and *lin-53*, two genes that antagonize a *C. elegans* Ras pathway, encode proteins similar to Rb and its binding protein RbAp48, Cell *95*, 981-91.

Luo, R. X., Postigo, A. A., and Dean, D. C. (1998). Rb interacts with histone deacetylase to repress transcription, Cell *92*, 463-73.

Magnaghi-Jaulin, L., Groisman, R., Naguibneva, I., Robin, P., Lorain, S., Le Villain, J. P., Troalen, F., Trouche, D., and Harel-Bellan, A. (1998). Retinoblastoma protein represses transcription by recruiting a histone deacetylase, Nature *391*, 601-5.

Mello, C. C., Kramer, J. M., Stinchcomb, D., and Ambros, V. (1991). Efficient gene transfer in *C.elegans*: extrachromosomal maintenance and integration of transforming sequences, Embo J. *10*, 3959-70.

Rea, S., Eisenhaber, F., O'Carroll, D., Strahl, B. D., Sun, Z. W., Schmid, M., Opravil, S., Mechtler, K., Ponting, C. P., Allis, C. D., and Jenuwein, T. (2000). Regulation of chromatin structure by site-specific histone H3 methyltransferases, Nature *406*, 593-9.

Reddien, P. W., and Horvitz, H. R. (2000). CED-2/CrkII and CED-10/Rac control phagocytosis and cell migration in *Caenorhabditis elegans*, Nat. Cell Biol. *2*, 131-6.

Riddle, D. L., Blumenthal, T., Meyer, B. J., and Priess, J. R., eds. (1997). *C. elegans* II (Cold Spring Harbor, New York: Cold Spring Harbor Laboratory Press).

Solari, F., and Ahringer, J. (2000). NURD-complex genes antagonise Ras-induced vulval development in *Caenorhabditis elegans*, Curr. Biol. *10*, 223-6.

Sternberg, P. W., and Han, M. (1998). Genetics of RAS signaling in *C. elegans*, Trends Genet. *14*, 466-72.

Sternberg, P. W., and Horvitz, H. R. (1986). Pattern formation during vulval development in *C. elegans*, Cell *44*, 761-72.

Sulston, J. E., and Horvitz, H. R. (1977). Post-embryonic cell lineages of the nematode, *Caenorhabditis elegans*, Dev. Biol. *56*, 110-56.

Sulston, J. E., and White, J. G. (1980). Regulation and cell autonomy during postembryonic development of *Caenorhabditis elegans*, Dev. Biol. *78*, 577-97.

Thomas, J. H., and Horvitz, H. R. (1999). The *C. elegans* gene *lin-36* acts cell autonomously in the *lin-35* Rb pathway, Development *126*, 3449-59.

Timmons, L., and Fire, A. (1998). Specific interference by ingested dsRNA, Nature *395*, 854.

Trimarchi, J. M., and Lees, J. A. (2002). Sibling rivalry in the E2F family, Nat. Rev. Mol. Cell Biol. *3*, 11-20.

von Zelewsky, T., Palladino, F., Brunschwig, K., Tobler, H., Hajnal, A., and Muller, F. (2000). The *C. elegans* Mi-2 chromatin-remodelling proteins function in vulval cell fate determination, Development *127*, 5277-84.

TABLES

Table 1: Loss of *lin-54* function causes a synMuv phenotype

Genotype	% Muv @ 15°C (n)	% Muv @ 20°C (n)
wild type	0 (231)	0 (302)
lin-15A(n433)	0 (280)	0 (350)
lin-15A(n767)	0 (411)	0 (272)
lin-54(n2231)	0.6 (169)	0 (327)
lin-54(n2990)	0 (203)	0 (541)
lin-54(n3423)	0 (111)	0 (242)
lin-54(n3424)	0 (169)	0 (271)
lin-54(RNAi)	0 (357)	0 (622)
lin-54(n2231); lin-15A(n433)	1.2 (173)	99.1 (227)
lin-54(n2231); lin-15A(n767)	88.9 (189)	100 (221)
lin-54(n2990); lin15A(n433)	2.6 (229)	100 (291)
lin-54(n3423); lin-15A(n433)	1.6 (123)	91.7 (96)
lin-54(n3423); lin-15A(n767)	98.6 (144)	100 (314)
lin-54(n3424); lin-15A(n767)	23.1 (26)	98.9 (87)
lin-15A(n433); lin-54(RNAi)	0 (107)	100 (576)
lin-15A(n767); lin-54(RNAi)	79.6 (191)	96.9 (196)

The penetrance of the Muv phenotype was determined after growing mutant strains at the indicated temperature for two or more generations. *lin-54(RNAi)* was performed at the indicated temperature as described in Materials and Methods. *lin-54(n3423)* and *lin-54(n3424)* were *cis*-marked with *unc-30(e191)*, and Unc progeny of heterozygous mutant parents were examined to score the penetrance of the Muv phentoype. ND, not determined.

Table 2: *let-60* Ras pathway activity is required for the *lin-54* Muv phenotype

Genotype	Vulval phenotype
lin-54(RNAi)	WT
lin-15A(n767); lin-54(RNAi)	Muv
lin-3(n378); lin-15A(n767)	Vul
let-23(sy97); lin-15A(n767)	Vul
let-60(n1876); lin-15A(n767)	Vul
lin-3(n378); lin-15A(n767); lin-54(RNAi)	Muv
let-23(sy97); lin-15A(n767); lin-54(RNAi)	Vul
let-60(n1876); lin-15A(n767); lin-54(RNAi)	Vul

The vulval phenotype reported was observed in greater than 85 percent of animals of a given genotype examined. To score *let-23(sy97)* and *let-60(n1876)* homozygotes, we examined the Unc progeny of *rol-6(e187) let-23(sy97) unc-4(e120) / mIn1[dpy-10(e128) mIs14]; lin-15A(n767)* and *let-60(n1876) unc-22(e66) / nT1; +/nT1; lin-15A(n767)* parents, respectively, that were placed on *lin-54(RNAi)* or control bacteria.

FIGURES

Figure 1. Molecular cloning of *lin-54*. Top panel, genetic map location of *lin-54* on linkage group IV. Middle and bottom panels, rescuing cosmids MMMC1 and JC8 and DNA subclones assayed for *lin-54* rescue. The number of transgenic lines rescued for the *lin-54(n2231); lin-15A(n433)* Muv phenotype over the number of lines assayed is shown on the right. The *lin-54* gene is indicated on the minimal rescuing fragment. The arrow indicates the direction of transcription. Coding sequences of *lin-54* are shaded.

Figure 1

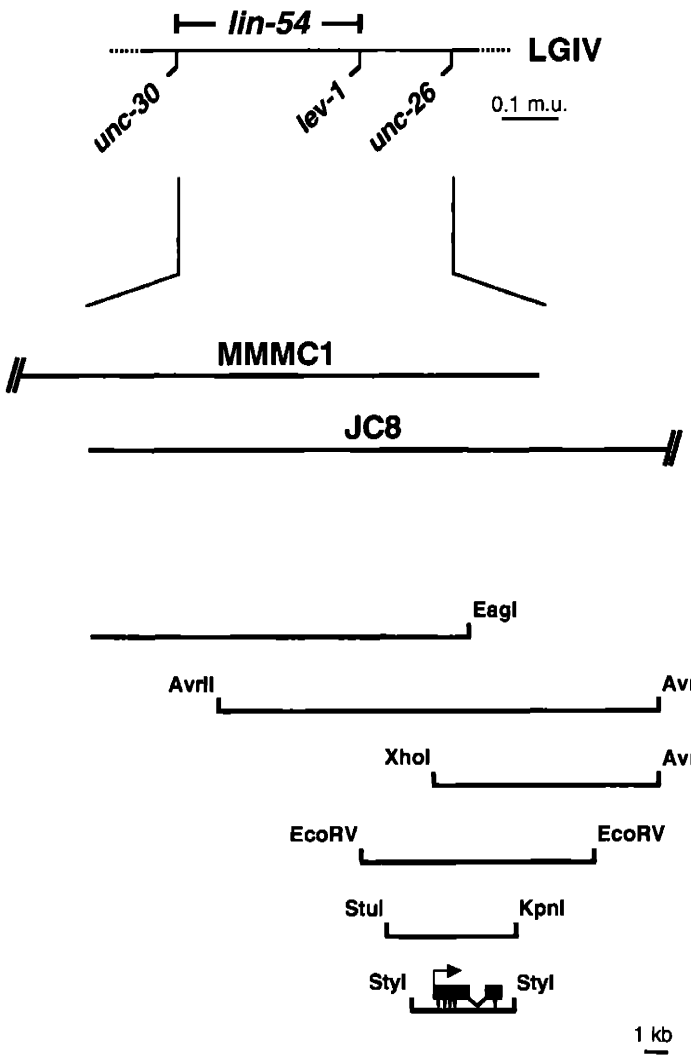
lin-54
LGIV
unc-30
lev-1
unc-26
0.1 m.u.
MMMC1
JC8
Lines Rescued
EagI
0/8
AvrII
AvrII
7/7
XhoI
AvrII
0/13
EcoRV
EcoRV
9/10
StuI
KpnI
3/4
StyI
StyI
4/4
1 kb

Figure 2. *lin-54* gene structure as deduced from cDNA and genomic sequences. Coding sequences are shaded, and 5' and 3' untranslated regions are indicated by open boxes. Predicted translation initiation and termination codons, the SL1 splice leader and the poly(A) tail are shown. The positions of *lin-54* missense mutations are indicated above (arrows) and deletion mutations below (brackets). Positions of alternative splicing are indicated by asterisks. In both cases, the use of alternative splice acceptors creates small differences in the *lin-54* coding sequence: alternative splicings of the first (ag/AACTTACAGGC versus agaacttacag/GC) and second (ag/CTTTTTCAGCC versus agctttttcag/CC) introns each differ by nine nucleotides. As described in Materials and Methods, the SL1 leader is also alternatively spliced.

Figure 2

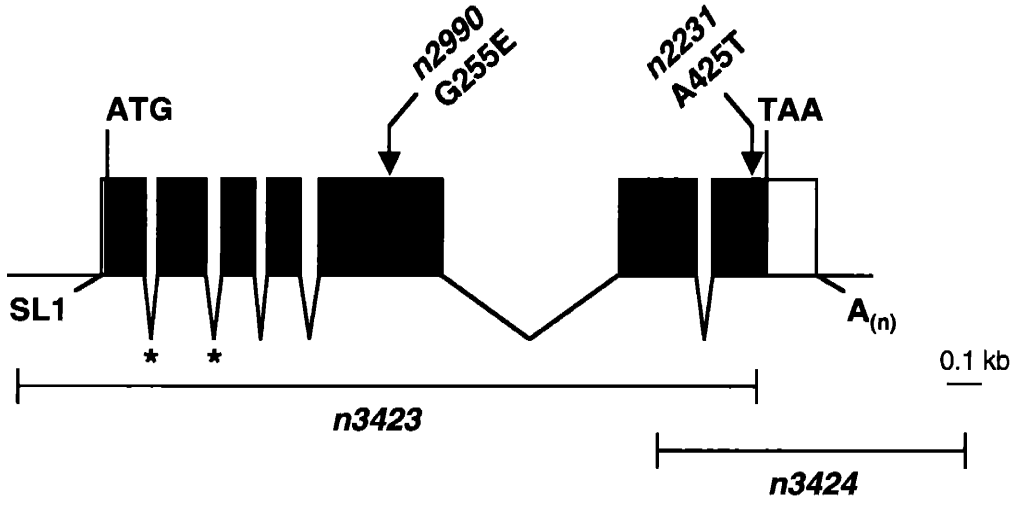

Figure 3. Alignment of LIN-54L with proteins predicted from human, mouse and *Drosophila* cDNA and genomic sequences. The predicted *Drosophila* AAF58365 protein has a large amino-terminal region that is not shown. Solid boxes indicate identities with LIN-54L. Arrowheads indicate the sites of the *n2231* and *n2990* missense mutations. The sequences removed by *n3423* and *n3424* are bracketed. The component cysteine residues of two cysteine-rich domains (amino acids 180-209 and 256-286) are shown by asterisks. Amino acids removed by alternative splicing are boxed.

Figure 3

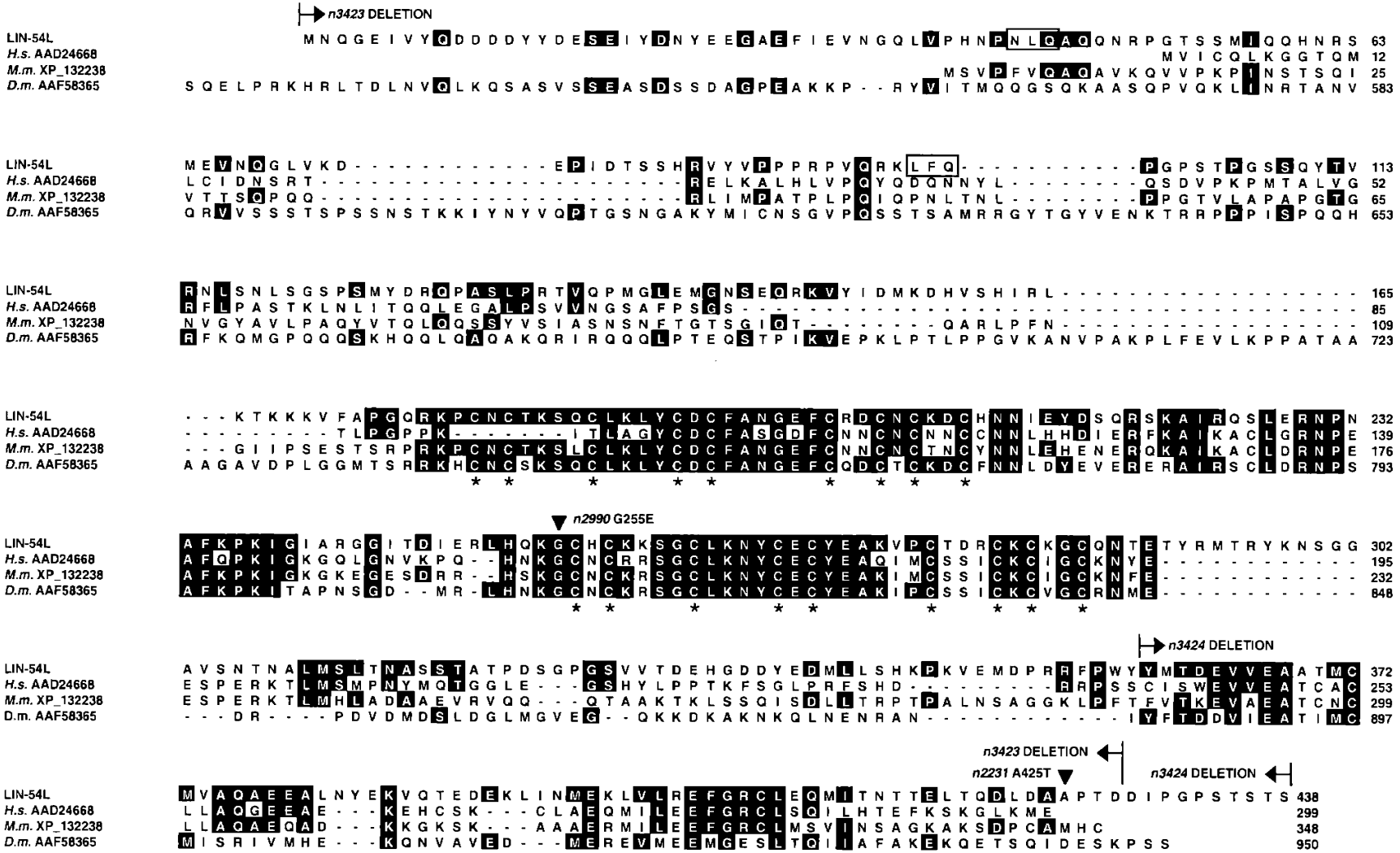
n3423 DELETION
LIN-54L
H.s. AAD24668
M.m. XP_132238
D.m. AAF58365
n2990 G255E
n3424 DELETION
n3423 DELETION
n2231 A425T
n3424 DELETION

Figure 4. *lin-54::gfp* expression. A *lin-54::gfp* L2 larva as viewed under transmitted light and Nomarski optics (A) and flourescent light (B). Midbody Pn.p cells are indicated with arrows. Anterior is to the left. The scale bar represents 10μm.

Figure 4

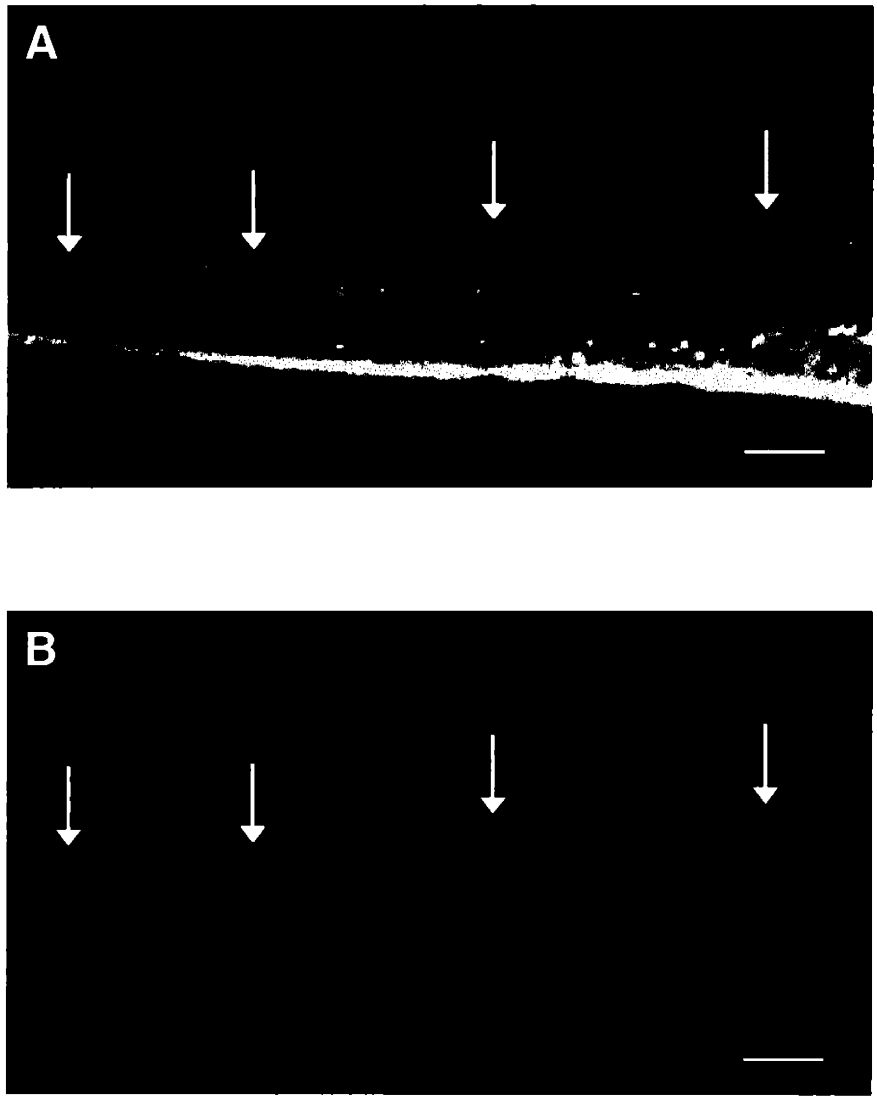

Figure 5. *lin-54* heat shock rescue. Temporal-specific expression of *lin-54* rescues the Muv phenotype of *lin-54(n2231); lin-15A(n433)* mutants. Animals were heat shocked at the stage indicated and scored as adults for rescue of the Muv phenotype. E, embryo.

Figure 5

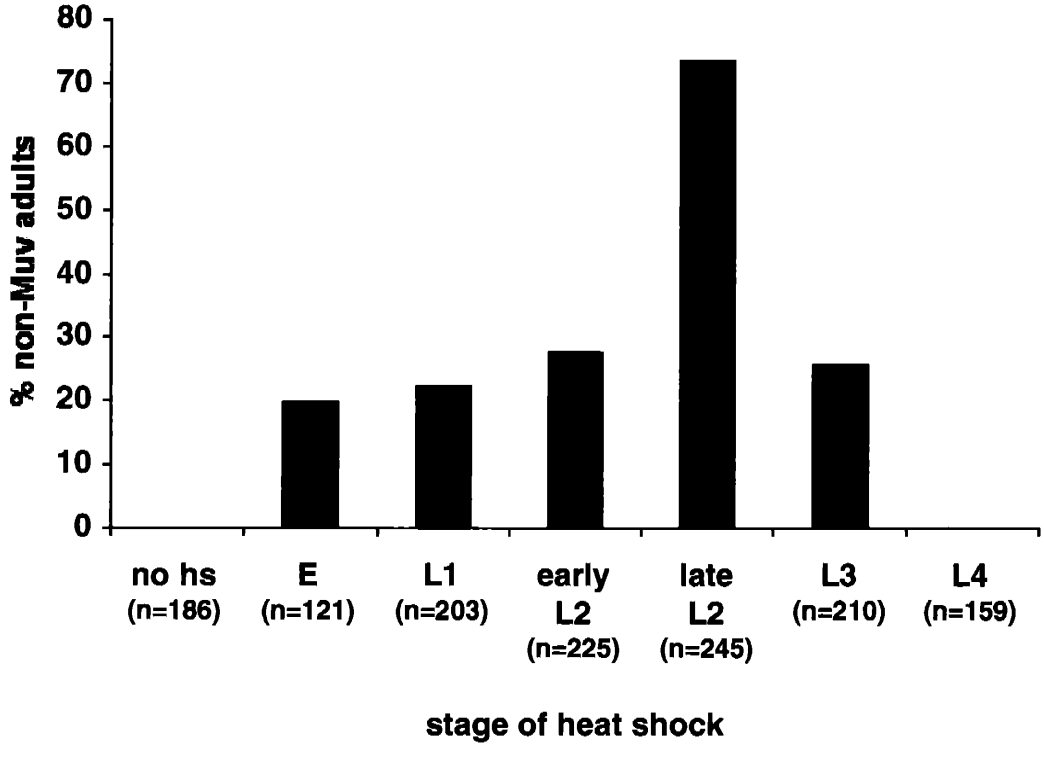
80
70
60
50
40
30
20
10
0
% non-Muv adults
no hs (n=186)
E (n=121)
L1 (n=203)
early L2 (n=225)
late L2 (n=245)
L3 (n=210)
L4 (n=159)
stage of heat shock

Figure 6. LIN-54 and LIN-36 *in vitro* interactions

(A) Full-length ^{35}S-labeled LIN-36 (lane 1) but not ^{35}S-labeled luciferase (lane 2) interacted with MBP-LIN-54. Full-length ^{35}S-labeled LIN-54 (lane 3) but not ^{35}S-labeled luciferase (lane 4) interacted with MBP-LIN-36. None of the ^{35}S-labeled proteins (lanes 5-7) interacted with MBP alone.

(B) Thirty percent of the ^{35}S-labeled proteins used in the binding reactions is shown.

(C) Coomassie blue staining of resin-bound MBP-LIN-36, MBP-LIN-54 and MBP proteins used in the binding reactions.

Figure 6

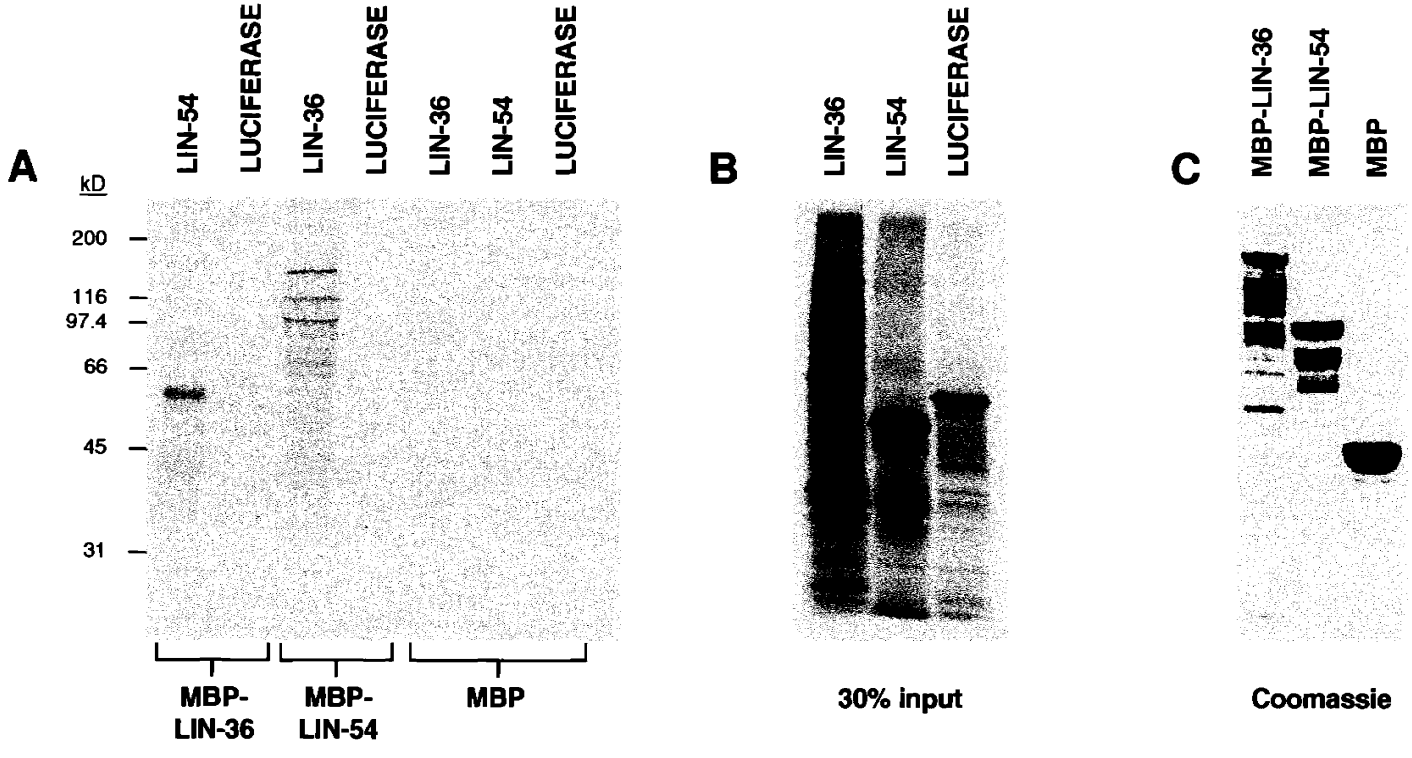
A
kD
200
116
97.4
66
45
31
LIN-54
LUCIFERASE
LIN-36
LUCIFERASE
LIN-36
LIN-54
LUCIFERASE
MBP-
LIN-36
MBP-
LIN-54
MBP
B
LIN-36
LIN-54
LUCIFERASE
30% input
C
MBP-LIN-36
MBP-LIN-54
MBP
Coomassie

CHAPTER 5

Newly-identified synthetic multivulva mutations affect the *lin-35* Rb pathway genes *lin-52* and *mep-1* and define genes that negatively regulate *let-60* Ras pathway signaling in *C. elegans*

Craig J. Ceol, Frank Stegmeier, Melissa Harrison and H. Robert Horvitz

This manuscript is being prepared for publication.

Frank Stegmeier and Melissa Harrison provided assistance in the isolation of synMuv mutants. Frank Stegmeier was a summer student and Melissa Harrison is a current graduate student in the Horvitz laboratory.

ABSTRACT

The synthetic multivulva (synMuv) genes negatively regulate Ras-mediated vulval induction in the nematode *C. elegans*. The synMuv genes are grouped into two classes, A and B, such that a mutation in a gene of each class is required to produce a multivulva phenotype. The class B synMuv genes include *lin-35*, a homolog of the retinoblastoma (Rb) tumor suppressor gene, and homologs of other genes that function with Rb in transcriptional regulation. We screened for additional synMuv mutations using a strategy different from that of previous synMuv genetic screens. Mutations we recovered affect previously identified synMuv genes and define seven new synMuv genes, some of which are putative components of a class B *lin-35* Rb signaling pathway. We present the molecular characterization of one previously identified and one new class B synMuv gene. A subset of mutations we recovered affect the gene *trr-1*. These mutations synthetically interact with both class A and class B synMuv mutations, indicating that *trr-1* defines a new class of synMuv genes.

INTRODUCTION

A fundamental issue in studies of development is how a group of cells that are initially equivalent in developmental potential can eventually adopt different fates. Genetic studies have indicated that cells within a developmental equivalence group often adopt different fates through the combined action of multiple and sometimes competing signals. For example, the initial step of R8 photoreceptor specification in *Drosophila* ommatidial development uses both positive and negative signals to properly select presumptive R8 photoreceptors from a field of developmentally equivalent cells in the eye imaginal disc (reviewed by FRANKFORT and MARDON 2002). An overlay of such signals can make a response in binary cell-fate decisions more precise or can increase the number of fates available to a particular cell.

Proper vulval development in the nematode *C. elegans* requires that ectodermal Pn.p cells with initially similar developmental potentials adopt different fates. The specification of Pn.p cells that eventually make vulval tissue occurs in two steps, each of which involves the selection of a subset of Pn.p cells from a larger Pn.p field (SULSTON and HORVITZ 1977). In the first step, which occurs in the L1 larval stage shortly after the Pn.p cells are generated, anterior and posterior Pn.p cells fuse with the syncytial hypodermis. After this first step, the unfused midbody P(3-8).p cells each have the capacity to adopt a vulval cell fate (STERNBERG and HORVITZ 1986). In a second step, however, only three of these cells, P(5-7).p, adopt such fates in which they undergo three rounds of division to generate seven or eight descendants. P3.p, P4.p and P8.p adopt non-vulval fates, typically dividing only once to generate two descendants that eventually fuse with the syncytial hypodermis. The decision to adopt vulval cell fates occurs during the L2 and early L3 larval stages and is followed by cell divisions and differentiation in the L3 and L4 larval stages, respectively (STERNBERG and HORVITZ 1986; FERGUSON *et al.* 1987).

Many genes that control the specification of Pn.p fates have been identified. Some of these genes act in a spatially-restricted fashion to select Pn.p cells for vulval development. The homeobox gene *lin-39* is expressed in the midbody and regulates the sequential steps of fusion and vulval cell-fate specification of the Pn.p cells in this region (CLARK *et al.* 1993; WANG *et al.* 1993; MALOOF and KENYON 1998). Strong loss-of-function *lin-39* mutations cause ectopic P(3-8).p cell fusion during the L1 stage. In partial loss-of-function *lin-39* mutants, unfused P(5-7).p cells are sometimes observed

and often show vulval-to-non-vulval cell-fate transformations (CLARK *et al.* 1993). *lin-39* activity therefore promotes unfused cell fates in the L1 stage and vulval cell fates in the L2 and early L3 stages. Genes in the *let-60* Ras signaling pathway also regulate the specification of Pn.p fates. In addition to *let-60* Ras, this pathway includes a number of genes, such as the receptor tyrosine kinase *let-23*, the SH2/SH3 adaptor *sem-5* and the MAP kinase *mpk-1*, that are broadly conserved in Ras signaling systems (reviewed by STERNBERG and HAN 1998). The role of *let-60* Ras signaling in the specification of vulval cell fates is well characterized. In wild-type animals, the *let-60* Ras pathway is specifically activated in P(5-7).p in response to an EGF-like signal, encoded by *lin-3*, that is produced by the neighboring gonadal anchor cell (HILL and STERNBERG 1992). Mutations that reduce *let-60* Ras pathway activity prevent P(5-7).p vulval cell fate specification, resulting in a Vulvaless (Vul) phenotype. Mutations that activate this pathway result in a Multivulva (Muv) phenotype in which P(3-8).p all adopt vulval cell fates (BEITEL *et al.* 1990; HAN and STERNBERG 1990; EISENMANN and KIM 1997).

The activities of *lin-39* and genes in the *let-60* Ras pathway are antagonized by the synthetic multivulva (synMuv) genes. The study of synMuv genes in vulval cell-fate specification led to the division of these genes into two redundant classes, A and B (FERGUSON and HORVITZ 1989). Animals carrying both a class A and a class B mutation are Muv, but animals with a mutation in a gene or genes of a single class have a wild-type vulva. Both classes of genes promote non-vulval cell fates in P(3-8).p. At present it is not clear whether the synMuv mutations cause an increase of *lin-39* or *let-60* Ras pathway activity in these cells or whether the synMuv genes make these cells more sensitive to normal levels of *lin-39* or *let-60* Ras pathway activity. Roles for synMuv genes in regulating Pn.p fusion have also been described. Some class B genes, but no class A genes, antagonize *lin-39*-mediated cell fusion of at least one Pn.p cell, P3.p (CHEN and HAN 2001).

Many synMuv genes have been cloned and molecularly characterized. The class B synMuv protein LIN-35 is similar to the mammalian tumor suppressor pRb (LU and HORVITZ 1998). Other class B synMuv proteins include DPL-1 and EFL-1, which are similar to mammalian DP and E2F proteins and, by analogy to their mammalian counterparts, likely function to target LIN-35 Rb to DNA (CEOL and HORVITZ 2001). The class B synMuv protein HDA-1 is similar to class I histone deacetylases and is likely targeted to specific genes by a DPL-1/EFL-1/LIN-35-containing protein complex (LU and HORVITZ 1998). Other class B synMuv proteins may function in the generation or as

components of this protein complex. The class A synMuv genes cloned to date encode novel proteins (CLARK et al. 1994; HUANG et al. 1994; E. DAVISON AND H.R.H., unpublished results) and less is known about their mechanism of action.

Using an approach that allowed the recovery of homozygous inviable mutations, we performed a genetic screen in a sensitized class A synMuv mutant background to identify new synMuv strains. We isolated mutations in seven new synMuv genes and in three genes that negatively regulate vulval development but were previously not known to function redundantly with synMuv genes. In addition, we cloned the class B synMuv gene *lin-52* and found that it encodes a protein that is similar to mammalian and Drosophila proteins of unknown function. Because *lin-52* acts in the same genetic pathway as *lin-35* Rb, these LIN-52 homologs may likewise be Rb pathway proteins.

MATERIALS AND METHODS

Strains and general techniques: Strains were cultured as described by BRENNER (1974) and grown at 20°C unless otherwise indicated. The wild-type parent of all the strains described in this study was the *Caenorhabditis elegans* Bristol strain N2. For some two and three-factor mapping experiments we used the polymorphic strain RW7000 (WILLIAMS *et al.* 1992). We also used strains containing the following mutations:

LGI: *bli-3(e767)*, *lin-17(n677)*, *unc-11(e47)*, *unc-73(e936)*, *lin-44(n1792)*, *unc-38(x20)*, *dpy-5(e61)*, *lin-35(n745)*, *lin-61(sy223)* (LU, HUANG, STERNBERG and HORVITZ, unpublished data), *unc-13(e1091)*, *lin-53(n833)* (FERGUSON and HORVITZ 1989; CHAPTER 2), *unc-54(e1092)* (DIBB *et al.* 1985)

LGII: *lin-31(n301)*, *dpy-10(e128)*, *tra-2(q276)*, *rol-6(e187)*, *dpl-1(n2994)* (CHAPTER 2), *unc-4(e120)*, *unc-53(n569)*, *mex-1(it9)*, *rol-1(e91)*

LGIII: *dpy-17(e164)*, *lon-1(e185)*, *sma-3(e491)*, *lin-13(n770)* (FERGUSON and HORVITZ 1989; CHAPTER 2), *lin-37(n758)*, *lin-36(n766)*, *unc-36(e251)*, *lin-9(n112)*, *unc-32(e189)*, *unc-16(e109)*, *sqv-3(n2842)*, *lin-52(n771)* (FERGUSON and HORVITZ 1989; CHAPTER 2), *unc-47(e307)*, *unc-69(e587)*, *dpy-18(e364)*

LGIV: *lin-1(e1275)*, *unc-5(e53)*, *unc-24(e138)*, *mec-3(e1338)*, *lin-3(n378)*, *sem-3(n1900)* (STERN and HORVITZ, unpublished data), *dpy-20(e1282)*,*unc-22(e66)*, *dpy-26(n198)*, *unc-31(e169)*, *unc-30(e191)*, *lin-54(n2231)* (CHAPTER 2), *dpy-4(e1166)*

LGV: *tam-1(cc567)* (HSIEH *et al.* 1999), *unc-46(e177)*, *let-418(s1617)*, *dpy-11(e224)*, *rol-4(sc8)*, *unc-76(e911)*, *efl-1(n3318)* (CEOL and HORVITZ 2001), *dpy-21(e428)*

LGX: *sli-1(sy143)*, *aex-3(ad418)*, *unc-1(e1598n1201)* (PARK and HORVITZ, unpublished data), *dpy-3(e27)*, *gap-1(ga133)* (HAJNAL *et al.* 1997), *unc-2(e55)*, *lon-2(e678)*, *unc-10(e102)*, *dpy-6(e14)*, *unc-9(e101)*, *unc-3(e151)*, *lin-15A(n767)*, *lin-15AB(n765).*

Unless otherwise noted, the mutations used are described by RIDDLE (1997). In addition, we used strains containing the following chromosomal aberrations: *mnDf57 II* (SIGURDSON *et al.* 1984), *mnDf90 II* (SIGURDSON *et al.* 1984), *mnDf29 II* (SIGURDSON *et al.* 1984), *mnDf87 II* (SIGURDSON *et al.* 1984), *mIn1[dpy-10(e128)mIs14] II* (EDGLEY and RIDDLE 2001), *mnC1[dpy-10(e128) unc-52(e444)] II* (HERMAN 1978), *nDf40 III* (HENGARTNER *et al.* 1992), *qC1[dpy-19(e1259)glp-1(q339)] III* (AUSTIN and KIMBLE, 1989), *sDf63 IV* (CLARK and BAILLIE 1992), *sDf62 IV* (CLARK and BAILLIE 1992), *sDf10 IV* (ROGALSKI *et al.* 1982), *eT1(III;V)* (ROSENBLUTH and BAILLIE 1981), *nT1(IV;V)* (FERGUSON

and HORVITZ 1985). *mIs14*, an integrated transgene linked to the chromosomal inversion *mIn1*, consists of a combination of GFP-expressing transgenes that allow *mIs14*-containing animals to be scored beginning at the 4-cell stage of embryogenesis (EDGLEY and RIDDLE 2001).

Isolation of new alleles: We mutagenized *lin-15A(n767)* hermaphrodites with ethyl methanesulfonate (EMS) as described by BRENNER (1974). We allowed these animals to recover on food for between 15 minutes to one hour, and then transferred individual P_0 larvae in L4 lethargus to 50 mm plates. After three to five days, 20 F_1 L4 larvae per P_0 were individually transferred to 50 mm plates, and, subsequently, F_2 animals on these plates were screened for a Muv phenotype. We screened the progeny of 3380 F_1 animals using this procedure.

Linkage group assignment: We used the following markers to determine linkage of newly isolated synMuv mutations to autosomes: *dpy-5 I*, *rol-6 II*, *unc-32 III*, *dpy-20 IV*, *rol-4 V*. We generated animals heterozygous for the new synMuv mutation and for at least two of these markers. For fertile synMuv mutants we picked Muv progeny and determined if these progeny segregated the markers, whereas for sterile synMuv mutants we picked single marker homozygotes and determined if these animals segregated the synMuv mutation. We also mapped some mutations using polymorphisms present in the RW7000 strain. We generated animals heterozygous for the new synMuv mutation and for RW7000 markers. We picked individual Muv progeny of these animals, performed lysis and used the resulting template DNA to monitor linkage to each of the autosomes by PCR (WILLIAMS *et al.* 1992). We tested for sex linkage to assign some new synMuv mutations to the X chromosome. Briefly, we generated heterozygous or hemizygous mutant males and mated them with marked *lin-15A(n767)* hermaphrodites. We then determined whether all, indicating sex linkage, or roughly half, indicating autosomal linkage, of the cross progeny hermaphrodites of this mating segregated the synMuv mutation. Some *lin-15B* mutations were not tested for sex linkage. Instead, we tentatively assigned X-chromosome linkage based on the presence, when *lin-15A(n767)* males were mated with these mutants, of cross-progeny males with pseudovulval ventral protrusions. Such protrusions are often observed in hemizygous *lin-15AB* mutant males (FERGUSON and HORVITZ 1985) but are found at a much lower penetrance in *lin-15A(n767)* males that are hemizygous for an X-linked synMuv mutation affecting genes other than *lin-15B*. The mutations we assigned in this manner were later determined by complementation tests to affect *lin-15B*.

Complementation tests: We typically performed complementation tests by mating males heterozygous for the new mutation and hemizygous for *lin-15A(n767)*, or, if X-linked, males hemizygous for both the new mutation and *lin-15A(n767)*, into marked synMuv mutant hermaphrodites, all of which contained a *lin-15A* mutation. Hemizygous *lin-15B(n3711)lin-15A(n767)* males could not mate. To perform complementation tests with this mutation, we mated *tra-2(q276); lin-15B(n3711)lin-15A(n767)/++* XX males into marked *lin-15AB* hermaphrodites. For new mutations that caused recessive sterility, we generated heterozygous males by starting matings with wild-type L4 males and individual gravid, putative heterozygous mutant hermaphrodites. For complementation tests we used cross-progeny males derived from plates that had self-progeny Muv animals present. In all complementation tests, unmarked cross-progeny hermaphrodites were scored.

Construction of deficiency heterozygotes: To construct *trr-1(n3712)* heterozygotes with *mnDf57*, *mnDf90* and *mnDf29*, *Df/mIn1; lin-15A(n767)* males were generated. These males were mated into *rol-6 trr-1(n3712)/mIn1; lin-15A(n767)* hermaphrodites and non-Rol, non-Gfp cross-progeny were scored. *mnDf87* heterozygous males do not mate so in this case we generated *trr-1(n3712)/mnDf87; lin-15A(n767)* animals by mating *trr-1(n3712)/mIn1; lin-15A(n767)* males into *unc-4 mnDf87/mIn1; lin-15A(n767)* hermaphrodites. To construct the *lin-52* heterozygote with *nDf40*, we mated *nDf40 dpy-18/unc-36; lin-15A(n767)* males into *unc-36 lin-52(n771); lin-15A(n767)* hermaphrodites and scored non-Unc cross progeny. *mep-1/Df* animals were constructed by mating *Df/nT1; +/nT1* males into *dpy-20 mep-1; lin-15A(n767)* hermaphrodites and scoring non-Dpy cross progeny.

Transgenic animals: Germline transformation was performed, as described by MELLO (1991), by injecting cosmid (5-10 ng/μL) or plasmid (50-80 ng/μL) DNA into *lin-52* or *mep-1* mutants. Either pRF4, which causes a dominant Rol phenotype, or pPD93.97 (A. FIRE, personal communication), which expresses *gfp* under the control of the *myo-3* promoter, was used as a coinjection marker.

***lin-52* cDNA isolation:** We obtained a partial *lin-52* cDNA clone (kindly provided by YUJI KOHARA), yk253b12, that included 249 nucleotides of the *lin-52* open reading frame and also included the 3' untranslated region and a polyA tail. We used the 5' RACE system v2.0 (GIBCO-BRL) to determine the 5' end of the *lin-52* transcript. We ligated the two portions of the *lin-52* cDNA together to generate a full-length cDNA

clone. The *lin-52* 5' RACE products were *trans*-spliced to the SL2 leader sequence consistent with observations made by ZORIO *et al.* (1994).

Allele sequence: We used PCR-amplified regions of genomic DNA as templates in determining gene sequences. For each gene investigated, we determined the sequences of all exons and splice junctions. Whenever observed, the sequence of a mutation was confirmed using an independently-derived PCR product. All sequences were determined using an automated ABI 373 DNA sequencer (Applied Biosystems).

RESULTS

Isolation of new synMuv mutants: A variety of genetic studies revealed that sterility is often associated with a severe reduction of class B synMuv gene function: 1) In a genetic screen for alleles that did not complement the synMuv phenotype of *lin-9(n112)*, FERGUSON and HORVITZ (1989) recovered the alleles *lin-9(n942)* and *lin-9(n943)*, that, when homozygous, caused sterility; 2) We performed gene dosage studies and observed that, in comparison to the wild type, *lin-52(n771)/Df* (THIS STUDY) and *dpl-1(n2994)/Df* (CHAPTERS 2, 3) heterozygotes had markedly reduced brood sizes; 3) Deletion mutations of synMuv genes that showed recessive sterility were recovered by reverse genetic approaches (*e.g.* alleles of *lin-53* (LU 1999), *lin-54* (CHAPTER 4) and *dpl-1* (CEOL and HORVITZ 2001).

Previous genetic screens for synMuv mutants (FERGUSON and HORVITZ 1989; CHAPTER 2) were performed before a link between loss of synMuv gene function and sterility was well established. These screens required that isolates be fertile and viable in order to recover mutant alleles. In addition to not recovering recessive sterile mutations of the genes described above, these screens failed to recover mutations of the class B synMuv genes *efl-1* and *let-418*, both of which can mutate to a sterile phenotype (VON ZELEWSKY *et al.* 2000; CEOL and HORVITZ 2001). These results suggested that additional synMuv genes might be identified in a screen that allowed the recovery of homozygous sterile mutations through phenotypically wild-type heterozygous siblings.

To screen for new synMuv mutants, we examined the F_2 progeny of individually plated F_1 animals after EMS mutagenesis of *lin-15A(n767)* mutants. This screen represented 6760 haploid genomes examined for mutations that either alone or in combination with *lin-15A(n767)* showed a recessive Muv phenotype. Using this strategy we identified 95 Muv mutations, 24 of which were maintained as heterozygotes due to recessive sterility that cosegregated with the Muv phenotype. Three mutations caused a Muv phenotype in the absence of *lin-15A(n767)* and were found to affect the previously studied genes *lin-1* and *lin-31*, both of which function downstream of *let-60* Ras in vulval induction (FERGUSON *et al.* 1987). These mutations, *lin-1(n3443)*, *lin-1(n3522)* and *lin-31(n3440)* were not characterized further. Additionally we recovered 29 mutations that, together with *lin-15A(n767)*, caused a weakly penetrant (< 30%) Muv phenotype. To date we have been unable to convincingly map these

mutations to linkage groups and their characterization is not presented. The remaining 63 mutations were assigned to 21 complementation groups, which include the previously known genes *ark-1*, *dpl-1*, *efl-1*, *gap-1*, *let-418*, *lin-9*, *lin-13*, *lin-15B*, *lin-35*, *lin-36*, *lin-52*, *lin-53*, *lin-61* and *sli-1*, and the new genes *lin(n3441)*, *lin(n3542)*, *lin(n3628)*, *lin(n3681)*, *lin(n3707)*, *mep-1* and *trr-1*.

Phenotypes of new mutants: We characterized the penetrance of the Muv phenotype for each strain at 15°C and 20°C (Table 1). The penetrance at 25°C is not shown because all strains had a highly penetrant (>90%) Muv phenotype at this temperature. Since a heat-sensitive Muv phenotype is characteristic of most synMuv strains, including those with null mutations in synMuv genes (FERGUSON and HORVITZ 1989; CHAPTER 2), it is likely that many synMuv mutations are not particularly temperature sensitive, but rather that the synMuv genes regulate a temperature sensitive process.

A subset of our synMuv strains also exhibited a sterile phenotype. In these strains, the sterile phenotype cosegregated with the Muv phenotype during backcrosses and two- and three-factor mapping experiments. For those mutations tested, which included six *let-418* and two *lin-53* homozygous inviable mutations, we found that our new mutations did not complement the sterile phenotypes caused by previously isolated, allelic synMuv mutations (data not shown). These observations suggest that the sterile and Muv phenotypes of these strains were caused by the same mutation.

We observed an unusual aspect to the sterility of one of our strains. We examined the *mep-1(n3680); lin-15A(n767)* strain and found that its sterile phenotype showed maternal-effect rescue. When derived from heterozygous parents, the sterility of the *mep-1(n3680); lin-15A(n767)* animals was 3.2% penetrant (n=62) but was 55% penetrant (n=69) when these animals were derived from homozygous parents. Mutations that affect the Mes (Mes, maternal-effect sterility) genes also show maternal-effect rescue of sterility (CAPOWSKI *et al.* 1991). Some Mes genes encode homologs of *Drosophila* polycomb group proteins and are proposed to function in X chromosome transcriptional silencing in the germline (HOLDEMAN *et al.* 1998; KORF *et al.* 1998; FONG *et al.* 2002). A functional relationship between the synMuv and Mes genes has not been reported.

New synMuv genes: Using two-factor crosses and sex chromosome transmission tests (see MATERIALS AND METHODS), we mapped the new mutations to linkage groups (Table 2). We then determined if a given mutation failed to complement

mutations of known synMuv genes on the same linkage group. Mutations that were not assigned to known synMuv complementation groups were tested against unassigned mutations within the same linkage group for complementation. These tests defined seven new synMuv loci: *trr-1*, *mep-1*, *lin(n3441)*, *lin(n3628)*, *lin(n3681)*, *lin(n3707)* and *lin(n3542)*. We used three-factor crosses to map most of these new synMuv genes within their respective linkage groups (Table 3). In addition we thus far have isolated *trr-1*, *mep-1*, *n3441*, *n3628* and *n3681* mutations away from the parental *lin-15A(n767)* mutation. *mep-1*, *n3441*, *n3628* and *n3681* mutations alone do not cause a Muv phenotype (data not shown), and *trr-1* mutations alone cause only weak ectopic vulval induction (CHAPTER 6). Thus, these mutations synergize with *lin-15A(n767)* and are indeed synMuv mutations.

We identified mutations in *gap-1* and *sli-1*, two genes that were originally identified in screens for mutations that suppressed the Vul phenotype caused by a reduction in *let-60* Ras pathway signaling (JONGEWARD *et al.* 1995; HAJNAL *et al.* 1997). We also identified mutations in *ark-1*, a gene that was first identified in a screen for mutations that caused ectopic vulval induction in a *sli-1* mutant background (HOPPER *et al.* 2000). *gap-1*, *sli-1* and *ark-1* single mutants were previously isolated and found to have no (*sli-1*, *gap-1*) or subtle (*ark-1*) defects in vulval development. Our results indicate that *sli-1*, *gap-1* and *ark-1* act redundantly with *lin-15A* to negatively regulate *let-60* Ras signaling.

Molecular identification of *lin-52*: We have further characterized the class B synMuv gene *lin-52*. *lin-52* was originally identified by FERGUSON and HORVITZ (1989) and was subsequently mapped to an interval on LGIII (CHAPTER 2). Using standard three- and four-factor mapping techniques, we further mapped *lin-52* to a small genetic interval between *sqv-3* and the Tc1 transposon polymorphism *stP127* (Figure 1). We generated transgenic animals using DNA clones of this interval and found that the overlapping cosmids ZK630 and C26C12 and subclones of DNA common to both of these cosmids rescued the Muv phenotype of *lin-52(n771); lin-15A(n767)* mutants. Typically greater than 70 percent of transgenic animals in the first generation of a stable transgenic line (*i.e.* in the transgenic F_2 progeny of an injected animal) were rescued. However, in transgenic lines containing these cosmids or their subclones, we observed a progressive reduction in the penetrance of rescue in each subsequent generation. The reason for this trend is unknown, although we speculate that it may have resulted from transgene silencing. Such generation-dependent transgene silencing occurs in the

C. elegans germline and is thought to be due to the preferential recruitment of silencing factors to repetitive stretches of DNA (KELLY *et al.* 1997).

Because two complete predicted genes, ZK632.9 and ZK632.13, were present on the minimal rescuing fragment, we performed further experiments to define *lin-52* (Figure 1). Into the minimal rescuing fragment we cloned a small double-stranded oligonucleotide that is predicted to introduce an in-frame stop codon into the ZK632.13 gene. This subclone was unable to rescue the Muv phenotype of *lin-52(n771); lin-15A(n767)* mutants, whereas a subclone in which the oligonucleotide was removed, thereby restoring the ZK632.13 open reading frame, rescued like the clones described above. In addition, we found that RNA-mediated interference of ZK632.13 in a *lin-15A(n767)* background resulted in a highly penetrant Muv phenotype. Finally, we determined the sequence of ZK632.13 in *lin-52(n771)* and *lin-52(n3718)* mutants: *lin-52(n771)* mutants contain a missense mutation that is predicted to substitute a positively-charged lysine in place of a negatively-charged glutamate and *lin-52(n3718)* mutants contain a nonsense mutation that is predicted to truncate the ZK632.13 protein after 30 amino acids. These results together define ZK632.13 as *lin-52.*

We assembled a cDNA clone of *lin-52* (Figure 2A; see MATERIALS AND METHODS). It contains a 5' SL2 splice leader sequence and a polyA tail, indicating that it is a full-length clone. An SL2 leader sequence is often *trans*-spliced upstream of genes that are initially transcribed as downstream genes of an operon (ZORIO *et al.* 1994). The SL2 leader sequence and the proximity of *lin-52* to the gene immediately upstream of it suggest that *lin-52* is transcribed as part of a polycistron. The large open reading frame on this cDNA is predicted to encode a 161 amino acid protein that is similar to uncharacterized proteins predicted by human, mouse and Drosophila cDNA and genomic sequences (Figure 2B; C.J.C. and H.R.H., unpublished observations). LIN-52 is most similar to these proteins in a short carboxy-terminal domain. Over a stretch of 28 amino acids, LIN-52 is 50% identical and 75% similar to the human predicted protein LOC91750. This region of similarity may represent a functional domain within the LIN-52 protein.

Molecular identification of *mep-1*: We isolated three mutations, *n3680*, *n3702* and *n3703*, in a gene that we mapped to a small interval on linkage group IV in between *sem-3* and *dpy-20* (Figure 3). We attempted to rescue the Muv phenotype of *n3680; lin-15A(n767)* mutants using cosmid clones from this interval. Transgenic animals containing the cosmid M04B2 were rescued for the Muv phenotype and also showed

improved fertility relative to non-transgenic animals. Around this time we learned that two other laboratories were studying a gene called *mep-1* that was present on the M04B2 cosmid (PUOTI and KIMBLE; UNHAVAITHAYA and MELLO, personal communication). This gene was originally identified based on its interaction with the germline specification genes *mog-1*, *mog-4*, *mog-5* and *pie-1* in yeast two-hybrid screens. Because somatic tissues adopt germ cell-specific characteristics in *mep-1* mutants, *mep-1* is thought to repress germ cell fates in the soma. Recently, the MEP-1 protein was found to interact with LET-418, and the *mep-1* gene was found to have class B synMuv activity (UNHAVAITHAYA and MELLO, personal communication). We sequenced *mep-1* in our mutant strains to determine if the mutations we isolated affected this gene. *n3680* mutants have a missense mutation that, in the predicted MEP-1 protein, changes a polar serine residue to an asparagine. *n3702* mutants have a nonsense mutation and *n3703* mutants a splice acceptor mutation in the *mep-1* gene. Our genetic mapping data, cosmid rescue and DNA sequence results indicate that *n3680*, *n3702* and *n3703* are *mep-1* mutations.

mep-1 encodes a protein containing six zinc-finger motifs. Zinc fingers are known to mediate interactions of proteins with DNA and with other proteins. The zinc fingers of MEP-1 may mediate interactions with LET-418 or other synMuv proteins.

Sequences of synMuv mutations: We determined sequences of mutations that affected additional synMuv genes (Table 4). Most mutations are GC-to-AT transitions that are characteristic of EMS mutagenesis (ANDERSON 1995). Many of these mutations are predicted to truncate the corresponding synMuv proteins. The truncations predicted by *efl-1(n3639)*, *let-418(n3719)* and *lin-52(n3718)* are particularly severe, and the synMuv and sterile phenotypes caused by these mutations may represent the null phenotypes of these genes. In addition, we found missense mutations that disrupt predicted functional domains of synMuv proteins. For example, *n3536*, *n3626*, *n3629* and one of the two mutations of *n3636* affect the ATPase/helicase domain of LET-418. LET-418 is a member of the Mi-2 family of ATP-dependent chromatin remodeling enzymes (SOLARI and AHRINGER 2000; VON ZELEWSKY *et al.* 2000), and the LET-418 missense mutations suggest that LET-418 function is similarly dependent on ATP hydrolysis. At least one mutation affecting the LIN-13 protein, *n3642*, is predicted to disrupt a canonical zinc-finger motif. This missense mutation, along with those isolated previously (CHAPTER 2), indicate that at least some of the twenty-four LIN-13 zinc fingers are important for its synMuv activity. Missense mutations affecting other synMuv

proteins are not as easily linked to the disruption of predicted functional domains. These mutations may provide a useful starting point in identifying functional motifs within synMuv proteins that are not predicted by sequence comparisons.

DISCUSSION

Frequency of mutant isolation: The rate at which we isolated mutations was much higher than that observed in previous synMuv screens: counting only the 63 mutations described in this study, we recovered one synMuv mutation per 107 haploid genomes screened versus 1/750 (FERGUSON and HORVITZ 1989), 1/400 (CHAPTER 2) and 1/667 (CHAPTER 2) in previous screens. We believe the reasons for this difference are threefold. First, our screen design allowed the isolation of synMuv mutations that also caused sterility. Sterile synMuv mutants were observed previously, but because the heterozygous siblings of these mutants were present in a sea of genotypically unrelated animals, the underlying mutations could not be recovered. Second, our parental strain carried the strong class A mutation, *lin-15A(n767)*. The penetrance of a strain's Muv phenotype is dependent on the aggregate strengths of the component synMuv mutations (C.J.C. and H.R.H., unpublished observations). Therefore, even weak mutations may be identified in a strong synMuv background such as *lin-15A(n767)*. Although we have not formally tested this possibility, we believe that some of the mutations we recovered only weakly affect synMuv activity. Such mutations may not have been recovered in previous screens that were performed in partial loss-of-function synMuv backgrounds. Third, in screening a plate of many F_2 progeny derived from a single F_1 animal, we observed many genotypically identical animals per haploid genome screened. This type of screening likely accounts for our isolation of a number of partially penetrant synMuv mutations. Such mutations may not have been identified in earlier synMuv screens that typically observed fewer genotypically identical animals per haploid genome screened.

Our high rate of recovery indicates many genes can mutate to a synMuv phenotype. Including the ten genes that we found to have synMuv activity in this study, a total of 25 genes can act redundantly with class A synMuv genes. Many of these genes are represented by one or a few mutant alleles, indicating that screens for synMuv genes are not saturated.

The synMuv genes we identified likely act in different pathways: Class B synMuv mutations synergize with class A synMuv mutations but not with other class B synMuv mutations. Such genetic behavior led to the hypothesis that class B synMuv genes are part of a single genetic pathway (FERGUSON and HORVITZ 1989). In support of this hypothesis, mutations affecting different class B synMuv genes are similarly

suppressed by loss-of-function mutations in the *let-23* receptor tyrosine kinase and other *let-60* Ras pathway loss-of-function mutations (FERGUSON *et al.* 1987; LU and HORVITZ 1998; CEOL and HORVITZ 2001). Furthermore, a subset of class B synMuv gene products have been shown to interact *in vitro* and their homologs are known function together in other systems (LU and HORVITZ 1998; CEOL and HORVITZ 2001).

Because we conducted our screen in a class A synMuv background, we anticipated recovering mutations that affected genes of the class B synMuv pathway. In addition to Class B synMuv mutations, our results suggest that we recovered mutations that disable distinct genetic pathways. We recovered six mutations that affect the *trr-1* gene. Unlike typical class B synMuv mutations, *trr-1(n3712)* synergize not only with class A synMuv mutations, but also with class B synMuv mutations (CHAPTER 6). *trr-1(n3712)* single mutants also atypically show ectopic vulval induction. Because of its unusual genetic interactions, we propose that *trr-1* functions in a pathway distinct from the class B synMuv pathway. We also recovered mutations affecting the *sli-1*, *gap-1* and *ark-1* genes. These genes were previously characterized as negative regulators of *let-60* Ras pathway activity, acting genetically downstream of the *let-23* receptor tyrosine kinase (JONGEWARD *et al.* 1995; HAJNAL *et al.* 1997; HOPPER *et al.* 2000). The molecular identities of *sli-1*, *gap-1* and *ark-1* support their action downstream of *let-23*. *sli-1* encodes a homolog of the c-cbl proto-oncoprotein, which is thought to downregulate receptor tyrosine kinase levels though ubiquitin-mediated degradation (YOON *et al.* 1995; LEVKOWITZ *et al.* 1999). *gap-1* is a member of the GTPase-activating protein family (HAJNAL *et al.* 1997). GAPs enhance the catalytic function of Ras family GTPases, thereby facilitating the switch from active GTP-bound to inactive GDP-bound Ras. *ark-1* encodes a predicted cytoplasmic tyrosine kinase that interacts with the SEM-5 SH2/SH3 adaptor protein (HOPPER *et al.* 2000). Since *sem-5* acts downstream of the *let-23* receptor tyrosine kinase, *ark-1* is proposed to inhibit *let-60* Ras signaling downstream of *let-23*. These genetic and molecular data suggest that *sli-1*, *gap-1* and *ark-1* directly regulate *let-60* Ras pathway members and are likely not part of the canonical class B synMuv pathway, which is thought to regulate the *let-60* Ras pathway either upstream of, or in parallel to, the *let-23* receptor tyrosine kinase. We are currently placing our synMuv mutations into different genetic classes by examining interactions with class B synMuv and *let-23* mutations.

***lin-52* encodes a new putative Rb pathway protein:** *lin-35*, a member of the class B synMuv pathway, encodes a protein similar to the mammalian tumor suppressor

pRb (LU and HORVITZ 1998). Other genes with class B synMuv activity encode DP, E2F, RbAp48, histone deacetylase and HP1 family proteins (LU and HORVITZ 1998; CEOL and HORVITZ 2001; COUTEAU *et al.* 2002). Mammalian homologs of these proteins are known to functionally, and in some cases physically, interact with pRb. These and other parallels indicate that the class B synMuv pathway is an analog of Rb pathways in other systems. Consequently, additional class B synMuv genes may have homologs with analogous functions in other systems. One such gene is *lin-52*. By the genetic criteria outlined above, *lin-52* is a class B synMuv gene. *lin-52* mutations synthetically interact with class A mutations but not with class B mutations (CHAPTER 2). Furthermore, preliminary experiments indicate that the Vul phenotype of a *let-23* loss-of-function mutation is epistatic to the Muv phenotype caused by *lin-52* and *lin-15A* loss of function (C.J.C. and H.R.H., unpublished observations). *lin-52* encodes a small protein, portions of which are conserved in similarly small proteins predicted by the human, mouse and *Drosophila* genome sequences. The characterization of these and other class B synMuv protein homologs should help to determine whether they too function in Rb-mediated signaling.

ACKNOWLEDGMENTS

We thank Beth Castor, Na An and Andrew Hellman for expert technical assistance and Brendan Galvin for critical reading of this manuscript. We also thank Yuji Kohara for providing a *lin-52* cDNA clone and Neil Hopper for providing the *ark-1(sy247)* strain. Some of the strains used in this work were provided by the *Caenorhabditis* Genetics Center, which is supported by the National Institutes of Health National Center for Research Resources. This work was supported by National Institutes of Health grant GM24663 to H. R. H..

C. J. C. was a Koch Graduate Fellow. H. R. H. is an investigator of the Howard Hughes Medical Institute.

LITERATURE CITED

ANDERSON, P., 1995 Mutagenesis, pp. 31-58 in *Methods Cell Biol.*

AUSTIN, J., and J. KIMBLE, 1989 Transcript analysis of *glp-1* and *lin-12*, homologous genes required for cell interactions during development of *C. elegans*. Cell **58:** 565-571.

BEITEL, G. J., S. G. CLARK and H. R. HORVITZ, 1990 *Caenorhabditis elegans ras* gene *let-60* acts as a switch in the pathway of vulval induction. Nature **348:** 503-9.

BEITEL, G. J., E. J. LAMBIE and H. R. HORVITZ, 2000 The *C. elegans* gene *lin-9*,which acts in an Rb-related pathway, is required for gonadal sheath cell development and encodes a novel protein. Gene **254:** 253-63.

BRENNER, S., 1974 The genetics of *Caenorhabditis elegans*. Genetics **77:** 71-94.

CAPOWSKI, E. E., P. MARTIN, C. GARVIN and S. STROME, 1991 Identification of grandchildless loci whose products are required for normal germ-line development in the nematode *Caenorhabditis elegans*. Genetics **129:** 1061-72.

CEOL, C. J., and H. R. HORVITZ, 2001 *dpl-1* DP and *efl-1* E2F act with *lin-35* Rb to antagonize Ras signaling in *C. elegans* vulval development. Mol. Cell **7:** 461-73.

CHEN, Z., and M. HAN, 2001 *C. elegans* Rb, NuRD, and Ras regulate *lin-39*-mediated cell fusion during vulval fate specification. Curr. Biol. **11:** 1874-9.

CLARK, D. V., and D. L. BAILLIE, 1992 Genetic analysis and complementation by germ-line transformation of lethal mutations in the *unc-22 IV* region of *Caenorhabditis elegans*. Mol. Gen. Genet. **232:** 97-105.

CLARK, S. G., A. D. CHISHOLM and H. R. HORVITZ, 1993 Control of cell fates in the central body region of *C. elegans* by the homeobox gene *lin-39*. Cell **74:** 43-55.

CLARK, S. G., X. LU and H. R. HORVITZ, 1994 The *Caenorhabditis elegans* locus *lin-15*, a negative regulator of a tyrosine kinase signaling pathway, encodes two different proteins. Genetics **137:** 987-97.

COUTEAU, F., F. GUERRY, F. MULLER and F. PALLADINO, 2002 A heterochromatin protein 1 homologue in *Caenorhabditis elegans* acts in germline and vulval development. EMBO Rep. **3:** 235-41.

DIBB, N. J., D. M. BROWN, J. KARN, D. G. MOERMAN, S. L. BOLTEN et al., 1985 Sequence analysis of mutations that affect the synthesis, assembly and enzymatic activity of the *unc-54* myosin heavy chain of *Caenorhabditis elegans*. J. Mol. Biol. **183:** 543-51.

EDGLEY, M. L., and D. L. RIDDLE, 2001 LG II balancer chromosomes in *Caenorhabditis elegans*: *mT1(II;III)* and the *mIn1* set of dominantly and recessively marked inversions. Mol. Genet. Genomics **266:** 385-95.

EISENMANN, D. M., and S. K. KIM, 1997 Mechanism of activation of the *Caenorhabditis elegans* ras homologue *let- 60* by a novel, temperature-sensitive, gain-of-function mutation. Genetics **146:** 553-65.

FERGUSON, E. L., and H. R. HORVITZ, 1985 Identification and characterization of 22 genes that affect the vulval cell lineages of the nematode *Caenorhabditis elegans*. Genetics **110:** 17-72.

FERGUSON, E. L., and H. R. HORVITZ, 1989 The multivulva phenotype of certain *Caenorhabditis elegans* mutants results from defects in two functionally redundant pathways. Genetics **123:** 109-21.

FERGUSON, E. L., P. W. STERNBERG and H. R. HORVITZ, 1987 A genetic pathway for the specification of the vulval cell lineages of *Caenorhabditis elegans*. Nature **326:** 259-67.

FONG, Y., L. BENDER, W. WANG and S. STROME, 2002 Regulation of the different chromatin states of autosomes and X chromosomes in the germ line of *C. elegans*. Science **296:** 2235-8.

FRANKFORT, B. J., and G. MARDON, 2002 R8 development in the *Drosophila* eye: a paradigm for neural selection and differentiation. Development **129:** 1295-306.

HAJNAL, A., C. W. WHITFIELD and S. K. KIM, 1997 Inhibition of *Caenorhabditis elegans* vulval induction by *gap-1* and by *let-23* receptor tyrosine kinase. Genes Dev. **11:** 2715-28.

HAN, M., and P. W. STERNBERG, 1990 *let-60*, a gene that specifies cell fates during *C. elegans* vulval induction, encodes a ras protein. Cell **63:** 921-31.

HENGARTNER, M. O., R. E. ELLIS and H. R. HORVITZ, 1992 *Caenorhabditis elegans* gene *ced-9* protects cells from programmed cell death. Nature **356:** 494-9.

HERMAN, R. K., 1978 Crossover suppressors and balanced recessive lethals in *Caenorhabditis elegans*. Genetics **88:** 49-65.

HILL, R. J., and P. W. STERNBERG, 1992 The gene *lin-3* encodes an inductive signal for vulval development in *C. elegans*. Nature **358:** 470-6.

HOLDEMAN, R., S. NEHRT and S. STROME, 1998 MES-2, a maternal protein essential for viability of the germline in *Caenorhabditis elegans*, is homologous to a *Drosophila* Polycomb group protein. Development **125:** 2457-67.

HOPPER, N. A., J. LEE and P. W. STERNBERG, 2000 ARK-1 inhibits EGFR signaling in *C. elegans*. Mol. Cell **6:** 65-75.

HSIEH, J., J. LIU, S. A. KOSTAS, C. CHANG, P. W. STERNBERG et al., 1999 The RING finger/B-box factor TAM-1 and a retinoblastoma-like protein LIN-35 modulate context-dependent gene silencing in *Caenorhabditis elegans*. Genes Dev. **13:** 2958-70.

HUANG, L. S., P. TZOU and P. W. STERNBERG, 1994 The *lin-15* locus encodes two negative regulators of *Caenorhabditis elegans* vulval development. Mol. Biol. Cell **5:** 395-411.

JONGEWARD, G. D., T. R. CLANDININ and P. W. STERNBERG, 1995 *sli-1*, a negative regulator of *let-23*-mediated signaling in *C. elegans*. Genetics **139:** 1553-66.

KELLY, W. G., S. XU, M. K. MONTGOMERY and A. FIRE, 1997 Distinct requirements for somatic and germline expression of a generally expressed *Caernorhabditis elegans* gene. Genetics **146:** 227-38.

KORF, I., Y. FAN and S. STROME, 1998 The Polycomb group in *Caenorhabditis elegans* and maternal control of germline development. Development **125:** 2469-78.

LEVKOWITZ, G., H. WATERMAN, S. A. ETTENBERG, M. KATZ, A. Y. TSYGANKOV et al., 1999 Ubiquitin ligase activity and tyrosine phosphorylation underlie suppression of growth factor signaling by c-Cbl/Sli-1. Mol. Cell **4:** 1029-40.

LU, X., 1999. Molecular analyses of the class B synthetic multivulva genes of *Caenorhabditis elegans*, Ph.D. Thesis, Massachusetts Institute of Technology.

LU, X., and H. R. HORVITZ, 1998 *lin-35* and *lin-53*, two genes that antagonize a *C. elegans* Ras pathway, encode proteins similar to Rb and its binding protein RbAp48. Cell **95:** 981-91.

MALOOF, J. N., and C. KENYON, 1998 The Hox gene *lin-39* is required during *C. elegans* vulval induction to select the outcome of Ras signaling. Development **125:** 181-90.

MELENDEZ, A., and I. GREENWALD, 2000 *Caenorhabditis elegans lin-13*, a member of the LIN-35 Rb class of genes involved in vulval development, encodes a protein with zinc fingers and an LXCXE motif. Genetics **155:** 1127-37.

MELLO, C. C., J. M. KRAMER, D. STINCHCOMB and V. AMBROS, 1991 Efficient gene transfer in *C.elegans*: extrachromosomal maintenance and integration of transforming sequences. Embo J. **10:** 3959-70.

PAGE, B. D., S. GUEDES, D. WARING and J. R. PRIESS, 2001 The *C. elegans* E2F- and DP-related proteins are required for embryonic asymmetry and negatively regulate Ras/MAPK signaling. Mol. Cell **7:** 451-60.

ROGALSKI, T. M., D. G. MOERMAN and D. L. BAILLIE, 1982 Essential genes and deficiencies in the *unc-22 IV* region of *Caenorhabditis elegans*. Genetics **102:** 725-36.

ROSENBLUTH, R. E., and D. L. BAILLIE, 1981 The genetic analysis of a reciprocal translocation, *eT1(III; V)*, in *Caenorhabditis elegans*. Genetics **99:** 415-28.

SIGURDSON, D. C., G. J. SPANIER and R. K. HERMAN, 1984 *Caenorhabditis elegans* deficiency mapping. Genetics **108:** 331-45.

SOLARI, F., and J. AHRINGER, 2000 NURD-complex genes antagonise Ras-induced vulval development in *Caenorhabditis elegans*. Curr. Biol. **10:** 223-6.

STERNBERG, P. W., and M. HAN, 1998 Genetics of RAS signaling in *C. elegans*. Trends Genet. **14:** 466-72.

STERNBERG, P. W., and H. R. HORVITZ, 1986 Pattern formation during vulval development in *C. elegans*. Cell **44:** 761-72.

SULSTON, J. E., and H. R. HORVITZ, 1977 Post-embryonic cell lineages of the nematode, *Caenorhabditis elegans*. Dev. Biol. **56:** 110-56.

THOMAS, J. H., and H. R. HORVITZ, 1999 The *C. elegans* gene *lin-36* acts cell autonomously in the *lin-35* Rb pathway. Development **126:** 3449-59.

VON ZELEWSKY, T., F. PALLADINO, K. BRUNSCHWIG, H. TOBLER, A. HAJNAL et al., 2000 The *C. elegans* Mi-2 chromatin-remodelling proteins function in vulval cell fate determination. Development **127:** 5277-84.

WANG, B. B., M. M. MULLER-IMMERGLUCK, J. AUSTIN, N. T. ROBINSON, A. CHISHOLM et al., 1993 A homeotic gene cluster patterns the anteroposterior body axis of *C. elegans*. Cell **74:** 29-42.

WILLIAMS, B. D., B. SCHRANK, C. HUYNH, R. SHOWNKEEN and R. H. WATERSTON, 1992 A genetic mapping system in *Caenorhabditis elegans* based on polymorphic sequence-tagged sites. Genetics **131:** 609-24.

YOON, C. H., J. LEE, G. D. JONGEWARD and P. W. STERNBERG, 1995 Similarity of *sli-1*, a regulator of vulval development in *C. elegans*, to the mammalian proto-oncogene *c-cbl*. Science **269:** 1102-5.

ZORIO, D. A., N. N. CHENG, T. BLUMENTHAL and J. SPIETH, 1994 Operons as a common form of chromosomal organization in *C. elegans*. Nature **372:** 270-2.

TABLES

Table 1. Phenotypes of synMuv mutant strains

Genotype	Penetrance of Muv phenotype (n) 15° C	20° C	Additional phenotypes
ark-1(n3524) lin-15A(n767)	0 (251)	80 (171)	
ark-1(n3701); lin-15A(n767)	12 (190)	95 (160)	
dpl-1(n3643); lin-15A(n767)	99 (154)	100 (252)	
efl-1(n3639); lin-15A(n767)	93 (74)	100 (78)	Ste
gap-1(n3535) lin-15A(n767)	1.4 (143)	50 (236)	
let-418(n3536); lin-15A(n767)	0 (201)	55 (183)	hs Ste
let-418(n3626); lin-15A(n767)	1.6 (62)	97 (76)	Ste
let-418(n3629); lin-15A(n767)	0 (52)	86 (58)	Ste
let-418(n3634); lin-15A(n767)	0 (87)	92 (48)	Ste
let-418(n3635); lin-15A(n767)	0 (76)	71 (70)	Ste
let-418(n3636); lin-15A(n767)	0 (77)	92 (78)	Ste
let-418(n3719); lin-15A(n767)	0 (101)	100 (60)	Ste
lin-9(n3631); lin-15A(n767)	100 (42)	100 (72)	Ste
lin-9(n3675); lin-15A(n767)	43 (166)	100 (105)	
lin-9(n3767); lin-15A(n767)	100 (67)	100 (56)	Ste
lin-13(n3642); lin-15A(n767)	3.3 (60)	100 (63)	Ste
lin-13(n3673); lin-15A(n767)	61 (145)	97 (129)	
lin-13(n3674); lin-15A(n767)	78 (131)	100 (191)	hs Ste
lin-13(n3726); lin-15A(n767)	31 (225)	99 (149)	hs Ste
lin-15B(n3436) lin-15A(n767)	100 (193)	100 (212)	
lin-15B(n3676) lin-15A(n767)	18 (167)	72 (130)	
lin-15B(n3677) lin-15A(n767)	99 (111)	100 (122)	
lin-15B(n3711) lin-15A(n767)	100 (186)	100 (156)	
lin-15B(n3760) lin-15A(n767)	32 (171)	100 (150)	
lin-15B(n3762) lin-15A(n767)	63 (113)	97 (116)	
lin-15B(n3764) lin-15A(n767)	96 (232)	100 (199)	
lin-15B(n3766) lin-15A(n767)	55 (132)	100 (173)	

lin-15B(n3768) lin-15A(n767)	80 (159)	100 (302)	
lin-15B(n3772) lin-15A(n767)	100 (220)	100 (191)	
lin-35(n3438); lin-15A(n767)	100 (153)	100 (126)	partial Ste at 20°C, Rup
lin-35(n3763); lin-15A(n767)	100 (108)	100 (160)	partial Ste at 20°C, Rup
lin-36(n3671); lin-15A(n767)	65 (191)	100 (151)	
lin-36(n3672); lin-15A(n767)	98 (198)	100 (178)	
lin-36(n3765); lin-15A(n767)	0 (184)	37 (202)	
lin-52(n3718); lin-15A(n767)	100 (41)	100 (82)	Ste
lin-53(n3448); lin-15A(n767)	67 (130)	100 (211)	partial Ste at 20°C
lin-53(n3521); lin-15A(n767)	100 (34)	100 (125)	partial Ste at 20°C
lin-53(n3622); lin-15A(n767)	85 (61)	100 (66)	Ste
lin-53(n3623); lin-15A(n767)	24 (55)	100 (51)	Ste
lin-61(n3442); lin-15A(n767)	22 (130)	100 (152)	
lin-61(n3446); lin-15A(n767)	36 (124)	99 (191)	
lin-61(n3447); lin-15A(n767)	11 (121)	87 (207)	
lin-61(n3624); lin-15A(n767)	0 (152)	89 (231)	
lin-61(n3736); lin-15A(n767)	0 (193)	100 (201)	
n3441; lin-15A(n767)	80 (165)	99 (195)	
n3541; lin-15A(n767)	79 (242)	98 (137)	
n3543; lin-15A(n767)	85 (177)	100 (121)	
n3628; lin-15A(n767)	2.9 (103)	84 (188)	
n3681; lin-15A(n767)	0 (214)	72 (192)	
n3542 lin-15A(n767)	0 (127)	35 (218)	
n3707 lin-15A(n767)	3.8 (80)	77 (26)	
mep-1(n3680); lin-15A(n767)	4.9 (122)	97 (105)	hs Ste
mep-1(n3702); lin-15A(n767)	30 (61)	100 (141)	Ste
mep-1(n3703); lin-15A(n767)	25 (72)	100 (107)	Ste
sli-1(n3538) lin-15A(n767)	4.3 (138)	90 (173)	
sli-1(n3544) lin-15A(n767)	4.6 (153)	80 (265)	cs embryonic lethality
sli-1(n3683) lin-15A(n767)	5.0 (80)	88 (148)	cs embryonic lethality
trr-1(n3630); lin-15A(n767)	3.1 (131)	85 (212)	Ste, Gro
trr-1(n3637); lin-15A(n767)	1.1 (92)	80 (200)	Ste, Gro
trr-1(n3704); lin-15A(n767)	3.1 (96)	79 (244)	Ste, Gro
trr-1(n3708); lin-15A(n767)	2.0 (151)	84 (228)	Ste, Gro

trr-1(n3709); lin-15A(n767)	1.0 (97)	77 (154)	Ste, Gro
trr-1(n3712); lin-15A(n767)	5.8 (121)	77 (192)	Ste, Gro

The penetrance of the Muv phenotype was determined after growing synMuv mutant strains at the indicated temperature for two or more generations. For most strains in which a fully penetrant sterile phenotype was associated with the Muv phenotype, we scored the penetrance of the Muv phenotype by examining sterile progeny of heterozygous mutant parents. For *trr-1* mutant strains, we scored the penetrance of the Muv phenotype by examining non-Gfp progeny of *trr-1 / mIn1[dpy-10(e128)mIs14]; lin-15A(n767)* heterozygous parents. All strains were backcrossed to *lin-15A(n767)* twice prior to phenotypic characterization. In addition to the phenotypes described above, many of the strains exhibited heat sensitive inviability due to frequent rupture, sterility and/or general sickness. Ste, sterile; Gro, growth rate abnormal; Rup, rupture at the vulva; cs, cold sensitive; hs, heat sensitive.

Table 2. Chromosomal linkages of new synMuv mutations

A. Autosomal mutations

New mutation	Mutation used for selection of homozygous F_2 hermaphrodites	Genotype of selected F_2 hermaphrodites with respect to the linked, unselected mutation
ark-1(n3524)	*dpy-20(e1282) IV*	2/19 *ark-1(n3524)/+*
ark-1(n3701)	*ark-1(n3701)*	1/14 *dpy-20(e1282)/+ IV*
dpl-1(n3643)	*dpl-1(n3643)*	0/20 *rol-6(e187)/+ II*
efl-1(n3639)	*rol-4(sc8) V*	4/20 *efl-1(n3639)/+*
let-418(n3536)	*let-418(n3536)*	4/21 *rol-4(sc8)/+ V*
let-418(n3626)	*rol-4(sc8) V*	0/19 *let-418(n3626)/+*
let-418(n3629)	*rol-4(sc8) V*	1/20 *let-418(n3629)/+*
let-418(n3634)	*rol-4(sc8) V*	2/19 *let-418(n3634)/+*
let-418(n3635)	*rol-4(sc8) V*	5/20 *let-418(n3635)/+*
let-418(n3636)	*rol-4(sc8) V*	3/20 *let-418(n3636)/+*
let-418(n3719)	*rol-4(sc8) V*	2/30 *let-418(n3719)/+*
lin-9(n3631)	*unc-32(e189) III*	0/20 *lin-9(n3631)/+*
lin-9(n3675)	*lin-9(n3675)*	0/22 *unc-32(e189)/+ III*
lin-9(n3767)	*lin-9(n3767)*	0/16 *mgP21/+ III*
lin-13(n3642)	*unc-32(e189) III*	1/20 *lin-13(n3642)/+*
lin-13(n3673)	*lin-13(n3673)*	0/25 *unc-32(e189)/+ III*
lin-13(n3674)	*lin-13(n3674)*	0/25 *unc-32(e189)/+ III*
lin-13(n3726)	*lin-13(n3726)*	1/26 *unc-32(e189)/+ III*
lin-35(n3438)	*lin-35(n3438)*	0/30 *dpy-5(e61)/+ I*
lin-35(n3763)	*lin-35(n3763)*	0/22 *dpy-5(e61)/+ I*
lin-36(n3671)	*lin-36(n3671)*	1/23 *unc-32(e189)/+ III*
lin-36(n3672)	*lin-36(n3672)*	0/16 *unc-32(e189)/+ III*
lin-36(n3765)	*lin-36(n3765)*	0/9 *unc-32(e189)/+ III*
lin-52(n3718)	*lin-52(n3718)*	1/16 *mgP21/+ III*
lin-53(n3448)	*lin-53(n3448)*	1/22 *dpy-5(e61)/+ I*
lin-53(n3521)	*dpy-5(e61) I*	0/20 *lin-53(n3521)/+*

lin-53(n3622)	*dpy-5(e61) I*	5/30 *lin-53(n3622)/+*
lin-53(n3623)	*lin-53(n3623)*	4/16 *hP4/+ I*
lin-61(n3442)	*lin-61(n3442)*	0/20 *dpy-5(e61)/+ I*
lin-61(n3446)	*lin-61(n3446)*	1/23 *dpy-5/+ I*
lin-61(n3447)	*lin-61(n3447)*	0/13 *dpy-5(e61)/+ I*
lin-61(n3624)	*lin-61(n3624)*	0/15 *dpy-5(e61)/+ I*
lin-61(n3736)	*dpy-5(e61) I*	1/19 *lin-61(n3736)/+*
lin(n3441)	*lin(n3441)*	5/20 *dpy-5(e61)/+ I*
lin(n3541)	*lin(n3541)*	9/31 *dpy-5(e61)/+ I*
lin(n3543)	*lin(n3543)*	9/27 *dpy-5(e61)/+ I*
lin(n3628)	*lin(n3628)*	1/29 *dpy-5(e61)/+ I*
lin(n3681)	*lin(n3681)*	3/22 *rol-4(sc8)/+ V*
mep-1(n3680)	*mep-1(n3680)*	0/30 *dpy-20(e1282)/+ IV*
mep-1(n3702)	*mep-1(n3702)*	0/16 *sP4/+ IV*
mep-1(n3703)	*mep-1(n3703)*	0/16 *sP4/+ IV*
trr-1(n3630)	*rol-6(e187) II*	0/20 *trr-1(n3630)/+*
trr-1(n3637)	*rol-6(e187) II*	1/20 *trr-1(n3637)/+*
trr-1(n3704)	*rol-6(e187) II*	1/30 *trr-1(n3704)/+*
trr-1(n3708)	*rol-6(e187) II*	0/20 *trr-1(n3708)/+*
trr-1(n3709)	*rol-6(e187) II*	2/30 *trr-1(n3709)/+*
trr-1(n3712)	*rol-6(e187) II*	1/19 *trr-1(n3712)/+*

B. X- linked mutations

New mutation	Criteria for X linkage
lin(n3542)	transmission test
lin(n3707)	transmission test
gap-1(n3535)	transmission test
lin-15B(n3436)	males with pseudovulva
lin-15B(n3676)	transmission test, males with pseudovulva
lin-15B(n3677)	males with pseudovulva
lin-15B(n3711)	males with pseudovulva
lin-15B(n3760)	transmission test, males with pseudovulva

lin-15B(n3762)	males with pseudovulva
lin-15B(n3764)	transmission test, males with pseudovulva
lin-15B(n3766)	transmission test, males with pseudovulva
lin-15B(n3768)	transmission test, males with pseudovulva
lin-15B(n3772)	transmission test, males with pseudovulva
sli-1(n3538)	transmission test
sli-1(n3544)	transmission test
sli-1(n3683)	transmission test

Autosomal and sex chromosome linkages were determined as described (see Materials and Methods). *lin(n3541)* was also mapped relative to *bli-3(e767)* and *unc-54(e1092)*, mutations present on the extreme left and right arms, respectively, of linkage group I. Of 16 Muv progeny selected from a *lin(n3541) / bli-3(e767) unc-54(e1092); lin-15A(n767)* parent, none were *bli-3(e767)/+* whereas six were *unc-54(e1092)/+*, indicating *lin(n3541)* lies nearer to *bli-3(e767)*.

Table 3. Map data for newly-identified synMuv loci

A. Three- and four-factor mapping

Gene	Genotype of heterozygote	Phenotype of selected recombinants	Genotype of selected recombinants (with respect to unselected markers)
ark-1			
	+ + ark-1 / unc-5 dpy-20 +; lin-15A(n767)	Unc	10/10 *ark-1 / +*
		Dpy	0/1 *ark-1 / +*
	+ ark-1 + / dpy-20 + unc-30; lin-15A(n767)	Dpy	15/35 *ark-1 / +*
		Unc	17/33 *ark-1 / +*
	dpy-20 + + ark-1 / + lin-3 unc-22 +; lin-15A(n767)	Dpy	3/9 *unc-22 / +*
		Muv	3/3 *unc-22 / +*
	dpy-20 + ark-1 + / + unc-22 + unc-30; lin-15A(n767)	Dpy	1/3 *unc-22 / +*
		Muv	1/2 *unc-22 / +*
		Unc-22	2/3 *ark-1 / +*
		Unc-30	5/6 *ark-1 / +*
	dpy-20 + ark-1 + / + dpy-26 + unc-30; lin-15A(n767)	Dpy-20	4/7 *dpy-26 / +*
		Muv	3/8 *dpy-26 / +*
gap-1			
	+ + gap-1 lin-15A(n767) / unc-1 dpy-3 + lin-15A(n767)	Unc	17/17 *gap-1 / +*
		Dpy	0/8 *gap-1 / +*
	gap-1 + + lin-15A(n767) / + unc-2 lon-2 lin-15A(n767)	Unc	0/2 *gap-1 / +*
		Lon	6/6 *gap-1 / +*
	+ gap-1 + lin-15A(n767) / dpy-3 + unc-2 lin-15A(n767)	Unc	14/18 *gap-1 / +*
lin-52			
	+ lin-52 + / unc-16 + unc-47; lin-15A(n767)	Unc-47	7/9 *lin-52 / +*
	lin-52 + unc-69 / + stP127 +; lin-15A(n767)	Muv	3/12 *stP127 / +*
	sma-3 + lin-52 + / + sqv-3 + unc-69; lin-15A(n767)	Sma	9/9 *sqv-3 / +*
		Muv	1/27 *sqv-3 / +*
		Unc	14/16 *lin-52 / +*
lin(n3441)			
	+ lin(n3441) + / bli-3 + lin-17; lin-15A(n767)	Lin-17	9/19 *lin(n3441) / +*

bli-3 + lin(n3441) / + spe-15 +; lin-15A(n767)	Muv	10/18 *spe-15 / +*
+ lin(n3441) lin-17 / spe-15 + +; lin-15A(n767)	Lin-17	11/11 *spe-15 / +*
lin(n3628)		
lin(n3628) + + / + dpy-5 unc-13; lin-15A(n767)	Dpy	0/6 *lin(n3628) / +*
	Unc	6/6 *lin(n3628) / +*
+ lin(n3628) + / unc-11 + dpy-5; lin-15A(n767)	Unc	1/11 *lin(n3628) / +*
	Dpy	5/11 *lin(n3628) / +*
unc-11 + + lin(n3628) / + unc-73 lin-44 +; lin-15A(n767)	Muv	3/9 *unc-73 lin-44 / + +*
+ + lin(n3628) dpy-5 / unc-73 lin-44 + +; lin-15A(n767)	Muv	0/21 *unc-73 lin-44 / + +*
lin(n3628) + dpy-5 / + unc-38 +; lin-15A(n767)	Muv	3/7 *unc-38 / +*
unc-11 lin(n3628) + / + + unc-38; lin-15A(n767)	Muv	0/9 *unc-38 / +*
lin(n3542)		
+ + + lin(n3542) lin-15A(n767) / unc-10 dpy-6 lin-15A(n767)	Unc	8/8 *lin(n3542) / +*
+ lin(n3542) + lin-15A(n767) / dpy-6 + unc-9 lin-15A(n767)	Unc	4/40 *lin(n3542) / +*
mep-1		
+ mep-1 + / unc-5 + dpy-20; lin-15A(n767)	Unc	56/57 *mep-1 / +*
	Dpy	2/61 *mep-1 / +*
mep-1 + + / + dpy-20 unc-30; lin-15A(n767)	Dpy	0/51 *mep-1 / +*
	Unc	58/58 *mep-1 / +*
+ + mep-1 + / unc-24 mec-3 + dpy-20; lin-15A(n767)	UncMec	10/12 *mep-1 / +*
	Unc	17/17 *mep-1 / +*
	MecDpy	0/8 *mep-1 / +*
	Dpy	2/8 *mep-1 / +*
+ mep-1 dpy-20 + / lin-3 + + unc-22; lin-15A(n767)	Dpy	5/5 *lin-3 / +*
	Vul	3/10 *mep-1 / +*
+ + mep-1+ / mec-3 sem-3 + dpy-20; lin-15A(n767)	Mec	17/17 *mep-1 / +*
	Dpy	6/13 *mep-1 / +*
sli-1		
sli-1 + + lin-15A(n767) / + lon-2 unc-6 lin-15A(n767)	Lon	0/6 *sli-1 / +*
sli-1 + + lin-15A(n767) / + unc-2 lon-2 lin-15A(n767)	Lon	5/5 *sli-1 / +*
sli-1 + + lin-15A(n767) / + dpy-3 unc-2 lin-15A(n767)	Dpy	0/10 *sli-1 / +*
	Unc	6/6 *sli-1 / +*
sli-1 + + lin-15A(n767) / + unc-1 dpy-3 lin-15A(n767)	Unc	0/14 *sli-1 / +*
	Dpy	10/10 *sli-1 / +*

trr-1			
	+ rol-6 + trr-1 / dpy-10 + unc-4 +; lin-15A(n767)	Rol	3/14 *unc-4 / +*
		Dpy	3/3 *trr-1 / +*
		Unc	0/8 *trr-1 / +*
	+ trr-1 + / dpy-10 + rol-1; lin-15A(n767)	Rol	9/20 *trr-1 / +*
	+ + trr-1 / dpy-10 unc-53 +; lin-15A(n767)	Unc	0/17 *trr-1 / +*
	+ trr-1 + / unc-53 + rol-1; lin-15A(n767)	Unc	7/10 *trr-1 / +*
		Rol	7/10 *trr-1 / +*
	+ trr-1 + rol-1 / unc-4 + mex-1 +; lin-15A(n767)	Rol	12/14 *mex-1 / +*

B. Deficiency mapping

Gene	Genotype of heterozygote	Phenotype of heterozygote
lin-52		
	unc-36 lin-52 / nDf40 dpy-18; lin-15A(n767)	Muv
mep-1		
	mep-1 / sDf63 unc-31; lin-15A(n767) / +	PvlSte
	mep-1 / sDf62 unc-31; lin-15A(n767) / +	PvlSte
	mep-1 / sDf10; lin-15A(n767) / +	WT
trr-1		
	rol-6 trr-1 / mnDf57; lin-15A(n767)	WT
	rol-6 trr-1 / unc-4 mnDf90; lin-15A(n767)	WT
	rol-6 trr-1 / mnDf29; lin-15A(n767)	WT
	trr-1 / unc-4 mnDf87; lin-15A(n767)	Muv

Three- and four-factor crosses were performed using standard methods (BRENNER, 1974). Deficiency heterozygotes were constructed as described (see MATERIALS AND METHODS). WT, wild type; Pvl, protruding vulva; Ste, sterile.

Table 4. Selected synMuv proteins and allele sequences

A. Features of selected synMuv proteins

Protein	No. amino acids	Protein similarities and domains
DPL-1	598	Similar to DP family transcription factors; Contains DNA- and E2F-binding domains
EFL-1	342	Similar to E2F family transcription factors; Contains DNA-binding, DP-binding and transactivation domains
LET-418	1829	Similar to Mi-2 family ATP-dependent chromatin remodeling enzymes; Contains chromodomains, PHD finger motifs and a helicase domain*
LIN-9	LIN-9L: 644 LIN-9S: 642	Similar to *Drosophila* Aly cell cycle regulator and mammalian proteins of unknown function
LIN-13	2248	Protein has 24 Zn-finger motifs
LIN-35	961	Similar to Retinoblastoma (pRb) family transcriptional regulators; Contains "pocket" interaction domain
LIN-36	962	Novel protein with C/H-rich and Q-rich regions
LIN-52	161	Similar to *Drosophila* and mammalian proteins of unknown function
LIN-53	417	Similar to *Drosophila* p55, mammalian RbAp48 subunits of chromatin remodeling and histone deacetylase complexes; Contains WD repeats
LIN-61	491	Similar to *Drosophila* l(3)mbt and other MBT repeat-containing proteins
MEP-1	853	Protein has six Zn finger motifs
SLI-1	582	Similar to Cbl family ubiquitination-promoting proteins; Contains SH2 domain and RING finger motif
TRR-1	4064‡	Similar to mammalian TRRAP transcriptional regulator

B. Allele sequences

Mutation	Wild-type sequence	Mutant sequence	Substitution, splice site change or aberration	Domain affected by missense mutation
dpl-1(n3643)	TAT	TAA	Y341ochre	-
efl-1(n3639)	CAA	TAA	Q175ochre	-
let-418(n3536)	CCT	CTT	P675L	helicase/ATPase
let-418(n3626)	GGT	AGT	G1006S	helicase/ATPase
let-418(n3629)	TCC	TTC	S925F	helicase/ATPase
let-418(n3634)	TGG	TAG	W1128amber	-
let-418(n3635)	CAG	TAG	Q1594amber	-
let-418(n3636)	ACT	TCT	T807S	helicase/ATPase
	TGG	TGA	W1329opal	-
let-418(n3719)	TGG	TAG	W295amber	-
lin-9(n3631)	CAA	TAA	LIN-9L: Q594ochre	-
			LIN-9S: Q592ochre	-
lin-9(n3675)	GAT	AAT	LIN-9L: D305N	none predicted
			LIN-9S: D303N	none predicted
lin-9(n3767)	CAG	TAG	LIN-9L: Q509amber	-
			LIN-9S: Q507amber	-
lin-13(n3642)	CAT	TAT	H832Y	Zn finger
lin-13(n3673)	CAG	TAG	Q1988amber	-
lin-13(n3674)	CGA	TGA	R1250opal	-
lin-13(n3726)	GGA	GAA	G229E	none predicted
lin-35(n3763)[◊]	GCA	GTA	A555V	Pocket
	TTG AAA AAG	TTG AAA AAA G	K594frameshift and truncation after 611a.a.	-
lin-36(n3671)	CAT	CCT	H284P	C/H-rich region
	GAA	AAA	E424K	none predicted
lin-36(n3672)	CAG	TAG	Q467amber	-
lin-36(n3765)[†]	GCT	GTT	A242V	C/H-rich region
lin-52(n3718)	CAG	TAG	Q31amber	-
lin-53(n3448)	AGT	ATT	S384I	WD repeat

lin-53(n3521)	GAA	AAA	E174K	WD repeat
lin-53(n3622)	AAG/gtatgtgt	AAG/atatgtgt	Exon 1 donor	-
lin-53(n3623)	TGG	TAG	W337amber	-
lin-61(n3442)	aacttcag/AAT	aacttcaa/AAT	Exon 4 acceptor	-
lin-61(n3446)	CAA	TAA	Q412ochre	-
lin-61(n3447)	AGT	AAT	S354N	MBT repeat
lin-61(n3624)	CCG	TCG	P132S	none predicted
lin-61(n3736)	TTT	TCT	F247S	MBT repeat
mep-1(n3680)	AGT	AAT	S309N	none predicted
mep-1(n3702)	CAG	TAG	Q706amber	-
mep-1(n3703)	CTT/gtaagttt	CTT/ataagttt	Exon 3 donor	-
sli-1(n3538)	TCA	TTA	S305L	SH2
sli-1(n3544)	ttttccag/AAA	ttttccaa/AAA	Exon 6 acceptor	-
sli-1(n3683)	ttttttag/GAT	tttttta/GAT	Exon 4 acceptor	-
trr-1(n3630)	TGG	TAG	W2064amber	-
trr-1(n3637)	CAG	TAG	Q3444amber	-
trr-1(n3704)	CAA	TAA	Q694ochre	-
trr-1(n3708)	CGA	TGA	R1248opal	-
trr-1(n3709)	CGA	TGA	R2550opal	-
trr-1(n3712)	TGG	TAG	W2505amber	-

In the "Wild-type sequence" and "Mutant sequence" columns, exon and intron sequences are denoted by uppercase and lowercase script, respectively. Nucleotides altered by mutation are underlined.

* The predicted LET-418 protein contains a sequence described as a helicase domain. This domain was originally identified in helicases but has since been found in non-helicase proteins. Many of these proteins share a common ATPase activity, and this domain contains residues that are important for ATP binding and hydrolysis.

◊ The adenosine inserted by the *lin-35(n3763)* frameshift mutation is not underlined because it is unclear which nucleotide in the adenosine repeat was inserted.

† In addition to the missense mutation described, we found an additional mutation associated with *lin-36(n3765)*. This mutation, AG/gtaagaagaaaagc to AG/gtaagaagaaaagt, is present in the third intron of *lin-36* and creates a possible splice

donor sequence. If this splice donor were used, an in frame ochre (TAA) stop codon would be encountered, truncating the LIN-36 protein after 261 amino acids.

‡ Due to alternative splicing, *trr-1* encodes proteins that range in length between 4051 and 4061 amino acids (CHAPTER 6)

Molecular characterizations of the proteins described can obtained from the following sources: DPL-1, EFL-1 (CEOL and HORVITZ 2001; PAGE *et al.* 2001); LET-418 (SOLARI and AHRINGER 2000; VON ZELEWSKY *et al.* 2000); LIN-9 (BEITEL *et al.* 2000); LIN-13 (MELENDEZ and GREENWALD 2000); LIN-35, LIN-53 (LU and HORVITZ 1998); LIN-36 (THOMAS and HORVITZ 1999); LIN-52 (THIS STUDY); LIN-61 (LU, HARRISON & HORVITZ, unpublished results); MEP-1 (THIS STUDY); SLI-1 (YOON *et al.* 1995); TRR-1 (CHAPTER 6)

FIGURES

Figure 1. Molecular cloning of *lin-52*. The top panel shows the genetic map location of *lin-52* on linkage group III. The dashed portion of *nDf40* indicates that the left endpoint of this deficiency is not precisely known but maps in between *emb-30* and *sqv-3*. The middle and bottom panels show the rescuing cosmids ZK630 and C26C12 and subclones assayed for *lin-52* rescue. The restriction sites used to make subclones are indicated. "+" indicates that a majority of transgenic lines were rescued in the first generation of establishing the line. When rescue was observed, typically greater than 70% of animals in a line were rescued in this generation. Arrows indicate the direction of transcription. Coding sequences of predicted genes are shaded. An oligonucleotide encoding an in-frame stop codon was inserted into (arrowhead) and subsequently removed from (arrowhead with "X") the ZK632.13 predicted gene.

Figure 1

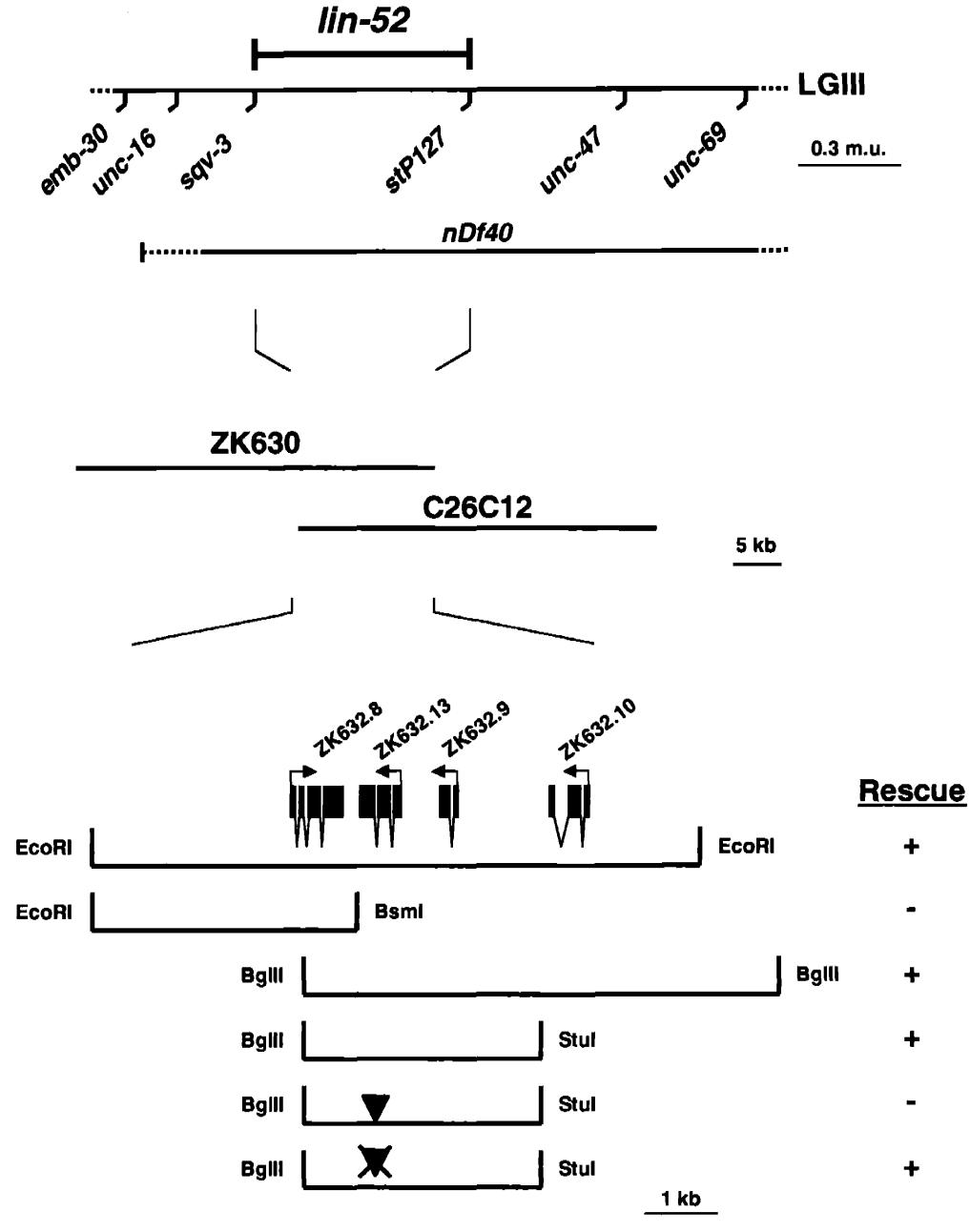
lin-52
LGIII
emb-30
unc-16
sqv-3
stP127
unc-47
unc-69
0.3 m.u.
nDf40
ZK630
C26C12
5 kb
ZK632.8
ZK632.13
ZK632.9
ZK632.10
Rescue
EcoRI
EcoRI
+
EcoRI
BsmI
-
BglII
BglII
+
BglII
StuI
+
BglII
StuI
-
BglII
StuI
+
1 kb

Figure 2. *lin-52* gene structure and translation

(A) *lin-52* gene structure as derived from cDNA and genomic sequences. Exons (closed boxes), 5' and 3' untranslated regions (open boxes), predicted translational start and stop codons, SL2 splice leader sequence and polyA tail are indicated. Arrows indicate the locations of the *n771* and *n3718* mutations.

(B) Alignment of the predicted LIN-52, human LOC91750 and *Drosophila* CG15929 proteins. Solid boxes indicate identities and shaded boxes indicate similarities. Arrowheads indicate the positions of *lin-52* mutations.

Figure 2

A.

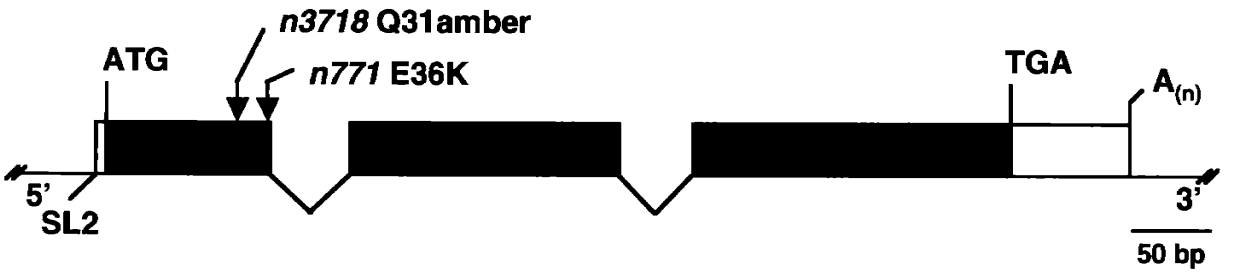
n3718 Q31amber
n771 E36K
ATG
TGA
A(n)
5'
SL2
3'
50 bp

B.

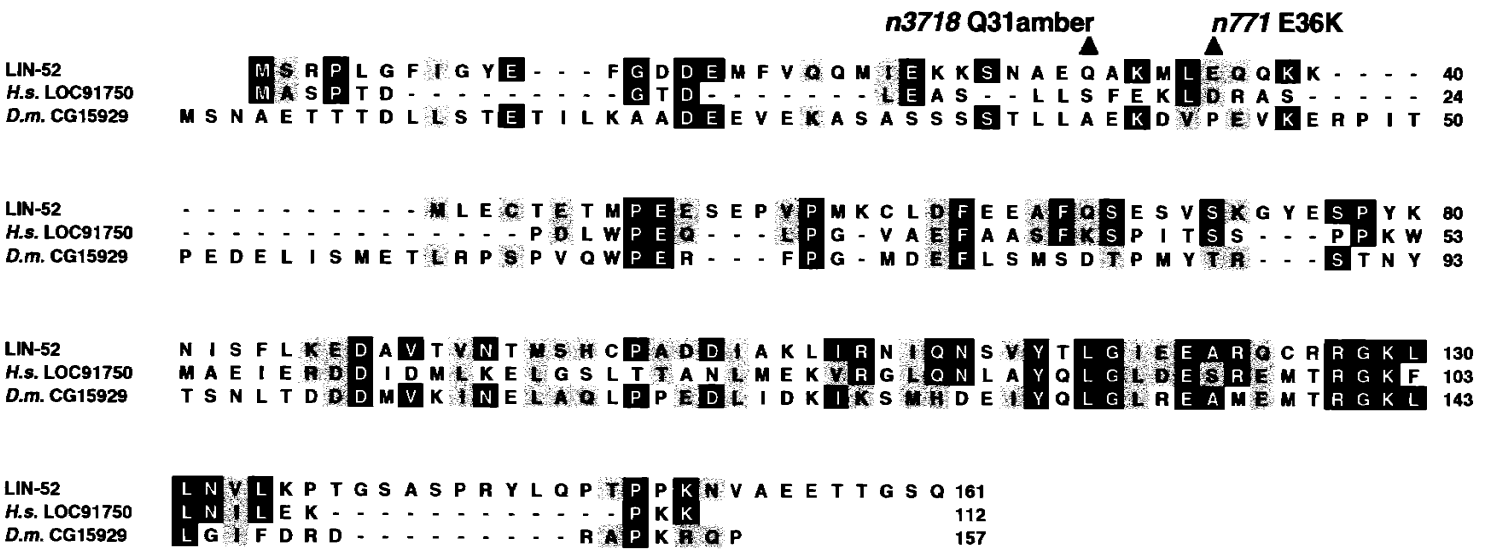
n3718 Q31amber
n771 E36K
LIN-52
H.s. LOC91750
D.m. CG15929
40
24
50
80
53
93
130
103
143
161
112
157

Figure 3. *mep-1* physical map location and translation

(A) Location of *mep-1* on the LGIV physical map in between *sem-3* and *dpy-20*. The *mep-1* rescuing cosmid M04B2 is shown in bold.

(B) Predicted MEP-1 protein. Zinc finger motifs are shaded, and the positions of *mep-1* mutations are indicated by arrowheads.

Figure 3

A.

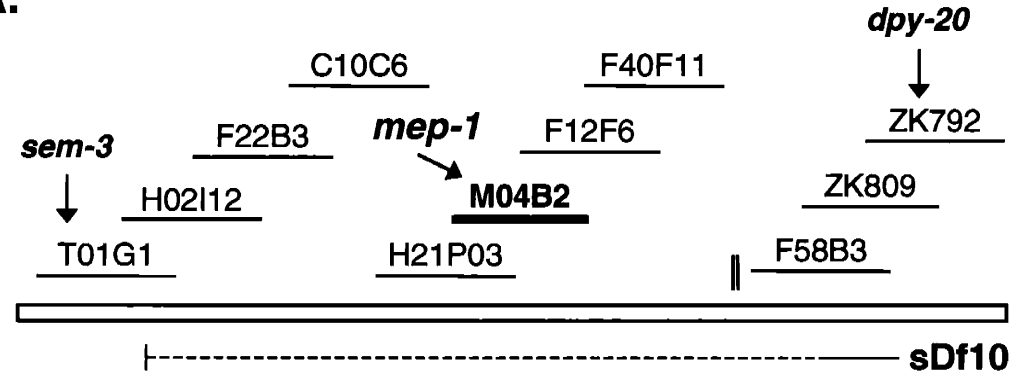

B.

```
M V T A D E T V L A T T T N T T S M S V E P T D P R S A G E  30
S S S D S E P D T I E Q L K A E Q R E V M A D A A N G S E V  60
N G N Q E N G K E E A A S A D V E V I E I D D T E E S T D P  90
S P D G S D E N G D A A S T S V P I E E E A R K K D E G A S 120
E V T V A S S E I E Q D D D G D V M E I T E E P N G K S E D 150
T A N G T V T E E V L D E E E P E P S V N G T T E I A T E K 180
E P E D S S M P V E Q N G K G V K R P V E C I E L D D D D D 210
D E I Q E I S T P A P A K K A K I D D V K A T S V P E E D N 240
N E Q A Q K R L L D K L E E Y V K E Q K D Q P S S K S R K V 270
L D T L L G A I N A Q V Q K E P L S V R K L I L D K V L V L 300
                ▼ n3680 S309N
P N T I S F P P S Q V C D L L I E H D P E M P L T K V I N R 330
M F G E E R P K L S D S E K R E R A Q L K Q H N P V P N M T 360
K L L V D I G Q D L V Q E A T Y C D I V H A K N L P E V P K 390
N L E T Y K Q V A A Q L K P V W E T L K R K N E P Y K L K M 420
H R C D V C G F Q T E S K L V M S T H K E N L H F T G S K F 450
                    ▼ n3703 splice
Q C T M C K E T D T S E Q R M K D H Y F E T H L V I A K S E 480
E K E S K Y P C A I C E E D F N F K G V R E Q H Y K Q C K K 510
D Y I R I R N I M M P K Q D D H L Y I N R W L W E R P Q L D 540
P S I L Q Q Q Q Q A A L Q Q A Q Q K K Q Q Q L L H Q Q Q A A 570
Q A A A A A Q L L R K Q Q L Q Q Q Q Q Q Q Q A R L R E Q Q Q 600
A A Q F R Q V A Q L L Q Q Q S A Q A Q R A Q Q N Q G N V N H 630
N T L I A A M Q A S L R R G G Q Q G N S L A V S Q L L Q K Q 660
M A A L K S Q Q G A Q Q L Q A A V N S M R S Q N S Q K T P T 690
                    ▼ n3702 Q706amber
H R T P T F V C E I C D A S V Q E K E K Y L Q H L Q T T H K 720
Q M V G K V L Q D M S Q G A P L A C S R C R D R F W T Y E G 750
L E R H L V M S H G L V T A D L L L K A Q K K E D G G R C K 780
T C G K N Y A F N M L Q H L V A D H Q V K L C S A E I M Y S 810
C D V C A F K C S S Y Q T L E A H L T S N H P K G D K K T S 840
T P A K K D D C I T L D D 853
```

CHAPTER 6

C. elegans TRRAP, Enhancer of Polycomb and MYST family histone acetyltransferase homologs act redundantly with *lin-35* Rb and other synthetic multivulva genes to antagonize *let-60* Ras pathway-mediated vulval induction

Craig J. Ceol and H. R. Horvitz

This manuscript is being prepared for publication. A note regarding the genes described: *trr-1*, *hat-1*, *epc-1* and *ssl-1* correspond to the *C. elegans* predicted genes *C47D12.1*, *VC5.4*, *Y111B2A.11* and *Y111B2A.23*, respectively. We intend to submit full-length cDNA and predicted protein sequences of these genes to GenBank prior to submission of this manuscript.

ABSTRACT

The class A and B synthetic multivulva (synMuv) genes are functionally redundant negative regulators of a Ras signaling pathway that induces *C. elegans* vulval development. The cell-fate specification events that underlie vulval development likely depend on proper regulation of chromatin structure, as the class B synMuv genes *hda-1* and *let-418* encode histone deacetylase and ATP-dependent chromatin remodeling enzyme homologs, respectively. The class B synMuv proteins EFL-1 and DPL-1, homologs of E2F and DP heterodimeric DNA-binding transcription factors, and LIN-35, a homolog of the mammalian Rb tumor suppressor, are proposed to target HDA-1 and other class B synMuv proteins to specific loci. In this manuscript, we describe the identification and characterization of a third class of synMuv genes. In genetic tests this class, which we have named the class C synMuv genes, acts redundantly with either class A or class B genes in vulval cell-fate determination and acts redundantly with class B genes to allow embryonic viability. The three class C synMuv genes we identified encode TRRAP, Enhancer of Polycomb and MYST family histone acetyltransferase homologs that may be components of a multisubunit histone acetyltransferase complex. We propose that a combination of deacetylase and acetyltransferase activities is required for cell-fate determination during vulval development.

INTRODUCTION

The fates of cells that arise during development must be properly specified to generate the correct numbers and types of cells that are present in an adult animal. Genes involved in the determination of cell fates may therefore control aspects of cell division and function. To identify and characterize such genes, we have studied *Caenorhabditis elegans* mutants in which homeotic cell fate transformations lead to the production of excess vulval tissue.

In the wild type, the vulva is produced from the twenty-two descendants of three ectodermal blast cells, P(5-7).p (Sulston and Horvitz, 1977). During larval development, these cells receive an inductive signal from the nearby gonadal anchor cell and each responds by dividing to generate seven or eight descendants (Sulston and White, 1980; Kimble, 1981). P(5-7).p adopt vulval fates. Although the flanking cells, P3.p, P4.p and P8.p, are competent to adopt vulval fates, they do not receive sufficient inductive signal and consequently adopt non-vulval fates (Sternberg and Horvitz, 1986). Cells adopting non-vulval fates typically divide once, generating descendants that fuse with the syncytial hypodermis. Vulval induction requires the activity of a conserved Ras signaling pathway (Sternberg and Han, 1998). Mutations that disable *let-60* Ras and other genes in this pathway result in a vulvaless (Vul) phenotype in which fewer than three P(3-8).p cells adopt vulval cell fates (Ferguson et al., 1987; Beitel et al., 1990; Han and Sternberg, 1990). Mutations that overactivate this pathway, for instance mutations that create the same G13E substitution found in oncogenic forms of human Ras, cause a multivulva (Muv) phenotype that is characterized by excessive induction whereby greater than three P(3-8).p cells adopt vulval cell fates (Beitel et al., 1990; Eisenmann and Kim, 1997).

Loss-of-function mutations in two functionally redundant pathways that are encoded by the class A and class B synthetic multivulva (synMuv) genes also cause a Muv phenotype (Ferguson and Horvitz, 1989). The class B synMuv gene *lin-35* encodes a homolog of the mammalian Rb tumor suppressor protein (Lu and Horvitz, 1998) and *efl-1* and *dpl-1*, which encode homologs of E2F and DP DNA-binding transcription factors, respectively (Ceol and Horvitz, 2001). Like their mammalian counterparts, the LIN-35 Rb protein binds to a heteromer composed of EFL-1 and DPL-1 (Ceol and Horvitz, 2001). LIN-35 Rb, EFL-1 and DPL-1, together with other class B synMuv proteins, are proposed to recruit the histone deacetylase HDA-1 to

promoters to regulate transcription of genes important for vulval development (Lu and Horvitz, 1998; Ceol and Horvitz, 2001). LET-418, a homolog of Mi-2 ATP-dependent chromatin remodeling enzymes, is also a class B synMuv protein (Solari and Ahringer, 2000; von Zelewsky et al., 2000), although whether it is present in a protein complex with LIN-35 Rb, EFL-1 and DPL-1 has not been established. The involvement of HDA-1 and LET-418 suggests that regulation of chromatin structure is important for proper vulval cell fate specification in *C. elegans*.

In this study we report the identification of a distinct class of genes, termed the class C synMuv genes, that negatively regulate vulval induction. Mutations in class C synMuv genes alone cause mild defects, but synergize with either class A or class B mutations to produce more severe vulval induction and other developmental defects. The genes in this new class, *trr-1*, *hat-1* and *epc-1*, encode homologs of the transcriptional coactivator TRRAP, the MYST family acetyltransferases TIP60 and Esa1p and the *Drosophila* Enhancer of Polycomb (E(Pc)) protein, respectively. Because of the predicted acetyltransferase activity of the HAT-1 protein and because orthologs TRRAP and E(Pc) family proteins have been copurified in histone acetyltransferase complexes, we propose that a combination of histone acetyltransferase and histone deacetylase activities is required to properly specify vulval cell fates in *C. elegans*.

MATERIALS AND METHODS

Strains and genetics

Strains were cultured as described by Brenner (1974) and maintained at 20°C unless otherwise specified. Bristol N2 was used as the wild-type strain. The following mutations were used: LGI: *lin-35(n745)*; LGII: *dpy-10(e128)*, *let-23(sy97)*, *rol-6(e187)*, *dpl-1(n2994, n3316)* (Chapters 2, 3), *unc-4(e120)*, *trr-1(n3630*, *n3637*, *n3704*, *n3708*, *n3709*, *n3712)* (This study), *mex-1(it9)*, *lin-38(n751)*; LGIII: *lon-1(e185)*, *sup-5(e1464)*, *lin-36(n766)*, *lin-37(n758)*; LGIV: *lin-3(n378)*, *let-60(n1876)* (Beitel et al., 1990); LGV: *dpy-11(e224)*, *rde-1(ne219)* (Tabara et al., 1999); LGX: *lin-15B(n744)*, *lin-15A(n433, n767)* (Ferguson and Horvitz, 1989) and, unless otherwise noted, are described in Riddle (1997). The deficiencies *mnDf90* and *mnDf87* (Sigurdson et al., 1984), translocation *nT1 n754 (IV;V)* (Ferguson and Horvitz, 1985; Ferguson and Horvitz, unpublished results) and chromosomal inversion *mIn1[dpy-10(e128) mIs14]* (Edgley and Riddle, 2001) were also used. *mIs14*, an integrated transgene linked to the chromosomal inversion *mIn1*, consists of a combination of GFP-expressing transgenes that allow *mIs14*-containing animals to be identified beginning at the 4-cell stage of embryogenesis (Edgley and Riddle, 2001).

P(3-8).p induction assay

In the wild type, P(5-7).p adopt vulval fates in which they divide during the L3 larval stage to generate seven or eight descendants. P3.p, P4.p and P8.p adopt non-vulval fates, typically dividing once to generate two descendants that fuse with the hypodermis. Induction was scored in L4 hermaphrodites using Nomarski DIC microscopy by counting the number of descendants produced by individual P(3-8).p cells. Different scores, 1, 0.5 and 0 cells induced, were assigned to cells that were fully, partially or not induced, respectively. Partially induced P(3-8).p cells have one daughter produce its complement of induced descendants and the other daughter remain undivided.

trr-1 cloning

We mapped *trr-1* to an interval on LGII between the right endpoint of the deficiency *mnDf90* and the *mex-1* gene (Chapter 5). To clone the *trr-1* gene, we performed transformation rescue as described by Mello (1991), using the pRF4 plasmid (80ng/μL)

as a coinjection marker. We rescued the *trr-1* Muv and sterile phenotypes by injecting the cosmid C47D12 (10ng/μL) into *trr-1(n3712)/ mIn1[dpy-10(e128) mIs14]; lin-15A(n767)* mutants and isolating Rol non-Gfp transgenic lines. *trr-1* corresponds to the predicted gene *C47D12.1.*

RNAi analyses

Templates for *in vitro* transcription reactions were made by PCR amplification of either cDNAs and their flanking T3 and T7 promoter sequences or coding exons from genomic DNA using T3 and T7-tagged oligonucleotides. *In vitro*-transcribed RNA was annealed and injected as described by Fire et al. (1998). In addition to the genes described in Results, we injected RNA corresponding to *C. elegans* genes that encode homologs of the TRRAP complex proteins TIP48/TAP54α (*C. elegans* predicted gene *T22D1.1*), TIP49/TAP54β (*C27H6.2*), Eaf3p (*Y37D8A.9*), p33ING (*Y51H1A.4*) and AF-9 (*M04B2.3*) (Loewith et al., 2000; Eisen et al., 2001; Fuchs et al., 2001; Nourani et al., 2001; Gavin et al., 2002; Ho et al., 2002). We did not observe vulval lineage defects after injection of these RNAs into either wild-type or synMuv single mutant backgrounds. Lastly, bacteria designed to express double-stranded RNA corresponding to the *Gcn5* homolog *Y47G6A.6* (Fraser et al., 2000) were fed to wild-type and synMuv single mutant hermaphrodites. As described below, we did not observe vulval defects following this treatment.

Deletion allele isolation

Genomic DNA pools from mutagenized worms were screened for deletions essentially as described by Plasterk (1997). Deletion mutant animals were isolated from frozen stocks and were backcrossed four times prior to use. *hat-1(n4075)* removes nucleotides +106 to +1115, *epc-1(n4076)* nucleotides +2014 to +2899 and *ssl-1(n4077)* nucleotides +5075 to +5757 of genomic DNA relative to their respective predicted translational start sites.

cDNA isolation

We used RT-PCR (Titan one-tube RT-PCR, Roche Diagnostics) to recover *trr-1* and *hat-1* cDNA clones. Existing cDNAs were obtained from the *C. elegans* EST project (kindly provided by Y. Kohara and coworkers) to determine gene structures of *epc-1*, the *trr-1* 3' end and the *ssl-1* 5' end. We used 5' RACE (5' RACE System v2.0, GIBCO)

to determine the 5' ends and SL1 *trans*-spliced leader sequences of *trr-1*, *hat-1* and *epc-1* transcripts.

Allele sequence

We used PCR-amplified regions of genomic DNA as templates in determining mutant allele sequences. For each allele investigated, we determined the sequences of all exons and splice junctions of the gene in question. All mutations were confirmed by determining the sequence of independently-derived PCR products. All sequences were determined using an automated ABI 373 DNA sequencer (Applied Biosystems).

RESULTS

trr-1 interacts with class A and class B synMuv mutations

We performed a genetic screen for synMuv mutants in a *lin-15A(n767)* background and identified six mutations in our pool of isolates that failed to complement each other and defined the gene *trr-1* (Chapter 5; our nomenclature will be explained below). To more precisely quantitate the Muv phenotype of *trr-1; lin-15A* strains, we scored the numbers of P(3-8).p cells induced per animal and found that all strains had a similarly penetrant, temperature-sensitive hyperinduced phenotype (Table 1A). The hyperinduction we observed occurred in P3.p, P4.p and P8.p to similar extents (data not shown). To determine if *trr-1* interacted with other class A synMuv genes, we constructed a *trr-1(n3712) lin-38* double mutant. These double mutant animals were also hyperinduced (Table 1A), suggesting that *trr-1* functions in parallel not only to *lin-15A* but to the class A synMuv pathway in general.

We also isolated *trr-1(n3712)* and the other *trr-1* mutations away from any other synMuv mutations. Nearly all class A and class B synMuv single mutants adopt a wild-type pattern of P(3-8).p fates (Table 1B; data not shown), however *trr-1* adults had a weakly penetrant hyperinduced phenotype (Table 1B). By examining the cell fates adopted by individual P(3-8).p cells in L4 animals, we determined that the vulval cell-fate transformations of *trr-1* single mutants always occurred in P8.p (Figure 1). In addition to ectopic vulval cell-fate transformations, all *trr-1* mutations caused slow growth and sterility, although some mutant animals occasionally produced a small number of eggs (<10, as compared to ~300 for the wild type), all of which died during embryogenesis.

To determine if *trr-1* interacts with class B synMuv genes, we constructed double mutant strains containing *trr-1(n3712)* and mutations of class B synMuv genes. Interestingly, double mutant strains combining *trr-1(n3712)* with mutations of *lin-15B*, *lin-35* Rb and *lin-37* showed a significant increase in the penetrance of P8.p transformation (Figure 2). In addition to the increase in P8.p transformation, we occasionally observed ectopic transformations of P3.p and P4.p (data not shown). Since *lin-15B(n744)*, *lin-35(n745)* and *lin-37(n758)* are strong loss-of-function and possibly null mutations of their corresponding genes, these results indicate that *trr-1* functions redundantly with at least a subset of class B synMuv genes.

No significant increase was observed in *trr-1(n3712); lin-36(n766)* double mutants (Figure 2). By various genetic criteria, this loss-of-function *lin-36* mutation behaves unlike mutations in other class B synMuv genes (Hsieh et al., 1999; Fay et al., 2002). There are at least two possibilities to explain the unusual behavior of *lin-36(n766)*. First, the lack of enhancement could be allele specific, with the *lin-36(n766)* mutation disrupting a function that is redundant with a class A synMuv function but not disrupting a separable *lin-36* function that is redundant with *trr-1* activity. Alternatively, our observations with *lin-36* could reflect a gene-specific lack of enhancement. For example, the strength of the *lin-36* defect may not be equivalent to that of other class B synMuv gene defects such that lack of *lin-36* activity may be readily observable in a class A synMuv background but, unlike other class B synMuv defects, not observable in a *trr-1* background. Enhancement tests using additional *lin-36* alleles will help to resolve this issue.

trr-1 encodes a protein similar to mammalian TRRAP

We mapped *trr-1* to a small region of LGII and cloned the gene using transformation rescue (see Materials and Methods). To confirm the identity of *trr-1*, we obtained a partial cDNA and, using RNA derived from this cDNA, found that RNA-mediated interference (RNAi) of this gene caused a highly penetrant hyperinduced phenotype in *lin-15A* and *lin-38* mutant backgrounds (Table 1). As determined by RT-PCR and 5' RACE, the *trr-1* gene consists of 22 exons, four of which are alternatively spliced (Figure 3A). Since the sites of alternative splicing are separated by only six or nine nucleotides, the most exclusive (4054 amino acids) and inclusive (4064 amino acids) isoforms differ slightly in size.

The predicted TRR-1 proteins are similar to mammalian myc-associated protein TRRAP (transformation/transcription domain-associated protein) and its yeast homolog Tra1p throughout most of their lengths (McMahon et al., 1998; Saleh et al., 1998). TRRAP and Tra1p are similarly large proteins, extending 3828 and 3744 amino acids, respectively. The largest predicted TRR-1 isoform is 25 percent identical to TRRAP and 19 percent identical to Tra1p. TRR-1, TRRAP and Tra1p share limited regions of homology with other proteins (Figure 3B). One of these regions is located at the carboxy terminus and is similar to the catalytic domains of ATM and PI-3-like kinases. However, the DXXXXN and DFG motifs critical for kinase activity are not present in TRR-1, TRRAP or Tra1p (Hunter, 1995). Instead of having an enzymatic function, this

domain of TRRAP has been proposed to mediate protein-protein interactions (McMahon et al., 1998). All six *trr-1* mutations introduce nonsense codons (Figure 3B). *trr-1(n3637)* is predicted to truncate the protein just prior to the ATM/PI-3 kinase-like domain. The strength of *trr-1(n3637)* is similar to that of other alleles, suggesting that deletion of the ATM/PI-3 kinase-like domain alone results in a severe loss of protein function. Finally, *trr-1(n3630)*, *trr-1(n3637)* and *trr-1(n3712)* introduce amber stop codons, and we observed that the sterility associated with these alleles was reduced by the *sup-5(e1464)* informational suppressor tRNA mutation. This suppression, along with the partially penetrant sterility caused by *trr-1(RNAi)* (data not shown), confirms that the sterility observed in *trr-1* mutants is truly due to loss of *trr-1* function.

trr-1(RNAi) is synthetically lethal with mutations in *lin-35* Rb and other class B synMuv genes

trr-1(RNAi) caused more severe phenotypic consequences than did *trr-1* mutations. For example, the ectopic induction phenotype of *lin-15A; trr-1(RNAi)* mutants was much stronger than that of *trr-1; lin-15A* mutant strains (Table 1). We do not believe this difference is reflective of a partial loss of gene function caused by all of the *trr-1* mutations. Instead we propose that at least some of the mutations cause a severe loss of gene function and that the difference is due to an effect of *trr-1(RNAi)* on maternally-provided gene activity. In support of this proposal, *trr-1(n3704)/mnDf87; lin-15A* and *trr-1(n3712)/mnDf87; lin-15A* mutants that were severely deficient in zygotically-provided *trr-1* activity but retained maternally-provided *trr-1* activity had phenotypic penetrances that were similar to those of *trr-1; lin-15A* homozygotes and were weaker than those of *lin-15A; trr-1(RNAi)* mutants (data not shown). Also arguing that *trr-1; lin-15A* homozygotes have significantly reduced zygotically-provided *trr-1* gene activity, the protein truncations predicted by *trr-1(n3704)* and other *trr-1* mutations are likely to remove functional domains and compromise TRR-1 activity.

We further characterized the effects of *trr-1(RNAi).* In wild-type and class A synMuv genetic backgrounds, *trr-1(RNAi)* caused retarded growth, adult sterility and weakly penetrant embryonic and larval lethalities (Table 2). Interestingly, *trr-1(RNAi)* caused highly penetrant embryonic and larval lethalities in combination with many class B synMuv mutations. Most of the dead embryos arrested at the late embryonic pretzel stage and those that hatched died shortly thereafter. We have not yet determined a basis for this lethality. It is important to note that many of the class B synMuv mutations

tested are predicted to have severe effects on their cognate class B synMuv proteins. Since *trr-1(RNAi)* can synthetically interact with strong reduction-of-function or null class B synMuv mutations, these data indicate that *trr-1* functions redundantly with class B synMuv genes not only in vulval cell-fate determination but also in an essential process earlier in development.

trr-1(RNAi) causes synthetic lethality in a *lin-36(n766)* background although the penetrance of this lethality is not as high as in other class B synMuv backgrounds. This assay therefore unmasks a redundancy between *trr-1* and *lin-36* that we did not observe in the P8.p induction assay. As discussed above, the strength of the *lin-36* defect may not be equivalent to the strengths of defects of other class B synMuv genes. This difference in strengths may explain why, relative to other class B synMuv genes, *lin-36* shows weaker interactions with *trr-1* in terms of synthetic lethality and synthetic P8.p induction.

trr-1 synthetically interacts with *dpl-1* DP

Mammalian TRRAP and yeast Tra1p are thought to function as coactivator proteins that bridge transcription factors to histone acetyltransferases (McMahon et al., 1998; Brown et al., 2001). Based on coimmunoprecipitation and functional assays, E2F transcription factors were linked to TRRAP (McMahon et al., 1998; Lang et al., 2001). *In vivo*, E2F and DP family proteins form heterodimers that are bound by Rb family proteins via a direct interaction with the E2F subunit (reviewed by Dyson, 1998; Trimarchi and Lees, 2002). We previously determined that one of two *C. elegans* E2F family members, *efl-1*, and the sole DP family member, *dpl-1*, are class B synMuv genes (Ceol and Horvitz, 2001). As noted above, *lin-35* Rb was also characterized as a class B synMuv gene, and the LIN-35 Rb protein was found to form a complex with DPL-1 and EFL-1 *in vitro* (Lu and Horvitz, 1998; Ceol and Horvitz, 2001). LIN-35 Rb and Rb proteins in other species are thought to recruit histone deacetylase complexes to regulate E2F-dependent transcription (Brehm et al., 1998; Luo et al., 1998; Magnaghi-Jaulin et al., 1998). Coupling these results with our genetic finding that *trr-1* acts redundantly with *lin-35* Rb to negatively regulate vulval induction, one might speculate that EFL-1 and DPL-1 recruit distinct LIN-35-containing and TRR-1-containing complexes to appropriately regulate vulval cell fate determination. To examine this possibility, we wished to determine if *trr-1* acted through *efl-1* and *dpl-1* to negatively regulate vulval development.

Although we cannot rule out the possibility that *trr-1* functions only in part through *efl-1* and *dpl-1*, three lines of evidence argue that *trr-1* does not act solely through these transcription factors. First, the ectopic induction of P8.p in *dpl-1 trr-1* double mutants is greater than that observed in either single mutant (Figure 2). Because of the sterility conferred by the *dpl-1(n3316)* null and *trr-1(n3712)* mutations, these mutants were derived from *dpl-1(n3316) trr-1(n3712) / ++* mothers. However, it is notable that in this test we substantially reduced maternally-provided *dpl-1* activity by injecting mothers with *dpl-1* dsRNA and scoring *dpl-1(n3316 RNAi) trr-1(n3712)* progeny. Second, in a weak *lin-15A* mutant background at 15°C, *trr-1(RNAi)* greatly enhanced the ectopic induction observed in *dpl-1* mutant animals that were derived from *dpl-1* heterozygous mutant mothers (Table 3). Third, when performed in a homozygous *dpl-1* mutant background, *trr-1(RNAi)* caused synthetic lethality with *dpl-1* (Table 2). Since viable *trr-1(RNAi) dpl-1* progeny could be derived from heterozygous but not homozygous *dpl-1* mutant mothers, this synthetic lethality apparently required a lack of maternally-provided *dpl-1* activity. These results indicate that *trr-1* does not act only through *dpl-1* to regulate vulval development and embryonic and larval viability. Although all of these assays were conducted in *dpl-1* mutant backgrounds, we expect that, since reduction of *dpl-1* function is predicted to affect all *C. elegans* DP/E2F activity, these results similarly apply to *efl-1*.

In addition to these data, one other observation argues against the model that *trr-1* acts solely through *dpl-1*. Whereas double mutants containing *lin-35(n745)*, a putative null allele of *lin-35*, and *trr-1(n3712)* display highly penetrant ectopic induction of P8.p, the ectopic induction in *dpl-1(n3316 RNAi)* mutants is relatively weak (Figure 2). If both *lin-35* and *trr-1* were acting solely through *dpl-1*, defects of equivalent strengths would be expected.

The Muv phenotype of *trr-1* mutants requires *let-60* Ras pathway activity

Previous studies determined that a conserved Ras pathway induces vulval development in *C. elegans* (reviewed by Sternberg and Han, 1998). Loss-of-function mutations affecting genes in this pathway cause a vulvaless (Vul) phenotype characterized by P(3-8).p adopting hypodermal instead of vulval cell fates. To determine if Ras pathway activity is required for the *trr-1* mutant phenotype, we constructed strains in which the functions of *trr-1*, *lin-15A* and a Ras pathway gene were reduced. The uninduced phenotype caused by *let-23* receptor tyrosine kinase and *let-60* Ras mutations was

epistatic to the hyperinduced phenotype caused by *trr-1* and *lin-15A* loss of function (Table 4). These results indicate that Ras pathway activity is required to produce the *trr-1; lin-15A* Muv phenotype. By contrast, *trr-1; lin-3; lin-15A* triple mutants showed a wild-type level of induction in P(5-7).p and ectopic induction in P3.p, P4.p and P8.p. *lin-3* encodes an EGF-like protein that is produced by the gonadal anchor cell and is thought to act non-cell autonomously to stimulate Ras pathway activity in P(5-7).p (Hill and Sternberg, 1992). These findings suggest that a basal level of *lin-3*-independent Ras pathway activity, when combined with mutations in *trr-1* and *lin-15A*, is sufficient to induce vulval cell fates in P(3-8).p.

hat-1* and *epc-1*, but not *ssl-1*, loss of function phenocopies *trr-1

TRRAP and Tra1p are components of protein complexes that acetylate histones (Allard et al., 1999; reviewed by Brown et al., 2000). These complexes are distinguished by their histone acetyltransferase subunits: the mammalian TFTC and p/CAF and the yeast SAGA complexes contain Gcn5 family acetyltransferases, whereas the mammalian TIP60 and the yeast NuA4 complexes contain MYST family acetyltransferases.

To determine if TRR-1 might function with a histone acetyltransferase in *C. elegans*, we used RNA-mediated interference to inactivate such genes. Whereas inactivation of a *Gcn5* homolog *Y47G6A.6* had no effect, inactivation of a MYST family gene we have named *hat-1* produced a highly penetrant Muv phenotype in a *lin-15A* background (data not shown). To further characterize *hat-1*, we isolated a deletion allele, *n4075*, that removes 1010 base pairs from the *hat-1* locus and is predicted to produce a protein that contains the first 35 amino acids of HAT-1 followed by 52 unrelated amino acids prior to termination (Figure 4A). The predicted full-length HAT-1 protein is 458 amino acids long, and this deletion is expected to remove the conserved chromodomain and acetyltransferase catalytic domain (Figure 4B). *hat-1(n4075)* mutants exhibited the same spectrum of phenotypes and genetic interactions as *trr-1* mutants. *hat-1(n4075)* single mutants were slow growing and sterile. In combination with class A synMuv mutations, *hat-1(n4075)* caused a severe Muv phenotype characterized by P3.p, P4.p and P8.p ectopic induction (Table 4). Alone, *hat-1(n4075)* caused ectopic induction of P8.p (Figure 4C). In combination with a *lin-15B* mutation, the penetrance of this ectopic induction was greatly increased (Figure 4D).

The TIP60 and NuA4 complexes contain other proteins in addition to MYST family acetyltransferases. We inactivated *C. elegans* genes encoding homologs of

these proteins and identified *epc-1* as a negative regulator of vulval induction. *epc-1* encodes a homolog of the *Drosophila* Enhancer of Polycomb (E(Pc)) protein and similarly named mammalian and yeast proteins. Aside from their association with MYST family histone acetyltransferases, little is known about the molecular interactions of E(Pc)-like proteins. Inactivation of *epc-1* caused fully penetrant embryonic lethality in the broods of animals injected with RNA (data not shown). To study the effects of *epc-1* inactivation during postembryonic development, we injected *epc-1* RNA into RNAi-deficient hermaphrodites and subsequently mated these animals with RNAi-competent males, a procedure referred to as "zygotic RNAi" (Herman, 2001). For many genes that act during multiple stages of development, this scheme has been shown to provide sufficient gene activity for embryonic functions but inadequate gene activity for postembryonic functions. *epc-1(RNAi)* performed in this manner did not affect vulval induction in wild-type animals but produced a Muv phenotype in *lin-15A* and *lin-38* mutant backgrounds (Table 5). A low percentage of P8.p induction was observed in a *lin-15B* background.

We recently obtained a deletion allele that removes 886 bases from the *epc-1* locus, including the third and fourth *epc-1* exons (Figure 5A). If the second exon were spliced to the fifth exon, a truncated 137 amino acid protein would be produced that contains the first 109 amino acids of the 795 amino acid predicted EPC-1 protein. Preliminary studies indicate that *epc-1(n4076)* homozygotes die as embryos (data not shown).

TRRAP copurified with the p400 protein as part of the mammalian TIP60 and p400 complexes (Fuchs et al., 2001). The p400 complex was isolated based on its interaction with the adenovirus E1A oncoprotein and was also shown to associate with c-myc. The p400 protein itself is a member of the SWI2/SNF2 family of proteins, and, like many SWI2/SNF2 family members, was shown to possess ATPase activity. We identified a *C. elegans* homolog of p400, which we named *ssl-1* (*ssl*, SWI2/SNF2-like), and studied its function using RNAi. *ssl-1(RNAi)* caused an embryonic lethal phenotype reminiscent of that caused by *epc-1(RNAi)*. In both cases, dead embryos generally arrested just prior to morphogenesis and apparently lacked the hypodermal ridge that is a characteristic of enclosed embryos (data not shown). We are currently characterizing this phenotype further. "Zygotic" RNAi of *ssl-1*, using the same procedure as described above, caused no vulval defects in wild-type, *lin-15A* or *lin-15B* genetic backgrounds (Table 5). We similarly have not observed vulval defects in animals carrying a *ssl-1*

deletion allele, *n4077* (Figure 5B), although these animals were sterile. These results suggest that *ssl-1* may not act with *trr-1*, *hat-1* and *epc-1* to regulate vulval cell-fate determination, but may act with *epc-1* in an essential embryonic process.

DISCUSSION AND FUTURE EXPERIMENTS

trr-1 acts redundantly with *lin-35* Rb to antagonize *let-60* Ras signaling

Identifying factors involved in cell fate determination is important for understanding how cells that contain the same genomic information can adopt different cell fates during animal development. As they help to distinguish P3.p, P4.p and P8.p from P(5-7).p, *trr-1*, *hat-1* and *epc-1* are such cell fate determination genes. Given their molecular identities, *trr-1*, *hat-1* and *epc-1* likely act at the level of transcription, either in an instructive or permissive fashion, to create differences in gene expression in P3.p, P4.p and P8.p as compared to P(5-7).p.

Many of the pathways involved in regulating cell fate determination are conserved. In many cases, pathways that control cell fate determination in model organisms have been shown to regulate cellular proliferation in mammals. Pathways that regulate vulval cell fate specification in *C. elegans* provide clear examples. A conserved *let-60* Ras pathway induces vulval cell fates, and this pathway is antagonized by the class B *lin-35* Rb pathway. *trr-1*, and likely *hat-1* and *epc-1*, act in parallel to *lin-35* Rb to negatively regulate *let-60* Ras pathway signaling. These comparisons suggest that mammalian counterparts of *trr-1*, *hat-1* and *epc-1* may similarly act in parallel to Rb and antagonize Ras in the control of cell proliferation.

Do *trr-1*, *hat-1* and *epc-1* share a common function?

The vulval phenotypes and genetic interactions of *trr-1*, *hat-1* and *epc-1* mutants are strikingly similar. In light of the copurification of their mammalian and yeast counterparts, these data strongly suggest that TRR-1, HAT-1 and EPC-1 proteins function as part of a protein complex. Some further experiments will bolster this hypothesis. First, strains containing mutations in two of these genes will be constructed. If these mutants are acting in the same complex, one would not expect to observe synergism in double mutants. Second, protein-protein interaction studies will be performed. Out of all of the RNAi we performed to inactivate putative complex members, *trr-1*, *hat-1* and *epc-1* were the only candidates we identified. It is possible that these three genes encode an indispensable core of a putative HAT complex that associates with other proteins whose functions are dispensable for proper vulval development. The large size of TRR-1 may require it to be divided into fragments to perform protein interaction studies.

Do *hat-1* mutants have defects in histone acetylation?

The best studied MYST family acetyltransferases are the yeast Esa1p and mammalian TIP60 proteins. Esa1p was found to preferentially acetylate histone H4 (Smith et al., 1998; Clarke et al., 1999; Suka et al., 2001). Furthermore, depletion of Esa1p resulted in global reduction of the acetylation of H4 and, to a lesser extent, of other nucleosomal histones (Reid et al., 2000; Suka et al., 2001). If HAT-1 functions in an analogous manner, commercially available antisera that specifically recognize acetylated isoforms of histones may be useful in determining whether *hat-1* mutants have gross defects in histone acetylation. We will attempt to determine a difference in acetylation between *hat-1* mutants and wild-type animals by whole-mount staining of fixed animals or possibly by chromatin immunoprecipitation.

Does this putative HAT complex function in gene activation or gene silencing?

Histone acetyltransferases have been characterized as transcriptional coactivators (reviewed by Roth et al., 2001), and TRRAP and its yeast homolog Tra1p are proposed to bridge interactions between activation domains of DNA-binding transcription factors and histone acetyltransferases (Brown et al., 2001). Therefore, a putative TRR-1/EPC-1/HAT-1 complex may function in transcriptional activation (Figure 6). If so, one would expect it to activate genes that negatively regulate vulval development.

While most data support the link between acetylation and activation, additional observations suggest that at least some histone acetylation may be important for gene silencing. For example, loss-of-function mutations that affect the MYST family acetyltransferases Sas2p and Sas3p cause defects in silencing of mating type loci and telomeres in yeast (Reifsnyder et al., 1996; Ehrenhofer-Murray et al., 1997). Sas2p and Sas3p are proposed to acetylate newly-deposited nucleosomes, and the modified acetyllysine residues they create are thought to be important for establishing silencing following DNA replication (Meijsing and Ehrenhofer-Murray, 2001; Osada et al., 2001). These residues may include acetyllysine 16 on histone H4, which is implicated in mating type loci and telomeric silencing in yeast (Johnson et al., 1992; Meijsing and Ehrenhofer-Murray, 2001). Other acetylated histone isoforms are prevalent in silent chromatin. For instance, *Drosophila* heterochromatin is enriched in acetyllysine 12 of histone H4 (Turner et al., 1992). Just as a MYST family histone acetyltransferase is linked to silencing, loss-of-function studies in *Drosophila* indicate a role for E(Pc) in

transcriptional repression. *E(Pc)* mutations synergize with polycomb group mutations to strongly derepress homeobox genes and act alone as suppressors of variegation to derepress genes that are juxtaposed to heterochromatin (Sato et al., 1983; Sinclair et al., 1998). These observations allow us to consider the possibility that HAT-1, in association with TRR-1 and EPC-1, may normally downregulate transcription (Figure 6). By this model, one would expect a putative TRR-1/EPC-1/HAT-1 complex to silence genes that are required for vulval cell fates. Because we do not know the relevant targets of TRR-1/EPC-1/HAT-1, we cannot distinguish between transcriptional activating versus repressing models at this time.

How might a putative TRR-1/EPC-1/HAT-1 complex be targeted to DNA?

Their coimmunoprecipitation and cooperation in reporter gene activation suggest that mammalian TRRAP can be targeted by E2F proteins to DNA (McMahon et al., 1998; Lang et al., 2001). We investigated the possibility of TRR-1 targeting by DP/E2F heterodimers by studying genetic interactions between *trr-1* and *dpl-1*. *dpl-1* is the only DP family member in *C. elegans* and therefore loss of *dpl-1* activity is expected to effectively reduce all DP/E2F heterodimer function in the organism. *dpl-1* synthetically interacted with *trr-1* in vulval induction and viability assays. It is especially relevant that we observed synergism in some of these assays when using *dpl-1(n3316 RNAi)* mutants, which are severely compromised for *dpl-1* function. These results combined with the observation that the defects of *trr-1* single mutants are stronger than those of *dpl-1* single mutants suggest that *trr-1* acts only partially or not at all through *dpl-1*. If not only through DPL-1, how might a putative TRR-1/EPC-1/HAT-1 complex be targeted to DNA? Studies in yeast indicate that the TRRAP homolog Tra1p directly interacts with acidic activation domains of transcription factors (Brown et al., 2000). TRR-1 may similarly be targeted to DNA by transcription factors other than DPL-1. The assays we have used to characterize *trr-1* provide a means of identifying and evaluating candidate transcription factors and other proteins that may function with TRRAP family members in targeted histone acetylation.

ACKNOWLEDGMENTS

We thank Beth Castor for DNA sequence determination and Na An for strain management. We thank Peter Reddien, Rajesh Ranganathan and members of the laboratory for construction of, and Ezequiel Alvarez-Saavedra and Eric Miska for assistance in screening the deletion library. We thank Michael Hurwitz and Ignacio Perez de la Cruz for critical reading of this manuscript. We thank Yuji Kohara and coworkers for providing cDNA clones. Some of the strains used in this work were provided by Theresa Stiernagle of the *Caenorhabditis* Genetic Center, which is supported by the NIH National Center for Research Resources. C. J. C. was a Koch Graduate Fellow, and H. R. H. is an investigator of the Howard Hughes Medical Institute. This work was supported by NIH grant GM24663 to H. R. H.

REFERENCES

Allard, S., Utley, R. T., Savard, J., Clarke, A., Grant, P., Brandl, C. J., Pillus, L., Workman, J. L., and Cote, J. (1999). NuA4, an essential transcription adaptor/histone H4 acetyltransferase complex containing Esa1p and the ATM-related cofactor Tra1p, Embo J. *18*, 5108-19.

Beitel, G. J., Clark, S. G., and Horvitz, H. R. (1990). *Caenorhabditis elegans ras* gene *let-60* acts as a switch in the pathway of vulval induction, Nature *348*, 503-9.

Brehm, A., Miska, E. A., McCance, D. J., Reid, J. L., Bannister, A. J., and Kouzarides, T. (1998). Retinoblastoma protein recruits histone deacetylase to repress transcription, Nature *391*, 597-601.

Brenner, S. (1974). The genetics of *Caenorhabditis elegans*, Genetics *77*, 71-94.

Brown, C. E., Howe, L., Sousa, K., Alley, S. C., Carrozza, M. J., Tan, S., and Workman, J. L. (2001). Recruitment of HAT complexes by direct activator interactions with the ATM-related Tra1 subunit, Science *292*, 2333-7.

Brown, C. E., Lechner, T., Howe, L., and Workman, J. L. (2000). The many HATs of transcription coactivators, Trends Biochem. Sci. *25*, 15-9.

Ceol, C. J., and Horvitz, H. R. (2001). *dpl-1* DP and *efl-1* E2F act with *lin-35* Rb to antagonize Ras signaling in *C. elegans* vulval development, Mol. Cell *7*, 461-73.

Clarke, A. S., Lowell, J. E., Jacobson, S. J., and Pillus, L. (1999). Esa1p is an essential histone acetyltransferase required for cell cycle progression, Mol. Cell. Biol. *19*, 2515-26.

Dyson, N. (1998). The regulation of E2F by pRB-family proteins, Genes Dev. *12*, 2245-62.

Edgley, M. L., and Riddle, D. L. (2001). LG II balancer chromosomes in *Caenorhabditis elegans*: *mT1(II;III)* and the *mIn1* set of dominantly and recessively marked inversions, Mol. Genet. Genomics *266*, 385-95.

Ehrenhofer-Murray, A. E., Rivier, D. H., and Rine, J. (1997). The role of Sas2, an acetyltransferase homologue of *Saccharomyces cerevisiae*, in silencing and ORC function, Genetics *145*, 923-34.

Eisen, A., Utley, R. T., Nourani, A., Allard, S., Schmidt, P., Lane, W. S., Lucchesi, J. C., and Cote, J. (2001). The yeast NuA4 and *Drosophila* MSL complexes contain homologous subunits important for transcription regulation, J. Biol. Chem. *276*, 3484-91.

Eisenmann, D. M., and Kim, S. K. (1997). Mechanism of activation of the *Caenorhabditis elegans ras* homologue *let- 60* by a novel, temperature-sensitive, gain-of-function mutation, Genetics *146*, 553-65.

Fay, D. S., Keenan, S., and Han, M. (2002). *fzr-1* and *lin-35*/Rb function redundantly to control cell proliferation in *C. elegans* as revealed by a nonbiased synthetic screen, Genes Dev. *16*, 503-17.

Ferguson, E. L., and Horvitz, H. R. (1985). Identification and characterization of 22 genes that affect the vulval cell lineages of the nematode *Caenorhabditis elegans*, Genetics *110*, 17-72.

Ferguson, E. L., and Horvitz, H. R. (1989). The multivulva phenotype of certain *Caenorhabditis elegans* mutants results from defects in two functionally redundant pathways, Genetics *123*, 109-21.

Ferguson, E. L., Sternberg, P. W., and Horvitz, H. R. (1987). A genetic pathway for the specification of the vulval cell lineages of *Caenorhabditis elegans*, Nature *326*, 259-67.

Fire, A., Xu, S., Montgomery, M. K., Kostas, S. A., Driver, S. E., and Mello, C. C. (1998). Potent and specific genetic interference by double-stranded RNA in *Caenorhabditis elegans*, Nature *391*, 806-11.

Fraser, A. G., Kamath, R. S., Zipperlen, P., Martinez-Campos, M., Sohrmann, M., and Ahringer, J. (2000). Functional genomic analysis of *C. elegans* chromosome I by systematic RNA interference, Nature *408*, 325-30.

Fuchs, M., Gerber, J., Drapkin, R., Sif, S., Ikura, T., Ogryzko, V., Lane, W. S., Nakatani, Y., and Livingston, D. M. (2001). The p400 complex is an essential E1A transformation target, Cell *106*, 297-307.

Gavin, A. C., Bosche, M., Krause, R., Grandi, P., Marzioch, M., Bauer, A., Schultz, J., Rick, J. M., Michon, A. M., Cruciat, C. M., *et al.* (2002). Functional organization of the yeast proteome by systematic analysis of protein complexes, Nature *415*, 141-7.

Han, M., and Sternberg, P. W. (1990). *let-60*, a gene that specifies cell fates during *C. elegans* vulval induction, encodes a ras protein, Cell *63*, 921-31.

Herman, M. (2001). *C. elegans* POP-1/TCF functions in a canonical Wnt pathway that controls cell migration and in a noncanonical Wnt pathway that controls cell polarity, Development *128*, 581-90.

Hill, R. J., and Sternberg, P. W. (1992). The gene *lin-3* encodes an inductive signal for vulval development in *C. elegans*, Nature *358*, 470-6.

Ho, Y., Gruhler, A., Heilbut, A., Bader, G. D., Moore, L., Adams, S. L., Millar, A., Taylor, P., Bennett, K., Boutilier, K., *et al.* (2002). Systematic identification of protein complexes in *Saccharomyces cerevisiae* by mass spectrometry, Nature *415*, 180-3.

Hsieh, J., Liu, J., Kostas, S. A., Chang, C., Sternberg, P. W., and Fire, A. (1999). The RING finger/B-box factor TAM-1 and a retinoblastoma-like protein LIN-35 modulate context-dependent gene silencing in *Caenorhabditis elegans*, Genes Dev. *13*, 2958-70.

Hunter, T. (1995). When is a lipid kinase not a lipid kinase? When it is a protein kinase, Cell *83*, 1-4.

Jansen, G., Hazendonk, E., Thijssen, K. L., and Plasterk, R. H. (1997). Reverse genetics by chemical mutagenesis in *Caenorhabditis elegans*, Nat. Genet. *17*, 119-21.

Johnson, L. M., Fisher-Adams, G., and Grunstein, M. (1992). Identification of a non-basic domain in the histone H4 N-terminus required for repression of the yeast silent mating loci, Embo J. *11*, 2201-9.

Kimble, J. (1981). Alterations in cell lineage following laser ablation of cells in the somatic gonad of *Caenorhabditis elegans*, Dev. Biol. *87*, 286-300.

Lang, S. E., McMahon, S. B., Cole, M. D., and Hearing, P. (2001). E2F transcriptional activation requires TRRAP and GCN5 cofactors, J. Biol. Chem. *276*, 32627-34.

Loewith, R., Meijer, M., Lees-Miller, S. P., Riabowol, K., and Young, D. (2000). Three yeast proteins related to the human candidate tumor suppressor p33(ING1) are associated with histone acetyltransferase activities, Mol. Cell. Biol. *20*, 3807-16.

Lu, X., and Horvitz, H. R. (1998). *lin-35* and *lin-53*, two genes that antagonize a *C. elegans* Ras pathway, encode proteins similar to Rb and its binding protein RbAp48, Cell *95*, 981-91.

Luo, R. X., Postigo, A. A., and Dean, D. C. (1998). Rb interacts with histone deacetylase to repress transcription, Cell *92*, 463-73.

Magnaghi-Jaulin, L., Groisman, R., Naguibneva, I., Robin, P., Lorain, S., Le Villain, J. P., Troalen, F., Trouche, D., and Harel-Bellan, A. (1998). Retinoblastoma protein represses transcription by recruiting a histone deacetylase, Nature *391*, 601-5.

McMahon, S. B., Van Buskirk, H. A., Dugan, K. A., Copeland, T. D., and Cole, M. D. (1998). The novel ATM-related protein TRRAP is an essential cofactor for the c-Myc and E2F oncoproteins, Cell *94*, 363-74.

Meijsing, S. H., and Ehrenhofer-Murray, A. E. (2001). The silencing complex SAS-I links histone acetylation to the assembly of repressed chromatin by CAF-I and Asf1 in *Saccharomyces cerevisiae*, Genes Dev. *15*, 3169-82.

Mello, C. C., Kramer, J. M., Stinchcomb, D., and Ambros, V. (1991). Efficient gene transfer in *C.elegans*: extrachromosomal maintenance and integration of transforming sequences, Embo J. *10*, 3959-70.

Nourani, A., Doyon, Y., Utley, R. T., Allard, S., Lane, W. S., and Cote, J. (2001). Role of an ING1 growth regulator in transcriptional activation and targeted histone acetylation by the NuA4 complex, Mol. Cell. Biol. *21*, 7629-40.

Osada, S., Sutton, A., Muster, N., Brown, C. E., Yates, J. R., 3rd, Sternglanz, R., and Workman, J. L. (2001). The yeast SAS (something about silencing) protein complex contains a MYST-type putative acetyltransferase and functions with chromatin assembly factor ASF1, Genes Dev. *15*, 3155-68.

Reid, J. L., Iyer, V. R., Brown, P. O., and Struhl, K. (2000). Coordinate regulation of yeast ribosomal protein genes is associated with targeted recruitment of Esa1 histone acetylase, Mol. Cell *6*, 1297-307.

Reifsnyder, C., Lowell, J., Clarke, A., and Pillus, L. (1996). Yeast SAS silencing genes and human genes associated with AML and HIV-1 Tat interactions are homologous with acetyltransferases, Nat. Genet. *14*, 42-9.

Riddle, D. L., Blumenthal, T., Meyer, B. J., and Priess, J. R., eds. (1997). *C. elegans* II (Cold Spring Harbor, New York, Cold Spring Harbor Laboratory Press).

Roth, S. Y., Denu, J. M., and Allis, C. D. (2001). Histone acetyltransferases, Annu. Rev. Biochem. *70*, 81-120.

Saleh, A., Schieltz, D., Ting, N., McMahon, S. B., Litchfield, D. W., Yates, J. R., 3rd, Lees-Miller, S. P., Cole, M. D., and Brandl, C. J. (1998). Tra1p is a component of the yeast Ada.Spt transcriptional regulatory complexes, J. Biol. Chem. *273*, 26559-65.

Sato, T., Russell, M. A., and Denell, R. E. (1983). Homeosis in *Drosophila*: A new enhancer of Polycomb and related homeotic mutations, Genetics *105*, 357-70.

Sigurdson, D. C., Spanier, G. J., and Herman, R. K. (1984). *Caenorhabditis elegans* deficiency mapping, Genetics *108*, 331-45.

Sinclair, D. A., Clegg, N. J., Antonchuk, J., Milne, T. A., Stankunas, K., Ruse, C., Grigliatti, T. A., Kassis, J. A., and Brock, H. W. (1998). Enhancer of Polycomb is a suppressor of position-effect variegation in *Drosophila melanogaster*, Genetics *148*, 211-20.

Smith, E. R., Eisen, A., Gu, W., Sattah, M., Pannuti, A., Zhou, J., Cook, R. G., Lucchesi, J. C., and Allis, C. D. (1998). ESA1 is a histone acetyltransferase that is essential for growth in yeast, Proc. Natl. Acad. Sci. USA *95*, 3561-5.

Solari, F., and Ahringer, J. (2000). NURD-complex genes antagonise Ras-induced vulval development in *Caenorhabditis elegans*, Curr. Biol. *10*, 223-6.

Sternberg, P. W., and Han, M. (1998). Genetics of RAS signaling in *C. elegans*, Trends Genet. *14*, 466-72.

Sternberg, P. W., and Horvitz, H. R. (1986). Pattern formation during vulval development in *C. elegans*, Cell *44*, 761-72.

Suka, N., Suka, Y., Carmen, A. A., Wu, J., and Grunstein, M. (2001). Highly specific antibodies determine histone acetylation site usage in yeast heterochromatin and euchromatin, Mol. Cell *8*, 473-9.

Sulston, J. E., and Horvitz, H. R. (1977). Post-embryonic cell lineages of the nematode, *Caenorhabditis elegans*, Dev. Biol. *56*, 110-56.

Sulston, J. E., and White, J. G. (1980). Regulation and cell autonomy during postembryonic development of *Caenorhabditis elegans*, Dev. Biol. *78*, 577-97.

Tabara, H., Sarkissian, M., Kelly, W. G., Fleenor, J., Grishok, A., Timmons, L., Fire, A., and Mello, C. C. (1999). The *rde-1* gene, RNA interference, and transposon silencing in *C. elegans*, Cell *99*, 123-32.

Trimarchi, J. M., and Lees, J. A. (2002). Sibling rivalry in the E2F family, Nat. Rev. Mol. Cell Biol. *3*, 11-20.

Turner, B. M., Birley, A. J., and Lavender, J. (1992). Histone H4 isoforms acetylated at specific lysine residues define individual chromosomes and chromatin domains in *Drosophila* polytene nuclei, Cell *69*, 375-84.

von Zelewsky, T., Palladino, F., Brunschwig, K., Tobler, H., Hajnal, A., and Muller, F. (2000). The *C. elegans* Mi-2 chromatin-remodelling proteins function in vulval cell fate determination, Development *127*, 5277-84.

TABLES

Table 1. *trr-1* mutations cause a hyperinduced phenotype

A. *trr-1* interactions with synMuv mutations

Genotype	Temp (°C)	Ave. # P(3-8).p induced (±SE)	% animals hyperinduced	n
wild type	20	3.00 (±0)	0	31
lin-15A(n767)	20	3.00 (±0)	0	24
lin-38(n751)	20	3.00 (±0)	0	27
trr-1(n3630); lin-15A(n767)	20	4.52 (±0.15)	82	45
trr-1(n3637); lin-15A(n767)	20	4.52 (±0.14)	83	54
trr-1(n3704); lin-15A(n767)	20	4.20 (±0.13)	79	43
trr-1(n3708); lin-15A(n767)	20	4.71 (±0.14)	92	36
trr-1(n3709); lin-15A(n767)	20	4.81 (±0.13)	95	39
trr-1(n3712); lin-15A(n767)	20	4.07 (±0.12)	74	54
lin-15A(n767); trr-1(RNAi)	20	5.60 (±0.08)	100	44
trr-1(n3712) lin-38(n751)	20	4.14 (±0.23)	79	14
lin-38(n751); trr-1(RNAi)	20	5.66 (±0.08)	100	32
wild type	15	3.00 (±0)	0	29
lin-15A(n767)	15	3.00 (±0)	0	32
trr-1(n3704); lin-15A(n767)	15	3.13 (± 0.05)	21	24
trr-1(n3712); lin-15A(n767)	15	3.06 (± 0.03)	13	32
wild type	25	3.00 (±0)	0	36
lin-15A(n767)	25	3.02 (±0.02)	3.6	28
trr-1(n3704); lin-15A(n767)	25	5.87 (±0.06)	100	38
trr-1(n3712); lin-15A(n767)	25	5.47 (±0.14)	100	17

B. *trr-1* single mutants

Genotype	Temp (°C)	Ave. # P(3-8).p induced (±SE)	% animals hyperinduced	n
wild type	20	3.00 (±0)	0	31
trr-1(n3630)	20	3.03 (± 0.02)	6.1	33
trr-1(n3637)	20	3.08 (±0.04)	13	30
trr-1(n3704)	20	3.01 (±0.01)	2.6	39
trr-1(n3708)	20	3.05 (±0.03)	8.1	37
trr-1(n3709)	20	3.03 (±0.02)	6.3	32
trr-1(n3712)	20	3.10 (±0.03)	13	89
trr-1(RNAi)	20	3.09 (±0.05)	13	32
wild type	15	3.00 (±0)	0	29
trr-1(n3704)	15	3.08 (± 0.05)	12	26
trr-1(n3712)	15	3.06 (± 0.03)	12	25
wild type	25	3.00 (±0)	0	36
trr-1(n3704)	25	3.04 (±0.03)	3.9	51
trr-1(n3712)	25	3.07 (±0.03)	13	48

The number of P(3-8).p cells induced was scored as described in Materials and Methods. Induction was scored after raising strains at the indicated temperature for two generations. *trr-1* mutant homozygotes were scored by examining the non-Gfp progeny of *trr-1/mIn1[dpy-10(e128) mIs14]* heterozygous parents.

Table 2. *trr-1(RNAi)* is synthetically lethal with class B but not with class A synMuv mutations

Genotype	% dead embryos	% dead L1 larvae	Total % lethality (n)
wild type	0	0	0 (1062)
trr-1(RNAi)	6.6	1.2	7.8 (726)
lin-15A(n767)	0	0	0 (823)
lin-38(n751)	0.1	0	0.1 (1003)
lin-15B(n744)	0.2	0	0.2 (1002)
lin-35(n745)	0.6	0.2	0.8 (482)
lin-36(n766)	0.3	0	0.3 (890)
dpl-1(n2994)	14	1.1	15.1 (265)
lin-15A(n767); trr-1(RNAi)	3.2	0.9	4.1 (470)
lin-38(n751); trr-1(RNAi)	3.8	1.3	5.1 (628)
lin-15B(n744); trr-1(RNAi)	62.5	36.0	98.5 (469)
lin-35(n745); trr-1(RNAi)	66.2	33.8	100 (263)
lin-36(n766); trr-1(RNAi)	19.4	21.6	41.0 (444)
dpl-1(n2994); trr-1(RNAi)	45.1	53.6	98.7 (304)

Animals injected with *trr-1* dsRNA were individually plated 10-15 hours following injection. Injected animals were subsequently transferred to new plates every 24 hours until egg laying had ceased. Dead embryos and larvae on a plate were counted at least two days after eggs were laid. All of the mutant strains in which *trr-1(RNAi)* was performed are homozygous viable.

Table 3. *trr-1* acts redundantly with *dpl-1*

Genotype	Ave. # P(3-8).p induced (±SE)	% animals mutant (n)
lin-15A(n433); trr-1(RNAi)	3.17 (±)	20 (15)
dpl-1(n3316); lin-15A(n433)	3.00 (±0)	0 (35)
dpl-1(n3316); lin-15A(n433); trr-1(RNAi)	4.98 (±)	89 (45)

Animals were raised at 15°C, a temperature at which *dpl-1(n3316); lin-15A(n433)* mutants do not show hyperinduction. *dpl-1(n3316)* homozygous mutants were recognized as the Unc non-Gfp progeny of *dpl-1(n3316) unc-4(e120)/ mIn1[dpy-10(e128) mIs14]* heterozygous parents.

Table 4. *trr-1* epistasis with *let-23* RTK, *let-60* Ras and *lin-3* EGF

Genotype	Ave. # P(3-8).p induced (±SE)	% animals hyperinduced	n
wild type	3.00 (±0)	0	31
lin-15A(n767)	3.00 (±0)	0	24
lin-15A(n767); trr-1(RNAi)	5.60 (±0.08)	100	44
let-23(sy97); lin-15A(n767)	0.02 (±0.02)	0	28
let-23(sy97); lin-15A(n767); trr-1(RNAi)	0.05 (±0.03)	0	42
let-60(n1876); lin-15A(n767)	0 (±0)	0	17
let-60(n1876); lin-15A(n767); trr-1(RNAi)	0 (±0)	0	23
lin-3(n378); lin-15A(n767)	0.30 (±0.07)	0	40
lin-3(n378); lin-15A(n767); trr-1(RNAi)	4.35 (±0.20)	85	20

let-23(sy97) homozygous mutants were recognized as Rol Unc non-Gfp progeny of *rol-6(e187) let-23(sy97) unc-4(e120)/mIn1[dpy-10(e128) mIs14]; lin-15A(n767)* heterozygous parents, and *let-60(n1876)* homozygous mutants were recognized as Unc progeny of *let-23(n1876) unc-22(e66)/nT1; +/nT1; lin-15A(n767)* heterozygous parents

Table 5. *hat-1* and *epc-1* but not *ssl-1* loss of function phenocopies *trr-1* loss of function

Genotype	Ave. # P(3-8).p induced (±SE)	% animals mutant	n
wild type	3.00 (±0)	0	31
lin-15A(n767)	3.00 (±0)	0	24
lin-38(n751)	3.00 (±0)	0	27
lin-15B(n744)	3.00 (±0)	0	20
hat-1(n4075)	3.15 (±0.08)	15	20
hat-1(n4075); lin-15A(n767)	3.76 (±0.14)	76	25
hat-1(n4075); lin-15B(n744)	3.71 (±0.10)	77	31
rde-1/+; epc-1(RNAi)	3.00 (±0)	0	65
rde-1/+; lin-15A(n767); epc-1(RNAi)	3.32 (±0.10)	36	33
lin-38(n751); rde-1/+; epc-1(RNAi)	3.29 (±0.02)	31	65
rde-1/+; lin-15B(n744); epc-1(RNAi)	3.03 (±0.02)	4.2	48
rde-1/+; ssl-1(RNAi)	3.00 (±0)	0	37
rde-1/+; lin-15A(n767); ssl-1(RNAi)	3.00 (±0)	0	42
rde-1/+; lin-15B(n744); ssl-1(RNAi)	3.01 (±0.01)	2.9	70

hat-1(n4075) homozygous mutants were recognized as the non-Unc progeny of *+/nT1n754; hat-1(n4075)/nT1n754* heterozygous parents. Since RNAi of *epc-1* and *ssl-1* using standard methods causes highly penetrant embryonic lethality, we performed "zygotic RNAi" as described in the text.

FIGURES

Figure 1. *trr-1* single mutants were defective in P(8).p fate specification. Induction of individual P(3-8).p cells was scored in wild-type animals (top) and *trr-1(n3712)* mutants (bottom) as described in Materials and Methods. Certain cells in *trr-1* mutants adopted hybrid fates in which one of two Pn.p daughters divided like daughters of induced Pn.p cells and the other daughter remained undivided as in uninduced Pn.p cells. Ectopic induction in single mutant animals containing each of the other five *trr-1* mutations was similarly restricted to P8.p.

Figure 1

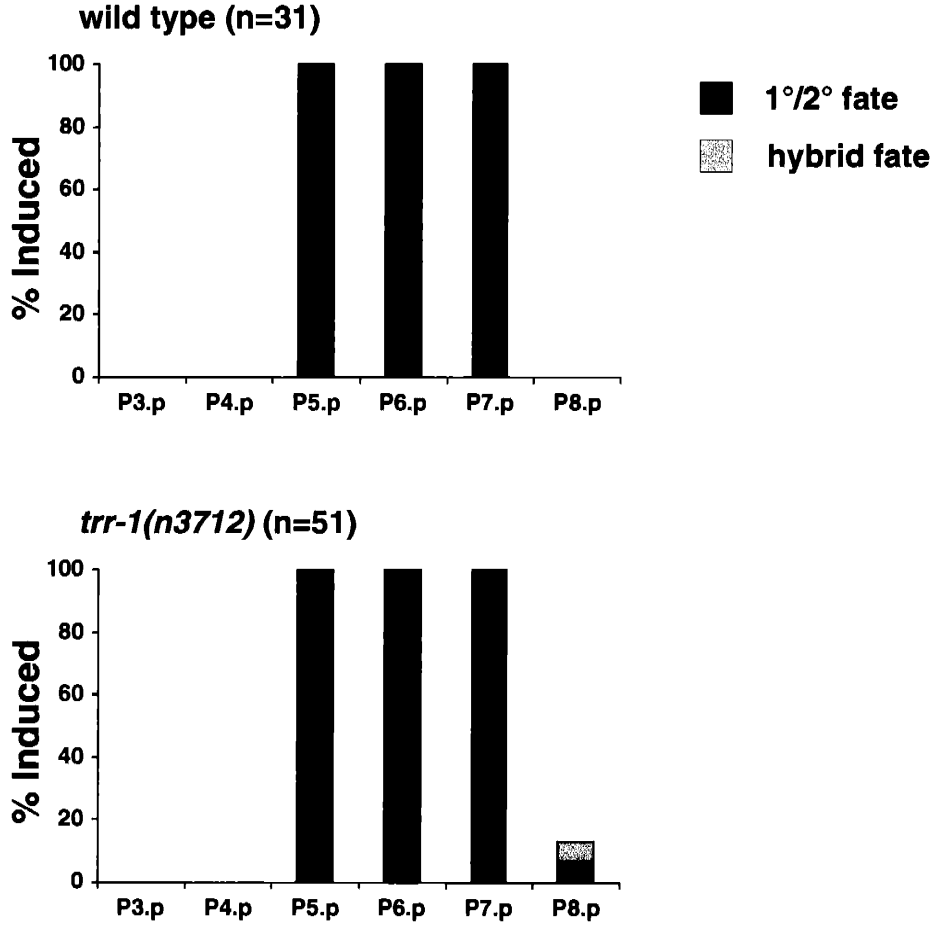
wild type (n=31)
% Induced
100
80
60
40
20
0
P3.p
P4.p
P5.p
P6.p
P7.p
P8.p
1°/2° fate
hybrid fate
trr-1(n3712) (n=51)
% Induced
100
80
60
40
20
0
P3.p
P4.p
P5.p
P6.p
P7.p
P8.p

Figure 2. *trr-1* and class B synMuv mutations are synthetically defective in P8.p cell-fate specification

P8.p induction was scored as described (see Materials and Methods). We recognized *trr-1* homozygous mutants as non-Gfp progeny of *trr-1/ mIn1[dpy-10(e128) mIs14]* heterozygous parents. *lin-15B(n744)*, *lin-35(n745)*, *lin-36(n766)* and *lin-37(n758)* are the strongest mutations of their corresponding genes. Strains homozygous for these mutations are viable. *trr-1; synmuvB* double mutant strains with these mutations were derived from parents that were homozygous for the *synmuvB* mutation and hence lacked maternal and zygotic function of the class B synMuv gene in question. The *dpl-1(n3316)* null mutation causes sterility. We combined *dpl-1(RNAi)* with the *dpl-1(n3316)* mutation to generate mutants that lacked both maternal and zygotic *dpl-1* activity and recognized these mutants as non-Gfp progeny of *dpl-1(n3316) trr-1/ mIn1[dpy-10(e128) mIs14]* heterozygous parents that were injected with *dpl-1* dsRNA.

Figure 2

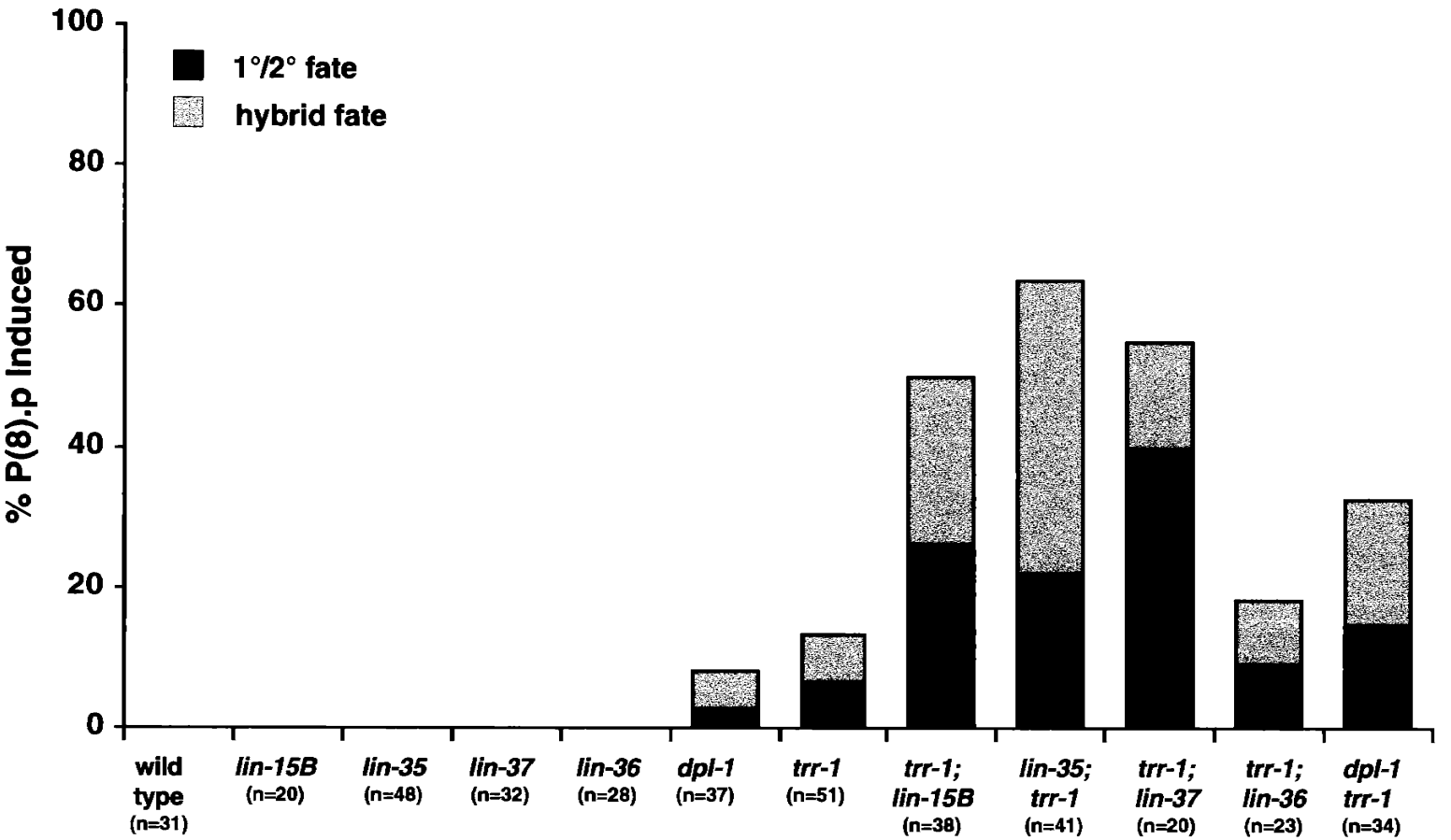
100
80
60
40
20
0
% P(8).p Induced
1°/2° fate
hybrid fate
wild type (n=31)
lin-15B (n=20)
lin-35 (n=48)
lin-37 (n=32)
lin-36 (n=28)
dpl-1 (n=37)
trr-1 (n=51)
trr-1; lin-15B (n=38)
lin-35; trr-1 (n=41)
trr-1; lin-37 (n=20)
trr-1; lin-36 (n=23)
dpl-1 trr-1 (n=34)

Figure 3. *trr-1* gene structure and mutations

(A) The *trr-1* gene structure as derived from cDNA and genomic sequences. Shaded boxes indicate coding sequence and open boxes indicate 5' and 3' untranslated regions. Predicted translation initiation and termination codons and the poly(A) tail are shown. Positions of alternative splicing are indicated by asterisks. In all cases, the use of alternative splice acceptors creates small differences in the *trr-1* coding sequence: alternative splicings of the fourth (ag/TTTCAGAC versus agtttcag/AC), fifth (ag/AATCTTCAGTC versus agaatcttcag/CC), eleventh (ag/AACTTTAAGAT versus agaactttaag/AT) and twelfth introns (ag/TTGCAGAA versus agttgcag/AA) differ by either six or nine nucleotides.

(B) A schematic of the TRR-1 protein. The positions of and substitutions caused by TRR-1 mutations are indicated above. TRR-1 is similar to mammalian TRRAP and yeast Tra1p thoughout the lengths of the proteins. Domains of similarity that these three proteins share with less similar proteins are indicated.

Figure 3

A.


SL1
1 kb

B.

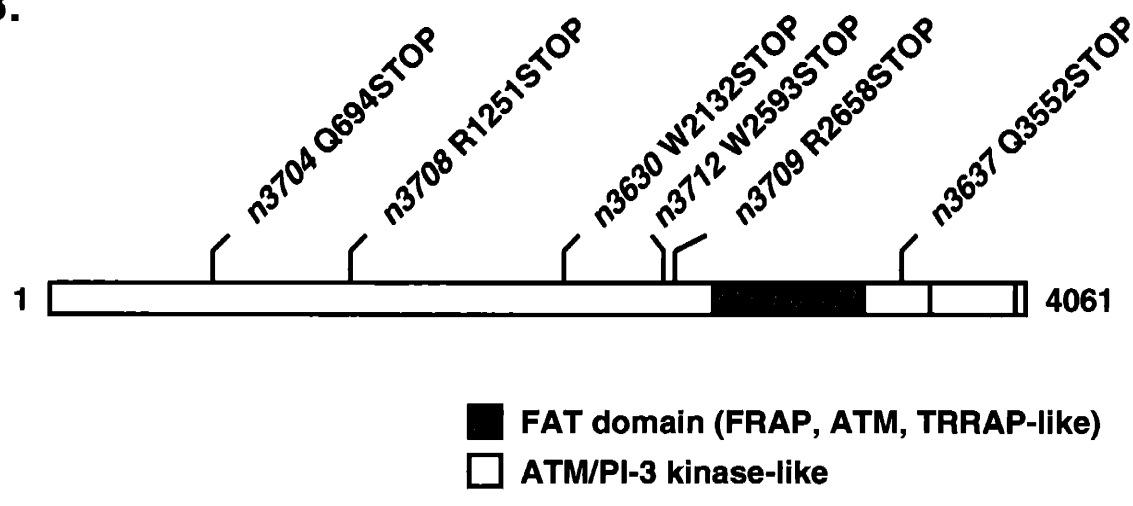
n3704 Q694STOP
n3708 R1251STOP
n3630 W2132STOP
n3712 W2593STOP
n3709 R2658STOP
n3637 Q3552STOP
1
4061
FAT domain (FRAP, ATM, TRRAP-like)
ATM/PI-3 kinase-like

Figure 4. *hat-1* encodes a putative MYST family histone acetyltransferase that is required for P(3-8).p cell-fate specification

(A) The *hat-1* gene structure as derived from cDNA and genomic sequences. Shaded boxes indicate coding sequence and open boxes indicate 5' and 3' untranslated regions. Predicted translation initiation and termination codons and the poly(A) tail are shown.

(B) A schematic of the HAT-1 protein. HAT-1 is similar to MYST family acetyltransferases, all of which contain a MOZ/SAS acetyltransferase domain and some of which contain a chromodomain. Animals containing the *hat-1(n4075)* deletion are expected to produce only the first 35 amino acids of the wild-type HAT-1 protein and additional frameshifted amino acids prior to truncation.

(C) *hat-1* single mutants were defective in P(8).p fate specification. Induction of individual P(3-8).p cells was scored in wild-type animals (left) and *hat-1(n4075)* mutants (right) as described in Materials and Methods. *hat-1* homozygous mutants were recognized as non-Unc progeny of *+/nT1n754; hat-1(n4075)/nT1n754* heterozygous parents.

(D) *hat-1* is synthetically defective in P8.p cell-fate specification with the class B synMuv mutation *lin-15B(n744)*. P8.p induction was scored as described (see Materials and Methods). *hat-1* homozygous mutants were recognized as in (C).

Figure 4

A.

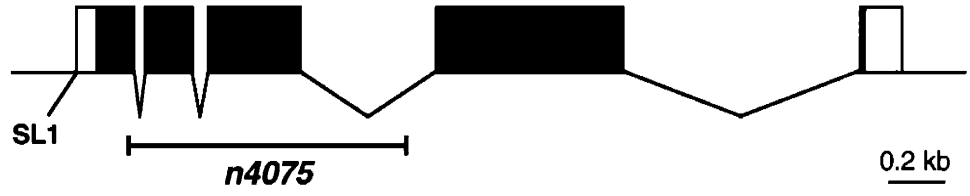

B.

C.

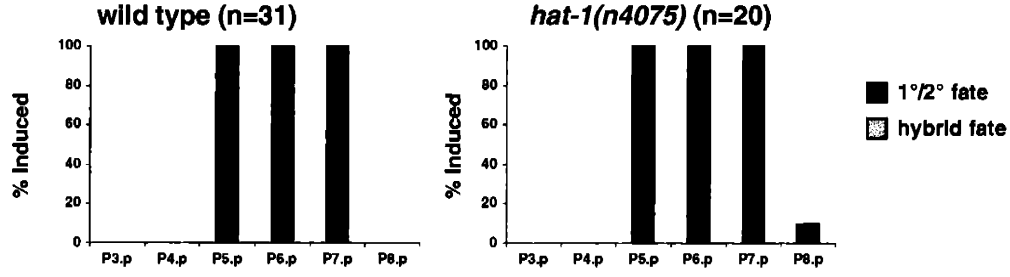

D.

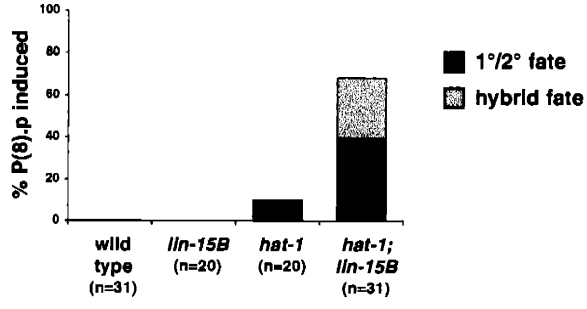

Figure 5. *epc-1* and *ssl-1* gene structures and deletion mutations
(A) *epc-1* gene structure and deletion mutation. The gene structure of *epc-1* was derived by comparing cDNA and genomic sequences.
(B) *ssl-1* gene structure and deletion mutation. The gene structure of *ssl-1* is partially derived from comparison of cDNA and genomic sequences (SL1 splice leader, 5' untranslated region, exons 1-12 and the beginning of exon 13) and partially predicted solely from genomic sequence (the end of exon 13). As we do not have cDNA clones representing the 3' end of *ssl-1*, we are unable to reliably assign a 3' untranslated region and poly(A) tail. Filled boxes indicate coding sequence and open boxes indicate 5' and 3' untranslated regions. SL1 splice leaders, predicted translation start and stop codons and poly(A) tail are shown. The regions of genomic sequence removed by the *epc-1(n4076)* and *ssl-1(n4077)* deletions are indicated.

Figure 5

A.

epc-1

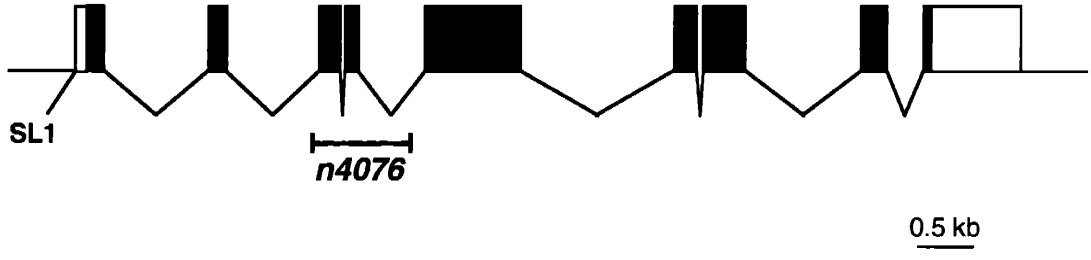

B.

ssl-1

Figure 6. Two models of TRR-1/HAT-1/EPC-1 function with respect to class B synMuv proteins

(A) MODEL 1: A TRR-1/HAT-1/EPC-1 complex and the class B synMuv proteins act on different targets and differentially regulate transcription. In this model a putative TRR-1/HAT-1/EPC-1 complex acts on targets that are different from those of a putative class B synMuv protein complex. A TRR-1/HAT-1/EPC-1 complex may promote transcription of genes that negatively regulate vulval development, whereas class B synMuv proteins may repress transcription of genes that promote vulval development. (B) MODEL 2: A TRR-1/HAT-1/EPC-1 complex acts on the same targets as do the class B synMuv proteins. Together these two putative protein complexes may specify an acetylation pattern on histones that is required for efficient silencing of genes that promote vulval development. A TRR-1/HAT-1/EPC-1 complex may act through DPL-1 and EFL-1, although genetic interactions suggest that not all TRR-1/HAT-1/EPC-1 complex activity goes through DPL-1 and EFL-1.

Figure 6

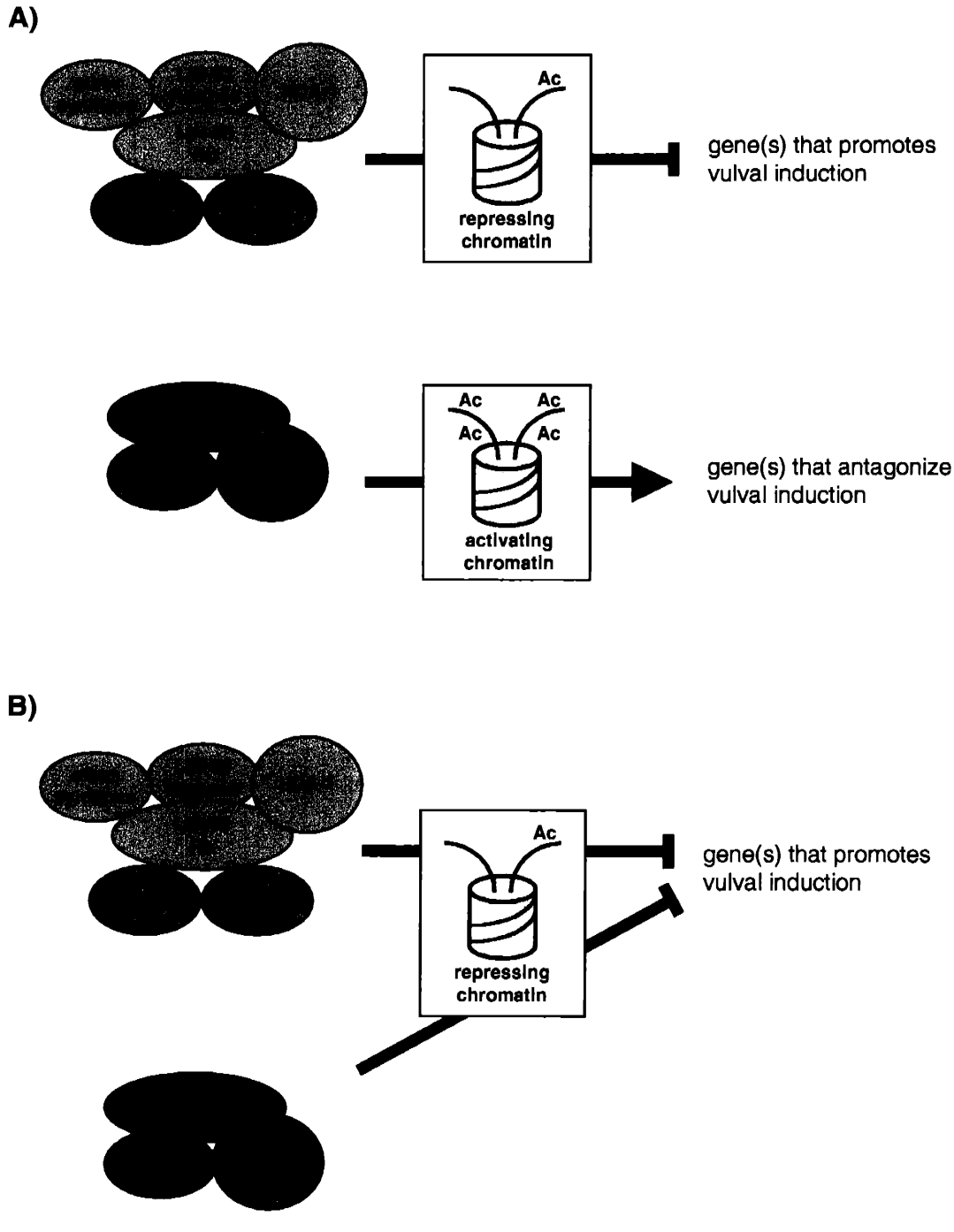
A)
Ac
repressing chromatin
gene(s) that promotes vulval induction
Ac
Ac
Ac
Ac
activating chromatin
gene(s) that antagonize vulval induction
B)
Ac
repressing chromatin
gene(s) that promotes vulval induction

CHAPTER 7

Discussion and future prospects

INVESTIGATIONS OF SYNTHETIC MULTIVULVA GENE FUNCTION

The studies described in this thesis and elsewhere have contributed to a model whereby the synMuv genes regulate vulval development by altering chromatin structure. I discuss this model in detail in the beginning of this chapter. In addition, I discuss issues regarding synMuv gene function that merit future attention. When appropriate, I suggest possible means of addressing these issues.

Model for class B synMuv function

The class B synMuv protein LIN-35 is a homolog of the tumor suppressor Rb (Lu and Horvitz, 1998), and other proteins with class B synMuv activity are homologous to mammalian Rb-associated proteins. These other proteins include DPL-1 and EFL-1, homologs of DP and E2F transcription factors (Ceol and Horvitz, 2001), LIN-53, a homolog of the Rb-binding proteins RbAp46 and RbAp48 (Lu and Horvitz, 1998), HDA-1, a histone deacetylase homolog (Lu and Horvitz, 1998) and HPL-2, a heterochromatin protein 1 homolog (Couteau et al., 2002). The functions of the corresponding mammalian proteins can be expanded to their *C. elegans* counterparts to formulate a model of class B synMuv function (Figure 1). In this model, the class B synMuv proteins act together to negatively regulate the transcription of genes that promote vulval development. Initially, DPL-1 and EFL-1 heterodimers bind DNA at specific regulatory sequences of vulval cell-fate determination genes. DNA-bound DPL-1 and EFL-1 heterodimers recruit LIN-35 Rb, which in turn recruits proteins that act to remodel chromatin. One of these proteins, HDA-1, is predicted to deacetylate lysines of nucleosomal histones. Deacetylation of lysine residues is required for their subsequent methylation. HPL-2, another protein that may be recruited by LIN-35 Rb, is expected to act like other HP1 family proteins and bind, via its chromodomain, to methylated lysine residues of nucleosomal histones.

To culminate in HPL-2 binding, this model predicts that an as yet unidentified histone methyltransferase (HMT) acts after HDA-1 to add methyl groups onto unmodified lysine residues. Searches of the complete *C. elegans* genome sequence indicate that there are at least seven putative HMTs (E. Andersen, C.J.C. and H.R. Horvitz, unpublished results). A subset of these HMTs are highly similar to mammalian SUV39H1 and related HMTs that target histone H3 lysine 9 residues (Rea et al., 2000). As HP1 proteins specifically bind methylated lysine 9 residues of histone H3 (Bannister

et al., 2001; Lachner et al., 2001), this subset represents the best candidate synMuv HMTs.

What are deacetylation, methylation and HPL-2 binding expected to do? As discussed in the Introduction, all three of these activities have been correlated with transcriptional repression. The mechanism by which binding of an HP1 family protein ultimately leads to transcriptional repression, however, is unclear. It is possible that HP1 proteins nucleate the formation of higher-order chromatin structures that are refractory to the general transcription machinery. For example, HP1 proteins may themselves create higher-order structures by self association (Nielsen et al., 2001) or they may recruit other proteins which create a refractory chromatin structure.

At a basic level, studies of the class B synMuvs have linked a group of genes together based on shared phenotypes and genetic interactions. Linking these genes together is interesting for a few reasons. First, many studies of Rb-associated proteins in other systems have relied on biochemical methods and genetic overexpression experiments to support a physiological link between the protein in question and Rb. Studies of the class B genes provide loss-of-function genetic data that functionally tie certain families of proteins to Rb. Such loss-of-function data are important in establishing the biological relevance of a suspected functional interaction. Second, that all class B synMuvs share a common phenotype suggests Rb-associated proteins representing different families can act together with Rb to regulate a single process. The genetic grouping of the synMuv genes suggests that studies of synMuv counterparts in other species, many of which focused on a single or a subset of Rb-associated proteins, can be more readily considered as a unit in order to formulate models of Rb-mediated transcriptional regulation. One such model is outlined above. It should be stressed, however, that this model describes regulation of just one process. It is possible that *lin-35* Rb can function with the class B synMuv proteins in this process, but need not act with some class B synMuv proteins in other processes. Indeed, the fact that certain pleiotropies associated with *lin-35* Rb mutations are not observed with mutations in other synMuv genes (Hsieh, Fay, Reddien thesis), suggests that *lin-35* Rb likely has functions independent of a subset of class B synMuv genes. Finally, the link between certain class B synMuv genes and *lin-35* Rb has defined families of genes whose functional interaction with Rb may be conserved across species. Included in this subset is *let-418*, which encodes a homolog of the Mi-2 chromatin remodeling ATPase (Solari and Ahringer, 2000; von Zelewsky et al., 2000).

By analogy to the interaction in *C. elegans*, a Mi-2-containing complex may interact with mammalian Rb to remodel chromatin. Also included in this subset are the novel, conserved class B genes *lin-52* and *lin-54*. Their counterparts in other species, which are described in Chapters 4 and 5, are excellent candidate Rb pathway proteins.

What is the relationship between different classes of synMuv genes?

As has been noted, the class A and class B genes act redundantly to negatively regulate vulval induction. There are many possible mechanisms by which two classes of genes might appear redundant. These mechanisms include: 1) biochemical redundancy of homologs in which both classes of genes encode similar sets of proteins with each set having the same biochemical function; 2) redundancy of unrelated proteins in which both classes of genes encode distinct sets of proteins with each set similarly regulating the same cell biological process; 3) redundancy of unrelated proteins in which both classes of genes encode distinct sets of proteins with each set regulating different cell biological processes. The first of these mechanisms likely does not apply to the class A and class B genes. Thus far, none of the cloned class A and class B genes are similar to one another. Furthermore, many of the cloned synMuv genes, including *lin-35* Rb and *dpl-1* DP, encode the sole *C. elegans* member of their respective gene families.

The second and third mechanisms are difficult to exclude, mainly because the biochemical activity (or activities) of the class A genes is obscure. Three of four known class A genes have been cloned (Clark et al., 1994; Huang et al., 1994; E. Davison and H.R. Horvitz, personal communication) and each encodes a novel protein that lacks homology to proteins of other species. However, recent observations suggest that *lin-8* and possibly other class A genes regulate transcription. The LIN-8 protein is localized to nuclei (E. Davison and H. R. Horvitz, personal communication), and in two-hybrid assays (M. Walhout and M. Vidal, personal communication) and *in vitro* (M. Harrison, E. Davison and H. R. Horvitz, personal communication) LIN-8 interacts with LIN-35 Rb. Furthermore, *lin-8* mutants show ectopic pharyngeal expression of a transgene that is normally restricted in expression to the two male-specific CEM neurons (H. Schwartz and H. R. Horvitz, personal communication). If *lin-8* and other class A genes were transcriptional regulators, the second mechanism of redundancy, that is, redundancy of unrelated proteins that regulate the same process, may apply.

RNAi of the recently-described gene *hpl-2* leads to a Muv phenotype in combination with mutations in class A and a subset of class B genes (Couteau et al., 2002). These results must be interpreted carefully. *hpl-2* may show redundancy with both classes because it possesses class A and class B activities. *hpl-2* encodes a member of the heterochromatin protein 1 (HP1) family (Couteau et al., 2002), and mammalian HP1 binds methylated lysine 9 of histone H3 and associates with Rb (Bannister et al., 2001; Lachner et al., 2001). The association of mammalian HP1 with Rb suggests that HPL-2 acts with LIN-35 Rb and that the synergism of *hpl-2(RNAi)* with class A mutations represents a decrease in *hpl-2* class B activity. Whether its redundancy with some class B genes means that *hpl-2* acts with class A genes is more of an open question. If it does, then some combination of the first two mechanisms of redundancy would apply. If it doesn't, then *hpl-2* would define another class of synMuv genes and the mechanism of redundancy would remain unresolved. Two factors argue towards the latter possibility. First, *hpl-2* interacts with a subset of class B genes (Couteau et al., 2002), whereas all of the class A genes characterized thus far interact with the range of class B genes. Second, *hpl-2(RNAi)* single mutants are non-Muv (Couteau et al., 2002), a result that would not be expected if both class A and class B activities were disabled.

How do these mechanisms of redundancy apply to the new class of synMuv genes defined by *trr-1*, *epc-1* and *hat-1*? Again, the first mechanism is unlikely: *trr-1* is the only TRRAP-like gene and *epc-1* is the only enhancer of polycomb-like gene in *C. elegans*. As discussed in Chapter 6, the second mechanism may explain the redundancy between this new class and the class B genes. To reiterate, this new class of genes and the class B genes may together specify an acetylation pattern at target promoters that is important for repressing the transcription of genes that are important for vulval cell fates. Alternatively, the third mechanism may apply. Again as previously discussed, this new class of genes may promote transcription of genes that negatively regulate vulval cell fates, whereas the class B genes may repress the transcription of genes that promote vulval cell fates. Clearly, it will be important in the future to identify synMuv targets.

Identifying synMuv targets

The class B synMuv genes and the class of synMuv genes defined by *trr-1*, *epc-1* and *hat-1* likely remodel chromatin to regulate transcription. Their effects on

transcription *in vivo*, however, cannot be measured without knowing the targets of their activity. The identification of targets of transcriptional regulators is a long-standing problem in biology. In the case of synMuv transcriptional regulation, this problem could be addressed by a variety of genetic and molecular approaches. For the purposes of simplicity, I will limit my discussion to targets of the class B synMuvs while noting that the approaches discussed could in principle be applied to the *trr-1/epc-1/hat-1* class of synMuvs or other transcriptional regulatory systems.

At least two genetic screens could be used to identify class B synMuv targets. Both screens are based on the assumption that the class B synMuv proteins negatively regulate transcription. Given this assumption, one would postulate that the Muv phenotype of synMuv mutants is due to the ectopic expression of class B targets. A simple F_2 suppression screen might identify these targets. In fact, two screens (Clark, 1992; X. Lu and H. R. Horvitz, personal communication) have identified synMuv suppressor mutations that may affect such genes. Many of the isolates from these screens are as yet uncharacterized. A second type of screen might also identify genes whose expression is negatively regulated by the class B synMuvs. In this second screen, mutagenized class A synMuv F_1 animals could be screened for a Muv phenotype. Dominant mutations expected from this screen might affect regulatory sequences bound by synMuv proteins and lead to ectopic expression of the target gene in question. Mutations of this type have been shown to affect the expression of *egl-1*, a gene that promotes programmed cell death in *C. elegans*. These *egl-1(gf)* mutations disrupt a binding site for the TRA-1 transcriptional repressor protein, leading to ectopic *egl-1* expression in the hermaphrodite specific neurons and subsequent programmed cell death (Conradt and Horvitz, 1999).

A major factor confounds the identification of transcriptional targets through genetic analysis. Transcription factors typically target multiple genes, and loss of function of one target may not suppress the phenotype caused by transcriptional repressor loss of function or, alternatively, recapitulate the phenotype caused by transcriptional activator loss of function. A means of addressing this problem is to perform the screen in a particularly sensitized genetic background so as to allow the observation of a small effect that may be caused by loss of one target. For example in one of the screens described above, Scott Clark suppressed the Muv phenotype caused by a temperature-sensitive *lin-15AB* allele (Clark, 1992). A similarly sensitized background is recommended for future F_2 suppression and F_1 synMuv screens.

Various molecular approaches involving microarrays may also be used to identify synMuv targets. In the simplest experiment, expression profiles of synMuv mutants could be compared to the wild type. A comparison of a synMuv double mutant to the wild type could be problematic because these animals have different amounts of vulval tissue. The generation of vulval tissue likely involves the differential regulation of many genes, only a subset of which might be direct targets of synMuvs. A better approach, perhaps, is to compare a synMuv single mutant to the wild type. This approach may not succeed if two classes of synMuvs must lose function in order for transcription to be differentially regulated. If mutations in two classes of synMuvs are desired, an appropriate comparison may, for example, be that of a synMuvA; synMuvB; *let-60* Ras triple mutant versus a *let-60* Ras single mutant. These animals would fulfill the requirements of having the same amount of vulval tissue and disabling two classes of synMuvs. Another final approach worth mentioning is that of chromatin immunoprecipitation (ChIP) combined with microarray analysis. For example, in a preparation of proteins crosslinked to DNA, DPL-1 or EFL-1 could be immunoprecipitated, the crosslink reversed and the resultant DNA amplified and applied to microarrays. This experiment relies on the specificity of anti-DPL-1 or anti-EFL-1 antibodies and on the availability of intergenic microarrays, which will not be available for a couple of years (J. Lieb and P.O. Brown, personal communication).

How do the synMuv genes interface with the *let-60* Ras pathway?

The synMuv genes antagonize *let-60* Ras pathway activity during vulval development; however, the point at which the synMuv genes interface with the *let-60* Ras pathway is unclear. Genetic epistasis results indicate that at least one class of synMuv genes acts upstream of or in parallel to the *let-60* Ras pathway. One possible mode by which the class B synMuv genes may act upstream is by direct transcriptional regulation of a *let-60* Ras pathway gene. Bioinformatic approaches thus far have identified few candidate DP/E2F binding sites in the vicinity of *let-60* Ras pathway genes (C.J.C. and H.R. Horvitz, unpublished results). Homologs of some of the genes examined can be studied in the related nematode *C. briggsae*, and, in these cases, none of the candidate regulatory sequences are conserved (C.J.C. and H.R. Horvitz, unpublished results). A mode by which the class B synMuv genes may act in parallel to the *let-60* Ras pathway is via the regulation of common target genes. Bioinformatic approaches to address this possibility are difficult, mainly because the regulatory sites

bound by ETS domain and winged helix transcription factors, including the LIN-1 ETS and LIN-31 winged helix transcription factors that act downstream of *let-60* Ras and the *C. elegans* MAP kinase homolog *mpk-1*, are either unknown or poorly defined.

There is some evidence that *let-60* Ras pathway activity is elevated in class B synMuv mutants. Alleles of *dpl-1* and *efl-1* were independently identified in surveys for mutants with a Mex (Mex, Muscle in excess) phenotype (Page et al., 2001). These mutations affect early embryonic asymmetry, leading to the production of muscle by AB, an embryonic founder cell that normally does not produce muscle. *dpl-1* and *efl-1* are thought to act in the maternal gonad to regulate *mpk-1* activation, which is dependent on a signal from sperm and is thought to promote asymmetry in progeny. In *dpl-1* mutants treated with sperm, the level of *mpk-1* activation, as judged by immunostaining with an antibody directed against the activated, diphosphorylated form of MPK-1, is elevated as compared to the level in wild-type, sperm treated animals. What does this result mean in terms of a class B synMuv - *let-60* Ras pathway interface? In the simplest interpretation, this result suggests that *dpl-1* interfaces with the *let-60* Ras pathway at or upstream of *mpk-1*. That is, a pathway component in between the sperm signal and *mpk-1* may be deregulated in *dpl-1* mutants, resulting in overactivation of *mpk-1*. However, an interface that may appear to be downstream of *mpk-1* cannot be ruled out as one cannot exclude the possibility of a positive feedback loop that may lead to overactivation of *mpk-1*.

How might the interface between synMuv genes and the *let-60* Ras pathway in vulval development be investigated? As done with MPK-1 in the gonad, levels of activated forms of *let-60* Ras pathway proteins could be compared in synMuv and wild type backgrounds. Unfortunately, preliminary studies using anti-diPMAPK antibodies and anti-activated LIN-1 antibodies have failed to detect these proteins in P(3-8).p (C. J. C., unpublished data, E. Davison, personal communication). Alternatively, a search for common transcriptional targets is possible. The microarray experiments described above may identify synMuv targets that could be compared to putative *let-60* Ras pathway targets as previously determined by microarray analyses (Romagnolo et al., 2002). Determining this interface is clearly an important issue as Rb and Ras pathways antagonize each other not only in *C. elegans* but also during cell cycle progression in cultured mammalian cells (Mittnacht et al., 1997; Peeper et al., 1997).

Do the synMuv genes act by regulating cell cycle progression?

Many studies of Rb and E2F in mammals have focused on the roles of these proteins in cell cycle regulation. Might the class B synMuv genes, and possibly other classes of synMuv genes regulate vulval development through direct regulation of P(3-8).p cell cycles? Certain observations argue towards this possibility. Most obviously, P3.p, P4.p and P8.p undergo extra cell divisions in synMuv mutants. Additionally, mutations in a subset of class B synMuv genes that includes *dpl-1*, *efl-1* and *lin-35* Rb have been shown to partially suppress the S phase and cell division defects caused by RNA-mediated interference of the *C. elegans* cyclin D homolog *cyd-1* (Boxem and van den Heuvel, 2002). There are other aspects of these observations that complicate a strict cell cycle regulation model. First, not only are there extra P3.p, P4.p and P8.p cell divisions in synMuv mutants, but there are also various changes in the differentiation of P3.p, P4.p and P8.p descendants in synMuv mutants. The synMuv genes therefore appear to regulate a cell fate decision, a component of which is the decision to progress through the cell cycle. Studies of Rb in mammals have indicated that Rb may have a role in halting cell cycle progression and stimulating differentiation during myogenesis (reviewed by Kitzmann and Fernandez, 2001). Second, whereas *dpl-1*, *efl-1* and *lin-35* Rb mutations can partially suppress defects caused by *cyd-1(RNAi)*, mutations in other class B synMuv genes cannot (Boxem and van den Heuvel, 2002). This observation suggests that, if the class B synMuv genes are cell cycle regulators, some of them act in a tissue-specific fashion, for example in P(3-8).p but not in the intestinal cells that were monitored in *cyd-1(RNAi)* studies. Clearly, a method of monitoring cell cycle progression in P3.p, P4.p and P8.p is required to address these issues.

Concluding remarks

Studies to date have identified a large number of synMuv genes. As evidenced by the questions put forward in this chapter, the functions of these genes in *C. elegans* remain largely unknown. In the future, development of assays to discover synMuv protein-protein interactions and transcriptional targets and to monitor synMuv and *let-60* Ras pathway protein activities, transcriptional regulation and cell cycle regulation in P(3-8).p will be important for assessing the functions of the synMuv genes.

REFERENCES

Bannister, A. J., Zegerman, P., Partridge, J. F., Miska, E. A., Thomas, J. O., Allshire, R. C., and Kouzarides, T. (2001). Selective recognition of methylated lysine 9 on histone H3 by the HP1 chromodomain, Nature *410*, 120-4.

Boxem, M., and van den Heuvel, S. (2002). *C. elegans* Class B Synthetic Multivulva Genes Act in G(1) Regulation, Curr. Biol. *12*, 906-11.

Ceol, C. J., and Horvitz, H. R. (2001). *dpl-1* DP and efl-1 E2F act with *lin-35* Rb to antagonize Ras signaling in *C. elegans* vulval development, Mol. Cell *7*, 461-73.

Clark, S. G. (1992) Intercellular signalling and homeotic genes required during vulval development in *C. elegans*, Ph.D. Thesis, Massachusetts Institute of Technology.

Clark, S. G., Lu, X., and Horvitz, H. R. (1994). The *Caenorhabditis elegans* locus *lin-15*, a negative regulator of a tyrosine kinase signaling pathway, encodes two different proteins, Genetics *137*, 987-97.

Conradt, B., and Horvitz, H. R. (1999). The TRA-1A sex determination protein of *C. elegans* regulates sexually dimorphic cell deaths by repressing the *egl-1* cell death activator gene, Cell *98*, 317-27.

Couteau, F., Guerry, F., Muller, F., and Palladino, F. (2002). A heterochromatin protein 1 homologue in *Caenorhabditis elegans* acts in germline and vulval development, EMBO Rep. *3*, 235-41.

Huang, L. S., Tzou, P., and Sternberg, P. W. (1994). The *lin-15* locus encodes two negative regulators of *Caenorhabditis elegans* vulval development, Mol. Biol. Cell *5*, 395-411.

Kitzmann, M., and Fernandez, A. (2001). Crosstalk between cell cycle regulators and the myogenic factor MyoD in skeletal myoblasts, Cell. Mol. Life Sci. *58*, 571-9.

Lachner, M., O'Carroll, D., Rea, S., Mechtler, K., and Jenuwein, T. (2001). Methylation of histone H3 lysine 9 creates a binding site for HP1 proteins, Nature *410*, 116-20.

Lu, X., and Horvitz, H. R. (1998). *lin-35* and *lin-53*, two genes that antagonize a *C. elegans* Ras pathway, encode proteins similar to Rb and its binding protein RbAp48, Cell *95*, 981-91.

Mittnacht, S., Paterson, H., Olson, M. F., and Marshall, C. J. (1997). Ras signalling is required for inactivation of the tumour suppressor pRb cell-cycle control protein, Curr. Biol. *7*, 219-21.

Nielsen, A. L., Oulad-Abdelghani, M., Ortiz, J. A., Remboutsika, E., Chambon, P., and Losson, R. (2001). Heterochromatin formation in mammalian cells: interaction between histones and HP1 proteins, Mol. Cell *7*, 729-39.

Page, B. D., Guedes, S., Waring, D., and Priess, J. R. (2001). The *C. elegans* E2F- and DP-related proteins are required for embryonic asymmetry and negatively regulate Ras/MAPK signaling, Mol. Cell *7*, 451-60.

Peeper, D. S., Upton, T. M., Ladha, M. H., Neuman, E., Zalvide, J., Bernards, R., DeCaprio, J. A., and Ewen, M. E. (1997). Ras signalling linked to the cell-cycle machinery by the retinoblastoma protein, Nature *386*, 177-81.

Rea, S., Eisenhaber, F., O'Carroll, D., Strahl, B. D., Sun, Z. W., Schmid, M., Opravil, S., Mechtler, K., Ponting, C. P., Allis, C. D., and Jenuwein, T. (2000). Regulation of chromatin structure by site-specific histone H3 methyltransferases, Nature *406*, 593-9.

Romagnolo, B., Jiang, M., Kiraly, M., Breton, C., Begley, R., Wang, J., Lund, J., and Kim, S. K. (2002). Downstream targets of *let-60* Ras in *Caenorhabditis elegans*, Dev. Biol. *247*, 127-36.

Solari, F., and Ahringer, J. (2000). NURD-complex genes antagonise Ras-induced vulval development in *Caenorhabditis elegans*, Curr. Biol. *10*, 223-6.

von Zelewsky, T., Palladino, F., Brunschwig, K., Tobler, H., Hajnal, A., and Muller, F. (2000). The *C. elegans* Mi-2 chromatin-remodelling proteins function in vulval cell fate determination, Development *127*, 5277-84.

FIGURE

Figure 1. Model for class B synMuv function
Class B synMuv proteins may modify and bind to exposed amino-terminal tails of histones in the sequence of events depicted. First, acetyl groups are removed from histones by HDA-1, which is targeted to DNA by EFL-1, DPL-1, LIN-35 Rb and other class B synMuv proteins. Next, an as yet unidentified histone methyltransferase is predicted to add methyl groups onto histone amino-terminal tails, thereby creating a docking site for the HP1 homolog HPL-2. Association of HPL-2 is ultimately predicted to lead to transcriptional repression.

Figure 1

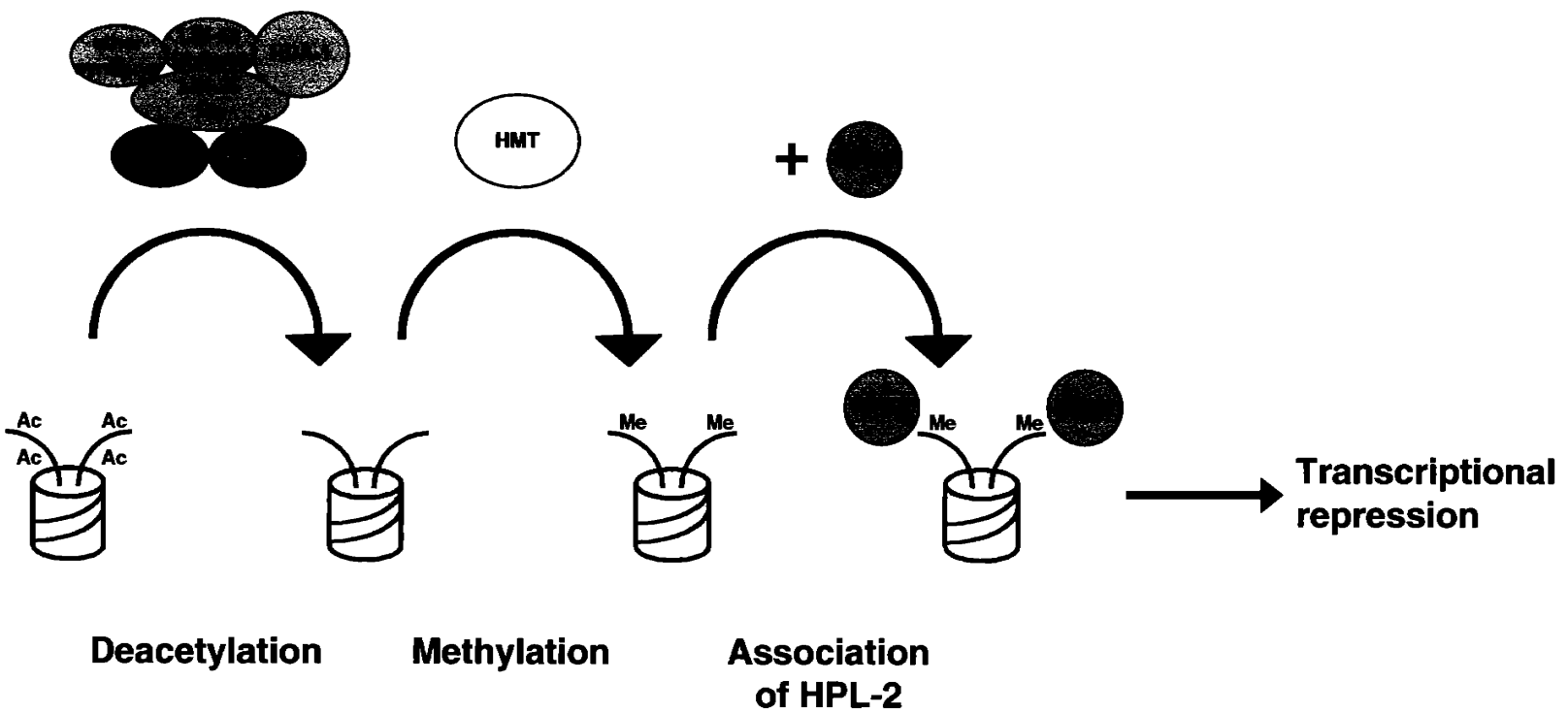
HMT
+
Ac
Ac
Ac
Ac
Me
Me
Me
Me
Transcriptional repression
Deacetylation
Methylation
Association of HPL-2

APPENDIX 1

The use of "wild-type" synMuv suppressor mutations to order class B synMuv genes into a genetic pathway

The class A and class B synMuv genes have been proposed to encode functionally redundant genetic pathways that negatively regulate Ras-mediated vulval induction (Ferguson and Horvitz, 1989). I was interested in determining whether the class B synMuv genes were indeed components of a genetic pathway and, if so, in what order these genes acted. The studies in this appendix describe my approach to address these issues.

BACKGROUND AND RATIONALE

Mosaic analyses suggest that the class B synMuv genes are components of a cell-cell signaling pathway. *lin-15B* and *lin-37* were proposed to act in the syncytial hypodermis, indicating that this tissue may be the source of a vulval cell fate inhibitory signal (Herman and Hedgecock, 1990; Hedgecock and Herman, 1995) As another class B synMuv gene, *lin-36*, is proposed to act in P(3-8).p, these cells may receive and transduce the signal from the hypodermis (Thomas and Horvitz, 1999).

Aside from the inference that *lin-15A* and *lin-37* may act upstream of *lin-36*, little is known about the order of gene action in a putative class B synMuv signaling pathway. This lack of knowledge stems in part from the inability to perform epistasis analyses, as all of the known class B synMuv mutations cause the same phenotype. Furthermore, none of the mutations that has been analyzed appears to cause an increase in function of a gene that positively regulates vulval induction. If such a mutation existed, one could isolate intragenic mutations that revert the synMuv phenotype and potentially use such mutations for epistasis analyses.

Mutations useful for ordering the class B synMuv genes may have been isolated as synMuv suppressors. Such mutations may inactivate a gene that normally positively regulates vulval cell-fate determination or overactivate a gene that negatively regulates vulval cell-fate determination. A former graduate student in the laboratory, Scott Clark, isolated a large number of mutations that suppressed the Muv phenotype of *lin-15AB* mutants (Clark, 1992). *lin-15* is a complex locus, most likely an operon, in which the *lin-15B* gene lies immediately upstream of the *lin-15A* gene (Clark et al., 1994; Huang et al., 1994). The *lin-15AB* suppressor mutations fell into two categories: ones that suppressed to a vulvaless (Vul) phenotype and ones that suppressed to a vulval phenotype closer to that of wild-type animals. Loss-of-function mutations affecting *let-60* Ras pathway genes were known to cause a Vul phenotype. For this reason, Scott Clark focused primarily on the Vul isolates and with a subset of them defined the *sem-5* gene, which encodes an SH2/SH3 adaptor protein similar to mammalian Grb2 (Clark et al., 1992). He also further characterized and cloned the *lin-39* gene, which encodes a homeobox protein similar to *Drosophila* Antennapedia and functions downstream of the *let-60* Ras pathway to promote vulval cell fates (Clark et al., 1993). All of the other Vul mutations were found to affect *let-60* Ras pathway genes or genes such as *lin-25* that appear to function downstream of *let-60* Ras but in parallel to the

lin-1 ETS and *lin-31* winged helix transcription factors. The so-called "wild-type" suppressors, in quotes because many of these mutations suppressed to a protruding, and not wild-type, vulval phenotype, were only partially characterized. We hypothesized that among these isolates there were mutations that could be used to order the synMuv genes into a genetic signaling pathway.

Mutations of interest would suppress the Muv phenotype caused by inactivation of some synMuv genes but not suppress the Muv phenotype caused by inactivation of other synMuv genes. Since the "wild-type" suppressor mutations were isolated based on their suppression of *lin-15AB*, one half of these criteria were met. To identify mutations that met the other half of these criteria, we performed RNA-mediated interference (RNAi) of the *dpl-1* gene in the suppressed strain. Suppressor strains that showed a Muv phenotype upon inactivation of *dpl-1* would contain suppressor mutations of interest. We chose to inactivate *dpl-1* over other class B synMuv genes primarily because of its molecular identity. *dpl-1* encodes a protein similar to mammalian DP transcription factors, which act in heterodimers with E2F proteins to regulate transcription of many genes, most notably those that promote cell cycle progression. Since many signaling pathways ultimately modulate transcription, we thought that the *dpl-1* gene would likely function at the terminus of a putative class B synMuv signaling pathway.

In this appendix, we present our identification of suppressor mutations that met the aforementioned criteria. Furthermore, we present genetic map locations of these mutations and epistasis analyses suggesting that our mutations suppress *lin-15AB* mutations in an allele-specific manner.

EXPERIMENTAL PROCEDURES

RNAi analyses

Templates for *in vitro* transcription reactions were made by PCR amplification of the *dpl-1* cDNA yk8d1 (kindly provided by Yuji Kohara and coworkers) and its flanking T3 and T7 promoter sequences. Single-stranded RNA was prepared using T7 RNA polymerase. *In vitro*-transcribed single-stranded RNA was injected as described by Fire et al. (1998).

Genetic mapping

Two-, three- and four-factor mapping crosses were performed according to standard methods (Brenner, 1974). All of these crosses were conducted in a *lin-15AB(n765)* background.

Construction of *sup, sup; lin-15(n309)* and *dpl-1(n3316); sup; lin-15A(n767)* mutants

sup single mutant strains were constructed after mapping individual suppressor loci to defined genetic intervals. Briefly, *sup/m1m2; lin-15AB(n765)/+* hermaphrodites were generated in which *m1* and *m2* were mutations in genes that flanked the suppressor mutation. These animals were selfed to obtain *sup/m1m2* hermaphrodites that produced phenotypically M1M2 progeny but no Muv progeny. Homozygous *sup* animals were obtained as progeny of *sup/m1m2* hermaphrodites. *sup; lin-15AB(n309)* double mutants were constructed by first mating *sup* single mutant males into *m1m2; lin-15(n309)* hermaphrodites. F_2 *sup/m1m2; lin-15AB(n309)* hermaphrodites were obtained and then selfed to generate *sup; lin-15AB(n309)* progeny. To generate *dpl-1(n3316); sup; lin-15A(n767)* mutants we first mated *sup* males into *dpl-1(n3316) unc-4(e120)/mnC1; m1m2; lin-15A(n767)* hermaphrodites then mated the F_1 males again into *dpl-1(n3316) unc-4(e120)/mnC1; m1m2; lin-15A(n767)* hermaphrodites. The resulting *dpl-1(n3316) unc-4(e120)/mnC1; sup/m1m2; lin-15A(n767)* hermaphrodites were selfed to obtain *dpl-1(n3316) unc-4(e120)/mnC1; sup; lin-15A(n767)* hermaphrodites.

RESULTS

dpl-1(RNAi) reduces the penetrance of suppression in a subset of "wild-type" suppressor strains

73 mutant strains in which the Muv phenotype of *lin-15AB(n765)* was suppressed to a wild-type-like, but not to a Vul, phenotype were isolated previously (Clark, 1992). We injected single-stranded *dpl-1* RNA into 69 of these strains and scored the penetrance of suppression in the F_1 progeny of injected animals. In 17 of 69 strains injection of *dpl-1* RNA caused a greater than 10% reduction in the penetrance of suppression. The reduction in suppression was characterized by a Muv phenotype reminiscent of the phenotype of synMuv mutants, including *dpl-1(RNAi); lin-15A* mutants. In an additional eight strains we observed growth defects, either embryonic lethality or arrest during larval development, that precluded scoring the vulval phenotype of adult animals. The defects underlying this apparent synthetic lethality are unknown.

We performed pairwise matings to assign the mutations to complementation groups. In general, we mated *supA/+; lin-15AB(n765)* heterozygous males into *supB; unc-3(e151) lin-15AB(n765)* hermaphrodites, where *supA* and *supB* were two different suppressor alleles. The largest complementation group contains five mutations, three complementation groups contain two mutations each and three complementation groups are defined by a single allele each. Due to its semidominant nature, we did not perform complementation tests with *n2059*.

Genetic mapping of suppressor isolates

We determined linkage group assignments for six loci defined by our complementation tests (Table 2). We further mapped the six loci within linkage groups using three- and four-factor crosses. Some loci mapped to large, gene poor intervals and could not be mapped further using standard phenotypic markers. However, since the time of this study, highly polymorphic, wild isolates of *C. elegans* have been characterized. The single nucleotide and other polymorphisms in these strains could be used to further map the suppressor loci.

"Wild-type" suppressor mutations do not suppress the Muv phenotype caused by *lin-15AB(n309)*

As noted above, we were ultimately interested in identifying genes that functioned downstream of some, but upstream of other, class B synMuv genes. In order to further test whether the genes we defined functioned downstream of *lin-15B*, we asked whether suppressor mutations could suppress the Muv phenotype caused by the *lin-15AB(n309)* null mutation. We constructed *sup; lin-15AB(n309)* mutant strains using mutations representing each of the six loci we had mapped to chromosomal intervals. The Muv phenotype caused by *lin-15AB(n309)* was not suppressed by any of the mutations tested (Table 4). Possible explanations why the suppressor mutations suppressed *lin-15AB(n765)* but not *lin-15AB(n309)* are discussed below.

DISCUSSION AND FUTURE DIRECTIONS

As outlined above, our goal was to identify mutations that could be used to separate class B synMuv genes into different parts of a putative class B synMuv genetic signaling pathway. In general, the mutations we best characterized suppressed *lin-15AB(n765)* well, suppressed *lin-15AB(n765); dpl-1(RNAi)* poorly and did not suppress *lin-15AB(n309)*. What might account for such suppression? One simple explanation is that the mutations were able to suppress a partial loss, but were unable to suppress a total loss, of class B pathway activity. This model assumes that the loss of class B pathway activity in the *lin-15AB(n765)* background is partial but is complete in the *lin-15AB(n765); dpl-1(RNAi)* and *lin-15AB(n309)* backgrounds. The molecular nature of the *lin-15AB(n765)* mutation argues against this possibility. This allele contains a roughly 200 base pair deletion within the *lin-15B* locus that is thought to result in a truncated LIN-15B protein and have severe consequences on *lin-15B* activity (Clark et al., 1994). It remains possible, however, that some residual *lin-15B* activity is present in the hypothesized LIN-15B truncated protein.

Another reason why *lin-15AB(n765)* may have more class B activity than *lin-15(n765); dpl-1(RNAi)* is because of partial genetic redundancy. There are multiple *lin-15B* homologs present in *C. elegans* and any one of these could provide *lin-15B*-like function. If so, one might expect a *lin-15B* null mutation to cause less of a reduction in class B synMuv pathway activity than a null mutation in a gene, *dpl-1* for example, with no worm homologs. The suppressor mutations we characterized might be sensitive to such a difference. This model unfortunately does not explain the lack of suppression of *lin-15AB(n309)*.

Some of our observations might also be explained by considering suppression of not just class B, but also class A synMuv activity. As judged by class-specific complementation tests, *lin-15AB(n765)* mutants are clearly defective in *lin-15A* activity. The lesion that causes this defect is unknown, although genetic criteria suggest that the loss of class A activity is only partial in *lin-15AB(n765)* mutants. By contrast, the loss of class A activity in *lin-15AB(n309)* mutants is likely to be total. *lin-15AB(n309)* mutants contain a deletion that removes most of the *lin-15B* locus and totally removes the *lin-15A* locus. These criteria, along with simple allele strength quantitation, indicate that *lin-15AB(n765)* causes a less severe defect in total synMuv activity than does *lin-15AB(n309)*. It is possible that the suppressors are sensitive to both class A and

class B activity. In this circumstance, the degree of suppression would depend on the combined strengths of the component class A and class B alleles. The suppressors we identified may be able to suppress the weaker class A plus class B defect of *lin-15AB(n765)* mutants but unable to suppress the stronger class A plus class B defect of *lin-15AB(n309)* mutants. Although this model might explain the difference in suppression we observed in *lin-15AB(n765)* and *lin-15AB(n309)* backgrounds, it does not explain the difference in suppression we observed in *lin-15AB(n765)* and *lin-15AB(n765); dpl-1(RNAi)* backgrounds, which have the same class A defect. A cumbersome but more complete explanation of our data might invoke a combination of this and the aforementioned models.

Allele-specificity is a hallmark of informational and interactional modes of suppression. It is possible that the mutations we characterized are acting to suppress *lin-15AB(n765)* via one of these modes. If the suppression were specific to the *lin-15B* locus, one could postulate that *lin-15AB(n765); dpl-1(RNAi)* and *lin-15AB(n309)* mutants would not be suppressed. How might informational or interactional suppression restore activity to a *lin-15B* locus that contains a deletion? An informational suppressor, for example, may alleviate a frameshift caused by the deletion, thereby creating a partially deleted LIN-15B protein with some activity. Alternatively, an interactional suppressor, for example, may stabilize a truncated or partially deleted LIN-15B protein and prevent its destruction. A number of other possible mechanisms exist. These modes of suppression could be evaluated by further testing the allele and gene specificity of suppression.

These studies were designed to characterize a putative class B synMuv genetic pathway. Genes arranged in a pathway have a sequence of action that could potentially be analyzed by epistasis analyses, which is what I hoped to do in these studies. The data regarding *lin-15B*, *lin-37* and *lin-36* genetic mosaics placed class B synMuv activity in two different tissues, clearly implying some sequence of gene action. More recent studies have suggested that these data must be interpreted more carefully. Aidyl Sanchez-Gerrichio and Paul Sternberg (personal communication) developed a technique for high resolution mosaic analysis that was based on the LacI/LacO system (Robinett et al., 1996). Using this technique these researchers determined that *lin-15B* activity, when present specifically in P(3-8).p cells, could rescue the ectopic induction of *lin-15AB* mutants. These results lead one to speculate whether the class B synMuv genes constitute a genetic pathway at all. For example, the class B genes may all act

together in one step to negatively regulate Ras signaling. At a molecular level this may occur if all of the class B synMuv proteins are present in a multisubunit complex that can no longer function if one of many critical subunits is dysfunctional or absent. The molecular identities of and interactions among synMuv proteins are consistent with this possibility.

REFERENCES

Brenner, S. (1974). The genetics of *Caenorhabditis elegans*, Genetics *77*, 71-94.

Clark, S. G. (1992) Intercellular signalling and homeotic genes required during vulval development in *C. elegans*, Ph.D Thesis, Massachusetts Institute of Technology.

Clark, S. G., Chisholm, A. D., and Horvitz, H. R. (1993). Control of cell fates in the central body region of *C. elegans* by the homeobox gene *lin-39*, Cell *74*, 43-55.

Clark, S. G., Lu, X., and Horvitz, H. R. (1994). The *Caenorhabditis elegans* locus *lin-15*, a negative regulator of a tyrosine kinase signaling pathway, encodes two different proteins, Genetics *137*, 987-97.

Clark, S. G., Stern, M. J., and Horvitz, H. R. (1992). *C. elegans* cell-signalling gene *sem-5* encodes a protein with SH2 and SH3 domains, Nature *356*, 340-4.

Ferguson, E. L., and Horvitz, H. R. (1989). The multivulva phenotype of certain *Caenorhabditis elegans* mutants results from defects in two functionally redundant pathways, Genetics *123*, 109-21.

Fire, A., Xu, S., Montgomery, M. K., Kostas, S. A., Driver, S. E., and Mello, C. C. (1998). Potent and specific genetic interference by double-stranded RNA in *Caenorhabditis elegans*, Nature *391*, 806-11.

Hedgecock, E. M., and Herman, R. K. (1995). The *ncl-1* gene and genetic mosaics of *Caenorhabditis elegans*, Genetics *141*, 989-1006.

Herman, R. K., and Hedgecock, E. M. (1990). Limitation of the size of the vulval primordium of *Caenorhabditis elegans* by *lin-15* expression in surrounding hypodermis, Nature *348*, 169-71.

Huang, L. S., Tzou, P., and Sternberg, P. W. (1994). The *lin-15* locus encodes two negative regulators of *Caenorhabditis elegans* vulval development, Mol. Biol. Cell *5*, 395-411.

Robinett, C. C., Straight, A., Li, G., Willhelm, C., Sudlow, G., Murray, A., and Belmont, A. S. (1996). In vivo localization of DNA sequences and visualization of large-scale chromatin organization using lac operator/repressor recognition, J. Cell Biol. *135*, 1685-700.

Thomas, J. H., and Horvitz, H. R. (1999). The *C. elegans* gene *lin-36* acts cell autonomously in the *lin-35* Rb pathway, Development *126*, 3449-59.

TABLES

Table 1. Effect of *dpl-1(RNAi)* on the penetrance of suppression of *sup; lin-15AB(n765)* strains

Genotype	% Sup w/o *dpl-1(RNAi)* (n)	% Sup w/ *dpl-1(RNAi)* (n)	% difference
n1481; lin-15AB(n765)	99 (95)	75 (169)	24
n1482; lin-15AB(n765)	100 (69)	99 (165)	1
n1483; lin-15AB(n765)	100 (131)	99 (82)	1
n1484; lin-15AB(n765)	100 (94)	99 (136)	1
n1485; lin-15AB(n765)	100 (102)	100 (86)	0
n1486; lin-15AB(n765)	22 (109)	24 (93)	-2
n1487; lin-15AB(n765)	100 (153)	100 (279)	0
n1521; lin-15AB(n765)	3.7 (107)	5.9 (169)	-2.2
n1522; lin-15AB(n765)	2.4 (41)	RNAi sick	ND
n1523; lin-15AB(n765)	100 (77)	100 (135)	0
n1524; lin-15AB(n765)	96 (132)	98 (184)	-2
n1525; lin-15AB(n765)	27 (78)	24 (153)	3
n1526; lin-15AB(n765)	6.3 (63)	40 (25)	-34
n1527; lin-15AB(n765)	sup?	ND	ND
n1528; lin-15AB(n765)	5.2 (97)	22 (176)	-17
n1529; lin-15AB(n765)	16 (81)	30 (43)	-14
n1609; lin-15AB(n765)	94 (161)	21 (281)	73
n1611; lin-15AB(n765)	100 (83)	100 (143)	0
n1617; lin-15AB(n765)	100 (73)	93 (177)	7
n1618; lin-15AB(n765)	100 (64)	100 (23)	0
n1620; lin-15AB(n765)	28 (131)	10 (106)	18
n1728; lin-15AB(n765)	100 (114)	98 (161)	2
n1729; lin-15AB(n765)	99 (94)	97 (123)	2
n1731; lin-15AB(n765)	100 (78)	100 (231)	0
n1732; lin-15AB(n765)	45 (92)	4.9 (185)	40
n1763; lin-15AB(n765)	100 (78)	97 (97)	3
n1764; lin-15AB(n765)	81 (180)	77 (192)	4

n1828; lin-15AB(n765)	100 (65)	100 (75)	0
n1829; lin-15AB(n765)	98 (215)	RNAi sick	ND
n1831; lin-15AB(n765)	97 (115)	83 (123)	14
n1865; lin-15AB(n765)	100 (171)	97 (60)	3
n1868; lin-15AB(n765)	100 (173)	95 (222)	5
n1869; lin-15AB(n765)	ND	ND	ND
n2051; lin-15AB(n765)	98 (52)	99 (81)	-1
n2052; lin-15AB(n765)	100 (36)	100 (117)	0
n2053; lin-15AB(n765)	98 (165)	RNAi sick	ND
n2054; lin-15AB(n765)	99 (68)	82 (74)	17
n2055; lin-15AB(n765)	100 (86)	97 (179)	3
n2056; lin-15AB(n765)	100 (60)	100 (91)	0
n2057; lin-15AB(n765)	97 (72)	RNAi sick	ND
n2058; lin-15AB(n765)	95 (136)	68 (160)	27
n2059; lin-15AB(n765)	54 (114)	15 (80)	39
n2060; lin-15AB(n765)	47 (91)	RNAi sick	ND
n2061; lin-15AB(n765)	100 (10)	100 (31)	0
n2062; lin-15AB(n765)	100 (216)	99 (209)	1
n2063; lin-15AB(n765)	100 (191)	100 (253)	0
n2064; lin-15AB(n765)	100 (137)	RNAi sick	ND
n2065; lin-15AB(n765)	100 (3)	70 (53)	30
n2066; lin-15AB(n765)	95 (134)	61 (150)	34
n2067; lin-15AB(n765)	100 (114)	97 (78)	3
n2068; lin-15AB(n765)	100 (67)	100 (51)	0
n2069; lin-15AB(n765)	sup?	ND	ND
n2070; lin-15AB(n765)	100 (23)	100 (69)	0
n2071; lin-15AB(n765)	100 (67)	RNAi sick	ND
n2072; lin-15AB(n765)	100 (133)	RNAi sick	ND
n2073; lin-15AB(n765)	99 (85)	80 (201)	19
n2074; lin-15AB(n765)	99 (131)	80 (117)	19
n2075; lin-15AB(n765)	100 (244)	44 (181)	56
n2118; lin-15AB(n765)	98 (115)	88 (154)	10
n2119; lin-15AB(n765)	99 (80)	100 (36)	-1
n2121; lin-15AB(n765)	97 (29)	97 (31)	0

n2122; lin-15AB(n765)	100 (129)	100 (162)	0
n2123; lin-15AB(n765)	69 (153)	50 (222)	19
n2124; lin-15AB(n765)	95 (120)	80 (94)	15
n2125; lin-15AB(n765)	92 (38)	81 (42)	11
n2126; lin-15AB(n765)	83 (12)	28 (85)	55
n2127; lin-15AB(n765)	100 (65)	100 (138)	0
n2128; lin-15AB(n765)	100 (47)	98 (192)	2
n2129; lin-15AB(n765)	100 (115)	95 (238)	5
n2130; lin-15AB(n765)	98 (44)	96 (84)	2
n2132; lin-15AB(n765)	100 (119)	97 (210)	3
n2133; lin-15AB(n765)	93 (70)	95 (203)	-2
n2139; lin-15AB(n765)	ND	ND	ND

dpl-1(RNAi) was performed as described in Materials and Methods. Percent Sup is scored as the percent of non-Muv animals in the progeny of uninjected or *dpl-1* RNA injected hermaphrodites. "RNAi sick" indicates strains in which injection of *dpl-1* RNA caused partially or fully penetrant lethality or larval arrest that precluded scoring of the Sup phenotype. "sup?" indicates strains that displayed a weak to undetectable Sup phenotype. ND, not determined.

Table 2. Chromosomal linkages of sup mutations

New mutation	Genotype of selected F_2 hermaphrodites with respect to the linked, unselected mutation
n2058	21/57 *dpy-20(e1282)/+ IV*
n2065	14/43 *dpy-20(e1282)/+ IV*
n2075	35/82 *dpy-20(e1282)/+ IV*
n2124	29/58 *dpy-20(e1282)/+ IV*
n1481	3/51 *dpy-20(e1282)/+ IV*
n1609	6/59 *dpy-20(e1282)/+ IV*
n2054	5/23 *unc-39(e369)/+ V*
n2066	6/21 *unc-39(e369)/+ V*
n2073	9/24 *unc-4(e120)/+ II*
n2074	31/77 *unc-4(e120)/+ II*
n1831	0/23 *unc-4(e120)/+ II*
n2125	3/17 *unc-4(e120)/+ II*

Chromosomal linkages were determined as described (see Materials and Methods). Due to difficulties working with strains containing these mutations, map positions of *n2059* and *n2126* were not determined.

Table 3. Three- and four-factor crosses

Gene	Genotype of heterozygote	Phenotype of selected recombinants	Genotype of selected recombinants (with respect to unselected markers)
sup(n1481)	*+ + n1481 / dpy-13 unc-24; lin-15AB*	Dpy	4/4 *n1481 / +*
		Unc	0/10 *n1481 / +*
	+ + n1481 / unc-44 unc-26 + ; lin-15AB	Unc-44	4/4 *n1481/+*
		Unc-26	0/12 *n1481/+*
	+ n1481 + / unc-30 + dpy-4 ; lin-15AB	Unc	2/13 *n1481/+*
		Dpy	18/23 *n1481/+*
		Dpy	1/23 *n1481/n1481*
	unc-30 + + n1481 / + ced-3 unc-26 + ; lin-15AB	Unc-30	1/1 *+ unc-26 / + +*
		Sup	4/4 *+ + / + +*
sup(n1831)	*+ n1831 + / bli-2 + unc-4 ; lin-15AB*	Bli	2/3 *n1831/+*
		Unc	4/7 *n1831/+*
	n1831 + + / + dpy-10 unc-4 ; lin-15AB	Dpy	0/10 *n1831/+*
		Unc	5/5 *n1831/+*
sup(n2054)	*+ n2054 + / + unc-46 sma-1 ; lin-15AB*	Unc	7/10 *n2054/+*
		Sma	3/8 *n2054/+*
	+ n2054 + / + dpy-11 unc-76 ; lin-15AB	Dpy	9/20 *n2054/+*
		Unc	9/10 *n2054/+*
	n2054 + + sma-1 / + rol-3 unc-42 + ; lin-15AB	Sup	3/10 *+ unc-42 / + +*
		Sup	7/10 *+ + / + +*
		Sma	4/5 *rol-3 unc-42 / + +*
		Sma	1/5 *rol-3 + / + +*
		Rol	1/1 *+ sma-1 / + +*
		Unc	4/4 *n2054 + / + +*
sup(n2058)	*n2058 + + / + dpy-13 unc-24 ; lin-15AB*	Dpy	0/5 *n2058/+*
		Unc	7/7 *n2058/+*
	+ + n2058 + / dpy-9 ced-2 + lin-1 ; lin-15AB	Dpy	6/19 *ced-2 n2058 / ced-2 +*
		Dpy	9/19 *+ n2058 / ced-2 +*
sup(n2073)	*+ + n2073 / bli-2 unc-4 + ; lin-15AB*	Bli	3/3 *n2073/+*
		Unc	0/4 *n2073/+*

	+ + n2073 / dpy-10 rol-1 + ; lin-15AB	Rol	1/14 *n2073/+*
		Rol	1/14 *n2073/n2073*
sup(n2125)	*n2125 + + / bli-2 unc-4 + ; lin-15AB*	Bli	0/3 *n2125/+*
		Unc	3/3 *n2125/+*

Three- and four-factor crosses were performed as described (see Materials and Methods).

Table 4. Phenotypes of *sup* single mutant, *sup; lin-15AB(n309)* double mutant and *dpl-1(n3316); sup; lin-15A(n767)* triple mutant strains

Suppressor mutation	Phenotype alone	Phenotype with *lin-15A(n309)*	Phenotype with *dpl-1(n3316); lin-15A(n767)*
n1732 IV	WT vulva	ND	ND
n2058 IV	Egl, WT vulva	ND	ND
n2065 IV	Egl, WT vulva	ND	ND
n2075 IV	WT vulva	ND	ND
n2124 IV	Egl, PVul	Muv	Muv
n1481 IV	PVul, Him	Muv	Muv
n1609 IV	PVul	ND	ND
n2054 V	PVul	Muv	Muv
n2066 V	PVul	Muv	Muv
n2073 II	WT vulva	Muv	ND
n2074 II	WT vulva	Muv	ND
n1831 II	PVul	Muv	ND
n2125 II	PVul, partial Ste	Muv	ND

sup; lin-15AB(n309) double mutants and *sup; dpl-1(n3316); lin-15A(n767)* triple mutants were constructed as described (see Materials and Methods). WT, wild type; Egl, egg-laying defective; PVul, protruding vulva; Him, high incidence of males; Ste, sterile.